THE STRUCTURAL GEOLOGY AND METAMORPHIC HISTORY OF THE LOWER PENNINE NAPPES, VALLE DI BOSCO, TICINO, SWITZERLAND.

by

WALTER DAVID MICHAEL HALL, M.Sc.(Hons), D.I.C.

A thesis submitted for the degree of Doctor of Philosophy in the University of London.

Imperial College.
June 1972.

SUMMARY

The geology of the Valle di Bosco is dominated by a major recumbent fold, the Wandfluhhorn Antiform, which closes to the north and plunges gently to the east. This structure distributes the different rock groups into three semi-concentric zones. The Antigorio Gneiss and Bosco Group are basement units occupying the outer and inner zones respectively, and are separated by a complex zone dominated by Mesozoic cover rocks. The Antigorio Gneiss is a granitic biotite gneiss with minor hornblende schist and dioritic gneiss, while the Bosco Group consists of semi-pelitic garnet and staurolite schist, hornblende schist with minor amphibolite and ultramafic schist, and muscovite gneiss. The Mesozoic rocks are dominantly calcareous schist and marble.

Basement and Mesozoic rocks were deformed three times during the early and middle Tertiary Alpine orogeny. During the F1 deformation the Antigorio Gneiss was thrust over the Bosco Group, but separated from it by a synclinal zone of Mesozoic rocks, named the Stella Syncline. During the F2 deformation the basement and tectonically intercalated Mesozoic rocks were intensely deformed under extremely ductile conditions. All rock types were penetrated by a powerful schistosity, and deformed xenoliths, flattened on the schistosity planes in the Antigorio Gneiss, have been used to calculated strains up to 77%. Large F2 recumbent folds are outlined by the zone of Mesozoic rocks between the two basement groups. F2 minor folds are usually isoclinal, single layer structures with thickened hinges and attenuated, sometimes boudinaged limbs. A strong mineral lineation is parallel to the axial direction of the F2 minor folds.

During the F3 deformation the basement and Mesozoic rocks were again refolded into a large north closing recumbent fold, the Wandfluhhorn Antiform. F3 minor folds are chevron-like, multilayer structures deforming the F2 schistosity. A poorly developed crenulation cleavage is associated with the folds. Crenulation lineation, mullion rods and an intersection lineation define the axial directions of the

folds. A slickenside lineation, lying at a high angle to the fold axes, shows that during the F3 deformation the layering of the rocks was obliquely inclined with respect to the bulk strain. The few examples of deformed lineations and small scale refolding structures show that the F2 and F3 deformations were closely co-axial.

Mineralised joints oriented NW-NNW and barren joints and faults oriented NNW and E - W cut across all earlier structures. The faults are dominantly normal, and have displaced the rocks up to 100 metres vertically. Most displacements are less than 5 metres.

Examination of the metamorphic textures shows that the main porphyroblasts crystallized under static conditions between the F2 and F3 deformations. Micas generally lie parallel to the F2 schistosity, while garnet, staurolite, kyanite and plagioclase grow randomly across the schistosity and have straight inclusion trails. The porphyroblasts were slightly rotated during the F3 deformation and the schistosity was deflected around them. Some plagioclase porphyroblasts grow across deformed schistosity, suggesting that minor crystallization continued after the F3 deformation.

A few lenses of basement rocks that escaped severe strain during the Alpine deformations provide an insight to the pre-Alpine geology. Undeformed granite dykes with chilled margins cut across strongly folded schists, unlike any deformed by Alpine structures.

ACKNOWLEDGEMENTS

To have completed a thesis in Structural Geology at the Imperial College of Science and Technology sees the fruition of a long-term, personal ambition. That this ambition has finally been realised is due in no small measure to the generous financial support of the Broken Hill Proprietary Co. Ltd., Melbourne, Australia. To Mr. D.G. Moye, Director of Exploration, I extend my very sincere thanks for arranging that support, and for his patience in awaiting my return. My thanks also go to Professor John G. Ramsay for his stimulating introduction to the concepts of modern structural geology and the fascinations of the Alps, and for his assistance during the preparation of this thesis. The following also deserve my thanks: Mrs. M. Queyrane for her meticulous typing; Mr. P. Zarenkus for his assistance with draughting; Mr. J. Gee for his assistance with the photography; Dr. W. Lindquist for the use of his wonderful microscope; and Mr. G. Grindley, who first introduced me to metamorphic rocks and structural geology in the mountains of western New Zealand over a decade ago, for his painstaking criticism of the manuscript during the initial stages of its creation. My thanks must also go to the people of Bosco-Gurin, particularly the family Kock-Sartori, who made my visit a memorable one. And finally, but not least, to Kerin and Andrew my thanks for their patience and perseverance during this protracted operation.

LIST OF CONTENTS

		Page
CHAPTER 1	GENERAL INTRODUCTION	
1:1	Location	1
1:2	Topography	3
1:3	Vegetation	5
1:4	Outcrops	5
1:5	Climate	6
1:6	Settlement	6
1:7	Field Work	7
CHAPTER 2	GEOLOGICAL INTRODUCTION	
2:1	Introduction	8
2:2	Basement and Cover	8
2:3	Lower Pennine Nappes	10
2:4	Valle di Bosco	11
2:5	Field Work	16
CHAPTER 3	DISTRIBUTION OF ROCK TYPES	
3:1	Introduction	18
3:2	Antigorio Gneiss	18
	(a) Biotite Gneiss	19
	(b) Muscovite Gneiss	20
	(c) Diorite Gneiss and Hornblende Schist	20
	(d) Schistose Gneiss	21
3:3	Bosco Group	22
	(a) Garnet Schist	23
	(b) Hornblende Schist	24
	(c) Staurolite Schist	25
	(d) Muscovite Gneiss	26
3:4	Mesozoic Rocks	27
CHAPTER 4	STRUCTURAL INTRODUCTION	33
CHAPTER 5	F1 DEFORMATION	35

CHAPTER 6	F2 DEFORMATION	Page
6:1	Introduction	39
6:2	Minor Folds	42
6:3	Schistosity	51
6:4	Lineation	52
6:5	Boudinage	54
CHAPTER 7	F3 DEFORMATION	
7:1	Introduction	60
7:2	Minor Folds	62
7:3	Comparison of F3 and F2 Minor Folds	74
7:4	Internal Boudinage	74
7:5	Crenulation cleavage	76
7:6	F3 Lineations	81
	(a) Lineations Parallel to Fold Hinges	81
	(b) Lineations Oblique to Fold Hinges	84
7:7	Deformation of Earlier Structures	86
	(a) Refolded Folds	86
	(b) Deformed Lineations	89
	(c) Deformed Boudinage	96
7:8	Ductility Contrasts During the F3 Deformation	96
CHAPTER 8	CORRELATION OF DEFORMATION HISTORY	100
CHAPTER 9	DEFORMATION AND METAMORPHISM OF THE ANTIGORIO GNEISS	
9:1	Introduction	105
9:2	Deformed Xenoliths	106
9:3	Deformed Dykes and Veins	115
9:4	Grain Size and Textures	120
9:5	Metamorphic Textures	135
9:6	Correlations and Conclusions	136

CHAPTER 10 UNDEFORMED PRE-ALPINE BASEMENT ROCKS

10:1 Introduction 139
10:2 Field Relations 139
10:3 Microtextural Relations 145
10:4 Outline of Structural and Metamorphic History 152

CHAPTER 11 POST F3 DEFORMATION

11:1 Introduction 153
11:2 Kink Folds 153
11:3 Tension Gashes 153
11:4 Chlorite-Filled Joints 154
11:5 Quartz-Filled Joints 154
11:6 Development of Mineralized Joints 154
11:7 Barren Joints 156
11:8 Faults 159

CHAPTER 12 REGIONAL METAMORPHIC HISTORY

12:1 Regional Setting 167
12:2 Metamorphic Textures 170

CHAPTER 13 METAMORPHIC TEXTURES, VALLE DI BOSCO

13:1 Introduction 174
13:2 Mesozoic Rocks 176
(a) Pelitic Schist 175
(b) Calcareous Schist 181
(c) Marble 183
(d) Quartzite 187

13:3 Bosco Group 187
(a) Semi-Pelitic Schist 188
(b) Hornblende Schist 196
(c) Amphibolite 201
(d) Ultramafic Schist 201

13:4 Antigorio Gneiss 205
(a) Diorite Gneiss 205
(b) Hornblende Schist 207

CHAPTER 14 TIME, TEMPERATURE AND TECTONICS 209

REFERENCES 215

LIST OF FIGURES

		Page
Geological Map 1:10,000		in pocket at back.
Geological Profile 1:10,000		in pocket at back.
1.	Location Map	2
2.	Locality Map, Valle di Bosco	4
3.	Geological correlations of Grutter (1929)	12
4.	Group correlations, Grutter and Wieland	14
5.	Detailed sections, Antigorio Gneiss - Bosco Group contact	31
6.	Detailed profile, Lago Superiore	36
7.	Interference pattern, Pizzo Bombogn	38
8.	Axial traces of major folds	40
9.	Profile section of major structures	41
10.	F2 minor folds, Antigorio Gneiss	43
11.	F2 minor folds, Mesozoic marble-calc schist	45
12.	Isogons and t'a plots, F2 minor folds	47
13.	Isogons and t'a plots, F2 minor folds	49
14.	Isogons and t'a plots, F2 minor folds	50
15.	Stereograms, F2 lineations	53
16.	F2 boudinage	55
17.	Progressive F2 deformation	57
18.	Rose diagram, F2 boudin neck orientation	58
19.	Regional extent of Wandfluhhorn Antiform	61
20.	F3 minor folds in garnet schist and calc schist	63
21.	F3 minor folds, schistose Antigorio Gneiss	64
22.	Symmetry of F3 minor folds (plan)	66
23.	Symmetry of F3 minor folds in profile section	64
24.	Isogons and t'a plots, F3 minor folds	69
25.	Isogons and t'a plots, F3 minor folds	71
26.	Isogons and t'a plots, F3 minor folds	73
27.	Internal boudinage; form and orientation	75
28.	Internal boudinage; garnet schist	77
29.	Internal boudinage; deformation of lineation trace	78
30.	F3 lineations and crenulation cleavage	80

31. F3 crenulation lineation and mullion structures 82
32. Trend of F3 lineations 83
33. F3 slickenside lineation on fold limb 85
34. F3 slickenside lineation and bulk strain 87
35. F3 slickenside lineation and minor folds 88
36. Interference patterns, F2 refolded by F3 90
37. Interference pattern, F2 refolded by F3 91
38. Interference patterns, axial traces and graphs 92
39. F2 lineation deformed by F3 folds 94
40. F2 lineation deformed by F3 folds 95
41. Hinge region of F3 fold, showing deformed F2 lineation 97
42. F2 boudins deformed by F3 folds 98
43. Regional correlation of fold phases 102
44. Deformed dioritic xenoliths in Antigorio Gneiss 107
45. Orientation of deformed xenoliths 108
46. Rf/ø diagrams, Wolfstaffel xenoliths 110
47. Rf/ø diagrams, Wandflühhorn xenoliths 111
48. Graphical representation of deformed xenoliths 113
49. Deformed xenoliths; diagrammatic shape changes 114
50. Aplite and pegmatite dykes in Antigorio Gneiss 116
51. Folded quartz vein in Antigorio Gneiss, isogons and t'a plots 118
52. Diagrammatic representation of deformed dykes and veins in Antigorio Gneiss 119
53. Grain size reduction in Antigorio Gneiss 122
54. Texture of coarse grained Antigorio Gneiss 124
55. Ra/ø diagrams, massive Antigorio Gneiss 125
56. Shear zones in massive Antigorio Gneiss 126
57. Ra/ø diagram, matrix and shear zone, Antigorio Gneiss 127
58. Antigorio Gneiss showing development of schistose texture 129
59. Ra/ø diagrams, slightly schistose Angitorio Gneiss 130
60. Texture of fine grained, schistose Antigorio Gneiss 131
61. Ra/ø diagrams, schistose Antigorio Gneiss 132

62. Quartz augen in schistose Antigorio Gneiss 133
63. Ra/ø diagrams, quartz augen in Antigorio Gneiss 134
64. Lenses of basement rocks undeformed during Alpine Orogeny 140
65. Granite dykes intruding pre-alpine schist 142
66. Strongly folded pre-alpine schist 143
67. Relationship between F2 schistosity and gneiss bands in Bosco Group schist 144
68. Mortar texture in pre-alpine granite 146
69. Mortar texture in pre-alpine granite 147
70. Textures of Bosco Group Gneiss 148
71. Textures of Bosco Group Gneiss 150
72. Pre-alpine schist showing fabric development 151
73. Mineralised joints and stress orientation 155
74. Strike and dip of barren joints 157
75. Barren joints, showing conjugate arrangement and slickensides 158
76. Principal faults 161
77. Strike and dip of faults. 162
78. Faults at Bann and on ridge between Valle di Campo and Valle di Bosco 164
79. View west along trace of Hendar Furggu fault 165
80. Metamorphic mineral zones of Lower Pennine nappes 169
81. Inclusion trails in garnet porphyroblasts in Mesozoic pelitic schist 177
82. Inclusion trails in garnet porphyroblasts in Mesozoic pelitic schist 178
83. Post F2 plagioclase porphyroblast in Mesozoic pelitic schist 180
84. Orientation of inclusion trails in garnet porphyroblasts in Mesozoic pelitic schist 182
85. Mesozoic marble with oriented phlogopite micas 184
86. Mesozoic quartzite with skeletal garnets 185
87. Mineral parageneses of Mesozoic rocks 186
88. Garnet porphyroblasts in semi-pelitic schist of Bosco Group 190

89. Inclusion trails in garnet porphyroblast in semi-pelitic schist of Bosco Group 191

90. Post F2 garnet and staurolite porphyroblasts in semi-pelitic schist of Bosco Group 193

91. Post F2 staurolite porphyroblasts in semi-pelitic schist of Bosco Group 194

92. Post F2 kyanite porphyroblast in semi-pelitic schist of Bosco Group. 195

93. Late crystallizing plagioclase porphyroblast in semi-pelitic schist of Bosco Croup 197

94. Texture of Bosco Group hornblende schist 199

95. Texture of Bosco Group amphibolite 202

96. Texture of Bosco Group ultramafic schist 203

97. Mineral parageneses of Bosco Group 204

98. Texture of dioritic gneiss, Antigorio Gneiss 206

99. Diagrammatic tectonic reconstruction 210

100. Time - temperature graph 213

CHAPTER 1

GENERAL INTRODUCTION

1:1 Location

The Valle di Bosco is a major tributary of the Valle Maggia of Southern Switzerland (fig. 1). It joins the Valle di Campo at the village of Collinasca, and opens onto the Valle Maggia three and a half kilometers to the east near the village of Cevio. Cevio is 20 kms upstream and to the northwest of the point where the Valle Maggia meets Lago Maggiore close to the city of Locarno.

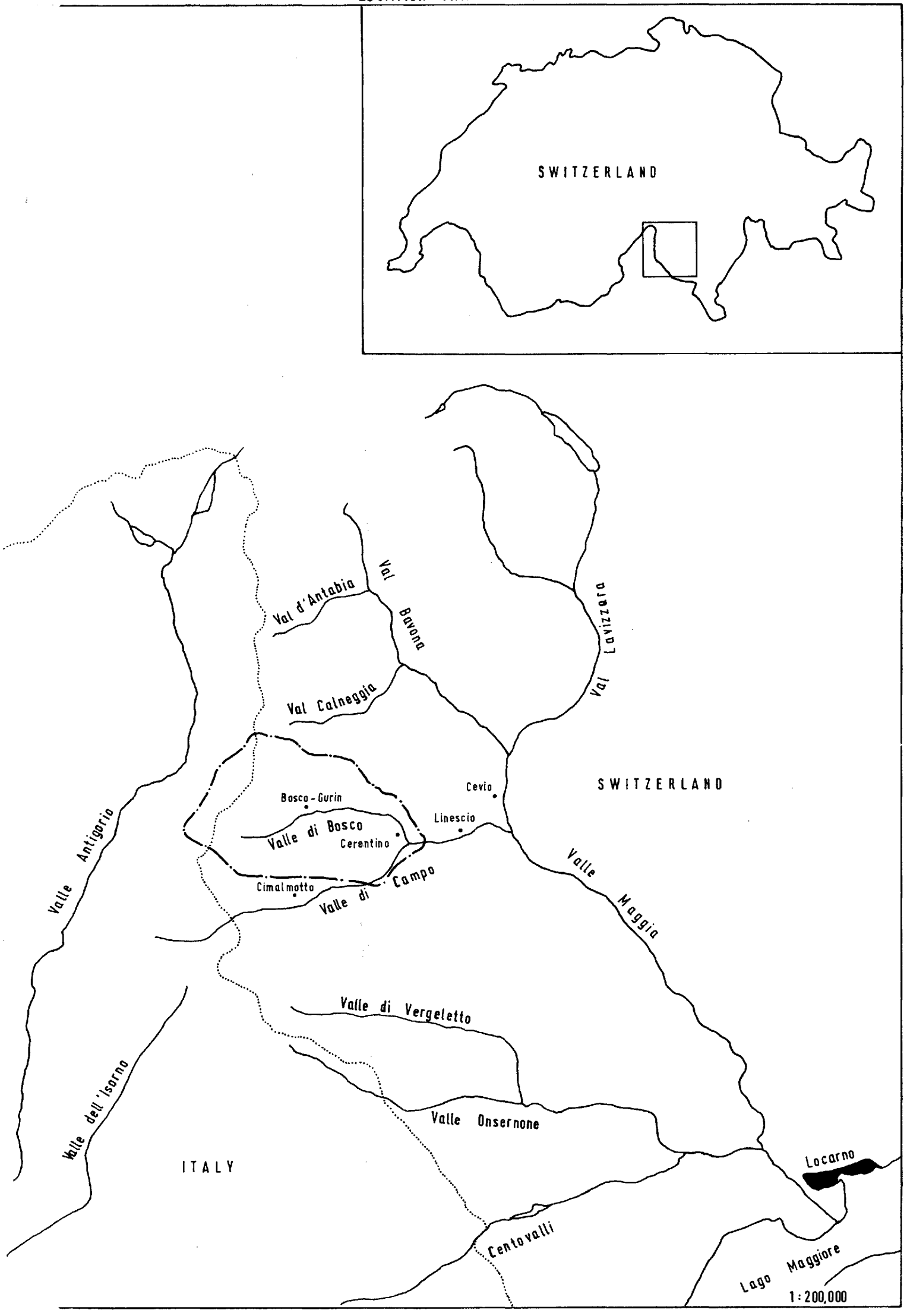
Access to the Valle di Bosco is by road along the Valle Maggia to Cevio, then by way of ten hairpin bends up the steep west wall of the valley to the village of Linescio, and up a further nine hairpin bends to the village of Cerentino, overlooking the junction of the Valle di Bosco with the Valle di Campo. Here the road divides, the northern branch serving the Valle di Bosco and ending at the village of Bosco-Gurin (elevation 1,503 m.), and the southern branch extending nine kms up the Valle di Campo to the village of Cimalmotto (elevation 1,405 m.). From Cevio to Bosco-Gurin the road rises almost 1,100 m. in a distance of 13 kms.

Bosco-Gurin (fig. 2) is three kms from the International boundary which runs along the north-south trending ridge at the head of the Valle di Bosco. The Italian Province of Novara lies to the west of the boundary, and the Swiss Canton of Ticino to the east. To the west the streams fall steeply into the Valle Antigorio, and to the east they lead to the Valle Maggia.

The area studied in this thesis includes the entire Valle di Bosco and the lower reaches of the Valle di Campo, as well as the east-west dividing ridge between them. It covers approximately 40 square kms, the boundaries of which extend from the village of Collinasca in the east, northwest up the valley side to Pizzo d'Orsalia, and west along the ridge between the Valle di Bosco and the Val Calneggia to just

LOCATION MAP

FIGURE 1



north of the Wandfluhhorn, the highest mountain in the area. It then extends south along the western side of the ridge marking the international boundary to the head of the small basin containing Lago del Cramec, and recrosses the international boundary between Pizzo Quadro and the Batnall. It continues southeast for about 1.5 kms, and then east to the junction of the Valle di Niva with the Valle di Campo, and finally along the lower reaches of the Valle di Campo back to Collinasca.

1:2 Topography

The topography of the area is strongly influenced by the extensive Quaternary glaciation, and the regional southeast dipping schistosity which gives rise to very steep north and west facing slopes and much more gentle south and east facing valley sides.

The Valle di Bosco is a typical U-shaped valley with a very steep south wall, and a steep, but much less pronounced north wall which quickly gives way to the extensive shoulders of Wolfstaffel, Bann, Bort, Grossalp and Chummuheij. These slope gently southeast parallel to the direction of dip, before rising abruptly to the sharp, bare ridges dividing the Valle di Bosco from the Val Calneggia and the Valle Antigorio. North and west of these divides, the steep slopes are interrupted only by a few small lake filled cirques, of which Lago Superiore, between the Martschenspitz and Wandfluhhorn, is the largest.

The highest peaks occur in the west of the area along the dividing ridge forming the international boundary. The Wandfluhhorn (2,863 m.) at the northern end of the ridge occurs at the junction of the Valle di Bosco, Val Calneggia and Valle Antigorio, and is separated from the Martschenspitz (2,688.1 m.) to the south by a deep, fault-controlled gash in the ridge at Hendar Furggu (2,419 m.). The Martschenspitz is isolated to the south by another deep fault-controlled gash at Passo di Bosco (2,323 m.). South of the pass the ridge rises gradually, with only a few small undulations in height, from the Ritzberg (2,591.6 m.) to the Batnall (2,748.4 m.) at the junction of the Valle Antigorio, Valle di Campo and Valle di Bosco.

FIGURE 2

676 677 678 679 680 681 682 683 684 685 686

133 132 131 130 129 128 127

Wandfluhhorn (2863m)

VAL CALNEGGIA

P.d'Orsalietta (2476 m)

P.d'Orsalia (2664·3 m)

STRAHL BANN

VALLE ANTIGORIO

2592 m

Camino (2488·6 m)

Hendar Furggu (2419m)

2528 m

BANN

WOLFSTAFFEL

Lago Superiore (2254m)

Bann (2104 m)

Martschenspitz (2688·1m)

2141m

ALPE MATER

Rota Balmu

Bodme (2241m)

BORT

Passo di Bosco (2823m)
(Guriner Furka)

Ritzberg (2591m)

2446 m

Ritana (1557m)

Pögga (1574m)

Bosco-Gurin (1503m)

Ubarab (1294m)

Cios (1206 m)

Corino (1093 m)

Camanoi (1136 m)

Krammegg pass (2518m)

GROSSALP

Grossalp

Piano del Vitetti

Pila (1075 m)

Alpe Cramec (1981m)
Lago del Cramec

VALLE DI BOSCO

Andatschei (1680 m)

Schwarza Brunna

Rovana

Passo della Stella

CHUMMUHEIJ

Alp Bobna (174 m)

Passo Pian Crosc (1925 m)

1850m

Pian Crosc (1955m)

Chumma (1855m)

2173 m

Cerentino (980 m)

Collinasca (761m)

Grosshorn (2150 m)

Batnall (2748·4 m)

P. Bombogn (2330·6 m)

Kleinhorn (2171m)

Sasso Rosso

Passo Quadrella (2137 m)

P. Quadro (2792·5 m)

Rio Colobiasca

SWITZERLAND
ITALY

ALPE DI QUADRELLA

VALLE DI CAMPO

Campo (1281 m)

Niva (955 m)

Piano (1187 m)

ONE KILOMETRE

1 : 25,000

Cimalmotto 200 ms

V. di Niva

LOCALITY MAP VALLE DI BOSCO

The highest peak along the ridge between the Valle di Bosco and Valle di Campo is Pizzo Bombogn (2,330.6 m.) which has a steep north face, and much gentler southern slopes.

1:3 Vegetation

The valley sides are generally covered by thick larch forest up to between 1,900 m. and 2,000 m., although a few scattered trees climb above this level beside some of the larger gullies. The most extensive forest is along the northern slopes of the Valle di Campo where only a few small patches have been cleared to provide pastures for summer grazing. Much of the forest has also been cleared from the area immediately surrounding the village of Bosco-Gurin.

The steepest slopes immediately above the floor of the Valle di Bosco, particularly those on the south side, support a very thick scrub cover, which makes access both difficult and unpleasant.

1:4 Outcrops

The best and most continuous outcrops occur above the timber line, although they are often covered by scree adjacent to the steepest faces. They are generally poor on the lower valley slopes, and mainly restricted to the steep, fault controlled gullies and streams which are negotiated with difficulty, especially where they are enclosed by forest. The steep waterfall-infested gullies on the south side of the Valle di Bosco are really only safely worked when they are still snow-filled in early summer.

Outcrops occur along the main streams in the valley floors only where they have cut narrow gorges, the most spectacular examples being along the lower reaches of both the Valle di Bosco and the Valle di Campo, and in the river downstream from their junction.

Continuous outcrops extend along the ridge east of the Batnall to Pizzo Bombogn, and for a kilometer east of Passo Pian Crosc, but over extensive areas on the southern slopes they are concealed beneath

tumbled, chaotic blocks and finer scree extending in most places to the floor of the Valle di Campo. The few isolated outcrops are mainly in deep fault-controlled gullies and on a few steep faces at the head of minor scree slopes.

The western face of the ridge forming the international boundary, the most critical area for an understanding of the structural geology, is particularly well exposed. Only a few of the very steepest parts are inaccessible, and one small portion is concealed by scree in the basin immediately southwest of the Wandfluhhorn.

1:5 Climate

In common with other areas in the mountains of Ticino the Valle di Bosco has a short, relatively warm summer and a long cold winter. Snow falls intermittently throughout the year, but only begins to lie from mid-October onwards, and has generally cleared by mid-June, except from the more sheltered north-facing basins. Cloud build-up is common during many of the warm summer days, particularly in August, and the late afternoons are often punctuated by thunderstorms with accompanying heavy downpours.

1:6 Settlement

The village of Bosco-Gurin, with a population of 120, is situated on a small moraine almost in the centre of the area and overlooks a series of small, cleared river terraces. It was first inhabited in the mid 13th century by Walser people, the descendants of whom still speak a mediaeval German dialect, and have given the valley it's distinctly German topographic names in what is otherwise an Italian influenced region.

Although the population has diminished considerably in the past 100 years, many of the older people still carry out their traditional summer tasks of cutting hay for winter feed for a small herd of milch cows, now dwindled to about 30, and tending small vegetable patches. Remnants of terracing on the hillsides immediately above the village testify to much more intensive activity in the past, and records exist of the valley having supported up to 500 cows. A small herd of cows

and goats is taken up to the Grossalp-Bann-Wolfstaffel pastures for three summer months from the time the snow disappears until the hunting season begins in early September, but many of the higher pastures have been unused for a number of years.

1:7 Field Work

Bosco-Gurin was an ideal base for field work, as the farthest point of work was only a four hour walk from the village, and the numerous, recently abandoned huts dotted throughout the area formed excellent high camps. The only tent camp necessary was at Lago Superiore.

A total of seven months were spent in the field, chiefly on detailed mapping within the thesis area, but also on reconnaissance work in adjacent parts of the region. During the 1969 summer three months field work was carried out between early July and the end of September, while the remaining four months were completed between early June and the end of September during the summer of 1970.

CHAPTER 2

GEOLOGICAL INTRODUCTION

2:1 Introduction

A century of geological research in the Western Alps has lead to an understanding of the basic stratigraphy and tectonic evolution, and made the region one of the classics of geology. The excellent exposure and many fascinating problems, together with the ease of access continue to make the region a fruitful stamping ground for the structural geologist.

South of the Molasse Basin of Northern Switzerland the Alps are divided into the Pre-Alpine and Helvetic Nappes, the External Massifs, and the Pennine Nappes. The Lower Pennine Nappes, about which this study is concerned, form the lowest structural zone of the Western Alps, and are exposed in the Lepontine Mountains between the Gotthard Massif to the north and the Insubric Line to the south. Thanks to the development of the nappe theory by Bertrand (1884) and the outstanding work of Lugeon (1901 and 1902), the Lower Pennine Nappes were early recognised as large, north facing recumbent folds.

2:2 Basement and Cover

The interpretation of the nappe structures depended on the fundamental distinction between basement and cover rocks. In the less deformed and only slightly metamorphosed external portions of the Western Alps, a major unconformity separates the crystalline basement and the covering sediments. Although the cover succession varies from place to place, Trumpy (1960) has shown that it is dominantly calcareous, and begins with quartzite, dolomite and limestone containing Triassic fossils. Radiometric dating of the basement rocks below the unconformity shows that they are generally Carboniferous and older. In the Gotthard Massif, just north of the lower Pennine area, Arnold (1970) dated basement paragneiss between 1,500 and 450 million years old, and orthogneiss between 560 and 420 million years old. These are intruded by Hercynian granites giving whole rock and zircon ages between 300 and 240 million years old. Locally the Triassic cover

rocks rest on weakly metamorphosed conglomerate, arkosic sandstone and carbonaceous shale with ignimbrite layers, dated from plant remains as Late Carboniferous. (e.g. Franks, 1968).

The basement-cover unconformity can be traced back into the frontal portions of the lower Pennine nappes. A persistent marble and locally developed quartzite lie on non-calcareous basement gneiss and schist, and are overlain by a thick, largely unfossiliferous and strongly folded succession of dark calcareous schsist, the Bündnerscheifer. Liassic fossils have been discovered near the base of the formation by Nabholz (1945), and Trumpy (1954) considers that the formation probably ranges high into the Cretaceous. The scarcity of fossils has been attributed by Bolli and Nabholz (1959) to the original sterility of the formation, but may also be due to the amount of recrystallization and tectonic reworking. However, Higgins (1964a) discovered fossils in kyanite-bearing Bündnerschiefer in the Basodino region, north of the Valle di Bosco, and confirmed the Mesozoic age.

In the lower Pennine area the Mesozoic rocks can be traced around north-closing basement lobes, and southwards in synclines which gradually become very tight and lose their stratigraphic symmetry. Eventually the synclines are represented by thin bands of marble enclosed in basement rocks. The marble bands become strongly refolded and recrystallized, and without them a sensible and realistic structural interpretation would be extremely difficult.

As the basement rocks are traced into the lower Pennine region they give consistently younger radiometric ages, suggesting that they were reheated above the isotopic stability point of individual minerals. A line drawn between biotites giving cooling ages less than 20 million years old and between 20 and 50 million years old corresponds closely to the kyanite isograd of Alpine metamorphism, and delineates the lower Pennine area (Jaeger, Niggli and Wenk, 1967). The very young ages and the relatively undeformed nature of some of the granitic basement led Wenk (1943, 1963) to the conclusion that many of the crystalline rocks were Alpine intrusives. However, they were never seen to cut Mesozoic rocks. The only definite Alpine granite occurs

in the Bergell Alps just east of the lower Penning region, and gives zircon ages of 30 million years and biotite cooling ages of 25 million years. The youngest biotites from the basement rocks of the lower Pennine area give cooling ages close to 10 million years. Hunziker (1969) has dated the peak of the Alpine metamorphism as occurring 38 million years ago during the Late Eocene-Early Oligocene.

2:3 Lower Pennine Nappes

The earliest studies of the lower Pennine region by Desor (1865), Heim (1878), Renevier (1879) and Schmidt (1894), summarized by Niggli et. al. (1936), depict gneissic massifs separated by synclinal zones of Mesozoic schists. Development of the nappe theory led to a better appreciation of the style of deformation, and close examination of the cross sections of Schmidt (1907) and Preiswerk (1918) reveals a faithful and factural portrayal of these new ideas. However, while the major structures were clearly outlined, no minor structural features were examined in detail.

The excellence of this early mapping, notably that of Schmidt, Preiswerk and Stella (1908), has provided a basis for a much more accurate evaluation of the structural pattern of the lower Pennine Nappes. From the early maps critical areas have been chosen for new work which has begun to provide many of the answers to long standing problems.

During the past fifty years work in the lower Pennine Nappes has been dominated by geologists from the University of Basel and the E.T.H., Zurich, but this has a very strong petrographic bias, and with the exceptions of Milnes (1965) and Kobe (1966) there is little published work on the structural complexity of the region.

The lower Pennine Nappes were named Monte Leone, Lebendun and Antigorio in descending structural order in the Simplon region by Lugeon and Argaud (1905). They can be divided into three zones; a northern frontal zone of generally steep dips in which the basement cores close and pass into a large area of strongly folded Mesozoic rocks; a flat-lying zone in which basement rocks contain long thin Mesozoic strips, and dip gently east and west across the Toce and

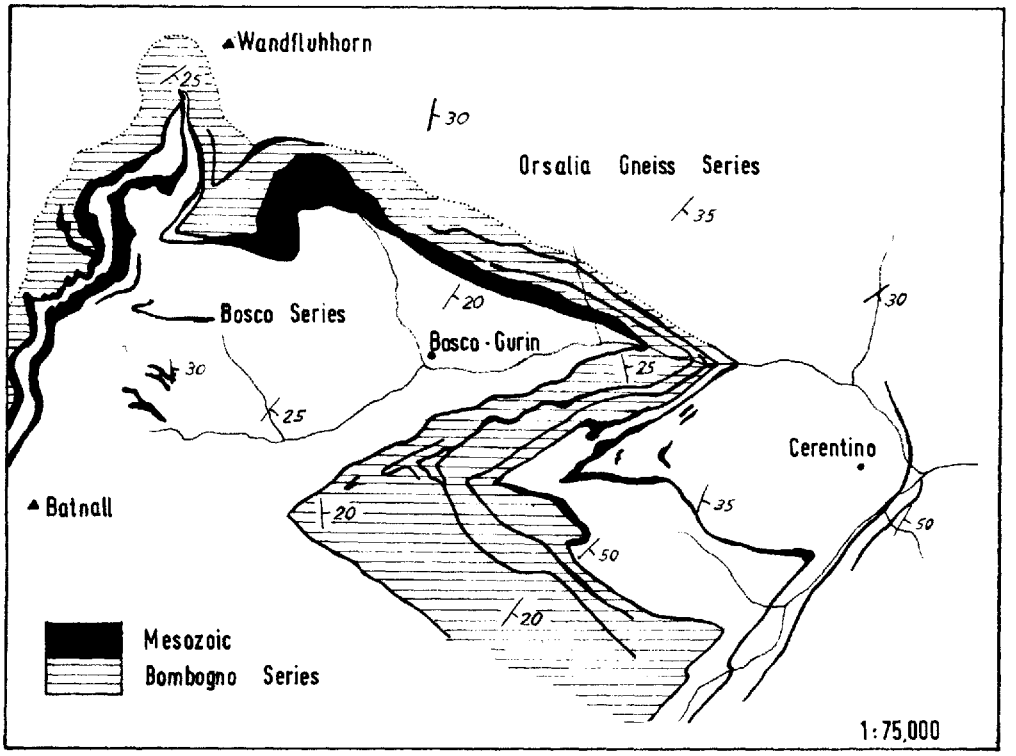
Ticino culminations (Preiswerk 1921); and a southern "root zone", a narrow zone of very steeply dipping basement rocks with thin Mesozoic bands, and classically depicted as the area from which the nappes originated (Argand 1916). The root zone is bounded to the south by a major fault, the Insubric Line. North of this line both basement and Mesozoic rocks were strongly folded and metamorphosed up to sillimanite grade during the Early to Middle Tertiary, while those to the south were unaffected by metamorphism and only gently folded.

2:4 Valle di Bosco

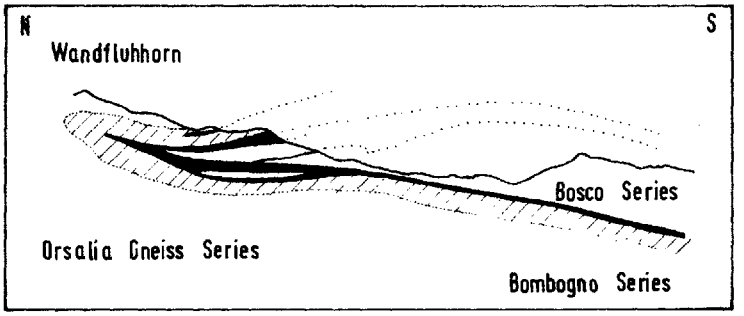
The Valle di Bosco is located roughly in the centre of the flat-lying zone, on the eastern side of the Toce culmination. The first detailed, but dominantly petrographic description of the geology of the region was published by Grutter in 1929. (see fig.3). He recognised a large north facing recumbent fold, here named the Wandfluhhorn Antiform, on the southwest face of the Wandfluhhorn, but considered it to be a relatively minor feature in which rocks of the Lebendun Nappe were involved in the complicated synclinal zone between the Monte Leone Nappe above and the Antigoric Nappe below.

Grutter divided the rocks of the Valle di Bosco into three groups. The outer Orsalia Gneiss Series was described as coarsely crystalline, mainly granitic gneiss with aplite dykes of igneous origin, and was divided petrographically into Wandfluhhorn, Strahlbann, Tosatal and Matero types depending on the quartz content and feldspar composition. Within the Orsalia Gneiss Series Grutter described bands of dioritic-gabbroic-amphibolite, and garnet-bearing paragneiss. The Bombogno Series, separating the outer gneiss from the inner Bosco Series, contained a number of thin bands of Mesozoic rocks, and was described as the tectonically reworked margin of the Orsalia Gneiss Series. It consists of fine grained, banded quartzo-feldspathic gneiss with a strong platey fabric. Grutter's inner Bosco Series consists of a heterogeneous complex of gneiss and schist, and includes light coloured schist containing garnet, staurolite and kyanite porphyroblasts, micaceous gneiss and a dark hornblende schist with coarse grained pods derived from peridotite and gabbro.

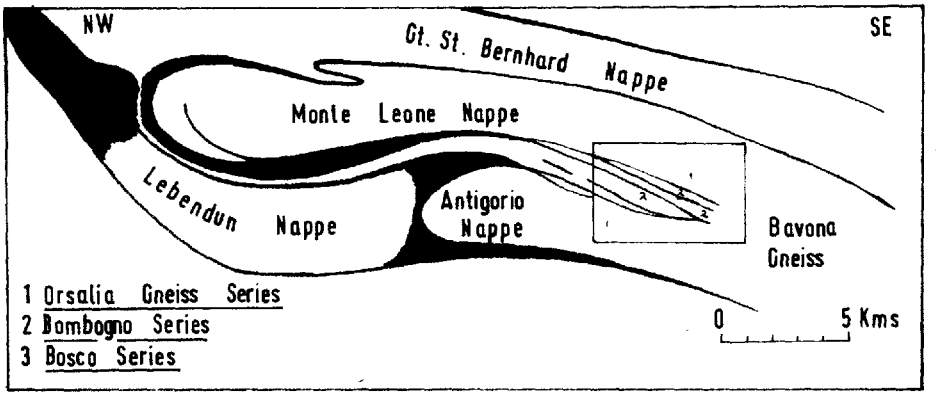
GEOLOGICAL CORRELATIONS OF GRUTTER (1929) FIGURE 3



(a) GEOLOGICAL SKETCH MAP SHOWING THREEFOLD DIVISION DESCRIBED BY GRUTTER



(b) SECTION THROUGH STRUCTURAL CLOSURES IN WANDFLUHHORN REGION



(c) SCHEMATIC REGIONAL PROFILE SHOWING POSITION OF AREA STUDIED IN DETAIL BY GRUTTER

The area immediately north of the Valle di Bosco was mapped by Gunthert (1957). The description (1958) is dominantly petrographic, and omits discussion of the structural geometry and significance of the minor structural features. Hunziker (1966), after a largely geochemical investigation, described the geology of an area along the Italian side of the international boundary immediately west of the Valle di Bosco. Although I find his structural conclusions difficult to follow, he, like the earlier workers, recognised the Wandfluhhorn Antiform, and concluded that it was the "knot" of the entire tectonic problem. He agreed with Wenk and Trommsdorff (1965) that crystallization outlasted the main Alpine deformation, and considered that this could be proved in the area he examined.

Recent work on the structural evolution and metamorphic textures (e.g. Higgins, 1964b; Chadwick, 1968) shows that this concept is an oversimplification, and that a major deformation occurred after the metamorphic peak. A similar conclusion is reached in Chapter 13 of this thesis.

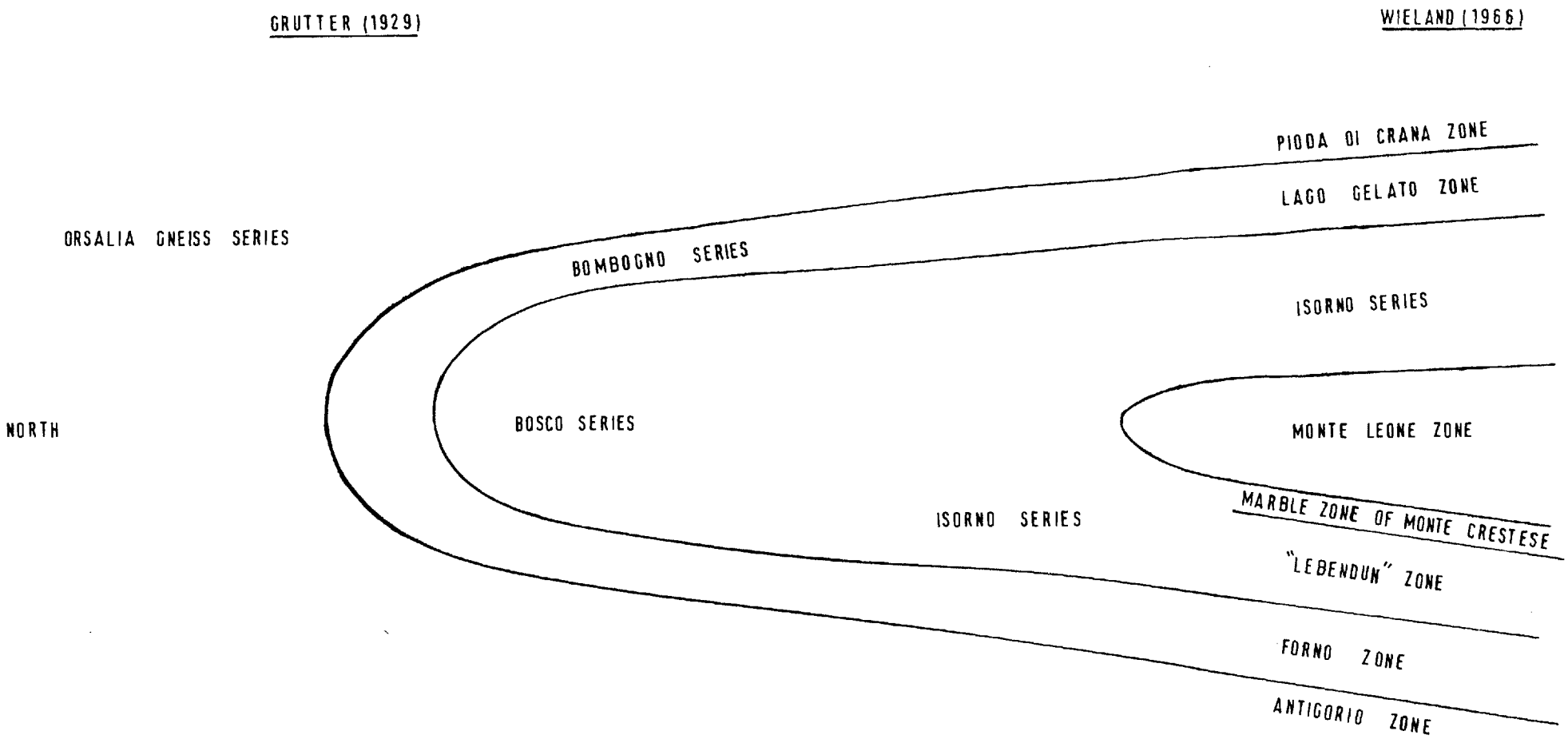
To the south of the Valle di Bosco Wieland (1966) distinguished seven zones, symmetrically disposed about the axial trace of the Wandfluhhorn Antiform, and showed that they continued northwards into those described by Grutter. From west to east the zones are: (see fig. 4).

1. Antigorio Zone; coarse grained, coarsely foliated biotite gneiss, passing north into Grutter's Orsalia Gneiss Series.

2. Forno Zone; alternating layers of carbonate rocks and gneiss, with rare amphibolite and mica schist, passing north along the inverted western limb of the Wandfluhhorn Antiform into Grutter's Bombogno Series.

3. "Lebendun" Zone; well banded, platey muscovite-biotite gneiss with marble and amphibolite bands, passing north into the Isorno Series.

4. Recumbent Limb of the Isorno Series; foliated biotite and biotite-muscovite schist, aplitic gneiss, mica schist with garnet, staurolite and kyanite, amphibolite with ultramafic lenses, and



GROUP CORRELATIONS GRUTTER (1929) AND WIELAND (1966)

FIGURE 4

Mesozoic marble and calc-mica schist, passing north into Grutter's Bosco Series.

5. Marble Zone of Monte Crestese; pure marble with minor mica schist, amphibolite and gneiss, separating the "Lebendun" Zone from the Monte Leone Zone.

6. Monte Leone Zone; dark, platy biotite gneiss, garnet-mica schist, amphibolite with ultramafic lenses, and a marble band, occupying the hinge region of the Wandfluhhorn Antiform.

The Isorno Series is again encountered east of the Monte Leone Zone, and is followed by 7. Lago Gelato Zone, equivalent of the Forno Zone, and 8. Pioda di Crana Zone, equivalent of the Antigorio Zone.

Hunziker (1966) followed Wieland in using these names, but as they duplicate those of Grutter, which clearly have historical priority, they are considered unnecessary. The Orsalia Gneiss Series of Grutter corresponds to Wieland's Antigorio Zone and Pioda di Crana Zone, but the term Antigorio Gneiss, as originally used by Schmidt (1907), has priority over all these names and should therefore be used as a group name to cover all the basement rocks of the Antigorio Nappe. Grutter's Bombogno Series correlates with the Lago Gelato Zone and Forno Zone of Wieland, but the terms series and zone are incorrectly used (American Geological Union, 1962). They apply to the structurally complicated transition between the Antigorio Gneiss and the Bosco "Series", and do not include any rock types unique to this particular horizon. Grutter's Bosco Series corresponds to Wieland's Isorno Series, which in turn appears to be equivalent of his "Lebendun" Zone and Marble Zone of Monte Crestese. The term Bosco Series clearly has historical priority, although it should be renamed Bosco Group as it includes a variety of lithological units. These rocks appear to form part of a basement nappe distinct from the Antigorio Nappe, but their precise correlation with other nappes in the region is unknown.

The correlation of the Bosco Group with the Lebendun Nappe, as shown on the Ticino 1:200,000 geological map (Commissione Geologica Svizzera, 1955) is now in considerable doubt. Dr. G. Milnes of the E.T.H., Zurich (pers. comm.) has recently discovered that the Lebendun

rocks along the west side of the Valle Antigorio die out just west of the southern portal of the Simplon Tunnel. Further, the Lebendun rocks are mainly conglomeratic gneiss and psammitic schist, quite different from the typical semi-pelitic schist and muscovite gneiss of the Bosco Group.

Wieland described his innermost unit as the Monte Leone Zone, a horizon which cannot be correlated directly with any in the Valle di Bosco. However, schist and amphibolite enclosed in the gneiss of this zone resembles that of the Bosco Group. Unfortunately, there is as yet no conclusive evidence that these rocks are connected with the Monte Leone Nappe, but Milnes (1968; 64) has shown that the Monte Leone rocks of the Simplon area consist of extensive, relatively homogeneous granitic gneiss alternating with complex heterogeneous zones of biotite rich gneisses, muscovite-garnet-staurolite schist, hornblende schists, ultramafic bodies and coarse grained augen gneiss. This description undoubtedly fits the Bosco Group.

The possible correlation of the rocks of the Bosco Group with those of the Monte Leone Nappe should not be greeted with too much surprise. The discovery of the regional significance of the Wandfluhhorn Antiform, and its complicated refolding of earlier large scale structures, has thrown wide open the question of the correlations of the individual lower Pennine Nappes across the Toce culmination, and indeed whether there are only three lower Pennine Nappes, and what their original structural order was. Until the Monte Leone - Bosco Group correlation is decided it is suggested that the name Bosco Group should be retained for the rocks on the east side of the Valle Antigorio, but with the proviso that it may become redundant when the correlations across the valley are firmly established by detailed field work.

2:5 Field Work

The Valle di Bosco was chosen for this thesis study after an examination of the Ticino 1:200,000 geological map revealed a large interference pattern in the region of the Wandfluhhorn. Two basement groups, one dominated by orthogneiss and the other by paragneiss

appeared to be involved in a complex structure with a number of thin bands of Mesozoic rocks. The work of Grutter (1929) and Hunziker (1966) further illustrated the structural complexity, and Higgins (1964b) had shown that the basement and cover rocks of the Basodino area to the north had been deformed at least three times.

An area of 40 square kilometres was remapped on a scale of 1:10,000, and one critical, excellently exposed area, 200 metres by 300 metres, near Lago Superiore, was mapped on a 1:500 scale. Measurements were made of all the structural features, and particular attention was paid to the fold styles and their relation to the major Wandfluhhorn Antiform. This led to an understanding of the complex structural geometry, and a tectonic pattern of three major deformations emerged. Each deformation has distinct minor features associated with it, and these are described in detail in the succeeding chapters. The first deformation saw the emplacement of two large basement nappes, separated by a complex, synclinal zone of Mesozoic rocks. The basement and cover rocks were intensely strained under very ductile conditions during the second deformation, and developed a powerful schistosity. During the third deformation the schistosity was folded into a major, north-closing recumbent fold, the Wandfluhhorn Antiform.

Samples were collected from all the lithological units in the area, and thin sections of these were examined with particular reference to the timing of growth of individual minerals in relation to the deformation episodes. The most significant conclusion was that the majority of the porphyroblasts crystallized under static conditions between the second and third periods of deformation.

When combined with a detailed analysis of the fold styles, boudinage relationships, grain size characteristics and strain calculations based on deformed xenoliths, the microtextural study led to an understanding of the processes of deformation, and the behaviour of the different rock types at each stage of the tectonic evolution. This was carried to a conclusion by a detailed examination of the faults and joints.

CHAPTER 3

DISTRIBUTION OF ROCK TYPES

3:1 Introduction

The rocks exposed in the Valle di Bosco are divided into three distinct groups, two of which are basement and one cover. The basement groups, the Antigorio Gneiss and Bosco Group, consist of gneiss and high grade schist, while the cover group is dominated by marble and calcareous schist. There is no direct evidence of a Mesozoic age for the cover rocks, but they resemble rocks generally regarded as Mesozoic in the lower Pennine area. Rocks of all three groups have been strongly folded and recrystallized, and are cut by a powerful schistosity. Despite the local masking of intrusive relationships within the basement, and the lack of positive evidence for an unconformity or thrust between the cover and basement the contacts between the groups remain sharp and well-defined.

The Wandfluhhorn Antiform distributes the basement groups into two semi-concentric zones, convex towards the north (see Geological Map, and Structural Profile). The outer zone is formed by the Antigorio Gneiss, and the inner zone by the Bosco Group. The Mesozoic rocks occur as thin bands at three structural levels, the most important being the complex synclinal zone between the Antigorio Gneiss and the Bosco Group.

The Antigorio Gneiss and the Bosco Group are thought to form part of separate basement nappes brought into contact during the first period of Alpine deformation. During this deformation the Mesozoic rocks were tectonically intercalated along the contact zone between the two nappes. This initially relatively simple relationship was complicated during two later periods of deformation.

3:2 Antigorio Gneiss

The Antigorio Gneiss is a relatively homogeneous massive rock derived from a Hercynian igneous complex. The igneous origin of the complex is depicted by the granitic appearance of the rocks, the common occurrence of xenoliths of a more basic composition, and

the thin, cross-cutting sheets of aplite and pegmatite. Chemical analyses and modal compositions listed by Grutter (1929) and Hunziker (1966) show that the dominant rocks vary slightly between granite and adamellite.

On the lower limb of the Wandfluhhorn Antiform the Antigorio Gneiss is exposed along the western (Italian) side of the ridge marking the international boundary from just below the summit to the floor of the Valle Antigorio. North of Lago Superiore, the gneiss is folded around the hinge of the antiform, and extends east along the north side of the Valle di Bosco. To the north the Antigorio Gneiss covers the entire Val Calneggia and extends to the Valle Antabbia, just south of Pizzo Basodino.

On the south side of the Valle di Bosco a band of massive gneiss extends from the valley floor at Piano dei Vitelli to the ridge top at Pian Crosc. This band is displaced 200 metres to the northwest by a fault at Passo Pian Crosc, but continues southwest to the summit ridge again just east of P. Bombogn. Although exposed for a short distance down the southern slopes of P. Bombogn its true extent is difficult to determine because of extensive forest and large landslides, but it appears to wedge out southwards.

A much thinner band of massive Antigorio Gneiss is exposed in the bed of Rovana Stream between 100 and 200 metres downstream from the bridge on the main road just southwest of Corino. The gneissic fabric of both this and the band to the west is very strongly folded, particularly in the area east of Passo Pian Crosc.

(a) Biotite Gneiss

The dominant biotite gneiss has a granitic appearance and composition (quartz, K feldspar and biotite). Grutter (1929) recognised Wandfluhhorn and Strahlbann "varieties", but these terms are considered unnecessary as they represent only small variations in the quartz and feldspar content that can only be distinguished microscopically. The biotite flakes are aligned parallel to the coarse schistosity along which good quartz and felspar augen are occasionally

developed. Lineation, apart from slickensiding on the biotite surfaces, is weak, but in the hinge region of the Wandfluhhorn Antiform the gneiss has a rod-like fabric, resulting from the intersection of the schistosity and a later crenulation cleavage.

The biotite gneiss is cut by thin aplite and pegmatite dykes and quartz veins rarely more than 10 cms thick. These usually lie sub-parallel to the schistosity and are penetrated by it, but a few are folded or boudinaged.

(b) Muscovite Gneiss

The white muscovite gneiss, equivalent to Grutter's quartz-rich Tosatal "type", usually occurs in patches too small to be outlined on a 1:10,000 scale. These often have irregular, probably originally intrusive boundaries with the biotite gneiss, but are cut by the same strong schistosity. The best exposures of the muscovite gneiss, showing its relationship with the biotite gneiss, are on the glaciated pavement just southeast of the Wandfluhhorn, and at Rota Balmu where many surfaces have been freshly exposed by blasting during the construction of avalanche barriers. At these localities the muscovite gneiss forms distinct compositional bands within an otherwise homogeneous unit, and is often strongly folded. It is generally coarser grained than the biotite gneiss, and much lighter coloured

A persistent band of muscovite gneiss extends along the western side of the ridge from the Batnall to just south of the Wandfluhhorn. It can be traced around the fold hinge and south to the Martschenspitz. It reappears north of Bann and extends along the steep valley side to Rota Balmu, east of which it could not be found. The thickness gradually decreases from 30 metres below Passo dell Stella to six metres at the Martschenspitz and three metres at Rota Balmu.

(c) Diorite Gneiss and Hornblende Schist

Within the Antigorio Gneiss are a number of lenses of dioritic gneiss and hornblende chist. These two rock types are basement units intruded by the granitic rocks and subsequently deformed with them. The hornblende schist was probably derived from a basic

igneous rock, and the diorite gneiss from a diorite or tonalite.

A band of fine grained, dark hornblende schist 10 m. in thickness can be traced for a kilometre around the ridge west of the Martschenspitz. Both its margins and internal fabric are parallel to the schistosity of the surrounding gneiss, but the band thins and wedges out to the south and is obscured beneath scree slopes to the north.

The diorite gneiss is a mottled black and white, medium grained rock, and also occurs in bands parallel to the schistosity of the granite gneiss. The thickest and most extensive band is exposed at the eastern end of Strahlbann, and extends southeast from the ridge top near point 2,689.3 m. to the Wolfstaffel slopes where it wedges out. Three thinner bands, each up to three metres thick, occur high on the Val Calneggia side of the ridge east of the Wandfluhhorn. These all end in horizons densely packed with xenoliths which eventually die out.

Similar dioritic xenoliths are common throughout the gneiss and have proved extremely useful for the determination of strain. They are relatively uniform in size, about 20 cms by 1.5 cms, and apart from the area just east of the Wandfluhhorn are very common on the Wolfstaffel slopes and below Krameggpass.

(d) Schistose Gneiss

As the Antigorio Gneiss is followed towards the zone of Mesozoic rocks separating it from the Bosco Group, its character changes noticeably through a transitional zone up to 300 m. thick. The gneiss becomes finer grained and grey coloured, and develops a very strong, often platey schistosity with a prominent mineral lineation. Common quartz and feldspar knots have long trails of disaggregated grains extending parallel to the lineation direction. The most distinctive mineralogical difference from the typical massive biotite gneiss is the abundance of muscovite. There are no obvious dykes in the schistose gneiss. Xenoliths are rare, and where they occur they are seen as paper thin relicts in the part of the transitional

zone furthest from the margin of the gneiss. Internal boudinage of the strong schistosity is common, but is completely absent in the massive biotite gneiss.

In the complexly folded area on the ridge east of P. Bombogna the schistose gneiss forms envelopes around the two tongues of massive Antigorio Gneiss.

3:3 Bosco Group

The Bosco Group is divided into four members in the Martschenspitz-Grossalp area. Muscovite gneiss in the core of the Wandfluhhorn Antiform is surrounded by semi-pelitic schist with abundant staurolite porphyroblasts, hornblende schist with small pods of amphibolite and ultramafic schist, and semi-pelitic schist with abundant garnet porphyroblasts. The garnet schist lies closest to the Antigorio Gneiss. This simple sequence does not persist south of Rovana Stream where the gneiss dominates the group.

The rocks of the Bosco Group are non-calcareous, and the few bands of marble and calcareous schist they enclose are probably tectonically intercalated Mesozoic rocks. The semi-pelitic schist members are possibly derived from sediments, as just south of the southwest corner of the thesis area they contain a few ellipsoidal granitic pebbles. The semi-pelitic staurolite schist is almost identical to the semi-pelitic garnet schist, and microscopically the two are indistinguishable. The main difference is that while small garnets are common in the staurolite schist, staurolite rarely occurs in the garnet schist. South of the Ritzberg the hornblende schist, lying between the semi-pelitic schist members, dies out, and the garnet schist passes up into the staurolite schist through a 15 m. thick transition zone with no macroscopically visible porphyroblasts. In the southwest of the area bands of staurolite schist enclosed in muscovite gneiss change laterally into garnet schist.

The hornblende schist was derived from a coarse grained, basic igneous complex. The few small pods of amphibolite are recrystallized gabbros, and grade into the hornblende schist as the grain size decreases and the schistosity develops.

The muscovite gneiss is derived from a leucocratic granitic rock intruding the semi-pelitic schist and hornblende schist. In the southwest corner of the thesis area the intrusive relationships are clearly displayed in a number of pods which escaped intense Alpine deformation. The network of granitic dykes cutting the schist suggests that the area was in the marginal zone of a large intrusion. The semi-pelitic schist in the pods was already strongly folded and recrystallized before the granitic rocks were intruded. Where the gneiss is the dominant member of the Bosco Group it encloses a few thin bands of schist which were probably caught at a deeper level in the intrusive body.

(a) Garnet Schist

The garnet schist member of the Bosco Group is a grey to brown, sometimes silvery semi-pelitic rock with a fine schistosity. It is characterised by abundant garnets knots up to 2 cms in diameter, and has a strong mica lineation especially conspicuous on the many flattened quartz rods.

On the lower limb of the Wandfluhhorn Antiform the garnet schist crops out as a band 40 m. to 50 m. thick along the western side of the ridge between the Batnall and Passo della Stella. At Passo della Stella the upper boundary crosses the ridge and can be traced eastwards across Grossalp to the Kleinhorn Fault. The lower boundary continues along the western side of the ridge to the Guriner Furgge Fault at Passo di Bosco. East of the ridge the garnet schist occupies much of the western portion of Grossalp, but is locally eroded to expose a small window of Mesozoic rocks.

North of the Guriner Furgge Fault the garnet schist continues as a single band along the western slopes of the Martschenspitz to Lago Superiore where it is folded around the hinge of the Wandfluhhorn Antiform. On the upper limb of the fold the schist crops out high on the western slopes of the Martschenspitz, and extends east across the very steep southern face to the gentler slopes of Bort. The upper contact with a band of Mesozoic rocks is easily traced across this area, but

the lower contact with hornblende schist is difficult to follow in the steeper, scree-covered and forested area along the edge of Bort. East of Bort the garnet schist is largely concealed beneath scree, except at the foot of the Rota Balmu cliffs where a small outcrop is separated from the underlying hornblende schist by 15 m. of muscovite gneiss. East of Ritana the garnet schist wedges out, and gneiss lies between the overlying Mesozoic rocks and the underlying hornblende schist.

On the south side of the Valle di Bosco the garnet schist is exposed only as a thin lens between hornblende schist below and muscovite gneiss above in the steep, gullied outcrops below Alpe Bobna. A further thin band, exposed on the ridge top 250 m. southwest of the Grosshorn, is surrounded by muscovite gneiss, and a similar band on the southwest face of P. Bombogn wedges out northwards just before reaching the ridge west of P. Bombogn.

Thin garnet schist bands, also surrounded by muscovite gneiss, are exposed in the steep forested area north and west of Cerentino.

(b) Hornblende Schist

The hornblende schist member of the Bosco Group is a fine grained, dark green to black rock containing abundant, minute hornblende needles are usually strongly oriented. The schist is often finely foliated with alternating hornblende- and quartz-plagioclase-rich layers.

On the lower limb of the Wandfluhhorn Antiform, south of the Guriner Furgge Fault, the hornblende schist is exposed along the ridge east of the Ritzberg and is repeated down the southwest face in the hinges of a series of small recumbent folds. North of the Guriner Furgge Fault the hornblende schist can be traced from just below Passo di Bosco to the western ridge of the Martschenspitz, around the hinge of the Wandfluhhorn Antiform and back to the Guriner Furgge Fault.

East of Passo di Bosco the hornblende schist is exposed in a broad area between the southern slopes of the Martschenspitz and the Guriner Furgge Fault, before being largely concealed in the forest and scree north of Bosco-Gurin. It reappears on the south side of the valley opposite Ubarab, and gradually rises to meet the ridge crest at the Kleinhorn. South of the Kleinhorn the hornblende schist is concealed beneath extensive scree.

South of Rovana Stream the hornblende schist is overlain by muscovite gneiss and underlain by interlayered muscovite gneiss and staurolite schist. The originally intrusive contact between the hornblende schist and the underlying muscovite gneiss is excellently exposed on the south face of the Kleinhorn. Thin fingers of muscovite gneiss extend into the basal 30 cms of the schist, and are slightly discordant to the schistosity.

In the steep gully eroded along the Kleinhorn fault on the north face of the Kleinhorn, the hornblende schist encloses a 10 m. thick lens of coarse grained epidote amphibolite. Pods of ultramafic schist up to 4 m. thick are also scattered through the hornblende schist. The rocks in the pods are strongly talcose and often have large, radiating aggregates of blade-like tremolite crystals. The most common occurrence of these rocks is on the ridge east of the Ritzberg.

(c) Staurolite Schist

The staurolite schist member of the Bosco Group is a grey to buff coloured, semi-pelitic rock with a fine schistosity. It contains abundant porphyroblasts of brown staurolite and a few of red garnet. The larger, stubby staurolite porphyroblasts are usually randomly oriented, but the smaller, more needle like forms are generally subparallel to the strong mica lineation on the numerous flattened quartz rods.

North of the Guriner Furgge Fault the staurolite schist is exposed only in the hinge zone of the Wandfluhhorn Antiform at Passo di Bosco, and is surrounded by hornblende schist. Immediately to the south, on the lower limb of the fold, it forms a small capping at the eastern end of the Ritzberg ridge, and reappears in the gently sloping area between Grossalp and Chummuheij. From Chummuheij

the staurolite schist rises gradually west to the ridge just south of Passo della Stella, and extends south along the western face of the Batnall into the basin between the Batnall and P. Quadro.

In the hinge region of the Wandfluhhorn Antiform east of the Batnall the staurolite schist occurs as bands up to 25 m. thick interlayered with muscovite gneiss. Immediately above and below the fold hinge garnet porphyroblasts become more dominant than staurolite. The schist bands extend east across the Kleinhorn Fault, along the steep, scrub covered south wall of the Valle di Bosco before being obscured by alluvium and moraine between Schwarza Brunna and Ubarab. At an isolated outcrop below Alpe Bobna staurolite schist with thin bands of muscovite gneiss occupies the hinge zone of the Wandfluhhorn Antiform.

The staurolite schist bands are repeated on the opposite side of the valley in the gently sloping, triangular area between the Kleinhorn Fault, Guriner Furgge Fault and the southeast edge of Grossalp. In the steep stream sections below Grossalp staurolite schist and muscovite gneiss are interlayered in bands 5 cms to 30 cms thick, parallel to the schistosity.

(d) Muscovite Gneiss

The muscovite gneiss member of the Bosco Group is a white to light grey granitic rock with abundant muscovite and common quartz and feldspar knots It has a strong planar fabric on which biotite and muscovite flakes and tourmaline needles up to 3 cms long are aligned to form a strong lineation.

On the lower limb of the Wandfluhhorn Antiform, north of Rovana Stream, the muscovite gneiss occurs as thin parallel bands within the staurolite schist of Grossalp and Chummuheij. These bands thicken towards the hinge zone of the antiform, and the gneiss becomes coarser grained and more biotite rich until it partly resembles the Antigorio Gneiss This darker, coarser facies of the gneiss

is exposed along the ridge between the Batnall and Passo Quadrella.

On the upper limb of the antiform the lighter coloured gneiss reappears above and below the hornblende schist at the Kleinhorn. It extends east along the ridge to a small peak 500 m. west of P. Bombogn, and is separated from schistose Antigorio Gneiss by a band of Mesozoic rocks. East of this peak the muscovite gneiss is largely concealed by forest and scree. A few exposures occur on the high southern slopes of P. Bombogn, in cliffs east of Cerentino and in gullies below Alp Bobna.

3:4 Mesozoic Rocks

The Mesozoic rocks consist dominantly of marble and calcareous schist, with minor pelitic garnet schist and quartzite. They were derived from strongly deformed, recrystallised sediments. The marble is generally white to light grey and coarsely crystalline. It is sometimes massive, but usually contains thin pelitic partings and aligned but isolated, phlogopite micas. In some outcrops it is banded grey and white, and the strong internal folding and boudinage is clearly visible. Many of the boudins consist of yellow-brown dolomitic marble.

The calcareous schist, the dominant Mesozoic rock, is typically a grey-brown rock with a strong schistosity, but weathers medium to dark brown and has a crumbly appearance. The calcareous schist grades into the marble both laterally and vertically, and all transitions between very pure, coarse-grained marble and slightly calcareous, fine grained quartz-mica schist were observed. The most siliceous varieties are chocolate coloured, and contain abundant biotite and a few small garnet porphyroblasts.

The pelitic schist is a fine grained, dark grey to black rock with a fine schistosity. It contains dark red to black garnet porphyroblasts, often with graphitic inclusion trails, and black kyanite. The Mesozoic pelitic schist differs from the semi-pelitic schist of the Bosco Group by its darker colour, complete absence of staurolite, and more common kyanite and rare calcite. It is always associated with marble and calcareous schist, often occurring as

thin, lenticular shaped boudins.

Mesozoic quartzite is very rare in the thesis area. It is a light grey to brown, finely banded rock and sometimes stained green with epidote.

Thin bands of hornblende schist are often intimately associated with Mesozoic rocks, particularly in the complex zone between the Antigorio Gneiss and Bosco Group (see fig. 6). They usually occur along the margins of the bands of Mesozoic rocks, but also occur as thin bands within the Mesozoic rocks and are often boudinaged. It is difficult to determine whether this hornblende schist is a Mesozoic or basement rock. It is identical to the hornblende schist of the Bosco Group, and also to the hornblende schist bands enclosed in the Antigorio Gneiss.

The Mesozoic rocks occur in bands 2 cms to 30 ms thick, tectonically intercalated at three structural levels in the basement rocks. The sharp boundaries of the bands are parallel to the schistosity in the enclosing basement rocks, and it was rarely possible to determine if they represent unconformable of thrust contacts. The number and thicknesses of the bands varies considerably at different localities. A few end in tight V-shaped forms or in a train of lenticular shaped boudins, but others were traced for a considerable distance and do not die out in the thesis area.

At the most important structural level bands of Mesozoic rocks are concentrated in the Antigorio Gneiss close to its contact with the Bosco Group. One thick and particularly persistent band lies at the contact, separating the two basement groups. It was traced along the lower limb of the Wandfluhhorn Antiform from the western slopes of the Batnall to Lago Superiore where it is refolded around the hinge of the Wandfluhhorn Antiform. It can then be followed across the western and southern slopes of the Martschenspitz onto the gentler slopes of Bann where it forms a prominent cliff. East of Bann it is exposed intermittently along the north side of the Valle di Bosco to just east of Ritana where it is concealed beneath scree. On the south side of the Valle di Bosco this band of Mesozoic rocks reappears on the scrub covered scree slopes immediately below

Alpe Bobna, and continues west along the edge of the basin below P. Bombogn. On the western ridge and poorly exposed southern slopes of P. Bombogn it appears to be folded around a north closing lobe of Bosco Group rocks and a south closing lobe of Antigorio Gneiss. East of Passo Pian Crosc it is strongly boudinaged and occurs only intermittently along the forest covered ridge. In Rovana Stream just below Camanoii it appears to be folded around another north closing lobe of Bosco Group rocks before extending southwest along the north bank of Rio Collobiasca to Niva. It is clearly exposed in the river bed just east of Niva, and reappears about 1.5 kilometres upstream. Brief reconnaissance showed that this band of Mesozoic rocks continues southwest along the south side of the Valle di Campo at least as far as Alpe di Sfii, in a small side valley opposite Cimalmotto.

Along the lower limb of the Wandfluhhorn Antiform, and on the upper limb between Lago Superiore and Ritana the Mesozoic band lies between the garnet schist member of the Bosco Group and schistose Antigorio Gneiss. South and east of Ritana the garnet schist wedges out, and the Mesozoic band lies between schistose Antigorio Gneiss above and schistose Bosco Group Gneiss below. This apparent "stepping over" from one member of the Bosco Group onto another suggests that the contact between the Mesozoic rocks and the Bosco Group is an unconformity.

At a number of localities along its outcrop this Mesozoic band exhibits a symmetric repetition of rock types suggesting that it is a major syncline. (see fig. 7). At Passo della Stella the garnet schist of the Bosco Group is underlain by, in order, 2 m. of hornblende schist, 2 m. of biotite-garnet quartzite, 6 m. of impure, brown weathering marble, 1.3 m. of dark grey schist with kyanite and black garnets, 1.3 m. of calcareous schist, a further 2 m. of garnet-kyanite schist, 10 m. of strongly folded marble with thin calc schist bands, and 2 m. of hornblende schist. Below the hornblende schist is 1 m. of biotite quartzite and 2 m. of hornblende schist, followed by schistose Antigorio Gneiss. Excluding the quartzite and hornblende schist bands, the sequence of Mesozoic rocks appears to be repeated on either side of the central calc schist band. The upper hornblende

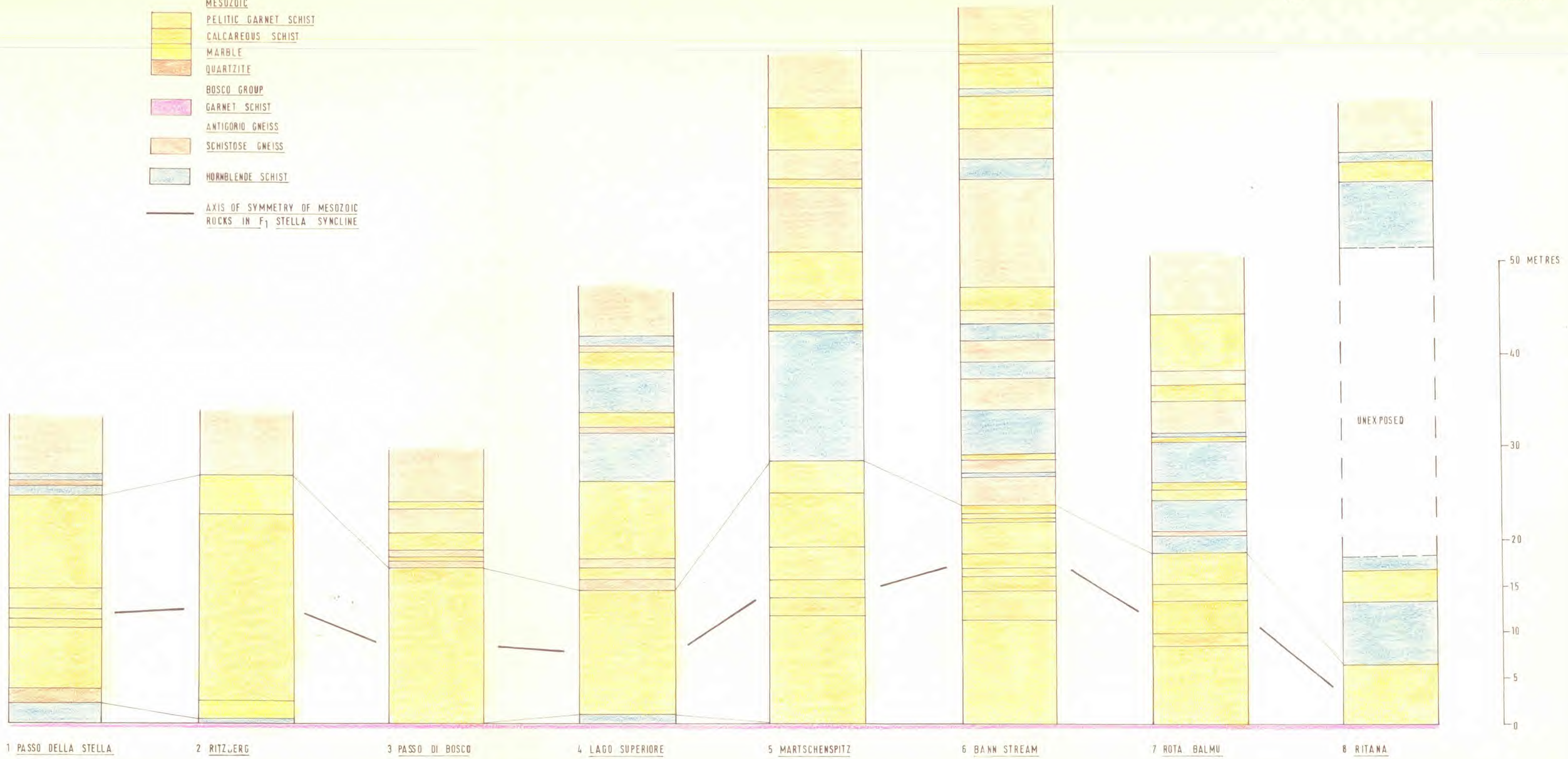
schist band wedges out a short distance to the south, and quartzite lies against the garnet schist. The quartzite in turn wedges out southwards so that marble lies against garnet schist. The hornblende schist and quartzite also wedge out to the north. The hornblende schist and quartzite at the base of the band of Mesozoic rocks also wedge out to the north and south. The contacts between the marble and Bosco Group and marble and Antigorio Gneiss at this locality thus appear to be sedimentary rather than tectonic. The quartzites may also be Mesozoic rocks, coincidentally preserved on opposite limbs of the syncline. The intimate association of the hornblende schist with the Mesozoic rocks strongly suggests that it, too, may have been derived from Mesozoic rocks.

Detailed sections of the rocks in the Mesozoic band were measured at a number of other localities and are also illustrated in fig. 5. The section at the Ritzberg in particular provides another excellent example of a possible stratigraphic repetition. Twenty metres of grey, crumbly calc schist with black garnets and thin marble bands is overalin by a 1 m. thick marble band and underlain by 4 m. of strongly folded marble. Thin bands of hornblende schist occur above and below the calcareous rocks, but extend for only a short distance north and south.

This band of Mesozoic rocks is named the Stella Syncline, after Passo della Stella, because of its position between the two groups of basement rocks and the apparently symmetric stratigraphic repetitions. In the tectonic profile, drawn when looking in the axial direction of the Wandfluhhorn Antiform, the Stella Syncline can be traced for about 20 kms. It extends south of the thesis area on both limbs of the Wandfluhhorn Antiform. No closure has yet been observed to confirm the synclinal structure, and there is no indication in the thesis area of the direction in which it either opens or wedges out.

At the two other structural levels in the basement rocks the bands of Mesozoic rocks are generally thinner and less continuous than those in the zone between the Antigorio Gneiss and Bosco Group. In the schistose edge of the Antigorio Gneiss, 60 to 140 m. from the Stella Syncline, thin bands of Mesozoic rocks have been traced from

FIGURE 5



DETAILED SECTIONS OF TRANSITION ZONE BETWEEN ANTIGORIO GNEISS AND BOSCO GROUP

the western slopes of the Batnall almost to the Wandfluhhorn. They are refolded around the hinge of the Wandfluhhorn Antiform and extend back along the ridge south of the Wandfluhhorn to the small peak immediately south of Hendar Furggu. They reappear at about the same structural level at Rota Balmu, and extend across the lower slopes of Wolfstaffel to just east of Pögga where they are concealed by scree. On the south side of the Valle di Bosco the bands of Mesozoic rocks can be traced from the valley floor opposite Cios to the north face of P. Bombogn. Between Andatschei and P. Bombogn they are partly boudinaged and folded by at least two sets of structures, and their complicated outcrop pattern is due to folds plunging gently eastwards across the steep NNW facing slopes.

On the southern slopes of P. Bombogn the Mesozoic bands were traced intermittently east to Passo Pian Crosc. East of Passo Pian Crosc the Mesozoic bands are difficult to trace along the poorly exposed, forest covered ridge, but they reappear on the south side of the Valle di Bosco opposite Corino and are refolded around a south closing tongue of Antigorio Gneiss and a north closing tongue of Bosco Group rocks. They are exposed again near Collinasca, from where they continue southwest along Rio Collobiasca for about a kilometre before being concealed beneath a large outwash fan. The clean, water-polished outcrops clearly display the internal structures of the Mesozoic rocks, particularly the marble which appears to have been folded by two, and possibly three sets of minor structures.

A third structural level of Mesozoic bands is associated with the hornblende schist member of the Bosco Group. The bands were mapped in detail just south of Lago Superiore, and are deformed by two sets of minor structures. The hornblende schist dies out on the lower limb of the Wandfluhhorn Antiform south of the Ritzberg, but one band of Mesozoic rocks continues south for about one kilometre in the garnet schist member of the Bosco Group just below the contact with the staurolite schist. On the upper limb of the Wandfluhhorn Antiform the Mesozoic bands in the hornblende schist extend around the southern slopes of the Martschenspitz to the steep forested area below Bort. On the south side of the Valle di Bosco thin boudinaged bands of Mesozoic rocks again occur in the hornblende schist in the vicinity of the Kleinhorn.

CHAPTER 4

STRUCTURAL INTRODUCTION

The structural features observed indicate that the rocks of the Valle di Bosco have suffered three major Alpine deformations. These deformations are designated, for convenience, F1, F2 and F3 in order of their development. The earliest deformation, F1, resulted in the emplacement of two large basement thrust sheets, separated by a major synclinal zone of Mesozoic rocks. These structures were severely deformed under extremely ductile conditions during the second, F2, movement, and flattening strains of up to 77% have been recorded. Basement and cover units were strongly refolded, and a regional schistosity was developed largely parallel to the lithological boundaries. During the F3 movement the F2 schistosity was folded into a major north-closing recumbent fold, the Wandfluhhorn Antiform. This structure was accompanied by the development of a cremulation cleavage.

The later brittle phases of the structural evolution are typified by NW-SE trending kink folds, chlorite-filled tension gashes and chlorite- and quartz-filled joints. Two sets of barren joints and faults trend NNW-SSE and E-W. Most faults are normal with throws of less than 5 m., but one major fault with a throw of 100 m. displaces the axial trace of the Wandfluhhorn Antiform.

The structural interpretation outlined in this thesis is based on a detailed study of the minor structures, particularly the fold styles. Recumbent, isoclinal F2 folds deform intrusive sheets in the basement rocks and also bands of Mesozoic rocks incorporated in the basement rocks. The hinge lines of the folds plunge gently east, while the axial planes dip gently southeast. A powerful, penetrative schistosity lying parallel to the axial planes of the folds is an important feature distinguishing the F2 folds from folds related to other deformations. A strong mineral lineation, parallel to the fold hinge lines, occurs on the schistosity surfaces. Deformed xenoliths in the Antigorio Gneiss show that the schistosity was a plane of flattening and the lineation a direction of stretching. Boudins with rectangular and lenticular cross sections lie in the plane of the schistosity, and many have their necks oriented normal

to the lineation direction.

F1 structures were recognised only in interference patterns in which F2 folds refold bands of Mesozoic rocks enclosed in basement. The Mesozoic bands lie parallel to the schistosity on the fold limbs, but are cut by the schistosity in the hinge regions, and must have been intercalated in the basement prior to the F2 deformation. No F1 minor structures were observed, and it is difficult to determine whether the Mesozoic bands occupy tight synclinal hinges or represent single limbs of structures whose opposing limbs were removed by thrusting.

Chevron-like F3 folds deform the F2 schistosity. They have the same general orientation as the F2 folds, but a wider spread in their plunge directions. A weak axial plane crenulation cleavage is associated with the minor folds in the hinge region of the Wandfluhhorn Antiform. Lineations parallel to the axial directions of the F3 folds include aligned crenulations of mica layers, mullions and the intersection of the F2 schistosity with the F3 crenulation cleavage. A slickenside lineation occurs on the schistosity surfaces at a high angle to the F3 fold hinges, and indicates the direction in which the layers slipped over each other during the F3 deformation. F3 folds folded the F2 lineation and refolded many F2 folds. Instabilities developed in the F2 schistosity which suffered internal boudinage. Most of the boudin necks are oriented normal to the F3 fold hinge lines.

CHAPTER 5

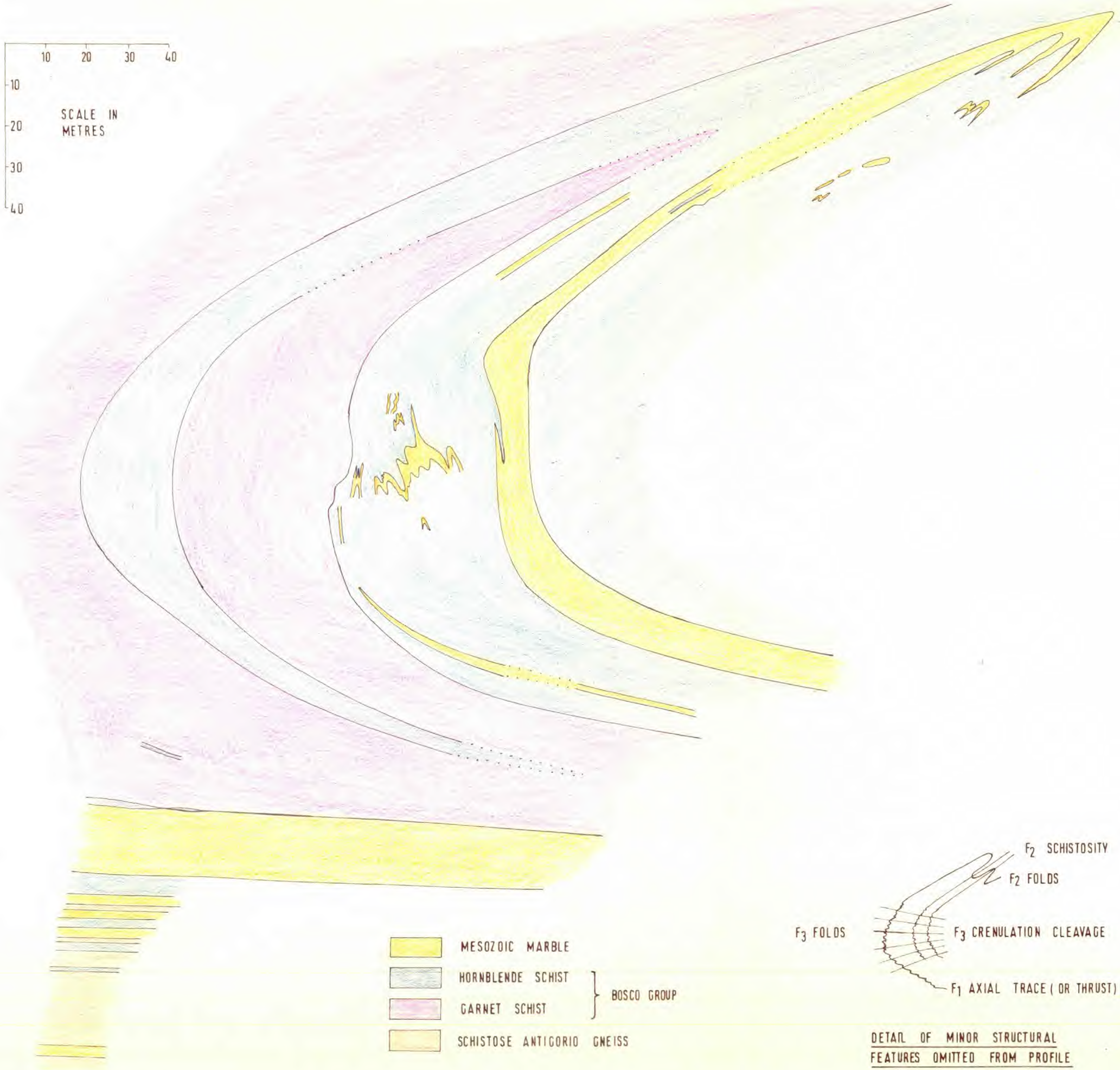
F1 DEFORMATION

Structures resulting from the first Alpine deformation have been recognised only when Mesozoic rocks are involved. It was shown earlier (see Chapter 3) that thin bands of Mesozoic rocks lie between the Antigorio Gneiss and Bosco Group, in schistose Antigorio Gneiss and in the hornblende schist member of the Bosco Group. The most persistent Mesozoic band, 6.5 m. to 26 m. thick, separates the Bosco Group and the Antigorio Gneiss. It is probably a major F1 syncline, and has been named the Stella Syncline from exposures immediately west of Passo della Stella where the Mesozoic rocks appear to form a stratigraphic sequence repeated on either side of a central band of calcareous schist. The extent of the Stella Syncline, and details of its internal stratigraphy have been described in Chapter 3.

Thin, sometimes discontinuous Mesozoic bands, parallel to the schistosity in the basement rocks on either side of the Stella Syncline, are also considered to have originated as F1 synclines or thrust slices derived from modified folds in which one limb was tectonically removed. The most convincing evidence that many of these bands are F1 structures is that some are refolded by F2 folds and cut by the associated schistosity.

The hornblende schist in the basin immediately south of Lago Superiore contains a number of Mesozoic marble and calc schist bands up to 17 m. thick (see fig. 6). One band occurs as a series of boudinaged folds with limbs parallel to the schistosity. In the fold hinges the schistosity of the enclosing hornblende schist cuts across the Mesozoic bands, showing that they must have already been enclosed in the schist before the F2 deformation. At the head of the basin a marble band 3.5 m. thick wedges out southwards parallel to the schistosity, but just before disappearing its lower contact with the hornblende schist is folded into lobe and cusp structures. The schistosity in the hornblende schist is axial planar to these folds, and cuts across the marble.

DETAILED GEOLOGY OF HINGE REGION OF WANDFLUHHORN ANTIFORM.
PROFILE VIEW LOOKING EAST, IN BASIN IMMEDIATELY SOUTH OF LAGO SUPERIORE.



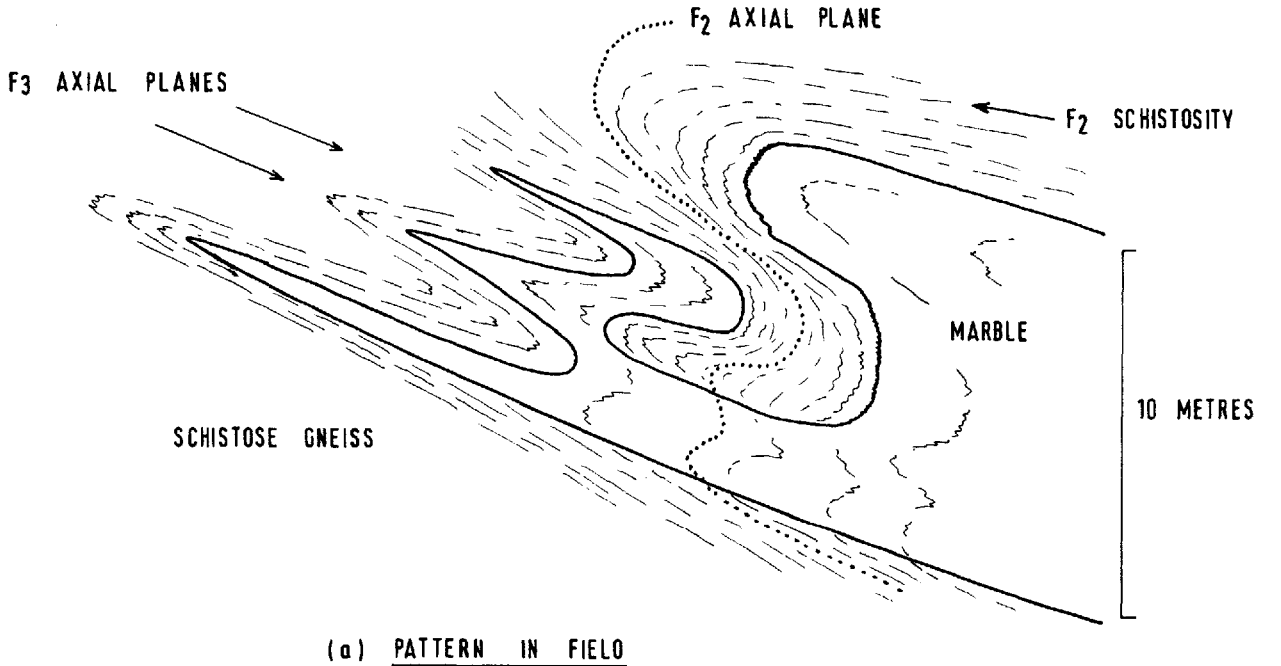
DETAIL OF MINOR STRUCTURAL FEATURES OMITTED FROM PROFILE

The only other example of a Mesozoic band which can be definitely proved to be an F1 structure occurs on the steep northern slopes of P. Bombogn in outcrops which show spectacular F1/F2/F3 interference patterns (fig. 7). The schistosity of the Antigorio Gneiss enclosing the Mesozoic rocks, and the Mesozoic-gneiss contact are folded into lobe and cusp structures by F3 minor folds. When the effects of these F3 folds are removed, the Mesozoic band appears to end in a hook shape. The Mesozoic-gneiss contact is parallel to the schistosity except in this hook-shaped hinge zone. This is considered to be an F2 structure resulting from the deformation of the wedge-shaped end of an F1 Mesozoic-filled syncline pinched into the Antigorio Gneiss.

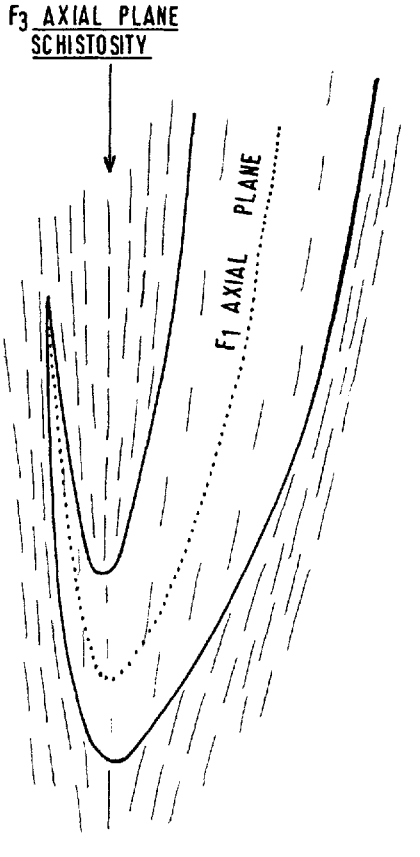
Apart from the Stella Syncline and the bands of Mesozoic rocks intercalated in the basement rocks, all evidence of the F1 deformation has been obliterated by later events. In a later chapter (see Chapter 10) it will be shown that during the F1 deformation basement rocks were emplaced without suffering large finite strains. The Stella Syncline and the bands of Mesozoic rocks immediately associated with it are thought to have developed between two large basement nappes, and been tectonically incorporated in the overriding nappe. The bands in the inner schistose margin of the Antigorio Gneiss are thought to have been tectonically incorporated at a higher level in the overriding nappe. The origin of the bands in the hornblende schist member of the Bosco Group is uncertain.

FIGURE 7

SKETCH OF INTEFERENCE PATTERN NORTHERN SLOPES P. BOMBOGN



(a) PATTERN IN FIELD



(b) PATTERN WITH F_3 FOLDS REMOVED SHOWING HOOK SHAPED F_2 FOLD WITH AXIAL PLANE SCHISTOSITY

CHAPTER 6

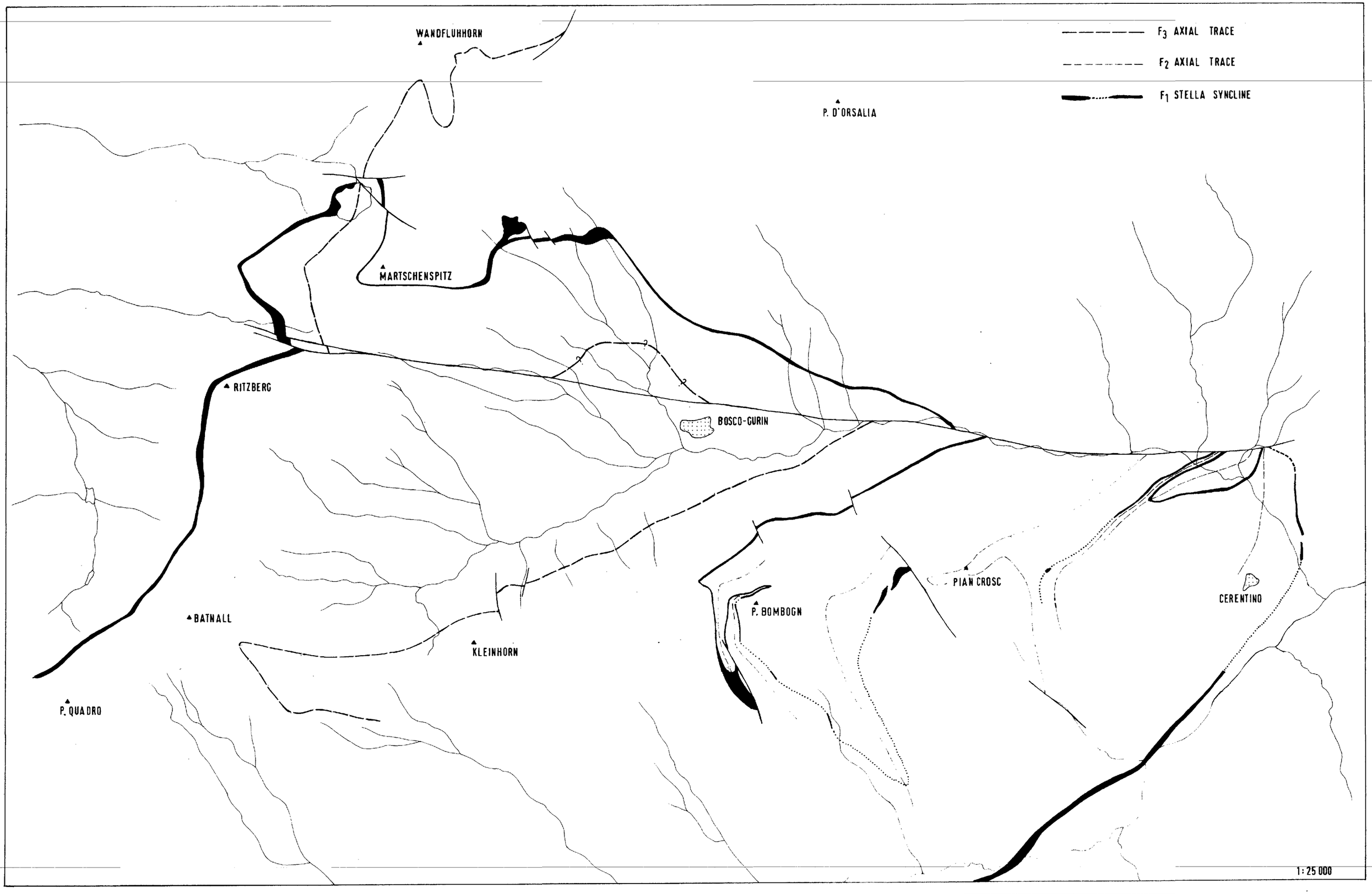
F2 DEFORMATION

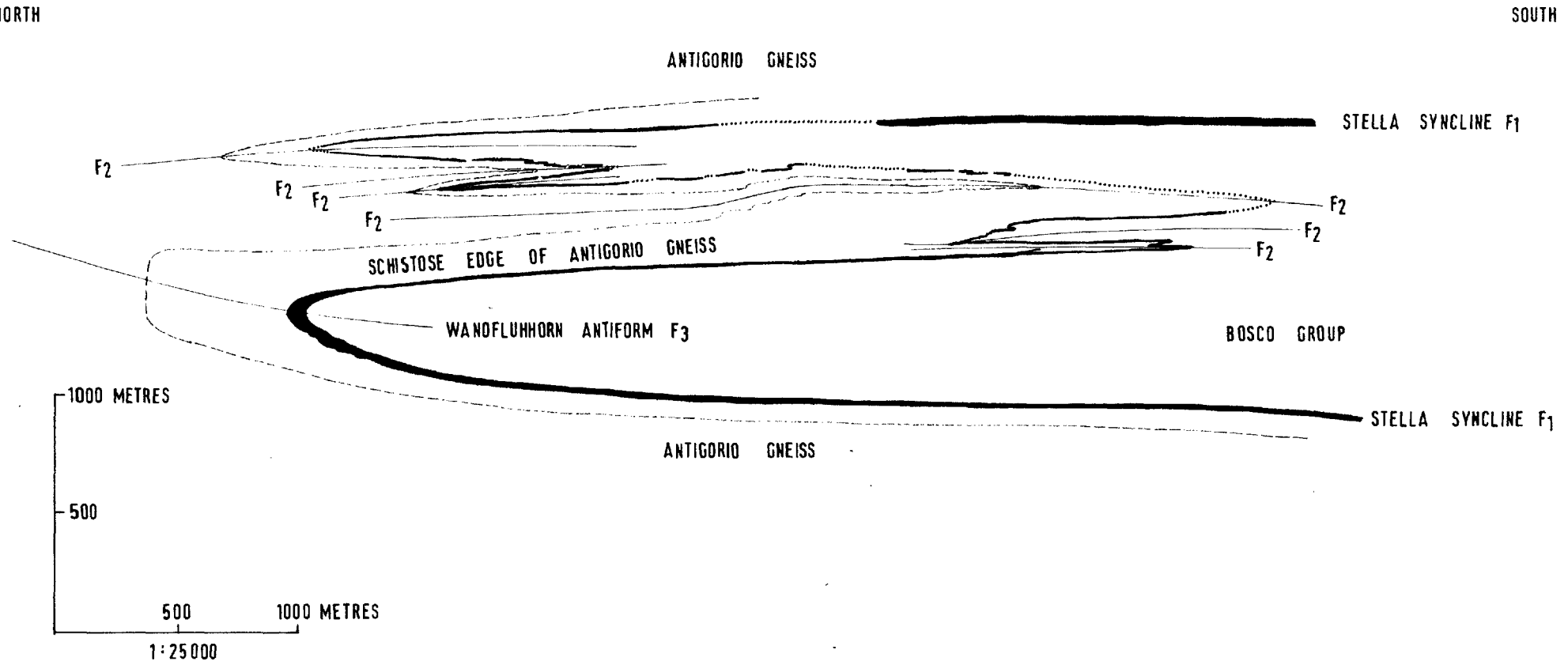
6:1 Introduction

During the F2 deformation the rocks of the Valle di Bosco suffered intense internal deformation, and underwent a change in shape under extremely ductile conditions. The bands of Mesozoic rocks in the synclinal zone between the Antigorio Gneiss and the Bosco Group were strongly refolded, and can now be traced around several large isoclinal structures (figs. 8 and 9). The minor folds developed during the F2 deformation have thickened hinges and attenuated, sometimes boudinaged limbs. The fold hinges are commonly lobe or cusp shaped. The folds are accompanied by a powerful, penetrative axial plane schistosity, which is parallel to the lithological layering except in the hinge regions of the folds. A strong mineral lineation, generally parallel to the axial direction of the minor folds, occurs on the schistosity surfaces.

A number of major F2 folds occur in the area between the Valle di Bosco and Valle di Campo east of the Grosshorn. The south-closing, synformal folds are recognised from their cores of massive Antigorio Gneiss, while the north-closing, antiformal folds are recognised from tongues of Bosco Group rocks surrounded by Antigorio Gneiss. The folds are recumbent. The hinge lines plunge gently east, and the axial planes dip gently southeast.

Two bands of massive Antigorio Gneiss are found on the south side of the Valle di Bosco downstream from Bosco-Gurin. The tectonically lower and more extensive band, 140 m. thick at river level, extends up the south side of the valley from Piano dei Vitetti. It is exposed along the ridge crest from Point 1,850 m. to just east of Passo Pian Crosc, where its base is displaced to the northwest. The gneiss climbs back along the western face of the ridge to the summit again approximately 370 m. east of P. Bombogn, and extends down the southern slopes as a narrow strip for 400 m. before becoming concealed by scree. The massive gneiss passes upwards and downwards into strongly schistose, muscovite rich gneiss with bands of Mesozoic rocks. The schistose


WANDFLUHHORN
P. D'ORSALIA
MARTSCHENSPITZ
RITZBERG
BOSCO-GURIN
BATNALL
KLEINHORN
P. QUADRO
P. BOMBOGN
PIAN CROSC
CERENTINO
F3 AXIAL TRACE
F2 AXIAL TRACE
F1 STELLA SYNCLINE
1:25 000



PROFILE SECTION OF MAJOR STRUCTURES

VIEW LOOKING DOWN PLUNGE OF F_2 AND F_3 MINOR FOLDS

FIGURE 9

gneiss is underlain and overlain by lighter coloured Bosco Group gneiss with thin bands of hornblende, garnet and staurolite schist.

The second, less extensive band of massive Antigorio Gneiss, approximately 50 m. thick, crosses Rovana Stream just below Corino. It also passes upwards and downwards into schistose gneiss with Mesozoic bands.

On the western ridge of P. Bombogn an antiformal hinge of Bosco Group garnet schist and gneiss is overlain and underlain by schistose Antigorio Gneiss with Mesozoic bands. A larger antiformal hinge occurs just north of Cerentino, where bands of Mesozoic rocks can be traced around a lobe of Bosco Group rocks enclosed by Antigorio Gneiss.

6:2 Minor Folds

Typical F2 minor folds are generally tight to isoclinal structures, with thickened, rounded hinges, attenuated limbs and, most important, a strong axial plane schistosity. Lobe and cusp forms (Ramsay 1967; 328-386) are common features of many of the folds.

In the massive Antigorio Gneiss folds of this generation can be found in aplite and pegmatite dykes and quartz veins, and along the contacts of the biotite-rich Antigorio Gneiss and irregularly-shaped, lighter coloured intrusions. Xenoliths and tectonically intercalated bands of Mesozoic rocks in the gneiss are also folded. Outstanding examples of gneisses of different composition having been folded together during the F2 deformation are seen in outcrops on the southern face of Rota Balmu (fig. 10). Cross-cutting sheets of white granitic gneiss show lobate folds protruding into the grey biotite gneiss, separated by tightly pinched cusps of the grey gneiss. Both rock types are cross-cut by a powerful schistosity sub-parallel to the axial surfaces of the folds. A thin quartz vein cutting across both varieties of gneiss also shows lobe and cusp folds. The lobe and cusp folds indicate that during the F2 deformation the more quartz-rich white gneiss and the quartz vein were more competent than the grey, biotite-rich gneiss.

On the cliffs immediately west of Passo della Stella, the interfaces between light coloured muscovite gneiss and grey biotite gneiss have been folded into recumbent forms, with irregular, wispy contacts sub-parallel to the strong schistosity.



Fig. 10(a) Lobe and cusp shaped F2 folds at interface between two varieties of Antigorio Gneiss. Note strong schistosity in grey gneiss and aligned micas in white gneiss. Rota Balmu (6810.51311).

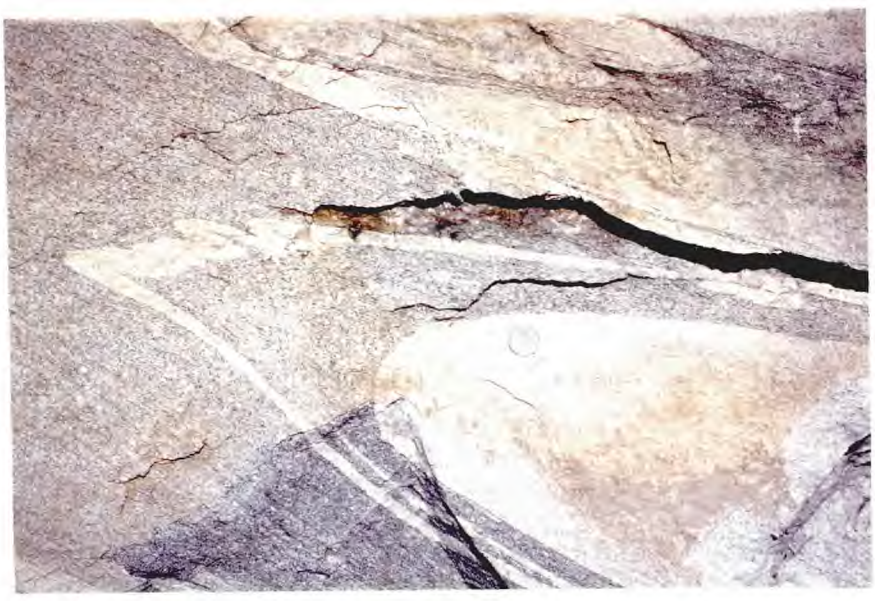


Fig. 10(b) F2 folds in Antigorio Gneiss. Note minor folds in aplite dyke, and strong schistosity in grey gneiss. Rota Balmu (6810.51311).

In the schistose margins of the Antigorio Gneiss the various rock types seen in the massive gneiss can no longer be distinguished. Thin bands of Mesozoic rocks in the schistose gneiss are isoclinally folded by F2 structures. The best examples may be viewed in the deeply incised upper reaches of Bann Stream; Mesozoic bands up to one metre thick alternate with bands of gneiss, and wedge out northwards. Both rock types have a strong schistosity sub-parallel to their contacts. F2 isoclinal folds are also seen in schistose gneiss with Mesozoic bands at Rota Balmu. Internal layering in the Mesozoic marble is weathered differentially to form small ridges which show tight folds with axial planes parallel to the schistosity in the surrounding Gneiss.

In the semi-pelitic schist of the Bosco Group F2 folds may be seen in quartz veins, and in thin intercalated layers of hornblende schist and Mesozoic rocks. The best exposed examples of minor folds occur in interlayered staurolite schist and muscovite gneiss. The muscovite gneiss, originally a leucocratic granitic rock, intruded the semi-pelitic schist as a network of dykes. The dykes were strongly deformed during F2, usually by being flattened parallel to the schistosity, but those lying initially sub-parallel to the compression direction were folded. The folded bands, generally less than one metre thick, have thickened hinges with alternating lobe and cusp shaped boundaries. The schistosity in the surrounding schist is parallel to the axial planes of the folds.

The compositional banding of the Mesozoic marble, together with veins of pre-F2 quartz, calcite and dolomite were all folded during the F2 movement. The minor folds are tight, and have rounded hinges and long, slender limbs (fig. 11). Thin layers of dark pelitic garnet schist contained within the marble are usually boudinaged, but occasionally occur as thick-hinged folds with extremely attenuated limbs.

No regional vergence pattern has been established from the F2 minor folds, partly because they are absent over wide areas, and because the structure is complicated by the F3 deformation. On a small scale vergences are consistent (e.g. within folded marble bands), but in the basement rocks the initial orientation of the originally cross-cutting bodies was such that adjacent folds often have both "S" and "Z" symmetry.

The hinge lines of F2 minor folds in the Mesozoic rocks, and



Fig. 11 F2 folds in Mesozoic marble and calcareous schist. Pizzo Bombogn (68291287).

at the contacts between the Mesozoic and basement rocks plunge sub-parallel to the F2 lineation. The few measurable hinge lines of F2 folded dykes in the Antigorio Gneiss and Bosco Group show more variable angles and directions of plunge, resulting from the initial orientation of the dykes with respect to the F2 bulk strain. Most of the hinge lines plunge between northeast and southeast, in the general direction of the F2 lineation.

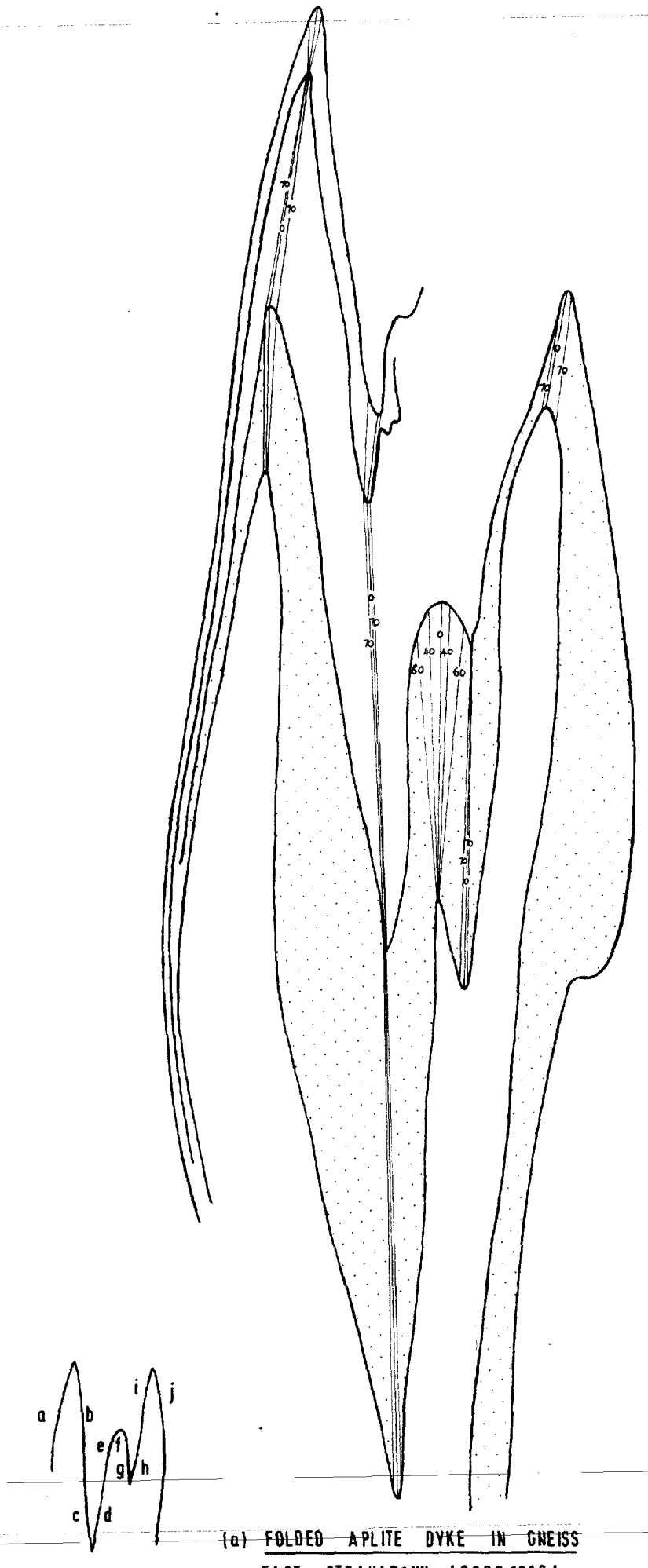
Examples of Typical F2 Minor Folds

F2 minor folds are usually single layer structures. Folds penetrating several lithological layers occur only in the Mesozoic marble or where a number of thin, originally intrusive sheets lay close together, as, for example, the white gneiss bands in the Antigorio Gneiss at Rota Balmu or the muscovite gneiss layers in the Bosco Group staurolite schist in the southwest of the thesis area.

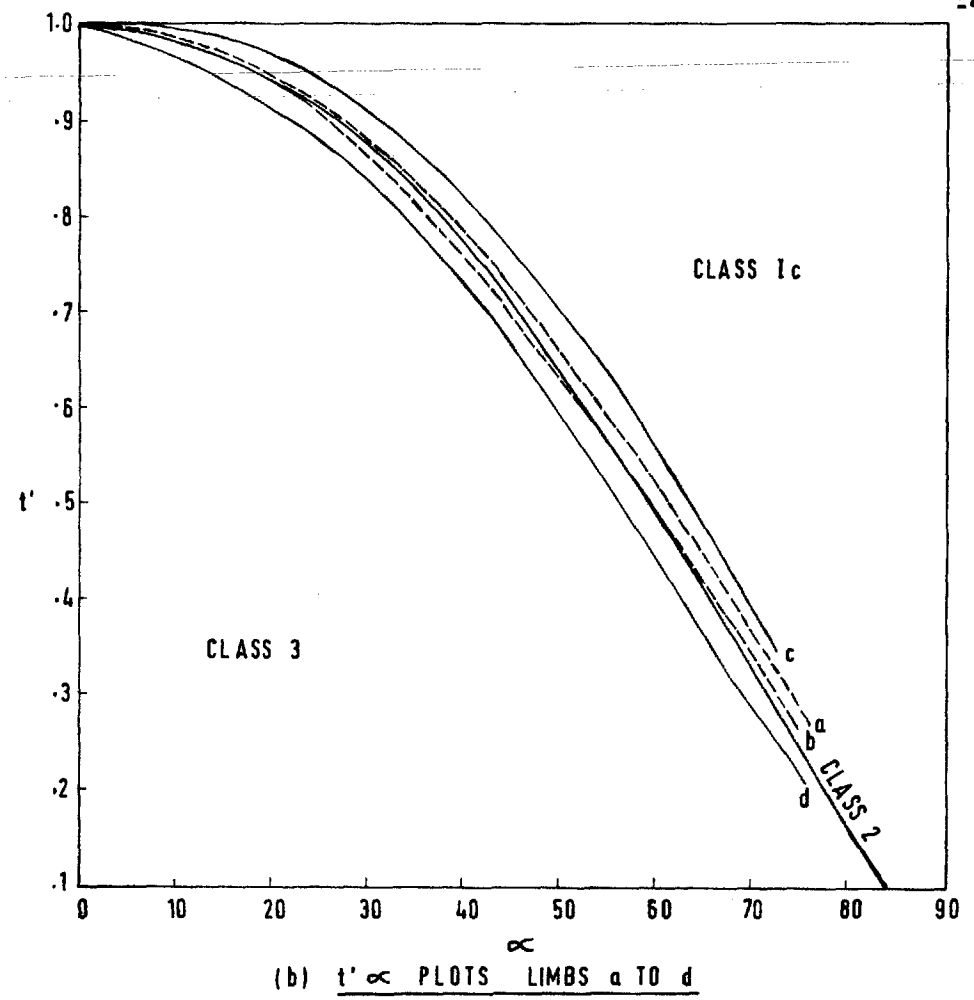
Example 1 is of a folded aplite dyke in the Antigorio Gneiss of East Strahlbann (68091318) (fig.12). The hinges are thickened and one limb is consistently much thinner than the other. The folds are tight to isoclinal, and commonly have pointed hinge zones with interlimb angles of between 30° and 17°. One rounded, lobe-shaped hinge zone shows that the dyke was locally more competent than the gneiss, but generally the fold geometry indicates that the two rock types had approximately the same ductility. Isogons for angles of dip up to 70° are generally sub-parallel.

The folded dyke was traced over five minor fold hinges. Over the first hinge the t'a plot (recording variation in thickness of a fold limb with change in angle of dip (Ramsay 1962) of the thin limb (a) was parallel to the class 2 line but just above it in the class 1c field, while the plot of the thick limb (b) was just below the class 2 line in the class 3 field. Over the second fold hinge, the thickest area of the layer, the plot of the thin limb (d) lay just below the class 2 line, while the plot of the thick limb (c) was slightly above it. A similar pattern occurs over the fourth and fifth fold hinges (limbs g, h, i and j). In all these cases the plots for opposing limbs of each fold lie equal distances above and below the class 2 line. Over the third fold hinge both plots are again parallel to the class 2 line, but that for the thicker limb (f) lies just below

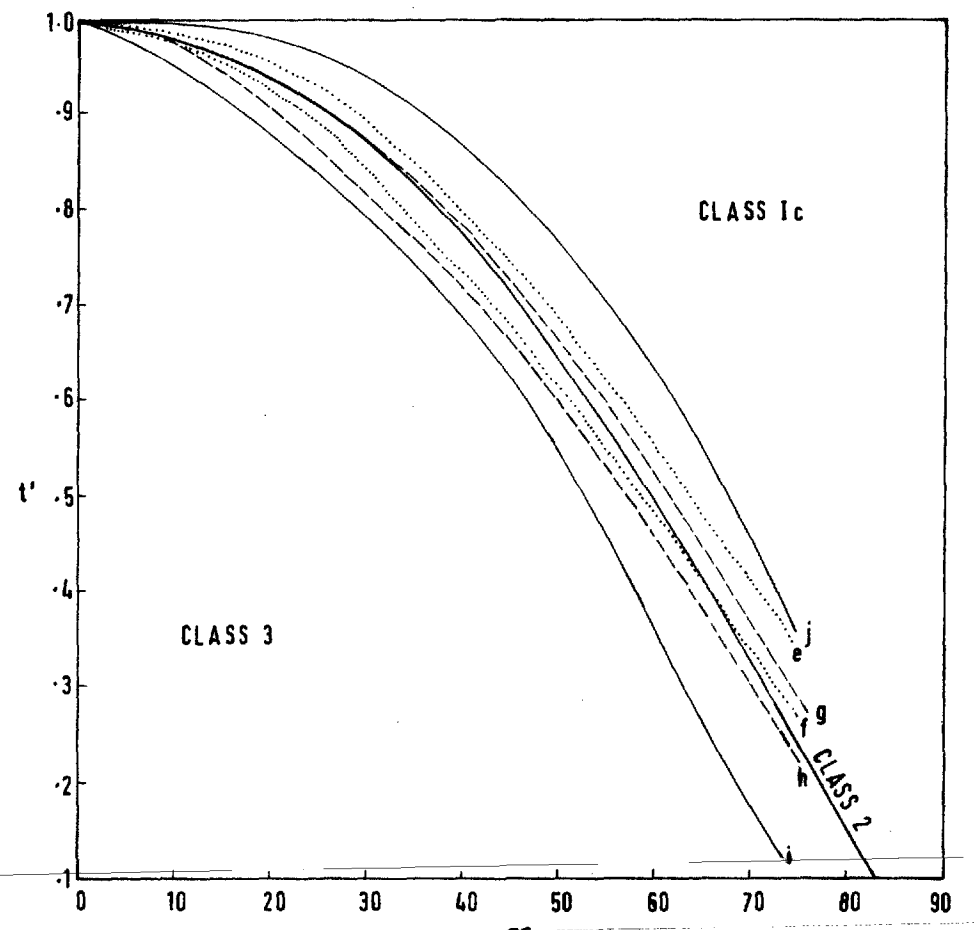
FIGURE 12
F2 MINOR FOLDS



(a) FOLDED APLITE DYKE IN GNEISS
EAST STRAHLBANN (6809 1318)



(b) t' ∝ PLOTS LIMBS a TO d



(c) t' ∝ PLOTS LIMBS e TO j

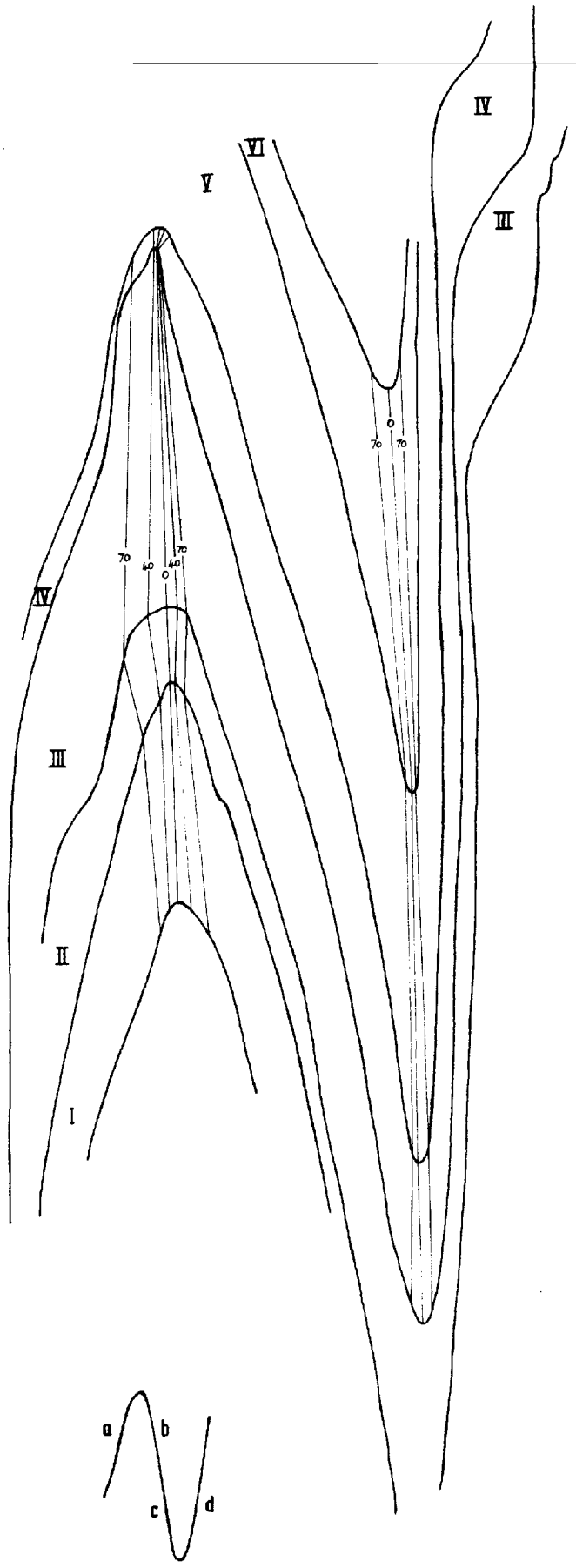
in the class 3 field while that for the thinner limb (e) lies the same distance above, in the class 1c field.

The minor folds are almost perfect examples of similar folds. They developed from asymmetric folds flattened parallel to their axial planes. The t'a plots suggest that there was little ductility contrast between the dyke material and the gneiss, and that, in general, the thicker portions of the dyke were slightly more competent than the thinner portions.

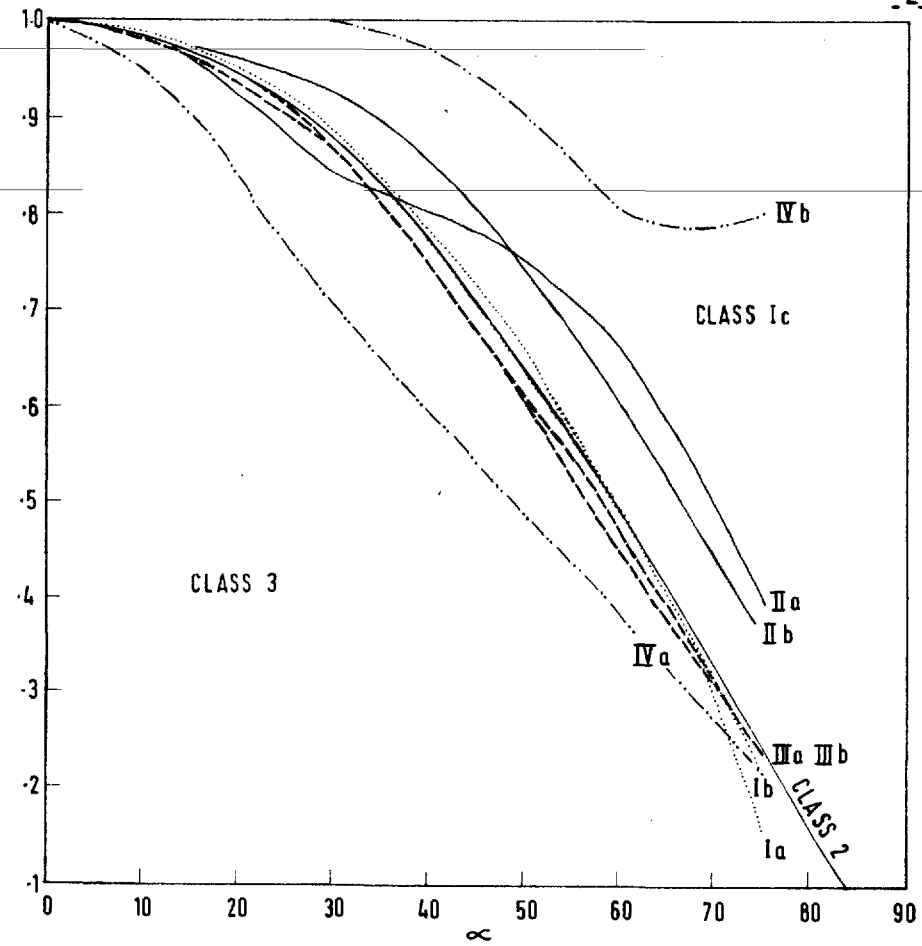
Example 2 is of some isoclinal folds developed in alternately layered grey and white gneisses at Rota Balmu (6810.51311) (fig.13). The dip isogons are sub-parallel, but slightly convergent across the white, quartz-rich layers and slightly divergent across the grey, biotite-rich layers. A strong mica fabric, parallel to the axial planes of the minor folds, is more strongly developed in the grey layers. Interlimb angles of the folds are between 13° and 35°.

The geometry of layers involved in two minor fold hinges was investigated. Over the first hinge the t'a plots for layers 1 and 3 (grey gneiss) lie along or very close to the class 2 line, but those for layers 2 and 4 (white gneiss) are more variable. On the thin limb (b) the plot for layer 2 lies in the class Ic field slightly above the class 2 line, while that for the thick limb (a) begins in the class 3 field and crosses to the class Ic field as the dip increases above 35°. Layer 4 is thicker on limb b, and the t'a plot lies in the class Ic field considerably above the class 2 line. The plot for layer 4 on the thin limb (a) lies in the class 3 field about the same distance below the class 2 line. Over the second fold hinge the t'a plots for all layers (4, 5 and 6) lie along or just below the class 2 line, but diverge slightly into the class 3 field as the dip increases above 65°.

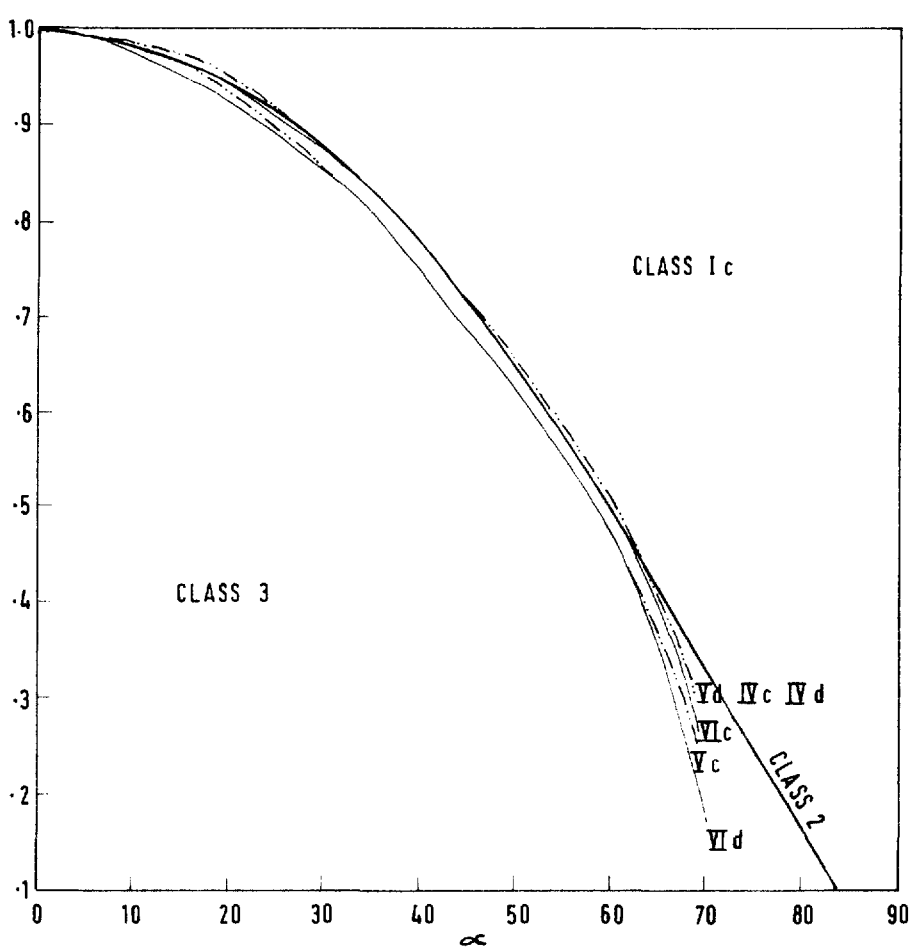
These minor folds, like those in the first example, are almost perfect similar folds resulting from asymmetric folds flattened parallel to their axial planes. The white gneiss was slightly more competent than the grey gneiss, but the ductility contrast between the two rock types diminished as the white layers became thinner.



(a) FOLDED GREY AND WHITE GNEISS
ROTA BALMU (6810-5 1311)

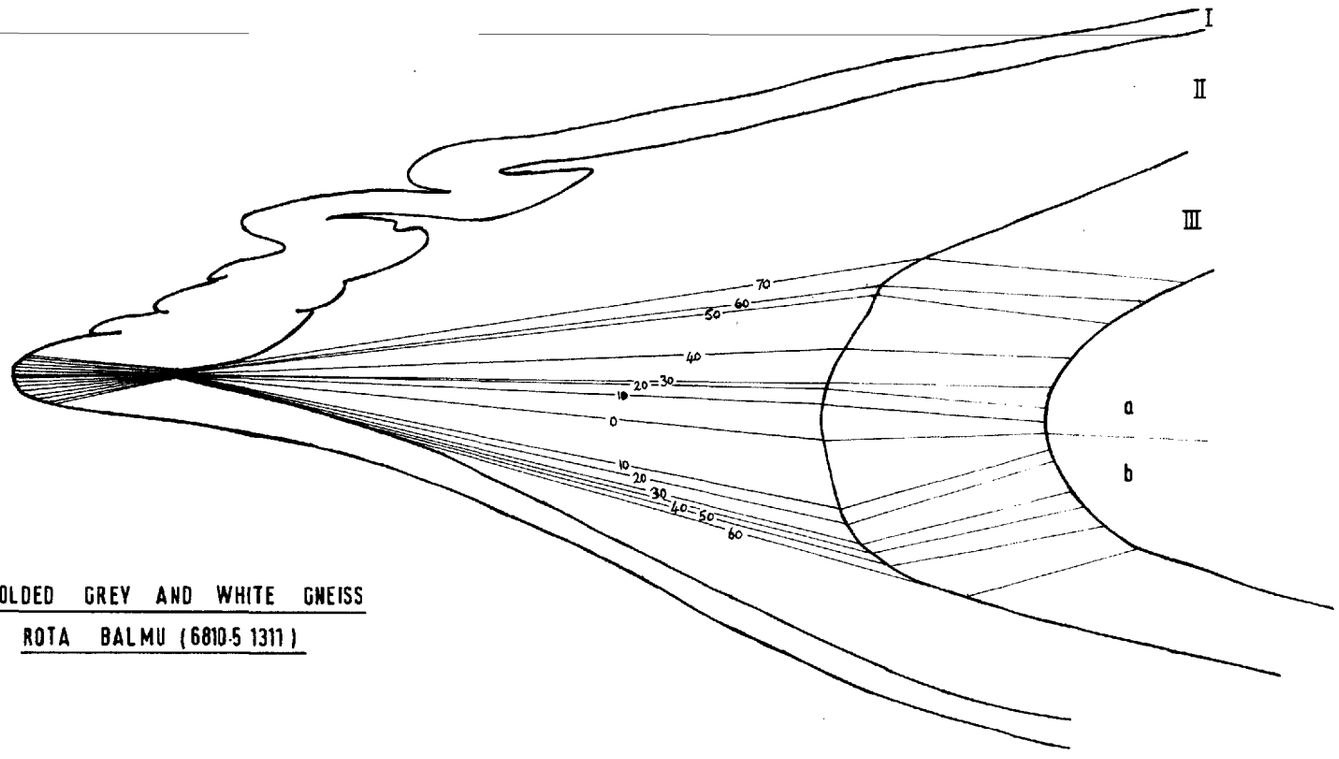


(b) $t' \propto$ PLOTS LIMBS a AND b

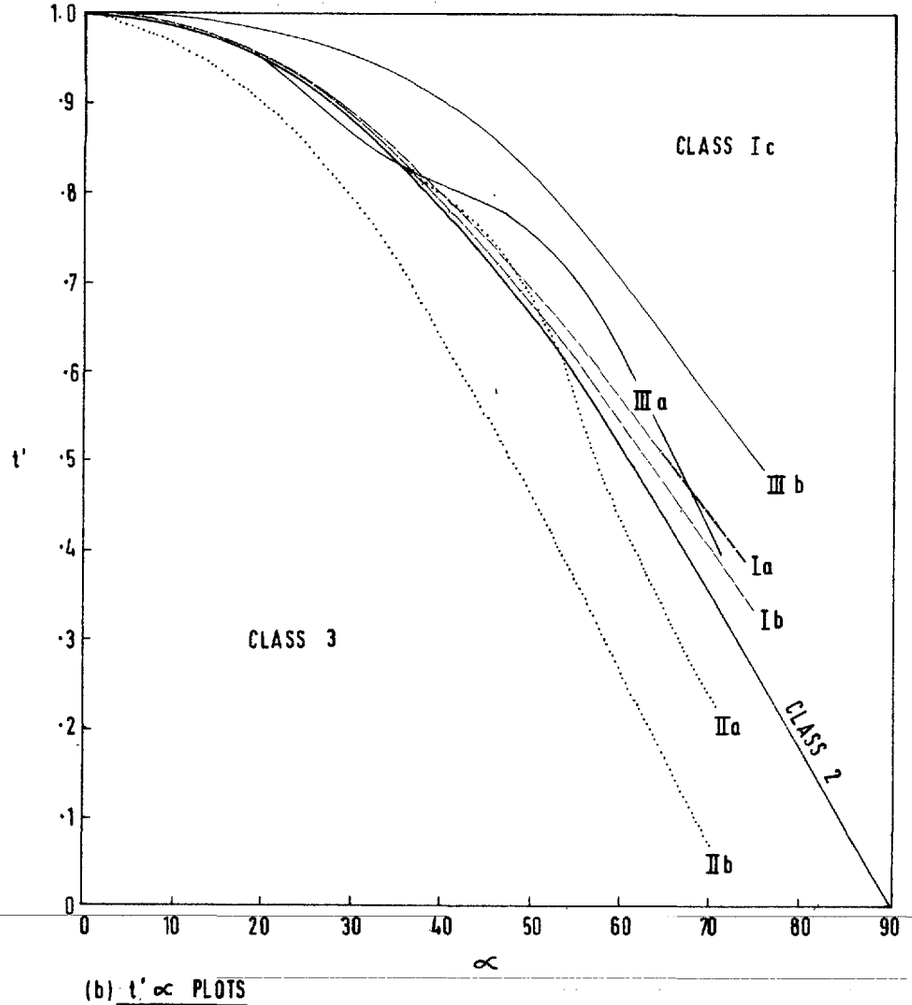


(c) $t' \propto$ PLOTS LIMBS c AND d

FIGURE 14
F_2 MINOR FOLDS



(a) FOLDED GREY AND WHITE GNEISS
ROTA BALMU (6810·5 1311)



(b) t' ∝ PLOTS

In Example 3, also in gneiss at Rota Balmu, the ductility contrasts between the layers were much stronger as the isogons show a conspicuous convergent-divergent pattern across the layers (fig. 14). The t'a plots for the more competent white layers (1 and 3) lie in the class 1c field just above the class 2 line, while those for the less competent grey layer (2) lie in the class 3 field.

6:3 Schistosity

As a result of the F2 deformation a powerful, penetrative schistosity was developed in all rocks in the Valle di Bosco. It is least intense in the centre of the massive Antigorio Gneiss, but becomes more strongly developed towards the margins of the gneiss. The pancake-shaped xenoliths in the gneiss lie in the plane of the schistosity, and become progressively thinner as the gneiss becomes more schistose.

In the schists of the Bosco Group the schistosity is accompanied by very thin, alternating quartz- and mica-(or hornblende-) rich layers. In the muscovite gneiss the micas and augen of quartz and feldspar are strongly aligned parallel to the schistosity. On the northeast slopes of the Batnall the schistosity refracts as it passes from semi-pelitic staurolite schist into thin bands of muscovite gneiss. Muscovite flakes in the gneiss make a higher angle with the lithological boundaries than do the micas in the semi-peltic schist.

In the Mesozoic rocks the schistosity is strongly developed in the pelitic schist, quartzite and the more siliceous calcareous schists. The marble retains a strong pre-F2 compositional banding, but in folded outcrops isolated phlogopite micas lie parallel to the axial planes of the F2 minor folds.

Over most of the area the F2 schistosity dips gently ESE, except where it is folded into a very steep attitude in the hinge zone of the Wandfluhhorn Antiform. The dip becomes gradually steeper towards the southeast, and angles of up to 50° are common near Collinasca.

6:4 Lineation

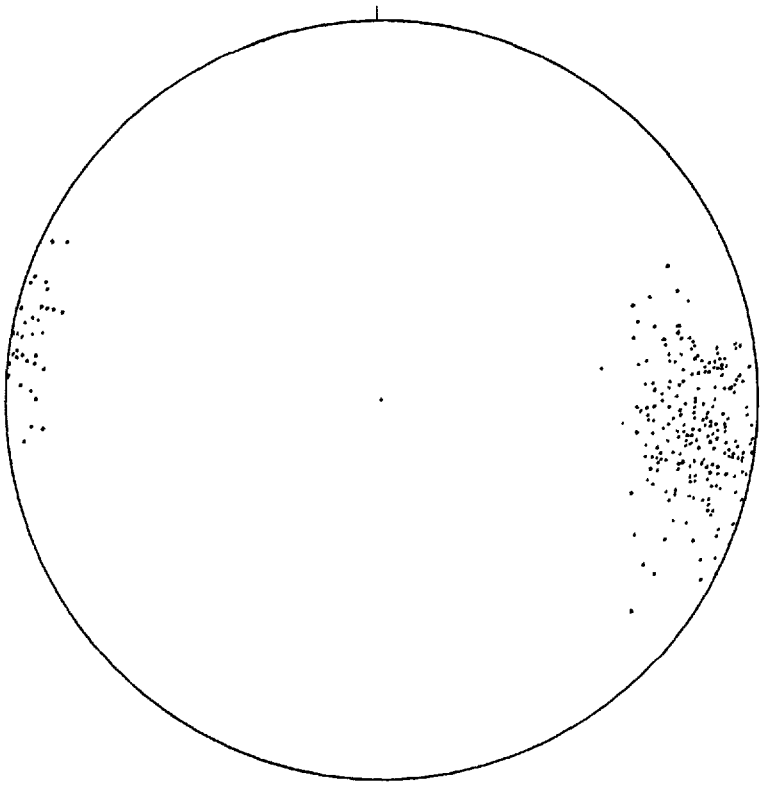
The F2 lineation, formed dominantly by aligned mica flakes, is the most strongly developed linear fabric in the region, and occurs on the schistosity surfaces of all rock types. It is most conspicuous in the schistose Antigorio Gneiss where the mica flakes stand out on the light coloured surfaces, and quartz augen have been streaked out into thin, sub-parallel lines. The lineation is only poorly developed in the massive Antigorio Gneiss, but dioritic xenoliths exposed on the schistosity surfaces generally have their longer axes oriented parallel to the lineation direction.

In the semi-pelitic schist of the Bosco Group thin, flat quartz sheets, probably originally pre-F2 quartz veins, have sub-parallel grooves and strongly aligned muscovite and biotite flakes on their surfaces. Kyanite needles and staurolite prisms may also be aligned parallel to the lineation, but they are generally randomly oriented. Black tourmaline needles up to 3 cms long and aligned mica flakes form the lineation on the muscovite gneiss of the Bosco Group, while in the hornblende schist the lineation is formed by the abundant, small, strongly oriented hornblende needles.

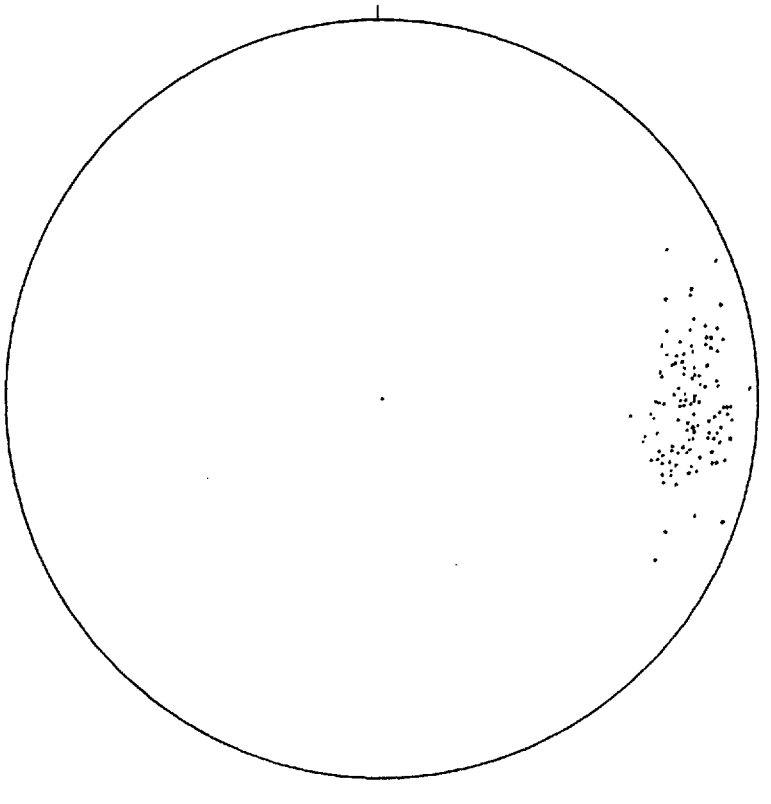
In the Mesozoic rocks the linear fabric is strongly developed in the pelitic schist and siliceous calcareous schist, but is less distinct in the marble and quartzite because of the lack of micaceous minerals.

The F2 lineation plunges gently eastwards (fig. 15). A few sub-horizontal WNW plunging lineations were recorded, mainly in the Bann area, where the schistosity has been tilted slightly by movement along small faults. The plots of the F2 lineations recorded from rocks on the upper and lower limbs of the Wandfluhhorn Antiform are almost identical, and plunge in the same direction as the hinge line of the Wandfluhhorn Antiform. This strongly suggests that the F2 and F3 deformations were closely coaxial.

FIGURE 15
F_2 LINEATIONS



(a) PLOTS OF F_2 LINEATIONS ON UPPER LIMB OF WANDFLUHHORN ANTIFORM (252 POINTS)



(b) PLOTS OF F_2 LINEATIONS ON LOWER LIMB OF WANDFLUHHORN ANTIFORM (120 POINTS)

6:5 Boudinage

Boudinage and pinch and swell structures are common features of the F2 deformation, and provide the best evidence of the relative ductilities of different rock types during the deformation. Individual boudins observed have two dimensional rectangular or lenticular shapes. Ramberg (1955) and Ramsay (1967, ch. 3) have shown that rectangular boudins, separating along tensile fractures, indicate a greater ductility contrast between the matrix and boudinaged layer than do lenticular boudins, resulting from a band being thinned by necking prior to separation. Rectangular boudins in the Valle di Bosco usually have smaller l/t (length/thickness) ratios than lenticular boudins. Typical F2 boudin shapes are illustrated in fig. 16. In general the more siliceous and coarser grained rocks appear to have been the most competent rock types, and were more likely to deform by boudinage than the calcareous rocks which were the least competent.

Boudinaged pre-F2 quartz veins have been found in marble (l/t ratios of 1.5:1), in massive Antigorio Gneiss, in schistose gneiss (l/t 3.9:1 to 7.3:1) and in semi-peltic schist. Boudins of quartz-rich white gneiss occur in both the massive Antigorio Gneiss and in the schistose edges (l/t 3:1), but disappear as the degree of deformation increases. Schistose gneiss boudins in marble are usually less than 60 cms thick, and represent the detached hinge zones of isoclinal F2 folds. They are generally lenticular and have l/t ratios of about 8:1.

The muscovite gneiss of the Bosco Group occurs as rectangular boudins with l/t ratios of 2.5:1 in semi-pelitic schist. Hornblende schist forms boudins with rectangular cross sections in marble (l/t 1.5:1 to 2:1) and lenticular cross sections in semi-pelitic schist (l/t 6:1). It is also deformed by pinch and swell structures in semi-pelitic schist. The Mesozoic pelitic schist and dolomitic segregations commonly occur as lenticular boudins enclosed in marble



Fig. 16(a) Rectangular shaped F2 boudins of hornblende schist in garnet schist. Krameggpass (67731299).



Fig. 16(b) Elliptically shaped F2 boudins of Mesozoic pelitic schist in marble and calcareous schist. Pizzo Bombogna (68181288).

and calcareous schist (l/t 6:1). The marble and calcareous schist were probably the most ductile rocks during the F2 deformation. However, on the northwest face of P. Bombogn (68141287) and at Rota Balmu (68111311) thin marble and calcareous schist bands enclosed in schistose gneiss are boudinaged into forms with thin lenticular cross sections and l/t ratios between 8:1 and 15:1. Marble and calcareous schist also occur as boudins and boudinaged folds in hornblende schist on the western slopes of the Martschenspitz (67821312), and a thick band of coarse grained, siliceous marble is boudinaged into rectangular forms (l/t 5:1) 300 m. WNW of Passo di Bosco (67791309). These observations imply that marble and calcareous schist bands were locally more competent than the enclosing basement rocks.

The boudinage relationships show that during the F2 deformation quartz veins were the most competent rock types, and were followed in order of decreasing competence by white gneiss (of the Antigorio Gneiss), massive biotite-rich Antigorio Gneiss, muscovite gneiss of the Bosco Group, hornblende schist, schistose gneiss, semi-pelitic schist, calcareous schist and marble.

In a series of spectacular water-worn outcrops of Mesozoic marble and pelitic schist in a stream bed just north of Ubarab (68221303), the structures show a complete range from F2 folds to boudinage (fig.17). Different outcrops show different stages of the progressive deformation. F2 folds become tighter until the limbs are parallel. Hinge zones of pelitic schist become isolated, and the closures are largely obliterated. Finally, the layers show undulations with pinch and swell structure and boudins.

The orientations of the F2 boudin necks have been plotted on a rose diagram (fig.18) which shows E-W, NNW-SSE and NNE-SSW peaks. The strongest peak, oriented NNE-SSW, and the NNW-SSE peak, are almost perpendicular to the trend of the F2 lineation. This is particularly significant as it suggests that the F2 lineation

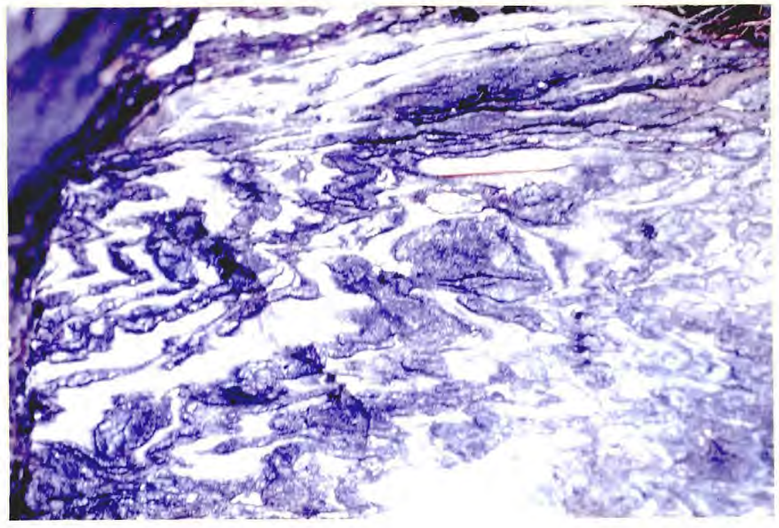


Fig.17(a) F2 folds in banded marble and pelitic schist Ubarab (68221303).

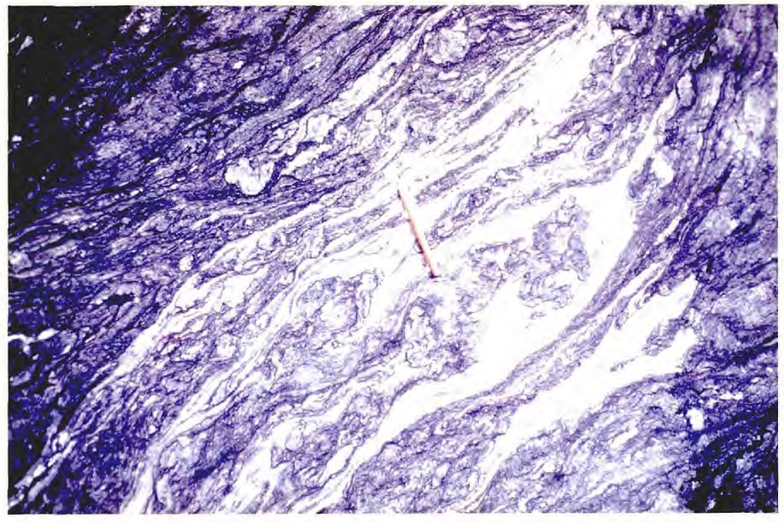


Fig.17(b) Progressive development of the folds showing attenuated limbs.

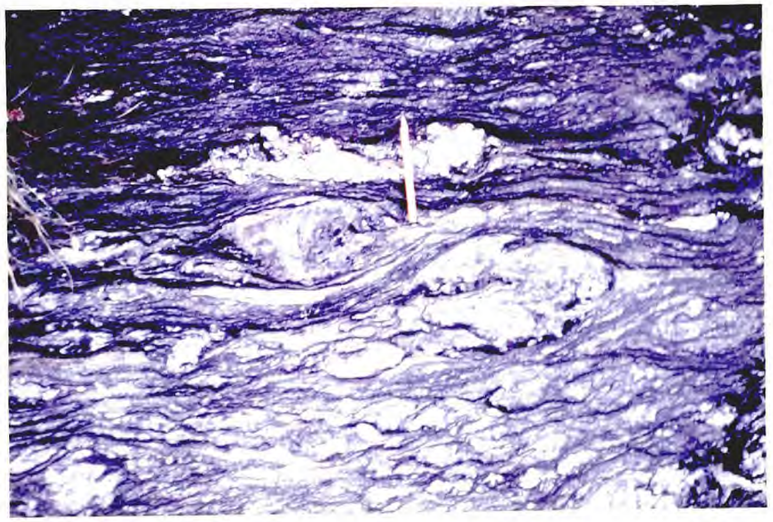


Fig.17(c) Extremely attenuated F2 fold limbs and isolated fold hinges.

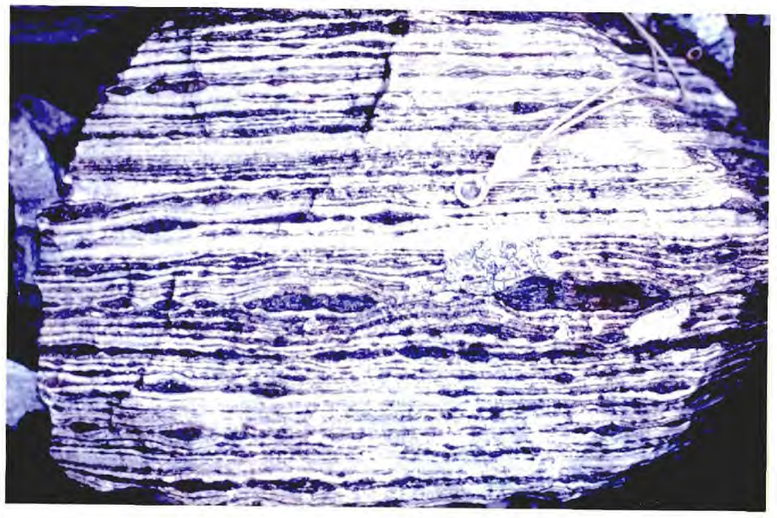
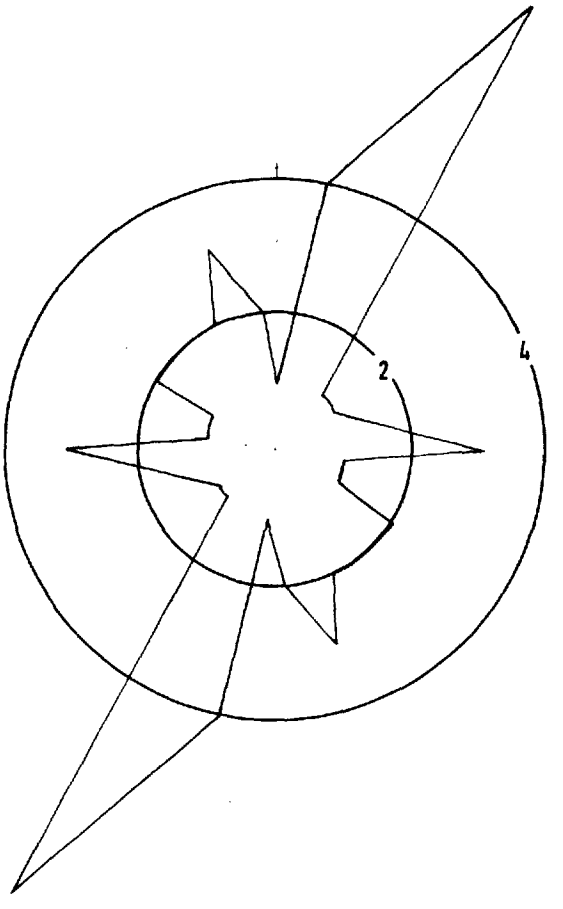


Fig.17(d) Final stage of progressive deformation, pinch and swell structures and pelitic schist boudins.

FIGURE 18



ORIENTATION OF NECKS OF F_2 BOUDINS AND PINCH AND SWELL STRUCTURES

direction represents the direction of greatest finite stretching. The E-W peak shows that stretching also occurred normal to the lineation direction. These observations confirm the conclusions of Ramberg that boudins have ellipsoid or parallelepiped shapes, which show that stretching occurred on the schistosity planes in both the X and Y directions of the bulk strain.

CHAPTER 7

F3 DEFORMATION

7:1 Introduction

The structural geology of the Valle di Bosco is dominated by a large recumbent F3 fold, the Wandfluhhorn Antiform, which closes to the north and plunges gently eastwards. The most outstanding features of this fold are its large size, extent and tightness. It is a major fold of regional importance which has deformed the F1 and F2 structures, and strongly folded the schistosity.

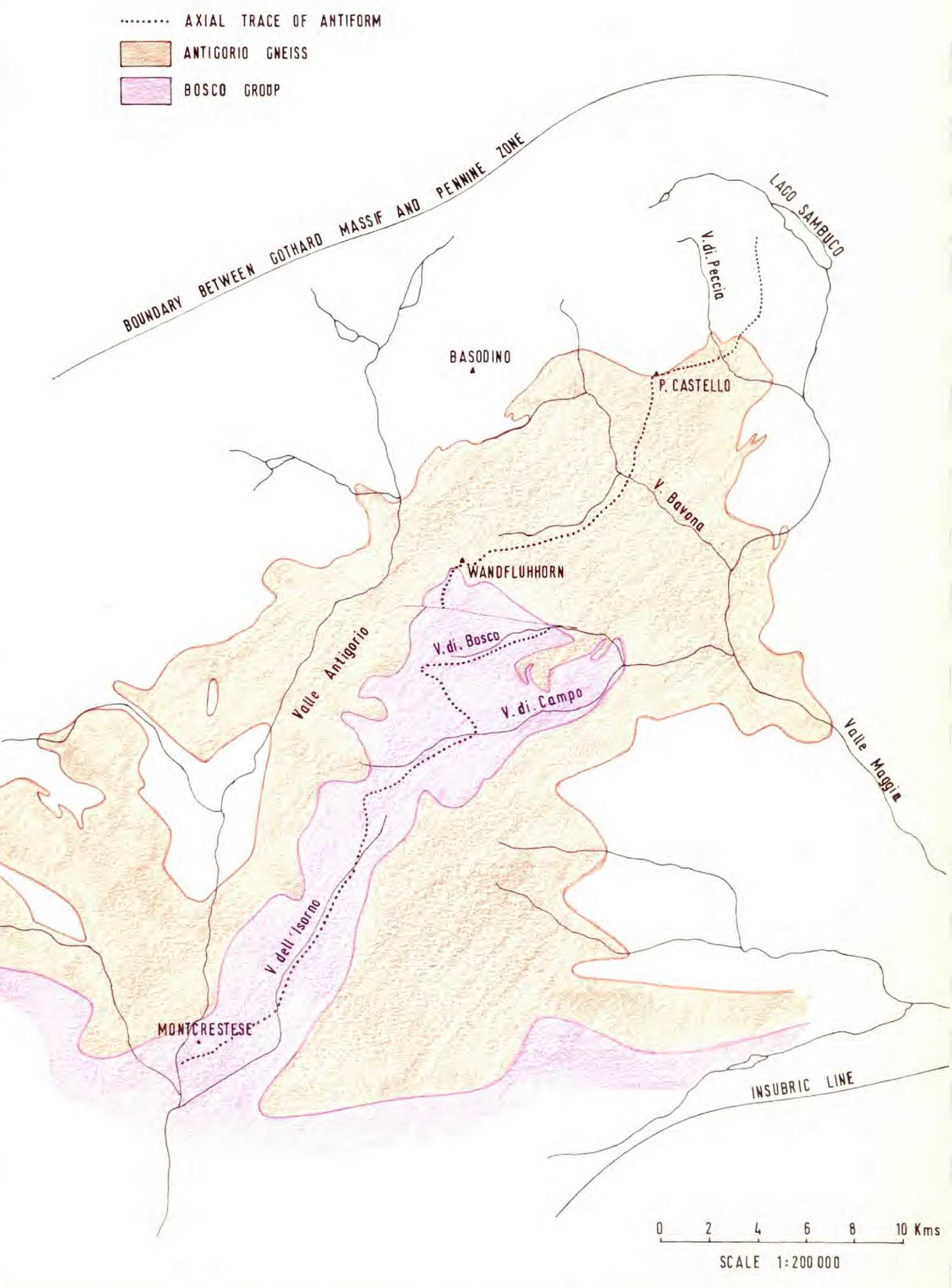
The Wandfluhhorn Antiform was discovered by Schmidt and Preiswerk (1908), and since this date further descriptions of the spectacular hinge zone on the western slopes of the Wandfluhhorn have been given by Grutter (1929) and Hunziker (1966). Wieland (1966) also described another excellent exposure of the hinge zone at Alpe Bosa, 9.5 SSW of the Wandfluhhorn.

The fold core in the thesis area is made up of Bosco Group schist and gneiss, and is surrounded by an outer zone of homogeneous, biotite-rich Antigorio Gneiss. The axial trace of the fold has been followed southwest from the basin east of the Wandfluhhorn to the ridge dividing the Valle di Bosco and the Val Calnegia. It then crosses a large gully to the ridge 500 m. south of the Wandfluhhorn, and continues south along the western (Italian) side of the ridge to the Guriner Furka Fault at Passo di Bosco. The hinge zone is exposed at a number of localities along this line, in particular in the basin immediately south of Lago Superiore (see fig. 6).

On the map of the area the axial trace is displaced 4.5 kms to the east across the Guriner Furka Fault, and reappears on the south side of the Valle di Bosco opposite Ubarab. The trace continues southwest along the steep valley side to just below Passo Quadrella, but the hinge zone is exposed only in isolated outcrops in the wooded terrain. West of Passo Quadrella the axial trace can be easily followed across almost continuous outcrops to the ridge crest 500 m.

FIGURE 19

REGIONAL EXTENT OF WANDFLUHHORN ANTIFORM



southeast of the Batnall. It then turns southeast along the southern face of the ridge before crossing into the head of Alpe di Quadrella. Southeast of this point the axial trace is hidden beneath extensive scree slopes which extend to the floor of the Valle di Campo.

Southwest of the thesis area the axial trace of the Wandfluhhorn Antiform extends along the upper reaches of the Valle di Campo before crossing into the head of the Valle dell' Isorno at Passo della Forcola. (fig. 19). It continues SSW along the Valle dell' Isorno to just south of Montecrestese and crosses the Toce River to Crevola d'Ossola. It has recently been traced northwest into the Simplon region by G. Milnes (pers. comm. 1971). The continuation of the axial trace north of the Valle di Bosco is less certain. It probably extends northeast along the south side of the Val Calnegia to the Val Bavona, and north along the east side of the Val Bavona to the vicinity of Pizzo Castello. From this point J. Ramsay (pers. comm. 1970) has traced it east to the Valle di Peccia, then northeast to the head of Lago Sambuco.

From its present known extent, the antiform appears to have an inverted (lower) limb at least 30 kms long when measured normal to the axial direction.

The Wandfluhhorn Antiform is accompanied by a distinct set of minor structures. The most common are small chevron-like folds, internal boudinage and a slickenside lineation. Crenulation cleavage, mullions and an intersection lineation were also observed. These minor structures deform the F2 schistosity, and are typical of those developed in strongly layered, statistically homogeneous but anisotropic rocks (Cobbold, Cosgrove and Summers, 1971; Paterson and Weis, 1961; Ramsay, 1967: 438).

7:2 Minor Folds

In the thesis area minor folds are concentrated in the hinge zone and upper limb of the Wandfluhhorn Antiform. Individual folds



Fig.20(a) F3 folds in garnet schist. Hinge zone of Wandfluhhorn Antiform, Lago Superiore (67831316).



Fig. 20(b) F3 folds in calcareous schist. Lago Superiore (67831318).



Fig. 21(a) F3 folds in schistose Antigorio Gneiss. Hendar Furggu (67881321).



Fig.21(b) F3 folds in schistose Antigorio Gneiss, North of Lago Superiore (67871322).

have straight limbs and sharp to rounded, slightly thickened hinges (figs. 20, 21). The fold shape of the different layers remains fairly constant around each hinge zone, resulting in an overall geometric form very close to a similar (class 2) model. Interlimb angles are commonly between 50° and 100°, with a strong concentration between 50° and 65° as predicted by De Sitter (1958), but angles as low as 20° were recorded. The axial surface of each fold generally bisects the angle between the fold limbs.

The wavelength of the minor folds rarely exceeds 3 metres, and the amplitude is usually less than 1.5 metres. Folds with the largest wavelength occur in coarse grained gneiss, while those with the smallest wavelengths were observed in the fine-grained, finely schistose rocks of the Bosco Group. When the minor folds are viewed looking east, their symmetry changes from M-shaped in the hinge region of the Wandfluhhorn Antiform to S-shaped on the upper limb and Z-shaped on the lower limb (figs. 22, 23). This simple vergence pattern was used to determine the position of the axial trace where the hinge zone was not exposed, but care was needed particularly in the gneiss where minor folds with a much smaller amplitude often occurred on the limbs of larger F3 minor folds.

Antigorio Gneiss with intercalated Mesozoic bands on the upper limb of the Wandfluhhorn Antiform south of Rovana Stream is strongly folded by minor folds of variable wavelength, two of which are particularly common. The majority of these folds have an M symmetry, but it was not possible to locate a major F3 fold hinge. In this area there is probably a very large but open S-shaped fold deforming the rocks, with congruous minor folds having M, S and Z symmetry. Unfortunately the area is extensively wooded, and the best outcrops are often on extremely steep, inaccessible faces. In these circumstances I cannot be completely confident that the interpretation given is the correct one.

AXIAL TRACE OF WANDFLUHHORN ANTIFORM

ARROW INDICATES DIRECTION OF PLUNGE

SYMMETRY OF MINOR FOLDS SHOWN WHEN VIEWED EAST IN DIRECTION OF PLUNGE

WANDFLUHHORN

P. D'ORSALIA

MARTSCHENSPITZ

RITZBERG

BOSCO - GURIN

BATNALL

KLEINHORN

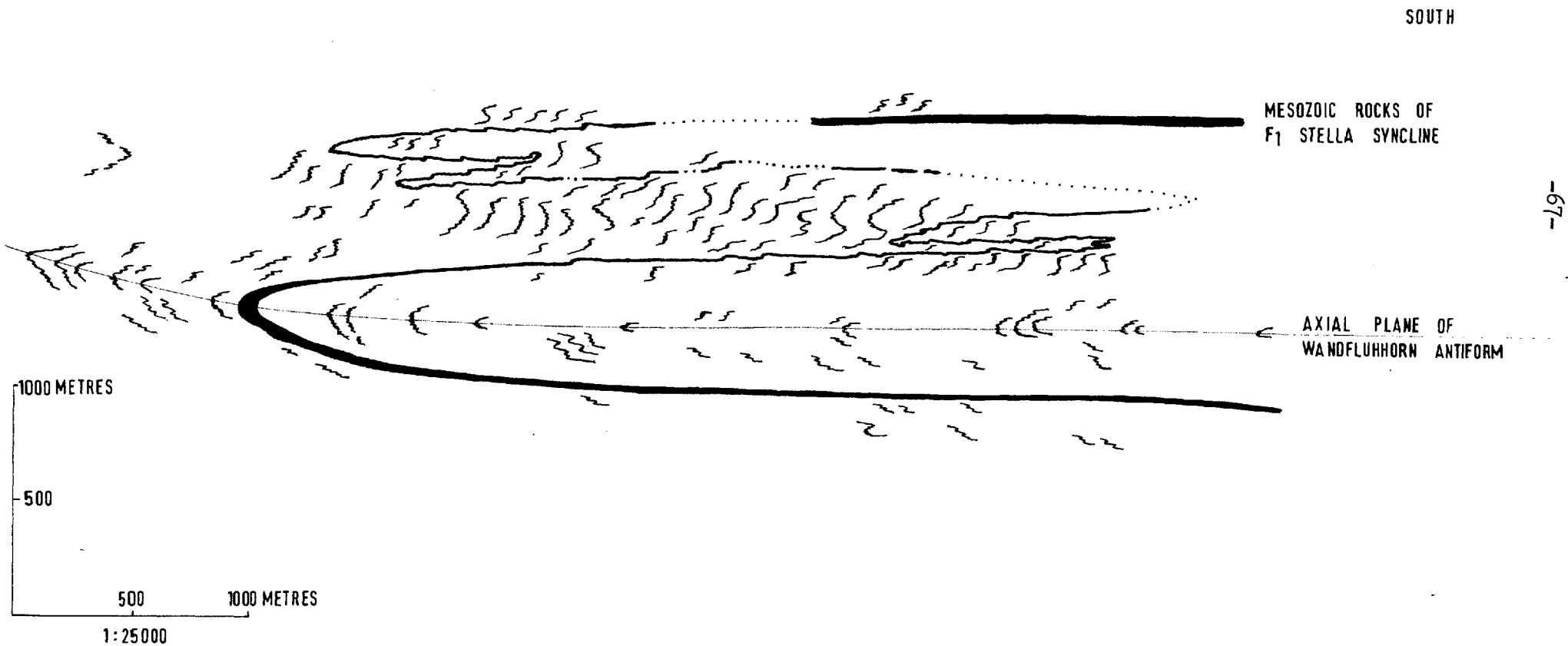
P. BOMBOGN

PIAN CROSC

CERENTINO

P. QUADRO

1:25000



SYMMETRY OF F_3 MINOR FOLDS IN PROFILE SECTION

NOTE IN PARTICULAR THE VERY STRONG FOLDING ON THE UPPER LIMB OF THE ANTIFORM

FIGURE 23

Estimates of the amount of shortening which caused the folding were obtained by measuring the arc lengths of a number of folded layers and comparing this value with the distances between the same two points normal to the axial surfaces. Values of between 29% and 63% were obtained, with a strong grouping between 40% and 50%. The amount of shortening of individual layers calculated in this way was independent of their thicknesses. The thickness of most layers varies slightly in the folds, and it is obvious that some modification of the initial thickness has occurred.

The geometry of a number of typical F3 minor folds was studied in detail, and the results are described below.

Schistose gneiss from west of Hendar Furggu (67881320)(fig.24)

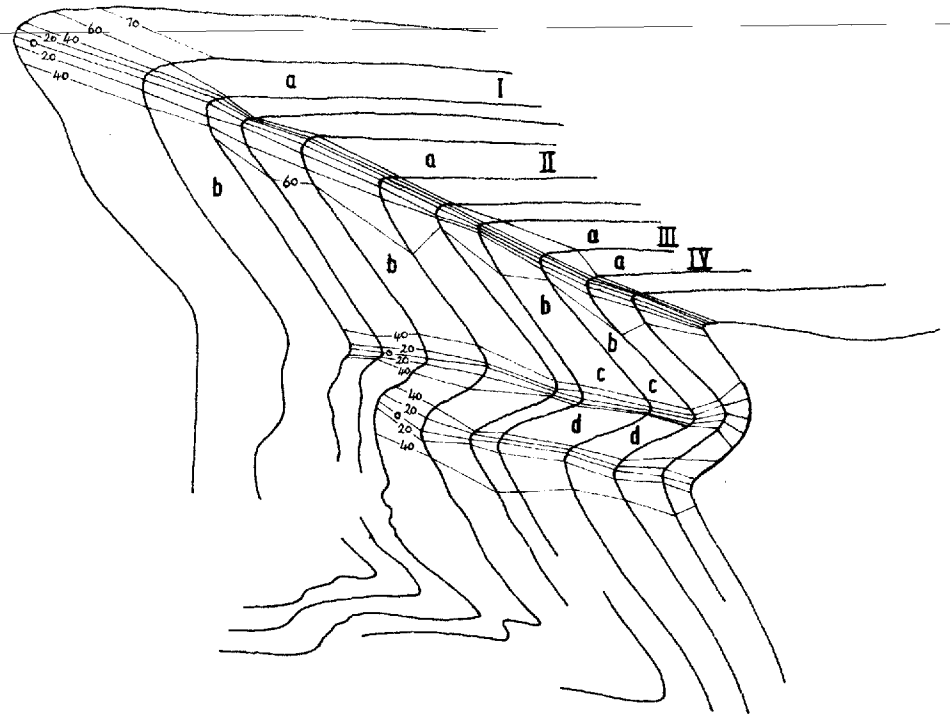
This is a very evenly layered rock, and probably one with the least ductility contrast between individual layers. The folds are chevron-like with interlimb angles of between 50° and 100°, and maximum limb dips of 70°. Isogons drawn for angles up to 40° are generally parallel to the axial surfaces of the folds, but where they deviate from the parallel form they are alternately divergent and convergent on successive layers.

Thickness variations in four layers were examined by plotting their variation in thickness against their angle of dip (i.e. t'a plots). Layers 1 and 2 were traced over one fold hinge, while layers 3 and 4 were traced over two fold hinges. Layers 1 and 2 were separated by two intervening layers, but layers 3 and 4 were in contact.

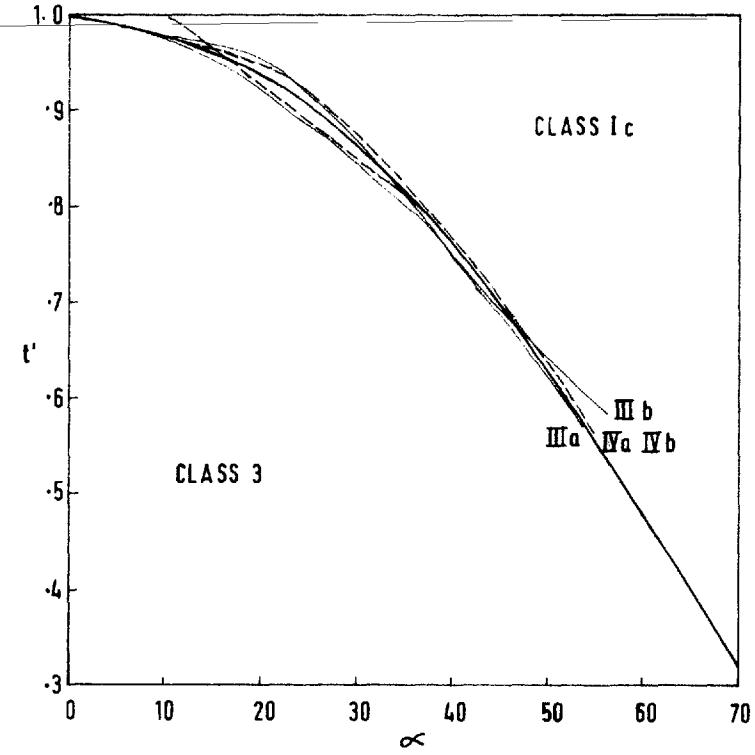
The plot for layer 1a begins in the class 3 field and crosses into the class 1c field before returning to the class 3 field. Layer 1b shows a complimentary plot, commencing and ending in the class 1c field after passing through the class 3 field. The intersection points, where the plots cross one another, lie on the class 2 line. The plots for layer 2 show a much simpler pattern, 2a following the class 2 line but deviating slightly into the class 1c field as the dip increases, while 2b deviates into the same field at a lower

FIGURE 24

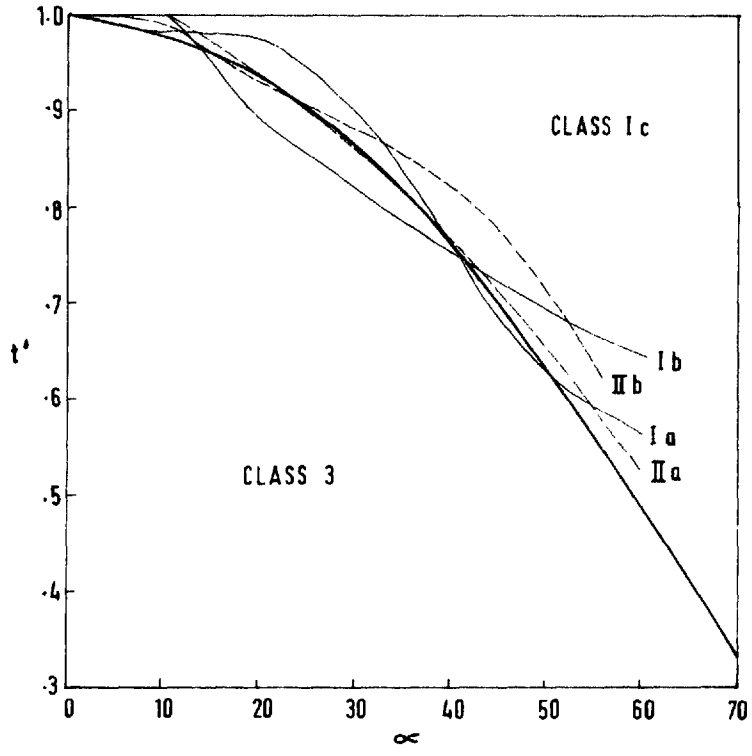
F3 MINOR FOLDS



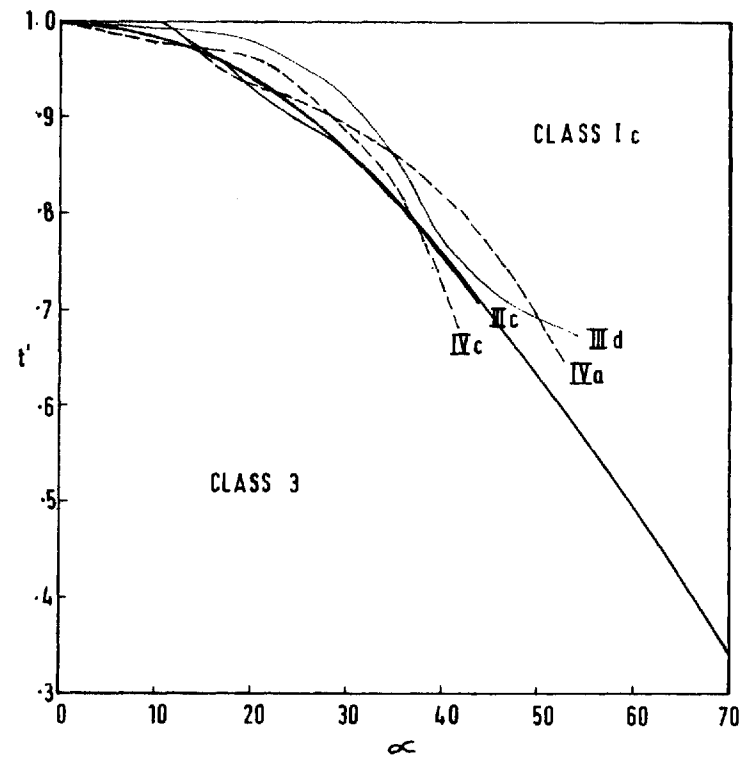
(a) F3 FOLDS SCHISTOSE GNEISS HENOAR FURGGU (67881320)



(c) t' ∝ PLOTS LAYERS III AND IV LIMBS a AND c



(b) t'∝ PLOTS LAYERS I AND II



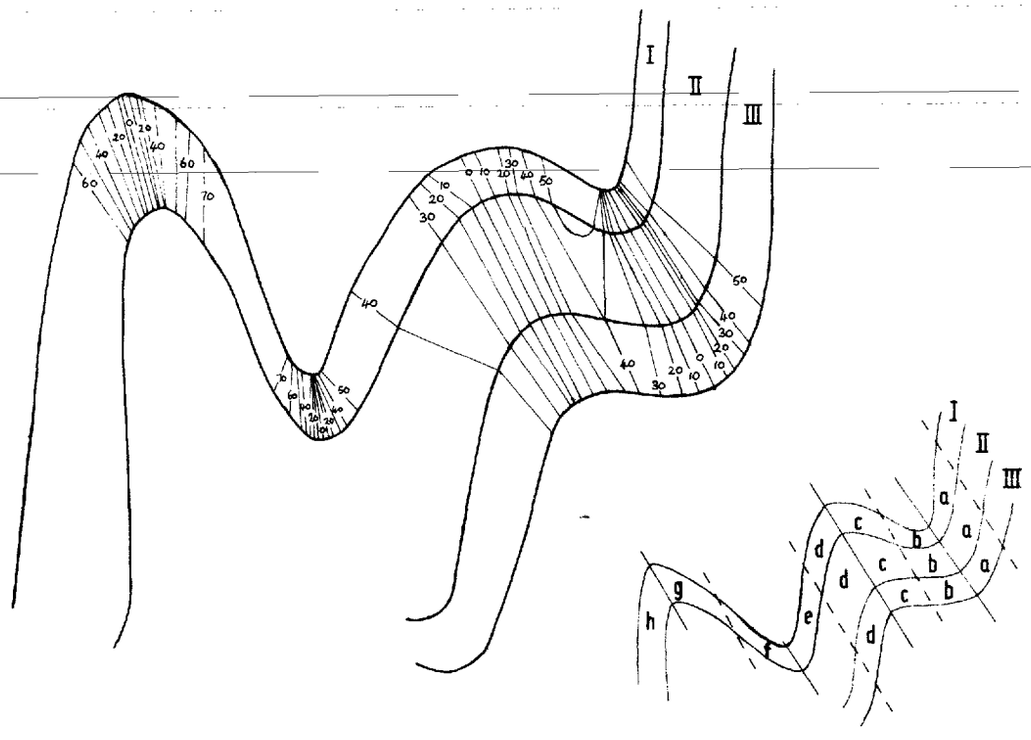
(d) t' ∝ PLOTS LAYERS III AND IV LIMBS c AND d

angle of dip. Over the first fold hinge the plot for layer 3a is parallel to the class 2 line, but just inside the class 3 field. Layer 3b is also largely parallel to the class 2 line, but crosses it slightly a number of times. Over the second fold hinge the plot for 3c begins in the class 1c field before lying along the class 2 line, but that for 3d deviates back into the class 1c field as the dip increases. Over the first fold hinge the plots for layers 4a and 4b lie very close to the class 2 line after beginning in opposite fields. At the second fold hinge the 4c plot begins in the class 3 field and crosses into the class 1c field before deviating back into the class 3 field. The 4d plot shows an exactly opposite pattern, and the intersection points of the two plots lie on or very close to the class 2 line. When layers 3 and 4 were considered as a single unit the plots from both fold hinges lay parallel to the class 2 line, but just inside the class 3 field.

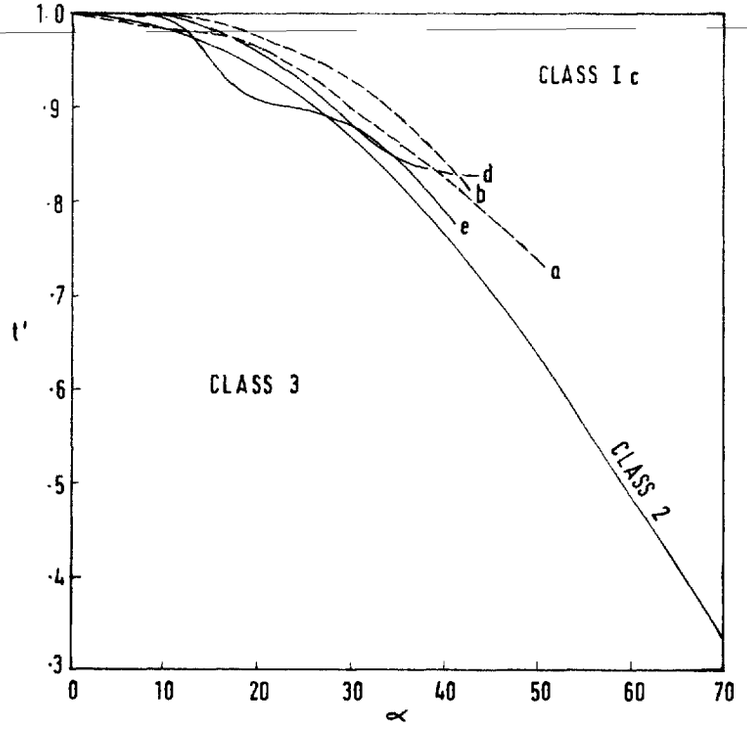
The t'a plots described above show that the F3 folds are almost perfect examples of class 2 (similar) folds (Ramsay, 1967: 432-4). The crossing of the plots of opposing limbs is probably due to slight changes in thickness of the schistosity planes along the fold limbs, resulting from the asymmetry of the folds. There appears to have been little competence difference between the layers, but alternate have been slightly thickened and thinned in the hinge regions of the folds to accommodate to the similar style.

Semi-pelitic schist from Lago Superiore (67841316) (fig.25).

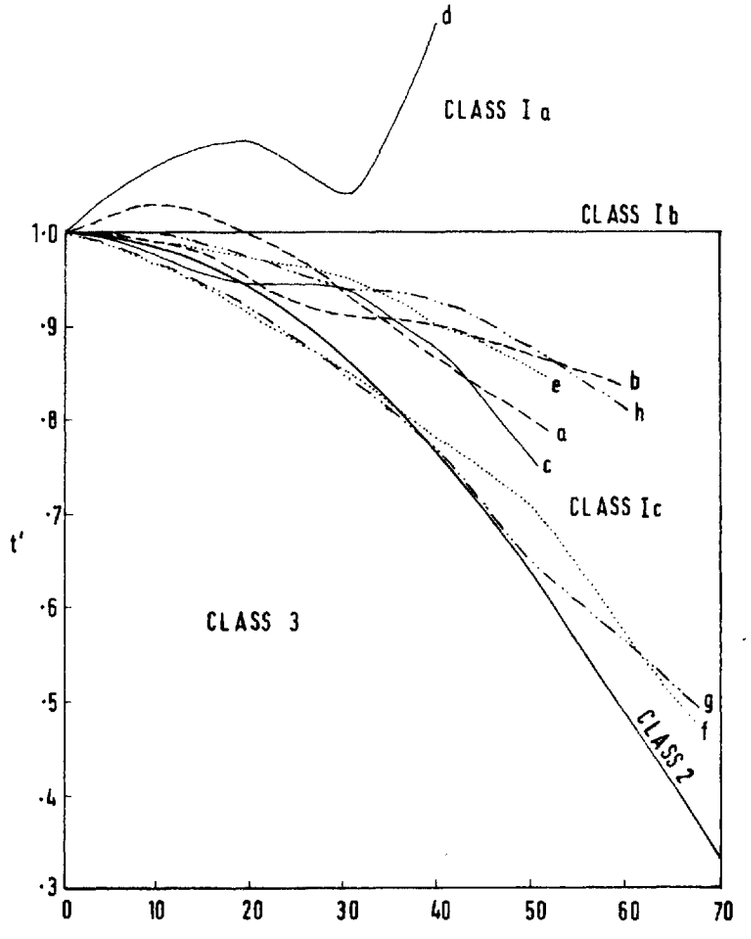
Isogons constructed from the minor folds are again almost parallel, but have slightly convergent traces over the quartz-rich layers and divergent traces over the micaceous layers. The plots for the quartz-rich layer 1 invariable lie in the middle and lower half of the class 1c field. However, on one fold limb the plot remained close to the class 2 line, and on another it fell in the class 1a field. The plots for the micaceous layer 2 also lie in the class 1c field, but much closer to the class 2 line. The plot for one fold limb deviates slightly into the class 3 field. The plots for the quartz-rich layer 3 vary from those lying almost parallel to the class 2 line to those lying in the upper part of the class 1c field.



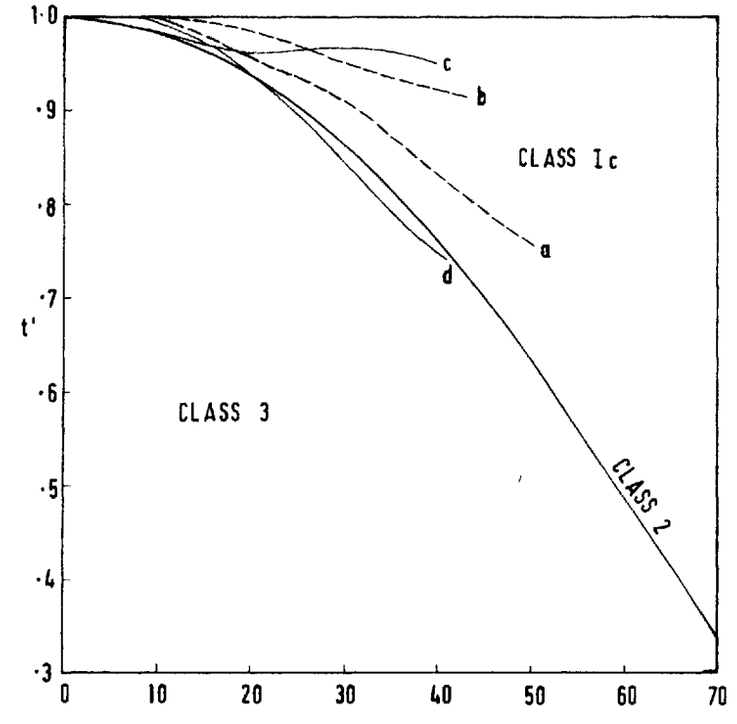
(a) F3 FOLDS SEMI-PELITIC SCHIST
LAGO SUPERIORE (6784 1316)



(c) t'∝ PLOT LAYER II MICACEOUS



(b) t'∝ PLOT LAYER I QUARTZOSE



(d) t'∝ PLOT LAYER III QUARTZOSE

The geometry of this example suggests that the layers were of differing competence. The plots for the quartz-rich layers generally lie further above the class 2 line than the plots for the micaceous layers, showing that the quartz-rich layers were the more competent. The variation in the plots for opposing limbs of the same fold reflect the difference in thickness of the limbs. The plots for the thinner limbs of each fold generally lie closer to the class 2 line than the plots for the thicker limbs. The alternately thin and thick limbs are a reflection of the asymmetry of the minor folds.

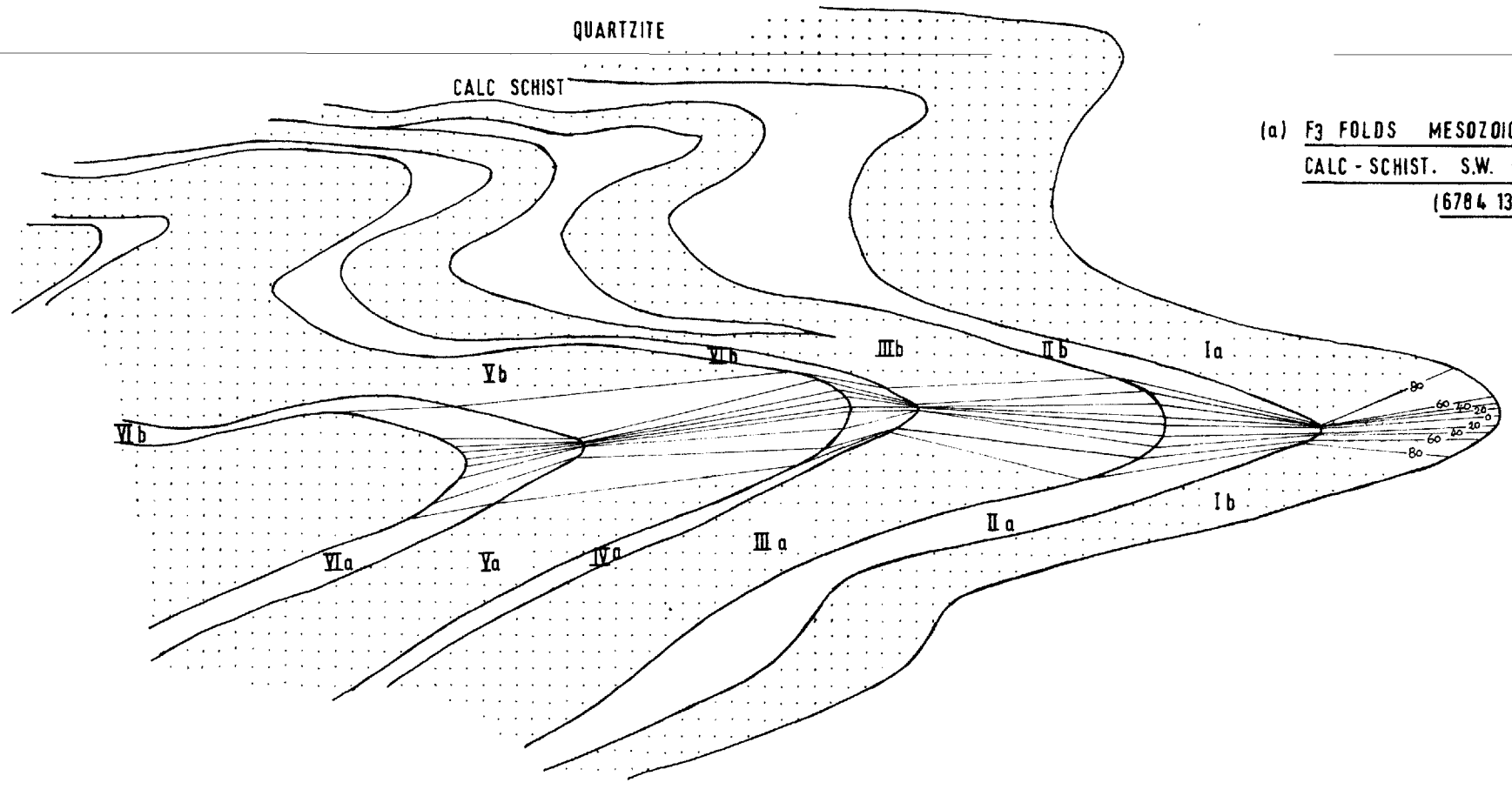
Banded Mesozoic rocks from southwest of the Wandfluhhorn (67841327) (fig.26).

Thin bands of quartzite and calcareous schist were traced around a single fold hinge. As each quartzite layer was traced around the fold hinge it was seen that one boundary formed a rounded U-shape while the other assumed a much tighter V-shape. The isogons converge across the quartzite layers and diverge across the schist layers. They meet at the peak of the V-shaped hinges. The plots for the quartzite layers lie initially along the class 2 line, but as the dip increases they deviate slightly into the class 1c field. The plots for the schist layers commence in the class 1c field or along the class 2 line, and deviate slightly into the class 3 field as the dip increases. The plots for each pair of layers lie along the class 2 line.

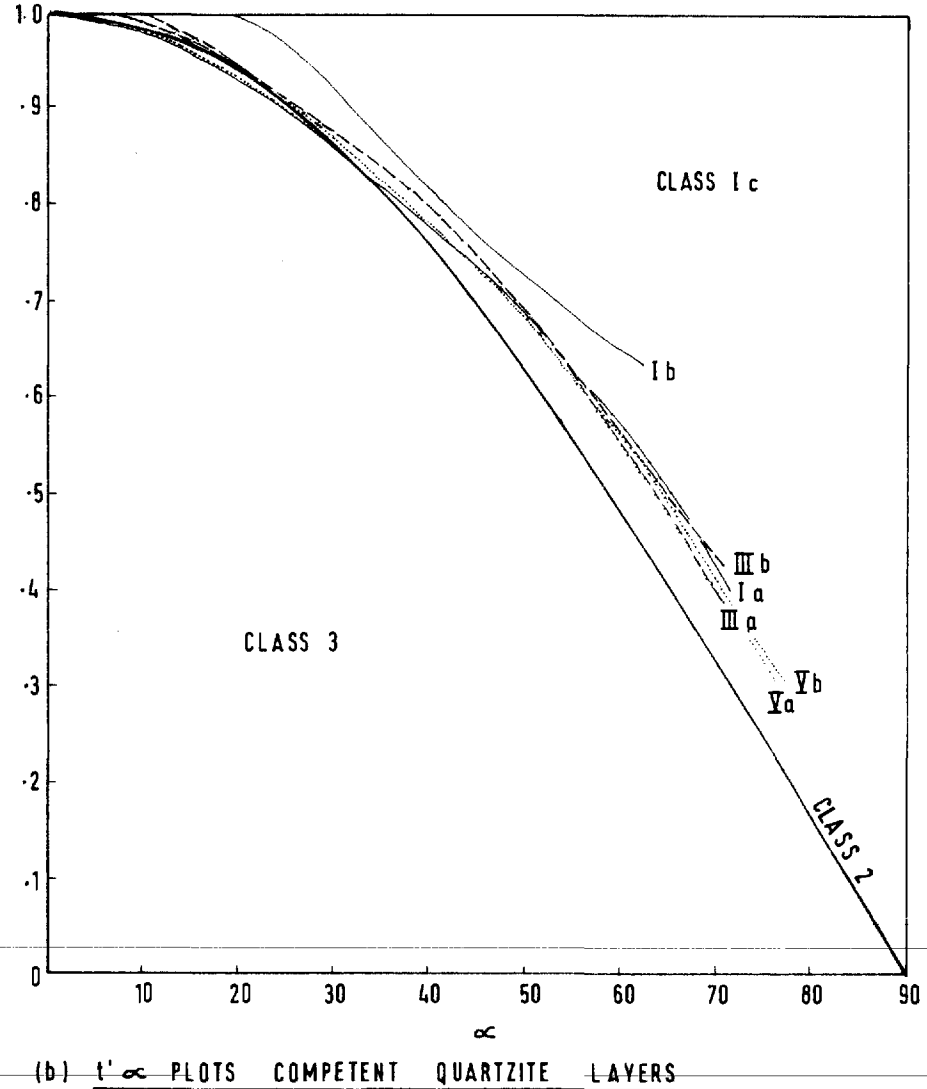
These folds are again almost perfect examples of similar folds. The geometric form is accommodated by alternate thinning and thickening of the layers in the fold hinges. The calcareous schist layers are thicker in the fold hinges than the quartzite layers, and as they were able to accommodate to the change in shape more readily than the quartzite layers they must have been less competent. This competence difference is reflected by the divergent-convergent isogon pattern on alternate layers.

FIGURE 26

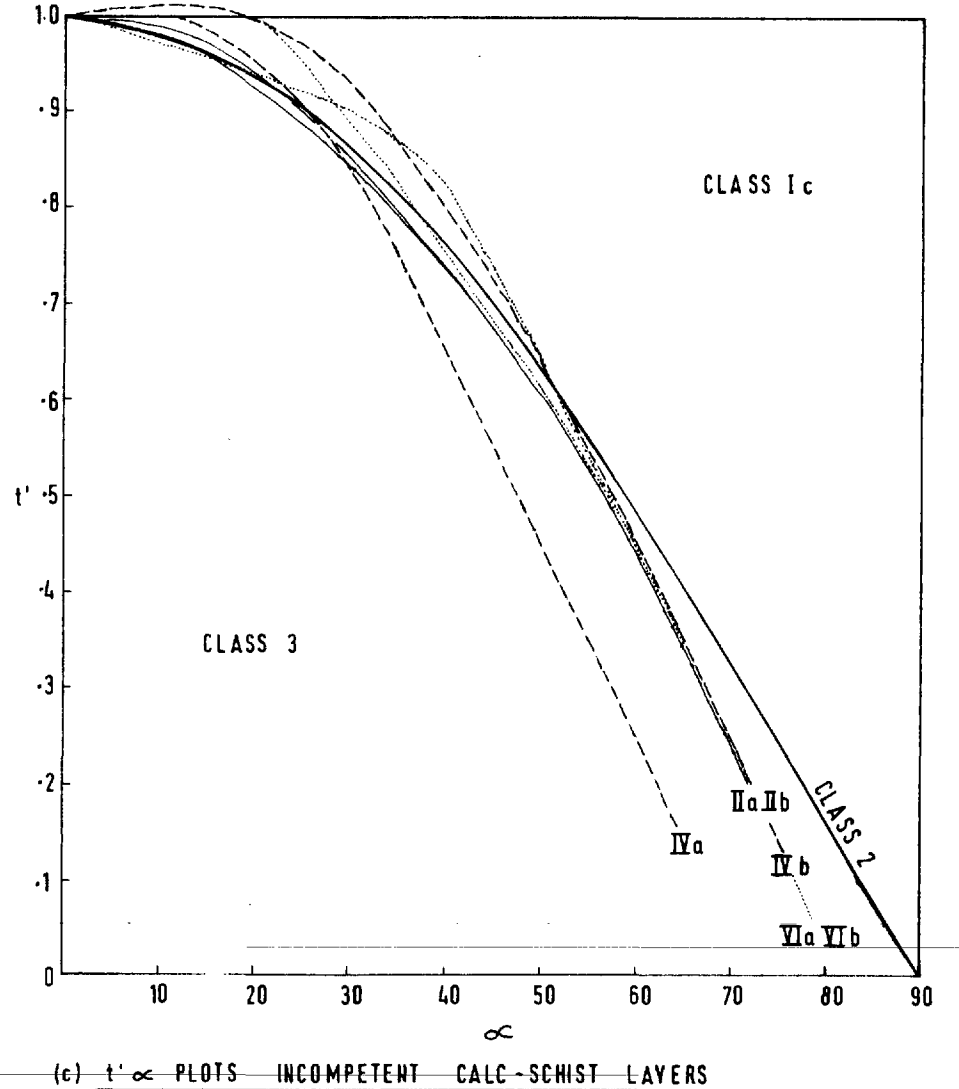
F3 MINOR FOLDS



(a) F3 FOLDS MESOZOIC QUARTZITE AND CALC - SCHIST. S.W. OF WANDFLUHHORN (6784 1327)



(b) t' ∝ PLOTS COMPETENT QUARTZITE LAYERS



(c) t' ∝ PLOTS INCOMPETENT CALC-SCHIST LAYERS

The geometric forms shownby the F3 minor folds are considered by Ramsay (1962) to develop when a multilayer complex is buckled, and the initial fold shapes are modified by superimposed strain normal to the axial planes. The final forms are flattened flexural folds.

7:3 Comparison of F3 and F2 Minor Folds

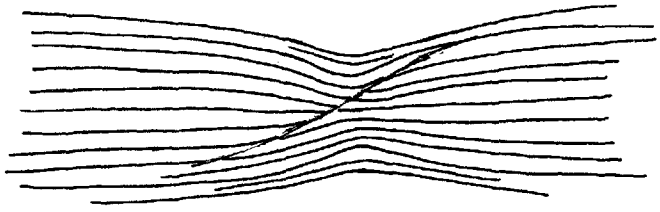
The F3 and F2 minor folds are best compared in the interference structures (figs. 36, 37). The most obvious difference is that the F3 folds are multilayer structures while the F2 folds, with the exception of those in the Mesozoic marble bands, are generally single layer structures. Both F2 and F3 folds have a similr (class 2) style geometry, but F2 folds are much tighter structures, with thicker hinges and longer limbs. The chevron-like form of the F3 folds is never observed in the F2 folds. The F2 folds have a strong axial plane schistosity, while the F3 folds in the hinge region of the Wandfluhhorn Antiform have a weak crenulation cleavage. The F3 folds deform the axial plane schistosity at the F2 folds.

7:4 Internal Boudinage

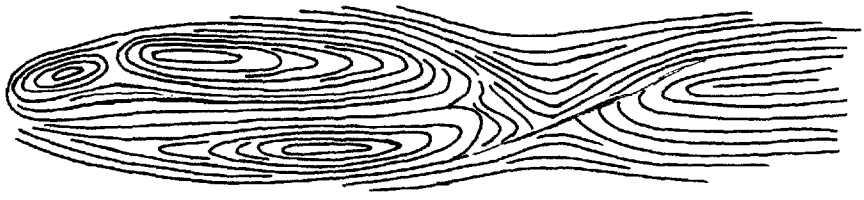
The term internal boudinage was proposed by Cobbold, Cosgrove and Summers (1971:49). They showed theoretically and experimentally that if a well layered rock was compressed normal to the layering the layering did not flatten uniformly, but developed pinch and swell structures. They considered that this resulted from different stress/strain properties for shear and compression in any given direction, as a result of the anisotropy of the material. They were also able to show that incipient shears connect the boudin "necks", and that the bisector of the obtuse angle between conjugate shears was normal to the layering.

Internal boudinage is a common feature of the most strongly layered rocks in the Valle di Bosco, particularly the marginal schists of the Antigorio Gneiss and the schists of the Bosco Group. It is uncommon in the Mesozoic rocks, and absent from the massive gneiss. The feature appears as small, slightly irregular, interlocking pinch and swell structures with small shears at angles of

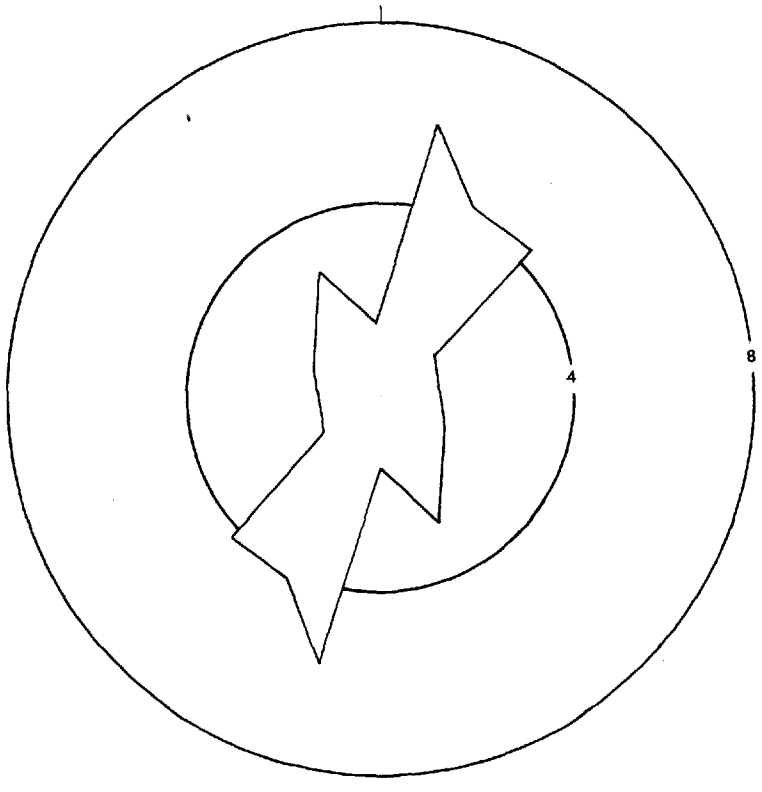
FIGURE 27
INTERNAL BOUDINAGE



(a) SKETCH OF USUAL FORM OF INTERNAL BOUDINAGE



(b) SKETCH OF MOST EXTREME FORM OF INTERNAL BOUDINAGE DEVELOPED IN HORNBLENDE SCHIST



(c) NECK ORIENTATIONS OF INTERNAL BOUDINAGE
(28 READINGS)

25^{o} to 35^{o} to the layering in the pinched areas (figs. 27a, 28). The most highly developed examples of the structure, found in hornblende schist, are seen to consist of very flat, elliptical bands parallel to the layering, and often separated from similar forms in the same layer by narrow shear zones making low angles to the layering (fig.27b). The neck orientations of the structures show a main NNE trend and a secondary NNW trend (fig. 27c). These trends are at a high angle to the hinge lines of the F3 minor folds, and suggest that stretching occurred in the axial directions of the folds.

The F2 lineation, lying on the F2 schistosity surface, is deformed in the neck regions of the internal boudinage structures. An example of this, taken from a garnet schist at Lago Superiore (67831317), is illustrated in fig. 29a. The orientations of the boudinage neck and the schistostiy plane have been plotted as if they were horizontal. There is an increase in the angle of plunge of the lineation as the neck region is approached, and a reduction in angle between the neck axis and lineation trace. In the neck region the layers are slightly thinned to compensate their increase in length (fig. 29b(i)). If the maximum shortening had been perpendicular to the layers, stretching in the neck region would increase the angle between the lineation trace and the neck axis (fig.29b(ii)). However, if this shortening was not completely perpendicular to the layers a slight component of displacement would take place parallel to them (fig. 29b(iii)). The resulting lineation trace would resemble that described from the Lago Superiore example.

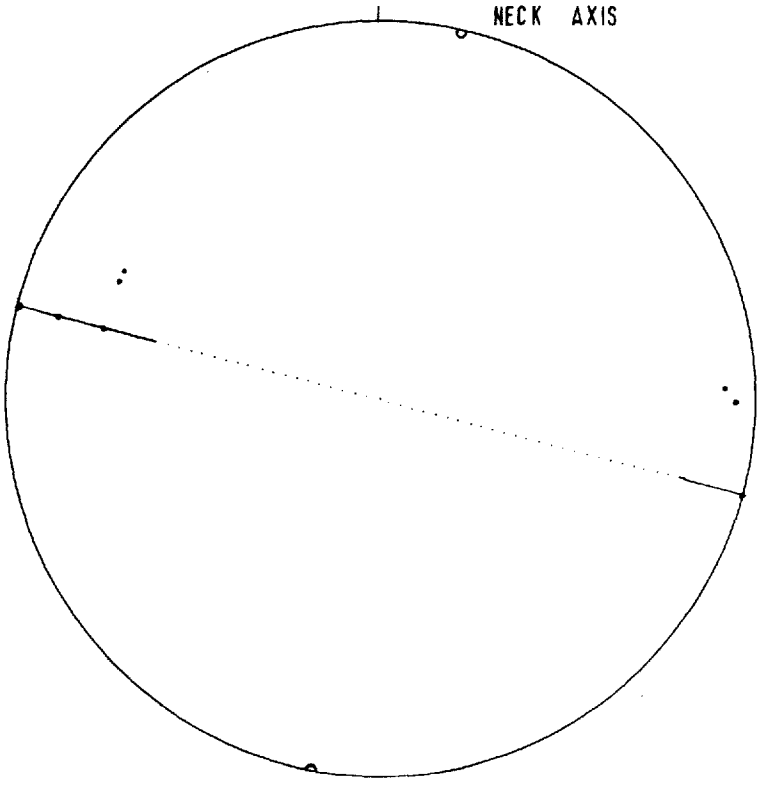
7:5 Crenulation Cleavage.

F3 axial plane crenulation cleavage is largely confined to the most strongly folded rocks in the hinge zone of the Wandfluhhorn Anti-form. The best development is in the semi-pelitic garnet schist exposed immediately south of Lago Superiore. Macroscopically the cleavage appears as thin lines joining the limbs of successive layers in the same minor fold, but there does not appear to be any new mineral growth, and the cleavage has not developed to the extent of forming microlithons

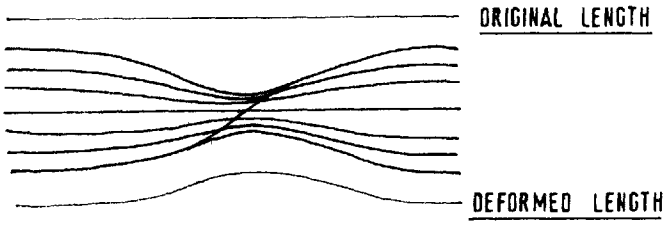


Fig. 28 Internal boudinage of schistosity planes in garnet schist. Lago Superiore (67831317).

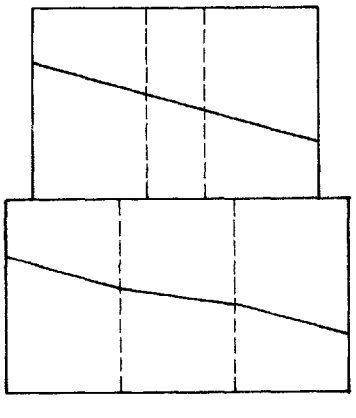
FIGURE 29
INTERNAL BOUDINAGE



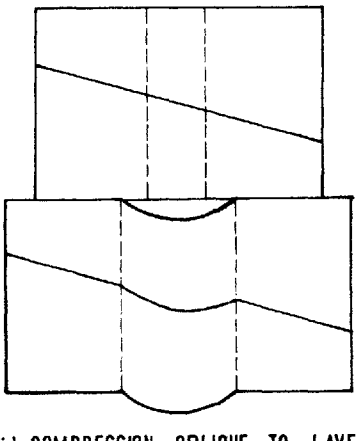
(a) PLOTS OF F_2 LINEATION DEFORMED IN NECK REGION OF INTERNAL BOUDINAGE. LAGO SUPERIORE (6783 1317)



(i) SECTION VIEW



(ii) COMPRESSION NORMAL TO LAYERING
PLAN VIEW



(iii) COMPRESSION OBLIQUE TO LAYERING
PLAN VIEW

(b) DEFORMATION OF LINEATION TRACE

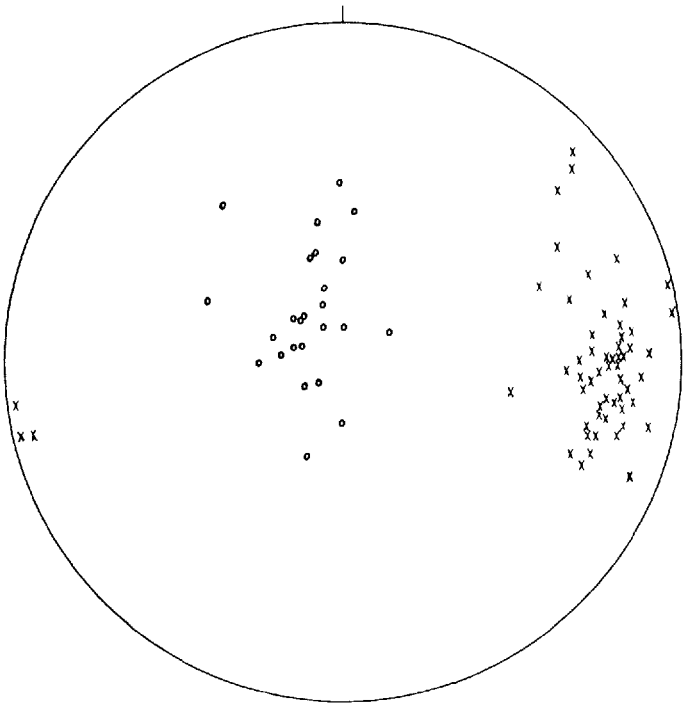
(De Sitter, 1954) (e.g. fig.37). In thin section the mica layers of the schist are seen to be strongly folded, and the quartz fabric in the hinge regions has been strongly reoriented. Individual grains have their long axes parallel to the axial surfaces of the F3 folds, and their boundaries are strongly sutured (e.g. fig. 72b, Chapter 10). On a regional scale the orientation of the cleavage shows a fan shaped pattern across the garnet schist, dipping gently south on the upper limb of the Wandfluhhorn Antiform and north on the lower limb.

In the strongly folded gneiss just below Passo Quadrella the F2 schistosity is very finely crenulated, and a new, evenly-spaced axial plane cleavage has developed. This occurs as thin, dark stripes resulting from both pressure solution and the growth of new, aligned biotite flakes. These lines break the rocks up into small rhomboid shaped blocks bounded by slightly curved F2 schistosity and the planar, semi-continuous F3 fabric.

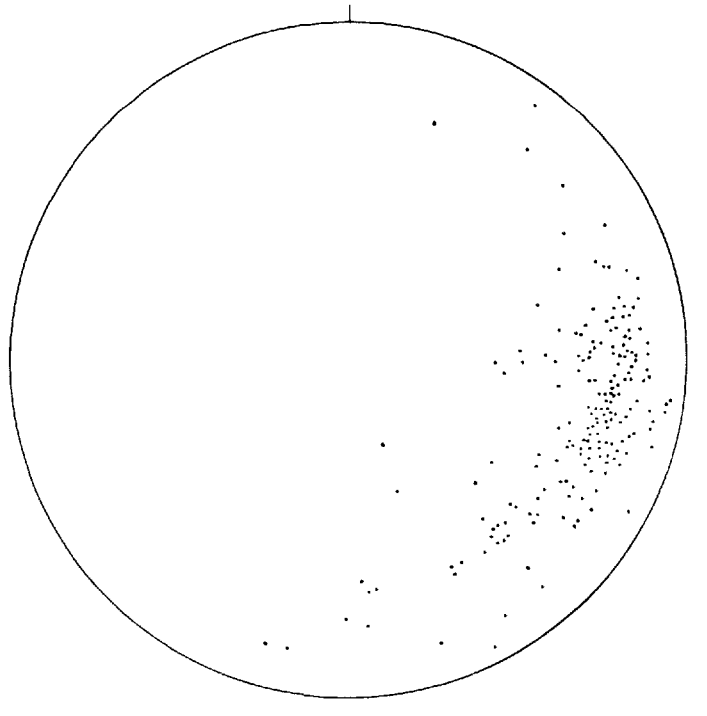
Biotite flakes aligned parallel to the axial surfaces of the F3 minor folds often occur in the most strongly folded gneiss, even where no crenulation cleavage has developed. In outcrops just below Lago Superiore (67841321) small biotite clusters grow along the limbs of F3 folds deforming quartz-rich bands lying parallel to the F2 schistosity. On the eastern side of the Rota Balmu ridge (68111314) the F2 fabric containing deformed xenoliths has been folded, and isolated biotite flakes have grown across the schistosity parallel to the axial surfaces of the F3 folds. A similar feature in muscovite flakes occurs in folded gneiss on the northeast slopes of the Batnall (67751286). At this locality crenulation cleavage has developed in semi-pelitic schist in the hinge zones of cuspate folds.

Crenulation cleavage also occurs in the strongly folded, schistose gneiss on the ridge east of P. Bombogna, but is not accompanied by any mineral growth. Throughout the remainder of the area crenulation cleavage is developed erratically. Near Bann, for example, it appears to have been accompanied by the removal of material by pressure solution from the limbs of asymmetric minor folds in the schistose gneiss, calcareous schist and talc schist.

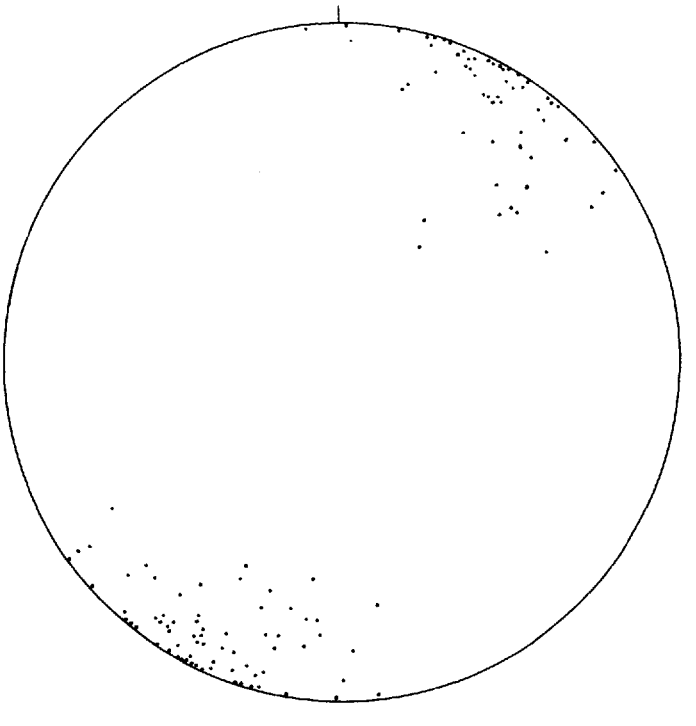
FIGURE 30
F3 LINEATIONS



(a) F3 axial plane cleavage ∘
and intersection lineation x



(b) F3 lineations parallel to fold axes



(c) F3 lineations oblique to fold axes

The poles to the F3 axial plane fabrics, plotted stereographically in fig.30a, show a dominantly gentle southeast dip.

7:6 F3 Lineations

Two distinct types of F3 linear structures were recognised; lineations parallel to the fold hinges of the F3 minor folds, and lineations oblique to the fold hinges.

(a) Lineations Parallel to Fold Hinges

Lineations parallel to F3 fold hinges have been recognised in all rock types. The most common are formed by the alignment of minute crenulations of thin mica layers (fig.31a). These are really small F3 fold hinges which vary in wavelength from 1 - 2 mm to approximately 3 cms, depending on the rock type and the thickness of the micaceous layers. They have the smallest wavelength in the thin pelitic partings in the gneiss and marble, and the largest wavelength on the hinges of isolated F3 folds in the semi-pelitic garnet and staurolite schist.

Mullion Structure (fig.31b) are also parallel to the hinges of F3 minor folds. They occur where the interface between bands of Bosco Group gneiss and semi-pelitic schist has been deformed into small lobe and cusp structures. The lobes stand out as parallel rod-like features on exposed faces of gneiss. They are uncommon features, occurring only in the hinge zone of the Wandfluhhorn Antiform on the northeast slopes of the Batnall and in the forested area 300 - 400 m. north of Alp Andatschei.

Another form of rodding, best named intersection lineation, occurs in the Antigorio Gneiss and Bosco Group gneiss in the hinge zone of the Wandfluhhorn Antiform, and in the strongly folded section between P. Bombogn and Collinasca. It forms where the F3 crenulation cleavage cuts the F2 schistosity and divides the rocks into a mosaic of small rods with rhomboid shaped cross sections. These rods lie parallel to the axial directions of the F3 minor folds. Rectangular biotite flakes on the surfaces of the rods also lie parallel to the F3 fold hinges, and appear to have been "smeared out" in that direction.

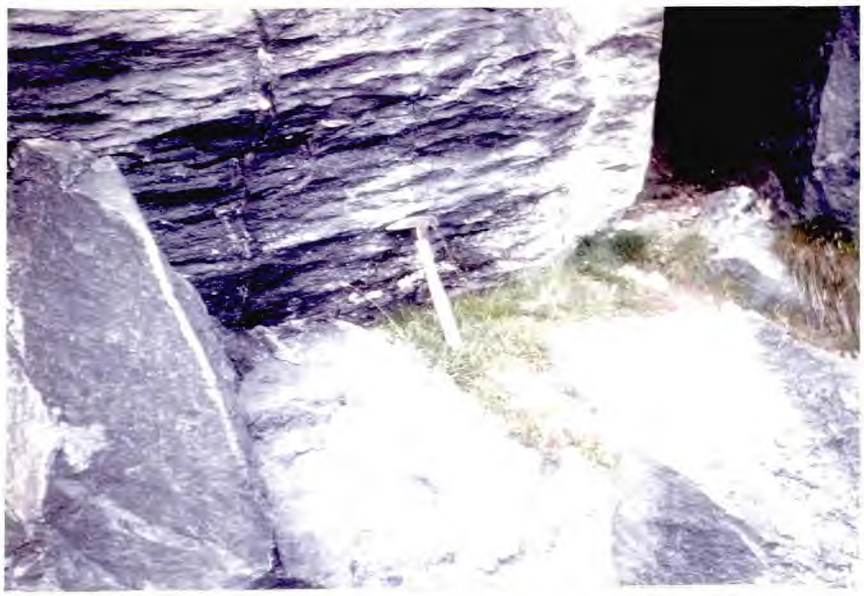


Fig.31(a) F3 crenulation lineation in schistose Antigorio Gneiss. Pizzo Bombogn (68181287).



Fig.31(b) F3 mullion structures in Bosco Group Gneiss. South side Valle di Bosco. (68241296).

Lineations parallel to fold axes

Lineations oblique to fold axes

Wandfluhhorn

P. d'Orsalia

Martschenspitz

Ritzberg

BOSCO-GURIN

Batnall

Kleinhorn

P. Bombogn

P. Pian Crosc

CERENTINO

1:25.000

An intersection lineation also occurs in the marble where crenulation cleavage is developed. It appears as a thin, dark and slightly irregular trace across the schistosity, and is parallel to the F3 fold hinges.

The trend of the F3 lineations parallel to the minor fold hinge lines has been plotted on a 1:25,000 base map of the Valle di Bosco (fig. 32) and is also shown stereographically on fig. 30b. There is a spread in the direction of plunge from NNE to SSW, with a concentration between ENE and SE. The angles of plunge are commonly between 15° and 30°. A few intersection lineations also plunge sub-horizontally WSW, where the schistosity has been bent by movement along small faults.

West of a line drawn northeast from P. Bombogn to midway between Cios and Corino the lineations have a fairly uniform E-W trend, and the plunge rarely exceeds 30°. To the east, however, the trend swings towards the southeast and plunges of up to 40° are common. This variation in the regional pattern may have been caused by either a gentle undulation in the F2 schistosity prior to the F3 deformation, or by straining after the F3 deformation. The F2 lineations does not show this change in direction.

(b) Lineations Oblique To Fold Hinges

F3 lineations lying oblique to the hinge lines of F3 minor folds appear as thin, scratch-like marks or very small slickensides 1 - 2 cms long on the schistosity planes, and are best named slickenside lineations (fig. 33). They are most common in the Antigorio Gneiss and gneiss of the Bosco Group, but are less obvious in the semi-pelitic schists and are never observed in the hornblende schist and calcareous Mesozoic rocks. They clearly post-date the F2 lineation, as they cut across it at a high angle, slightly indenting the surfaces of the micas defining the F2 lineation. No mineral growth is associated with the slickenside lineations.

The trend of the slickenside lineations is shown in figs. 30c and 32. It lies between north to northeast and south to southwest, and is almost perpendicular to the trend of the F3 lineations parallel



Fig.33 Slickenside lineations on limb of F3 minor fold. Hammer handle rests on fold hinge and points in axial direction of fold. Note angle between axial direction and slickenside lineations. Pizzo Bombogn (6818.51288).

to the F3 minor fold hinge lines. In the western portion of the area the average trend is about 020° - 200°, while in the eastern portion it is 030°/035° - 210°/215°. The accute angle between the trends of the slickenside lineations and lineations parallel to the fold hinges remains between 65° and 80° throughout the area. The majority of the slickenside lineations are subhorizontal.

The slickenside lineations are considered to have formed as the layers of schistosity slipped over each other during the F3 folding. They suggest that the folds formed by a flexural slip mechanism, but that the direction of slip was not always perpendicular to the axial directions of the folds. This oblique-slip is considered by Ramsay (1967; 396) to occur when the layers being folded are obliquely inclined to the principal axes of the bulk strain (fig. 34).

The relationship between the two F3 lineations can be seen in the small scale structures. In a typical example (fig. 35a), observed in schistose gneiss 200 - 300 m. east of P. Bombogn (68191288), a recumbent F3 minor fold plunges gently southeast, while the slickenside lineation locus lies on a plane striking northeast and dipping moderately steeply southeast. The X direction of the bulk strain, determined from the intersection of the lineation locus and the axial surface, plunges gently northeast, and lies at an angle of 82° to the axial direction of the fold.

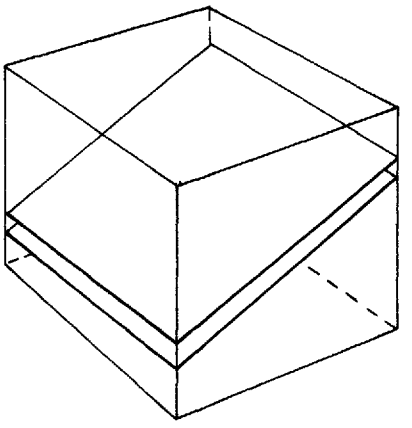
In another example (fig. 35b), taken from a recumbent fold plunging gently eastwards in a stream section 300 m. west of Chumma (67861289), the plane containing the slickenside lineations is vertical and cuts the axial plane of the fold at a very high angle. The X direction of the bulk strain plunges subhorizontally NNE, and lies at an angle of 88° from the axial direction of the fold.

7:7 Deformation of Earlier Structures

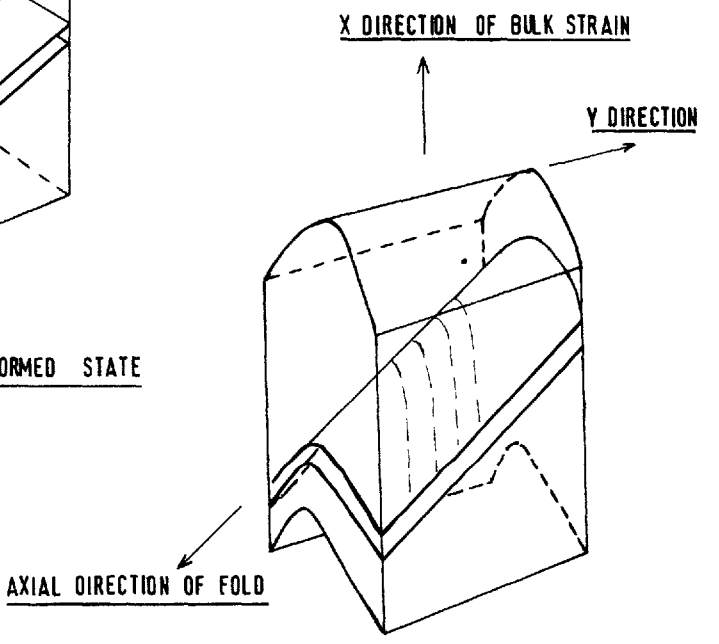
(a) Refolded Folds

The profile sections (figs 6, 9, 23 and 1:10,000 profile) show that on a regional scale the Wandfluhhorn Antiform refolds large structures of two earlier generations. In individual exposures, however, examples of F3 minor folds refolding earlier structures are uncommon, largely because of the relative scarcity of F2, and

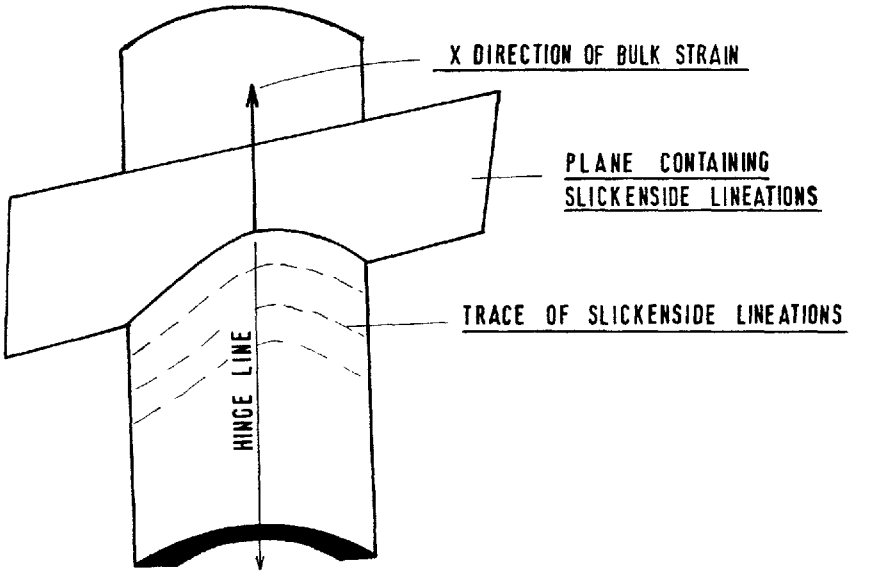
FIGURE 34



(a) INCLINED LAYERING IN UNDEFORMED STATE



(b) DEFORMED STATE SHOWING TRACE OF LINEATIONS LYING OBLIQUE TO AXIAL DIRECTION OF FOLD

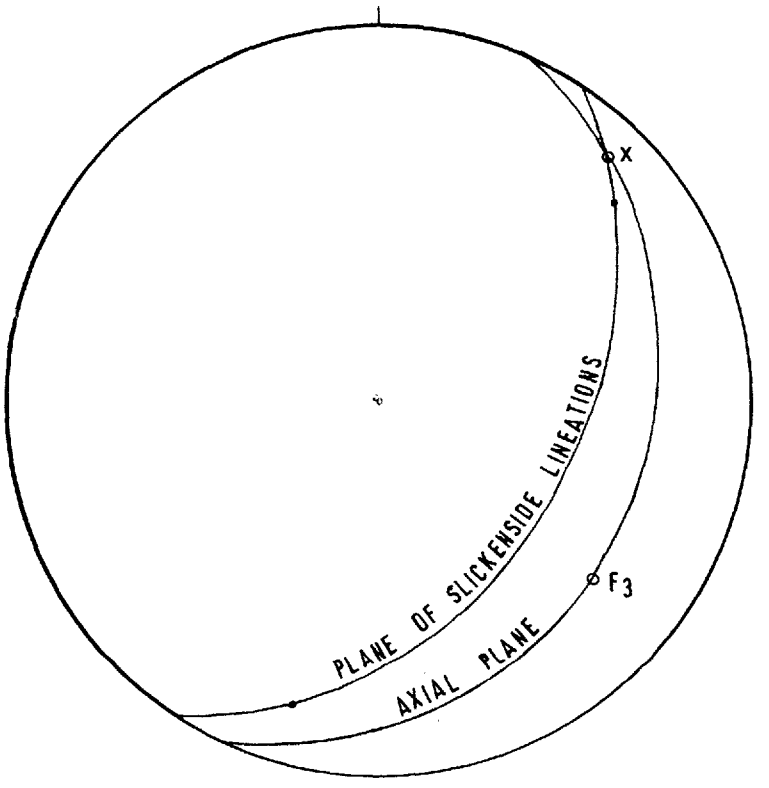


(c) VIEW DOWN ONTO FOLD HINGE

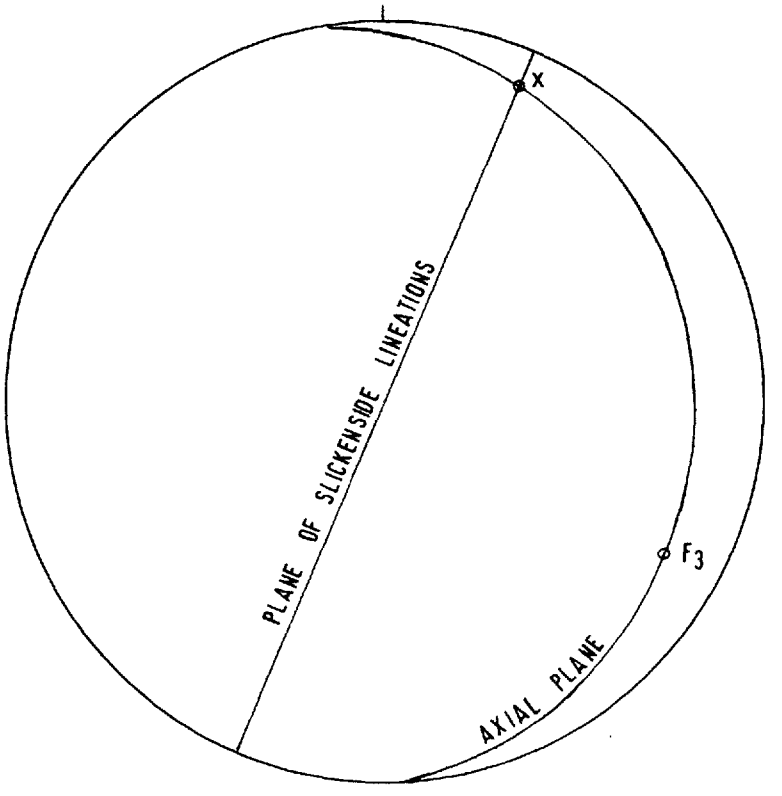
F3 SLICKENSIDE LINEATIONS

FIGURE 35

F_3 SLICKENSIDE LINEATIONS



(a) RELATIONSHIP BETWEEN SLICKENSIDE LINEATIONS AND F_3 MINOR FOLD. PIZZO BOMBOGN (6819 1288)



(b) RELATIONSHIP BETWEEN SLICKENSIDE LINEATIONS AND F_3 MINOR FOLD. CHUMMA (6786 1289)

particularly F1 minor folds. The few interference patterns caused by the superimposed folding are classified as type 3 after Ramsay (1967: 531) (figs. 36, 37). They result from the refolding of recumbent folds by later structures with axial surfaces at a high angle to those already existing. The axial directions of both sets of folds, illustrated by the lineation trends (compare figs. 15 and 30b), are largely coincident.

The interference patterns observed in the field usually consist of a single refolded layer, and in only a few examples could the variation in dihedral angle of the F2 fold be examined as described by Ramsay (1967: 511-2). The changes in dihedral angle of a refolded quartz layer in schistose gneiss from southwest of the Wandfluhhorn (67821321) were determined from the hinge to one limb of a small F3 fold. The plot of the dihedral angle of the F2 fold against the angle of dip of its axial plane (fig. 38a) is very similar to the example described by Ramsay (1967: fig. 9 - 36). The largest dihedral angle occurs where the axial plane of the F2 fold dips at almost 40°.

The plots for two further examples (fig. 38b and c) show only that the largest dihedral angles of the F2 folds occur on the limbs of the F3 folds slightly to one side of the hinge zones.

(b) Deformed Lineation

The F2 and F3 minor folds have already been shown to be largely coaxial, and examples of deformed lineations are consequently uncommon. Schistose gneiss just east of Rota Balmu (68131311) has a strong mica lineation which is folded around the hinge of a small F3 structure. On the fold limbs the angle between the lineation trend and the fold hinge is 21°, but as the lineation approaches the fold hinge the angle decreases, reaching a minimum of about 10° on the fold hinge itself. F3 slickenside lineations on one limb of the fold lie at an angle of 13° to a line drawn normal to the fold hinge in the plane of the axial surface (fig. 39a). The X direction of the bulk strain, calculated stereographically from the intersection of the axial surface and plane containing the slickenside lineations, plunges at 27° towards 014°.

A similar relationship of F2 lineations to F3 folds is seen on outcrop of schistose gneiss in a gully 400 m. west of Pogga (68251306). The F2 mineral lineation on the F3 fold limb lies at an angle of 14°

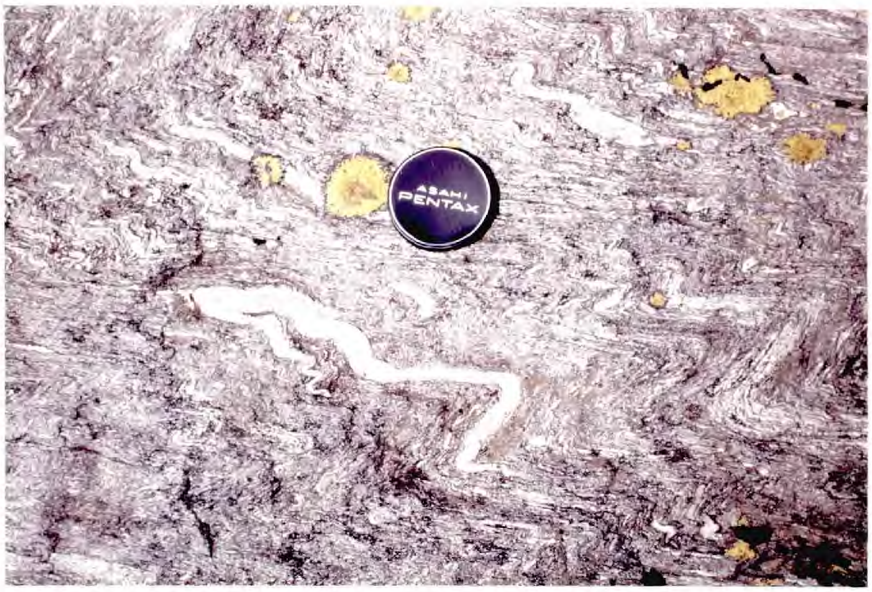


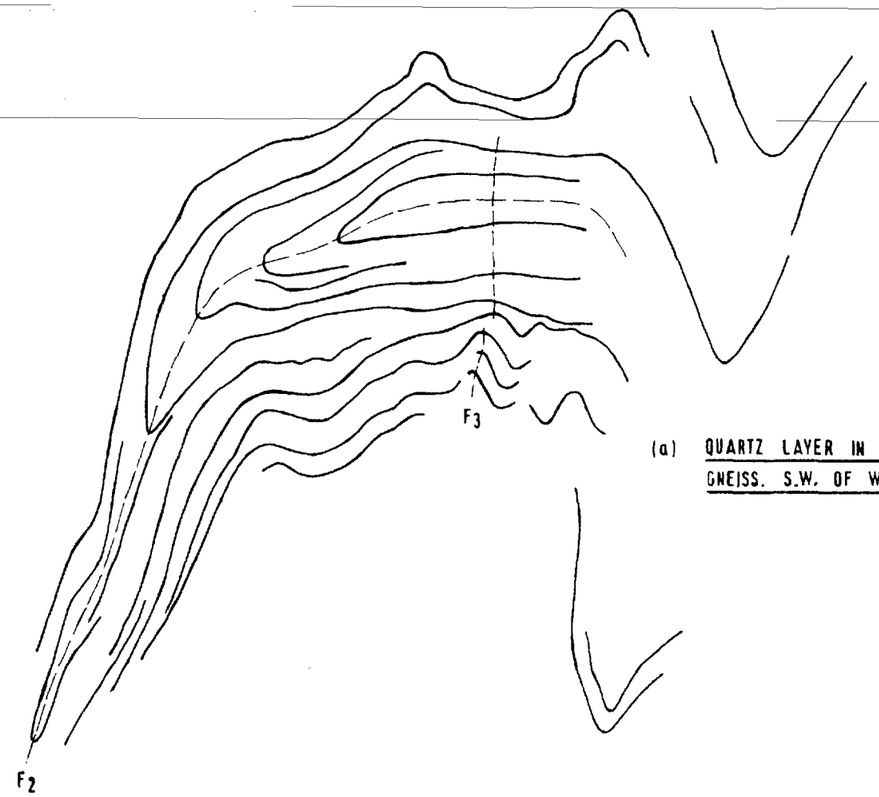
Fig.36(a) Chevron-like F3 folds refolding isoclinal F2 fold in Antigorio Gneiss. Lago Superiore (67841321).



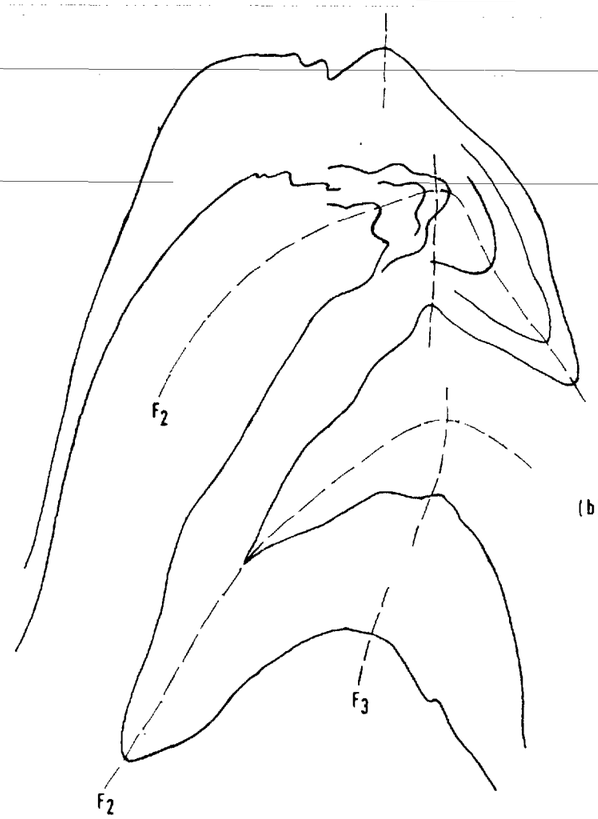
Fig.36(b) Isoclinal F2 folds in Mesozoic marble refolded by open F3 folds. South of Wandfluhhorn (67881325).



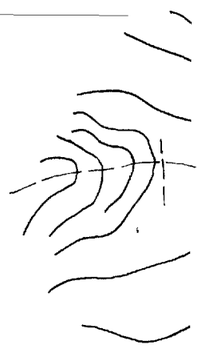
Fig. 37 F2 folds in schistose Antigorio Gneiss re-folded by F3 folds. Note sub-horizontal crenulation cleavage associated with F3 folds. Lago Superiore (67841320).

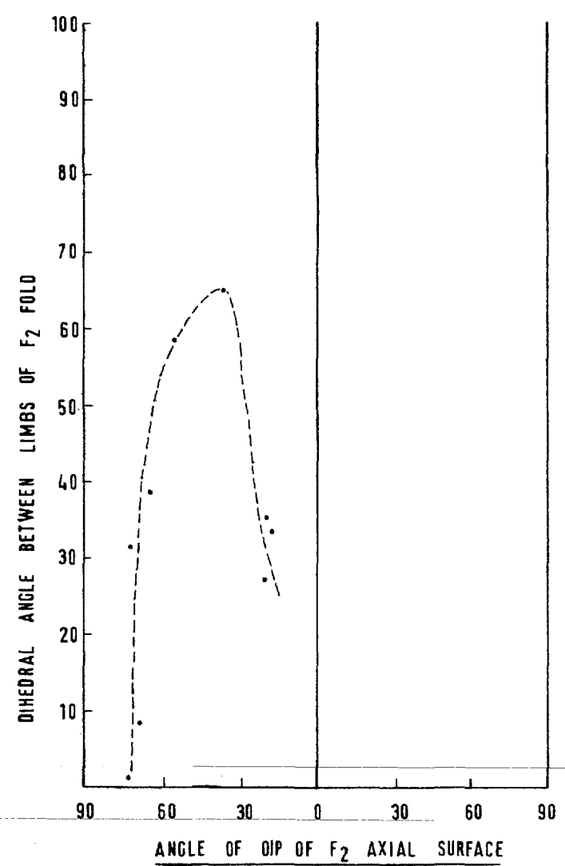


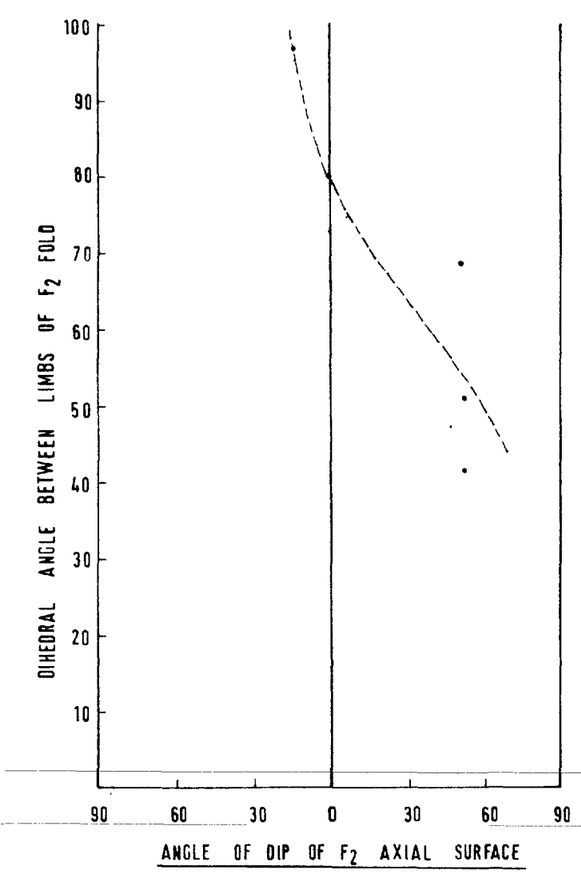
(a) QUARTZ LAYER IN SCHISTOSE GNEISS. S.W. OF WANOFLUHHORN (6782 1321)

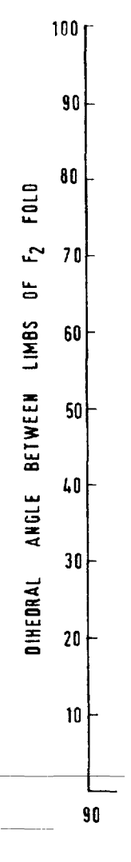


(b) QUARTZ LAYER IN SCHISTOSE GNEISS. LAGO SUPERIORE (6785 1320)









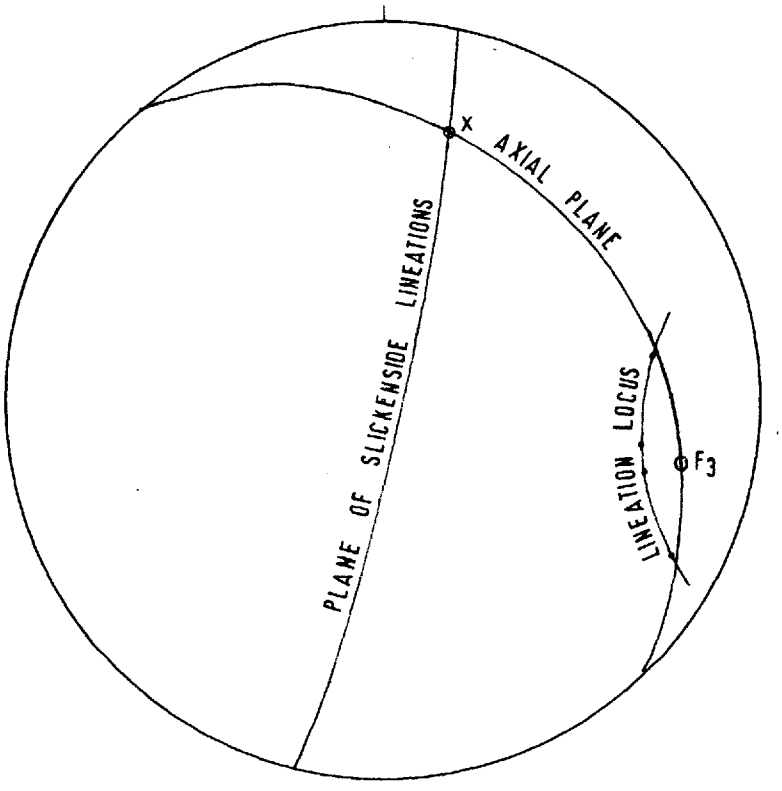
to the fold axis, but decreases to 5° as the lineation is traced around the fold hinge. In a folded gneiss band in garnet schist approximately 800 m. southwest of Grossalp village the angular difference between the F2 lineation and the F3 fold trend changes from 13° on the fold limbs to 5° on the hinge line.

Two further examples were found in the boulder strewn area just east of Krameggpass. Both were in gneiss bands from garnet schist, and show the typical pattern of the F2 lineation lying closer to the axial directions of the folds on the hinges than on the limbs. One of the folds had slickenside lineations lying on a plane making an acute angle of 87° with the hinge line, and cutting the axial surface with a 61° acute angle, again illustrating that the X direction of bulk strain was not normal to the fold hinge line (fig. 39b).

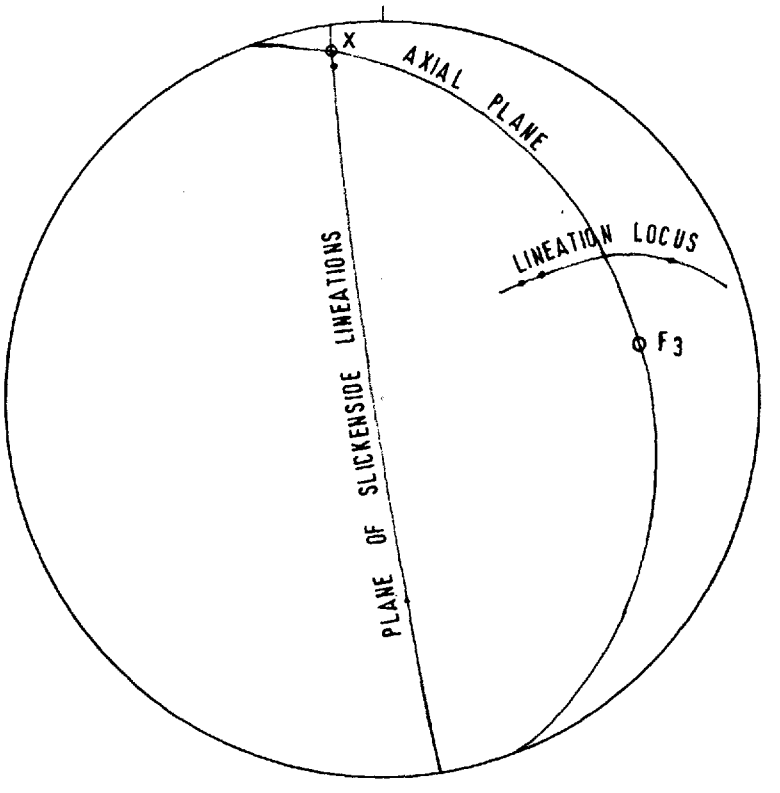
The pattern of the deformed lineations is typical of that described by Ramsay (1967:466) from flattened flexural folds. Where slickensides occur on the limbs of folds deforming the lineation they show that during the initial flexural slip stage of deformation the layers moved over each other in a direction at right angles to the fold hinge lines with a slight component parallel to the hinge lines. The resulting displacement vectors consequently vary from orientations normal to the fold hinges (i.e. 90°) to those at 60° from it. The flexural form of the folds was later modified by flattening normal to the axial planes, during which the angular relationship between the F2 lineations and the F3 fold hinge lines was changed.

Anomalous folded lineation patterns have been found at two localities. In a stream outcrop 800 m. southwest of Grossalp village (67891293) the F2 lineation on a gneiss band in staurolite schist is deformed by an F3 fold. The fold closes to the north and plunges gently southeast, and the locus of the deformed lineation lies on a plane dipping moderately steeply northeast (fig. 40a). As the lineation is traced around the fold hinge the angle between the fold axis and lineation trace increases to a maximum just above the hinge line, and decreases again as it crosses to the lower limb. The X direction of the bulk strain plunges at 24° towards 101°, and is perpendicular to the X direction calculated from the F3 slickenside lineations. This appears to be a very local feature, but there is no obvious explanation for its occurrence.

FIGURE 39
DEFORMED LINEATIONS



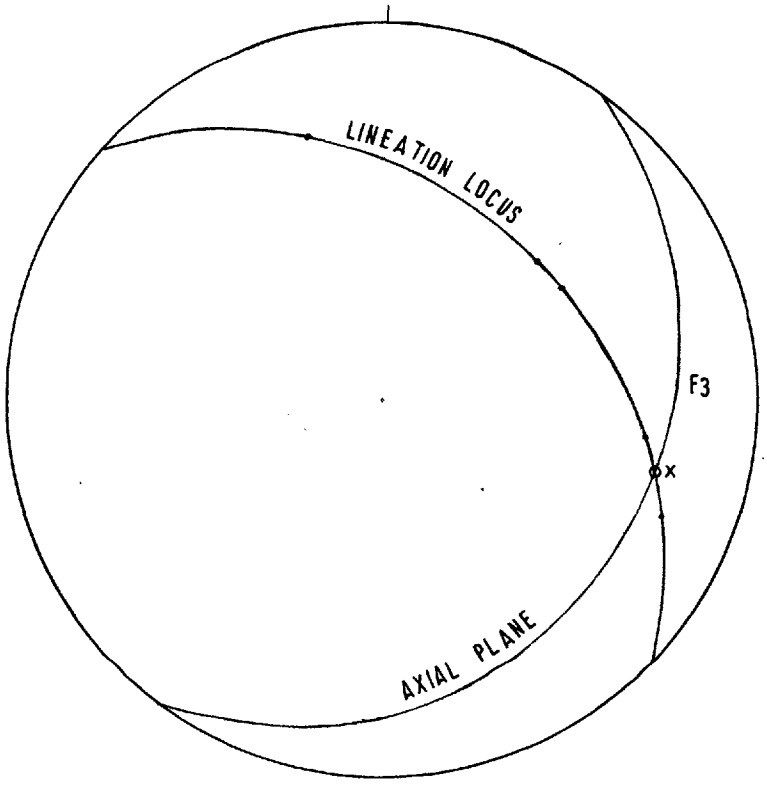
(a) F_2 LINEATION DEFORMED BY F_3 FOLD WITH SLICKENSIDE LINEATIONS ON LIMBS. ROTA BALMU (6813 1311)



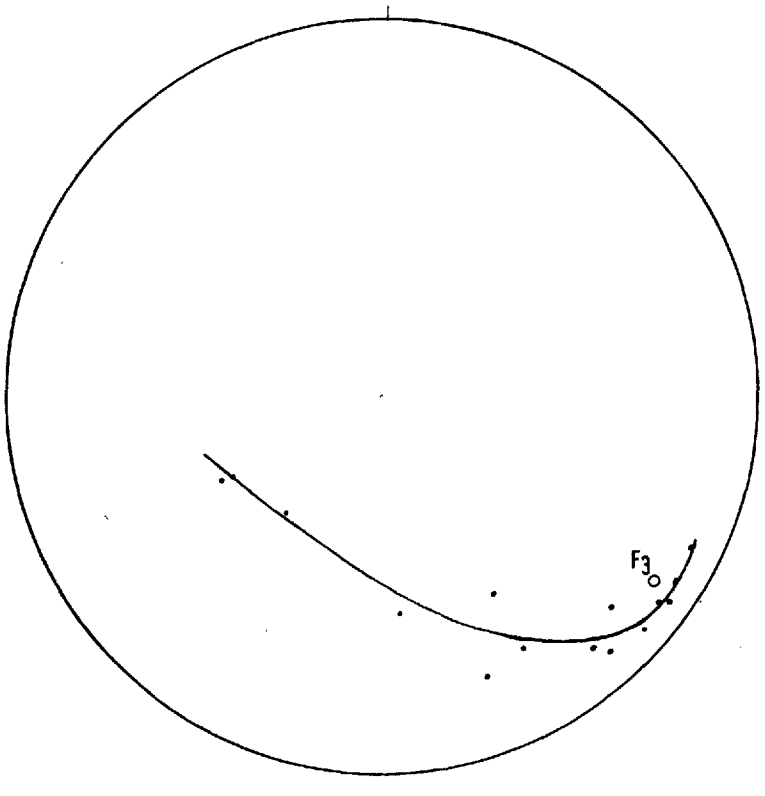
(b) F_2 LINEATION DEFORMED BY F_3 FOLD WITH SLICKENSIDE LINEATION ON LIMBS. DATA MEASURED FROM BOULDER EAST OF KRAMEGG PASS (67751299)

FIGURE 40

DEFORMED LINEATIONS



(a) F_2 LINEATION DEFORMED BY F_3 FOLD GROSSALP (6789 1293)



(b) F_2 LINEATION DEFORMED BY F_3 FOLD. MEASUREMENTS FROM BOULDER NEAR PASSO DELLA STELLA (6775 1292)

A similar example of this type of deformation pattern was found in a boulder of knotted garnet schist just below Passo della Stella (67751292) (fig. 41). The angle between the lineation trace and the fold axis again increases in the hinge region, but the lineation formed a locus partly resembling that of a cone with an elliptical base (fig. 40b). J. Watkinson, Imperial College (pers. comm., 1972) is at present studying deformed lineations and considers that this pattern could result from either folding an originally non-linear trace, or by oblique flexural-slip folding of a layer asymmetrically oriented with respect to the bulk strain.

(c) Deformed Boudinage

Boudinage is a common feature of the F2 deformation, but only one example was observed of boudins being deformed by F3 minor folds. This example, on the western ridge of P. Bombogn (68121288), is critical in illustrating the time relations of the structures, and shows that the "block" boudinage is an F2 feature. At this locality a marble band 2 m. thick contains two isolated hornblende schist boudins. These now occupy the hinge zones of F3 minor folds, and have been deformed into forms with arrow-head shaped cross sections (fig.42).

7:8 Ductility Contrasts During the F3 Deformation

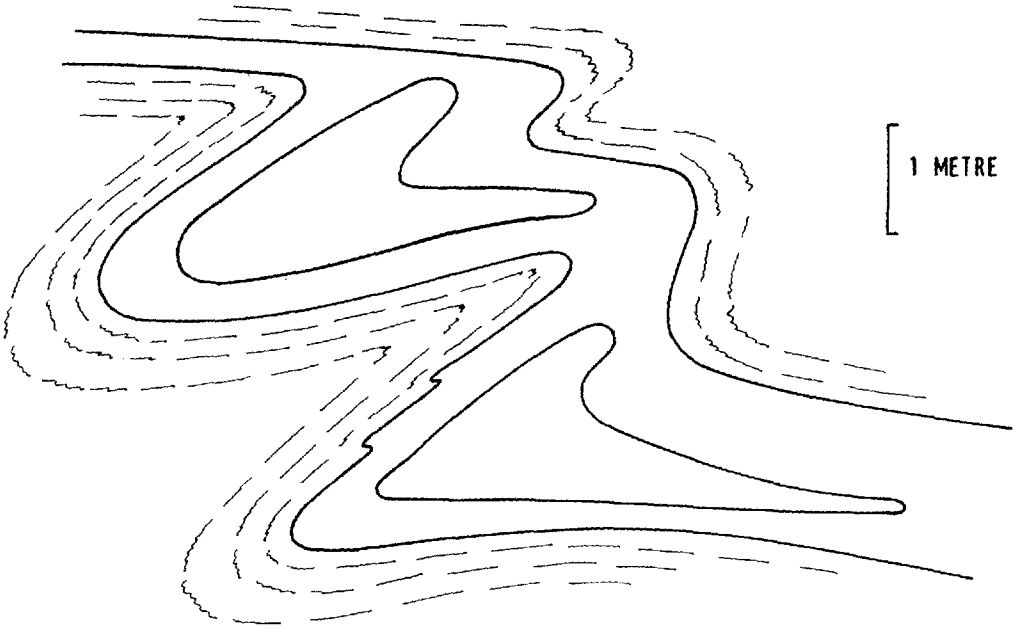
The ductility contrasts between the different rock types during the F3 deformation can be evaluated from the geometric forms of the F3 structures. The most obvious F3 ductility contrasts occur where the interface between two rock types was folded into lobe and cusp forms, and where lithological bands are slightly deformed by pinch and swell structures.

Quartz again appears to have been the most competent rock type, and folded layers exhibit slightly lobate forms in all lithologies with which they were folded during the F3 deformation. This is a similar relationship to that deduced from a study of the F2 structures. Pinch and swell structures show that horneblende schist behaved more competently than semi-pelitic schist, and that semi-pelitic schist was slightly more competent than marble. Where F3 folds deform the interface between schistose gneiss and marble, the marble is pinched into the tight hinges between lobate folded forms of schistose gneiss



Fig.41 F2 lineation deformed around hinge of F3 minor fold. Note that angle between lineation and axial direction of fold, shown by pencil, increases as lineation approaches fold hinge. Passo della Stella (67751292).

FIGURE 42



SKETCH OF HORNBLENDE SCHIST BOUDINS IN MARBLE, DEFORMED BY F_3 FOLDS WEST RIDGE OF P. BOMBOGN (68121288). THE MARBLE BAND IS ENCLOSED IN SCHISTOSE GNEISS

(e.g. fig. 7). Marble protrudes as lobate fold hinges into calcareous schist which is pinched into the intervening tight hinges.

The most probable order of relative ductilities during the F3 deformation, beginning with the most competent, appears to have been quartz, massive gneiss, hornblende schist, schistose gneiss, semi-pelitic schist, marble and calcareous schist. Evidence for the ductility contrasts during the F3 deformation is not as pronounced as that for ductility contrasts during the F2 deformation. While this may indicate an overall reduction in the relative ductilities during the F3 deformation it is probably also a reflection of the deformation of rocks penetrated by a strong planar fabric.

CHAPTER 8

CORRELATION OF DEFORMATION HISTORY

It is now almost a decade since the first modern, detailed account of the structural geology of the Lower Pennine region was presented. Previously there had been no description attempting to relate the numerous structural features to the regional geology, although Chatterjee (1961) had recognised minor folds of two generations.

Higgins (1964b), working in the Basodino - Nufenenpass area between 10 and 18 kms north of the Valle di Bosco, recognised four phases of Alpine folding which he named phases 1 to 4 in order of decreasing age. Phase 1 folds were recognised only in the Basodino area, and like the F1 structures of the Valle di Bosco were necessary to explain the apparently synclinal strips of Mesozoic rocks enclosed in basement. Phase 2 folds deform these Mesozoic bands and the basement lithological units. They are recumbent isoclinal folds plunging gently eastwards, and have a strong axial plane schistosity. Lobe and cusp structures are commonly associated with them. Higgins considered that the phase 3 folds were more open than those of the earlier phases, and had steep or vertical axial planes. They, like the phase 2 folds, plunge gently eastwards and have a strong mineral lineation parallel to their hinge lines. Phase 4 folds are open, recumbent structures plunging gently northeastwards and deforming the mineral lineation.

The phase 1 and phase 2 folds described by Higgins are equivalent to the F1 and F2 structures of the Valle di Bosco. The structures distinguished by Higgins as phase 3 have no equivalent in the Valle di Bosco, and appear to be F2 folds deformed into a vertical attitude by a later movement. Higgins' major phase 3 axial traces are parallel to isogons dividing the area into zones of subhorizontal and vertically dipping schistosity (fig. 43). The axial planes are implied to dip moderately steeply northwards, but are not accompanied by any planar or linear fabric development. Higgins' phase 4 folds, the most

abundant in the area, have the same structural and associated metamorphic features as the F3 folds of the Valle di Bosco.

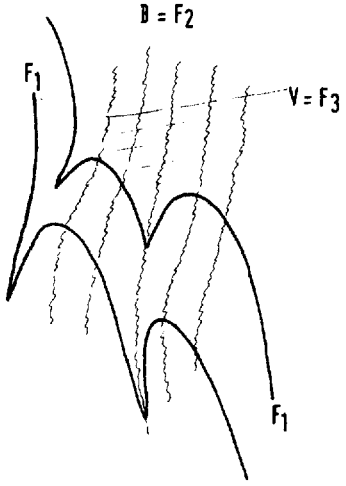
I interpret the rocks of the Basodino-Nufenenpass area as lying on the lower limb and part of the hinge zone of the Wandfluhhorn Antiform, and as a result of reconnaissance work in the area feel confident that it has undergone the same deformation history as the rocks of the Valle di Bosco.

Milnes (1965) recognised two Alpine deformations in the Monte Cistella area 20 kms WSW of the Valle di Bosco. The "main" Alpine movement gave rise to a strong axial plane schistosity and a lineation parallel to the minor fold hinges. These features were deformed during the "late" Alpine movement when distinct crenulation folds developed. These ideas were later developed when Milnes (1968) was able to work out a sequence of three movements in the Simplon region. The first involved the emplacement of basement thrust sheets which were later intensely folded and penetrated by a strong axial plane schistosity, formed by flattening during the "main" Alpine movement. The "later" movement folded the schistosity into generally upright structures with a locally developed crenulation cleavage.

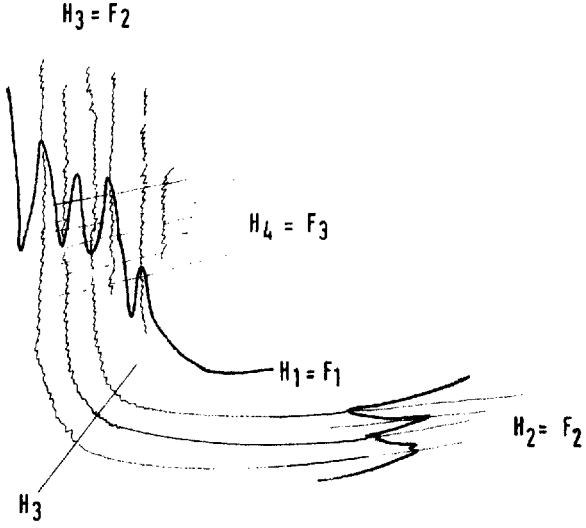
The deformation phases recognised by Milnes, and the minor structures associated with them, are very similar to those recognised by myself. Milnes' early nappe emplacement seems best correlated with the F1 deformation in the Valle di Bosco, while the "main" movement correlates with the F2 deformation and the "later" movement with the F3 deformation.

Chadwick (1968), working in the Lukmanier region 40 kms northeast of the Valle di Bosco, recognised that two successive phases of Alpine folding had deformed the Mesozoic rocks after the earliest northwards movement of the Lower Pennine Nappes. Phase B folds are accompanied by a powerful penetrative schistosity, and were formed during a 50% - 70% north-south shortening. They are probably equivalent to the F2 structures of the Valle di Bosco. The subsequent phase V structures deform the schistosity and lineation, and are very similar to the F3 structures of the Valle di Bosco. The earliest movement of the nappes can be correlated with the development of F1

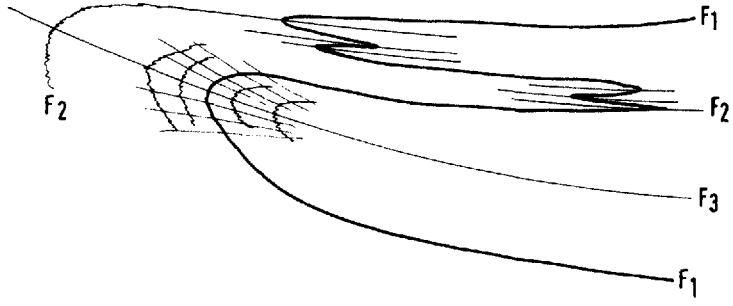
LUKMANIER
(CHADWICK 1968)



BASODINO
(HIGGINS 19646)



VALLE DI BOSCO



REGIONAL CORRELATION OF FOLD PHASES

F1 F2 ETC REFER TO AXIAL PLANES OF FOLDS

FIGURE 43

structures in the Valle di Bosco.

An identical Alpine deformation history was determined by Thakur (1971) who examined the area around Pizzo Molare, south of the Lukmanier region. F1 folds were recognised in interference patterns with F2 folds, while F2 folds were typically isoclinal and accompanied by a strong axial plane schistosity and mineral lineation. F3 minor folds were much more open, and typically chevron-like. They have an axial plane crenulation cleavage. Thakur also showed that coaxial interference patterns of type 3 (Ramsay, 1967) occurred where F2 structures were deformed during the F3 deformation.

Sibbald (1971) who examined the Val Piora, immediately west of and along strike from the ground covered by Chadwick, described four deformation phases, D1 to D4. His D1 and D2 phases correspond to the F1 and F2 movements of the Valle di Bosco, and his D4 structures include typical chevron folds, crenulation cleavage and internal boudinage now generally regarded as features of common age (F3) in the Lower Pennine region. D4 folds are common only where the sheet dip exceeds 50°, in the same way as equivalent F3 folds become very pronounced when the regional schistosity is folded around the hinge zone of the Wandfluhhorn Antiform.

Sibbald's conclusions differ from those of other workers in the region in one main aspect; his interpretation of the D3 deformation. The effects of this deformation are seen only in a strong lineation which is deformed by D4 (=F3) folds. This lineation represents an extension direction, and is oblique to linear fabrics Sibbald correlates with D1 and D2. The mechanism for the development of the lineation proposed by Sibbald is based on a theory of rotational deformation,but is inconsistent with regional evidence. It is more likely that the high angle between the "D3" lineation and the D2 fold hinges may be analagous to the relationship between the F3 minor fold hinges and the slickenside lineations in the Valle di Bosco. If this is correct, Sibbald's D3 lineation would simply be a stretching lineation on the limbs of the F2 folds,

normal to the axial direction of the folds. This explanation is that adopted by Chadwick and Thakur, and originally postulated by Higgins in the Nufenenpass area.

Summarising, it can now be stated with considerable confidence that three major phases of movement deformed the rocks of the lower Pennine region and the southern potion of the Gotthard Massif during the Alpine Orogeny. The first (F1) saw the formation and northwards displacement of sheet-like basement nappe structures. The second deformation (F2) resulted in a regional shortening of up to 77% (see chapter 9) with a consequent complete change in shape of the nappes, the development of very tight folds and a strong axial plane schistosity. During the F3 deformation further large structures, the so-called "back folds" (Argaud, 1916), were formed and the earlier formed schistosity was strongly crenulated. These latest folds lead to alternations of regions of flat-lying rocks (corresponding to the limbs of F3 structures), and regions of steeply dipping and generally much more strongly folded rocks (corresponding to the hinge zones of major F3 structures).

CHAPTER 9

DEFORMATION AND METAMORPHISM OF THE ANTIOGRIO GNEISS

9:1 Introduction

The Antigorio Gneiss is a relatively homogeneous, quartzo-feldspathic rock derived from a Hercynian granitic complex. It forms the basement of a large F1 Alpine nappe, and was strongly deformed under ductile conditions during the F2 deformation. This section of the thesis describes the deformation features of the Antigorio Gneiss and its transformation from an originally coarse grained igneous rock to an orthogneiss, and locally to a fine grained quartz-mica schist.

The least deformed Antigorio Gneiss in the Valle di Bosco has a granitic texture and mineralogy. A few of the cross cutting aplite and pegmatite dykes are folded, but most retain their tabular form and lie at high angles to the weak planar fabric in the surrounding rocks. Dioritic xenoliths in the gneiss occur as pancake-shaped ellipsoids lying subparallel to the planar fabric. They are slightly elongated subparallel to the weak mineral lineation.

The strain increases markedly towards the Mesozoic rocks separating the Antigorio gneiss from the Bosco Group. The granitic texture becomes strongly schistose as the average grain size decreases and individual grains develop distinct dimensional preferred orientation. A strong schistosity penetrated the rock, and a pronounced lineation appears on the schistosity planes. Aplite and pegmatite dykes are no longer visible, and xenoliths become extremely thin. The xenoliths lie in the plane of the schistosity, and are strongly elongated parallel to the lineation. No xenoliths were observed in the outer portion of the schistose gneiss.

As the average grain size decreases the mineralogy changes, and the quartz-orthoclase-microcline-oligoclase/andesine-biotite mineral assemblage of the gneiss changes to quartz-albite-biotite-muscovite-epidote (-ilmenite-chlorite-almandine-hornblende) in the schist. The change in mineralogy is due to the introduction of water into the metamorphic system.

9:2 Deformed Xenoliths

Deformed xenoliths in the Antigorio Gneiss have proved extremely useful for determining the strain. They occur throughout the gneiss, but are locally abundant and pass into thin bands of dioritic gneiss. They are commonly about 20 cms long and 2 cms thick, and their black colour is in sharp contrast to the light grey or pink of the granitic gneiss (fig. 44). Although the xenoliths differ mineralogically from the gneiss, they are thought to have deformed in a similar manner and by similar amounts.

Detailed measurements were made of the xenoliths over the western part of Wolfstaffel and on the east ridge of the Wandfluhhorn. At Wolfstaffel, where few xenoliths are found in individual outcrops, the readings from the entire area were grouped together. East of the Wandfluhhorn abundant xenoliths are packed into a band two metres thick. Both areas are on the upper limb of the Wandfluhhorn Antiform, about 300 m. to 400 m. structurally above the Mesozoic rocks of the Stella Syncline.

The measurements were made on good exposures displaying the principal planes of the strain. The principal strain axes (X and Y) of the xenoliths lay in the F2 schistosity plane, and the X axes, the directions of greatest extension, were parallel to the F2 lineation. The Z axes, the directions of greatest shortening, were normal to the schistosity. It was possible to examine only one principal plane of each xenolith (fig. 45a).

At each exposure the two principal axes of the xenoliths were measured, and the angles between the longer of these axes and the schistosity planes or lineation direction were recorded (fig. 45b). The data thus recorded from the xenoliths of the Wandfluhhorn and Wolfstaffel areas were plotted on Rf/ ϕ diagrams developed by Dunnet (1969), from curves calculated from Gay's (1968; 221) graph of the pure shear deformation paths of elliptical, randomly oriented particles with the same viscosity as their matrix. Evidence that the xenoliths and the enclosing matrix had similar viscosities was shown by the schistosity passing from the matrix through the xenoliths without being deflected.

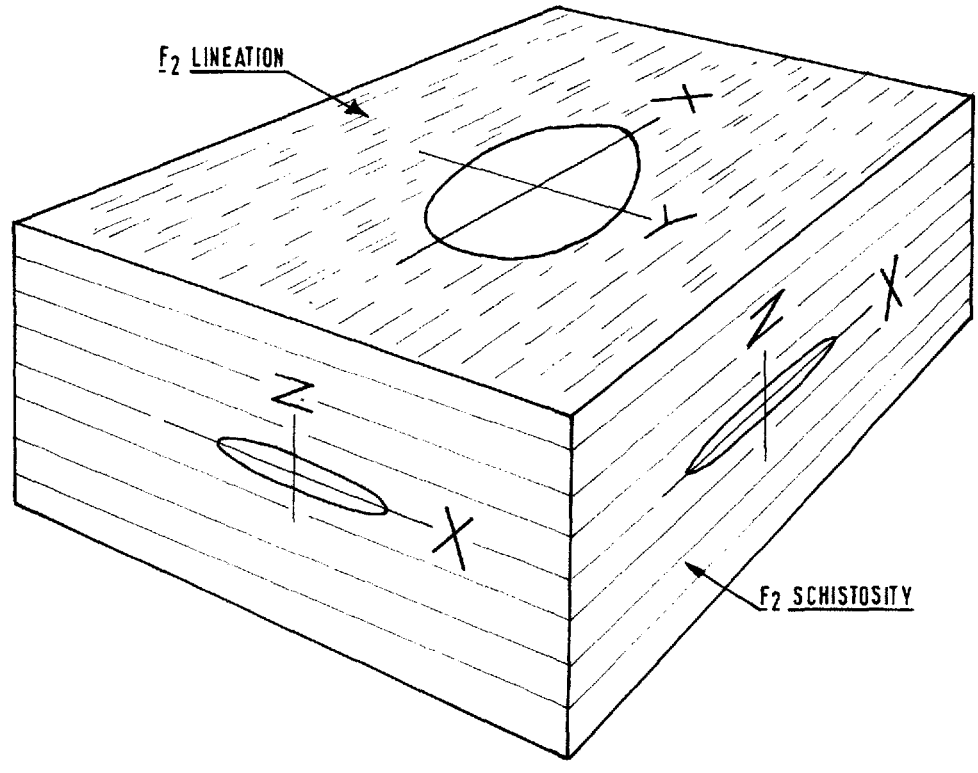


Fig.44(a) Flattened dioritic xenoliths lying parallel to planar fabric in Antigorio Gneiss. Wandfluhhorn (67941329).

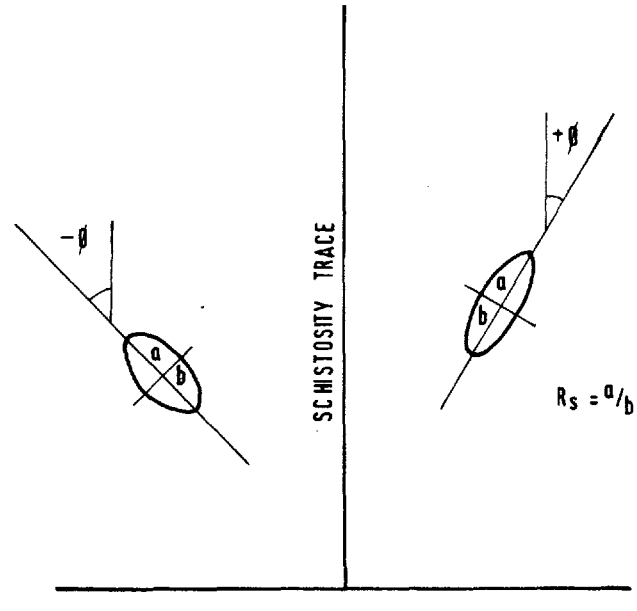


Fig.44(b) F2 folds with F2 schistosity containing flattened dioritic xenoliths. Rota Balmu (6810.51311).

FIGURE 45
DEFORMED XENOLITHS



(a) PRINCIPAL STRAIN AXES DETERMINED FROM DEFORMED XENOLITHS



(b) METHOD OF MEASURING DEFORMED XENOLITHS

A separate diagram was constructed for each principal plane. The ratios of the axial lengths of the xenoliths (Rs) were plotted on a logarithmic scale on the ordinate, while the corresponding angular fluctuations (ϕ) were plotted on a linear scale on the abscissa, east and west of a vertical line representing the schistosity or lineation trace. The points on each diagram were divided into numerically equal north-south and east-west sectors. The symmetric mid-point always lay on or within a degree or two of the schistosity trace, and was used as a guide in determining the finite strain ratio.

Siddans (1971) slightly modified Dunnett's method by introducing a precisely calculated 50% data line to replace the east-west dividing line. For low strain values the 50% data line is close to the east-west dividing line, but for higher strain values it becomes U-shaped and eventually V-shaped. Computer-printed curves (supplied by Dr. A. Siddans, Imperial College) for finite strain ratios close to those indicated by the symmetric mid-point were fitted over the diagrams until one was found which had a 50% data line equally dividing the points on the diagram. The value of the finite strain ratio occurs at the lowest point on the 50% data line, where it intersects the line representing the schistosity trace.

The statistical values obtained from the Rf/ ϕ diagrams are outlined below:

1. Wolfstaffel (fig.46)

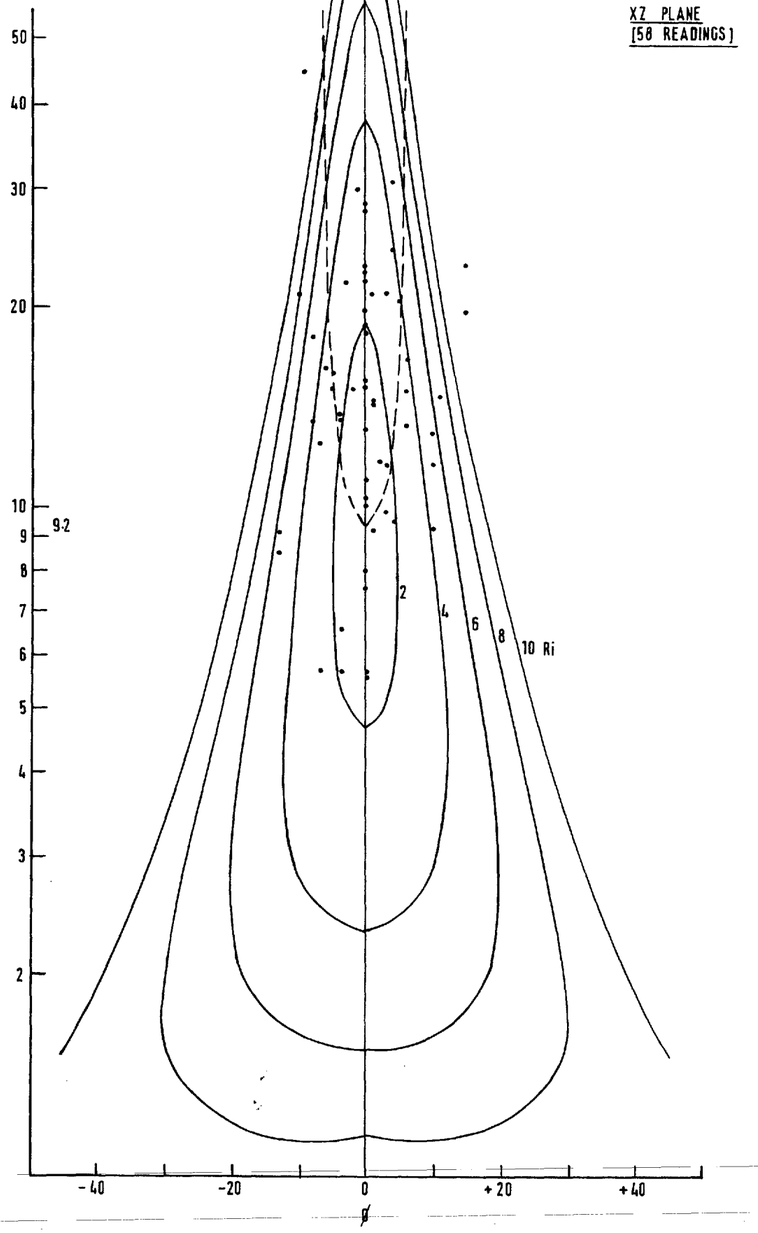
(a) XZ plane Rf = 9.2 from 58 readings, including a maximum fluctuation of 15° and Rs of 44.1. 40% of the xenoliths had initial axial ratios (Ri) between 1:1 and 2:1, and a further 38% had Ri's between 2:1 and 4:1.

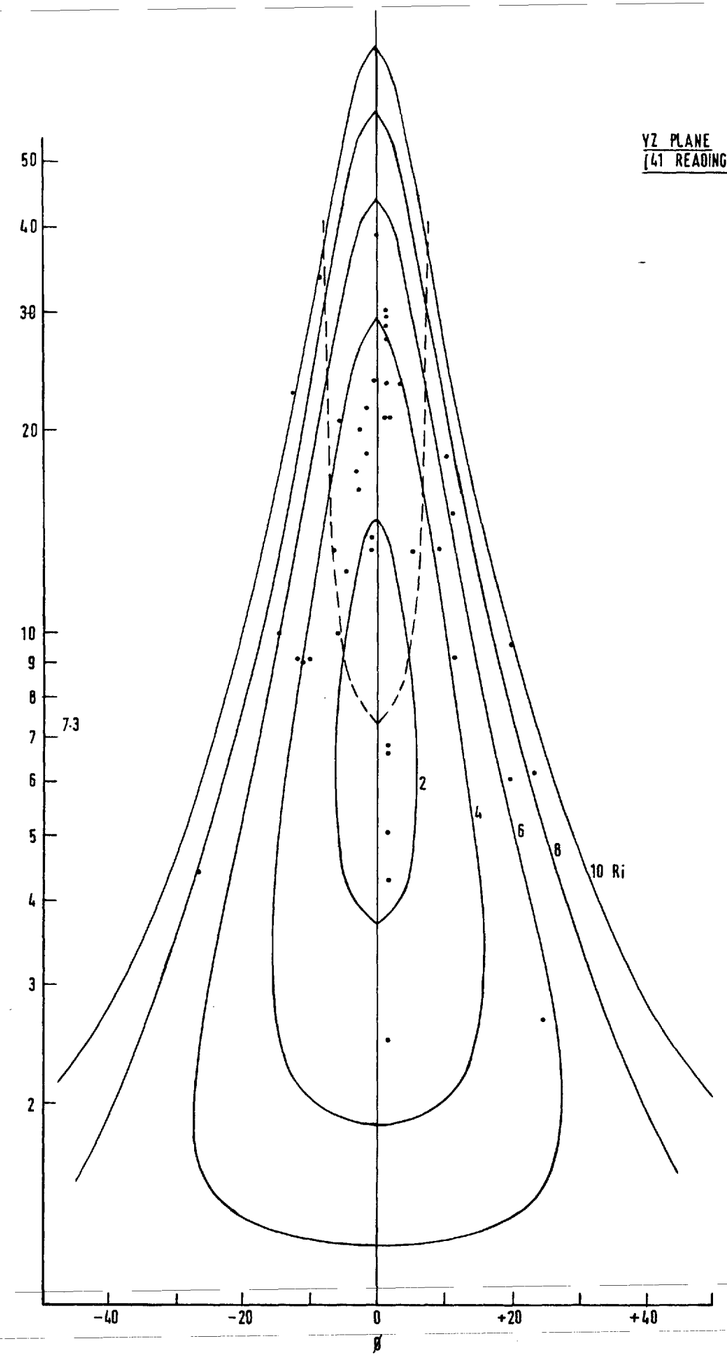
(b) YZ plane Rf = 7.3 from 41 readings. The maximum fluctuation is 28° and the greatest Rs is 39:1. 15% of the Ri's were between 1:1 and 2:1, 42% between 2:1 and 4:1, and 19% between 4:1 and 6:1.

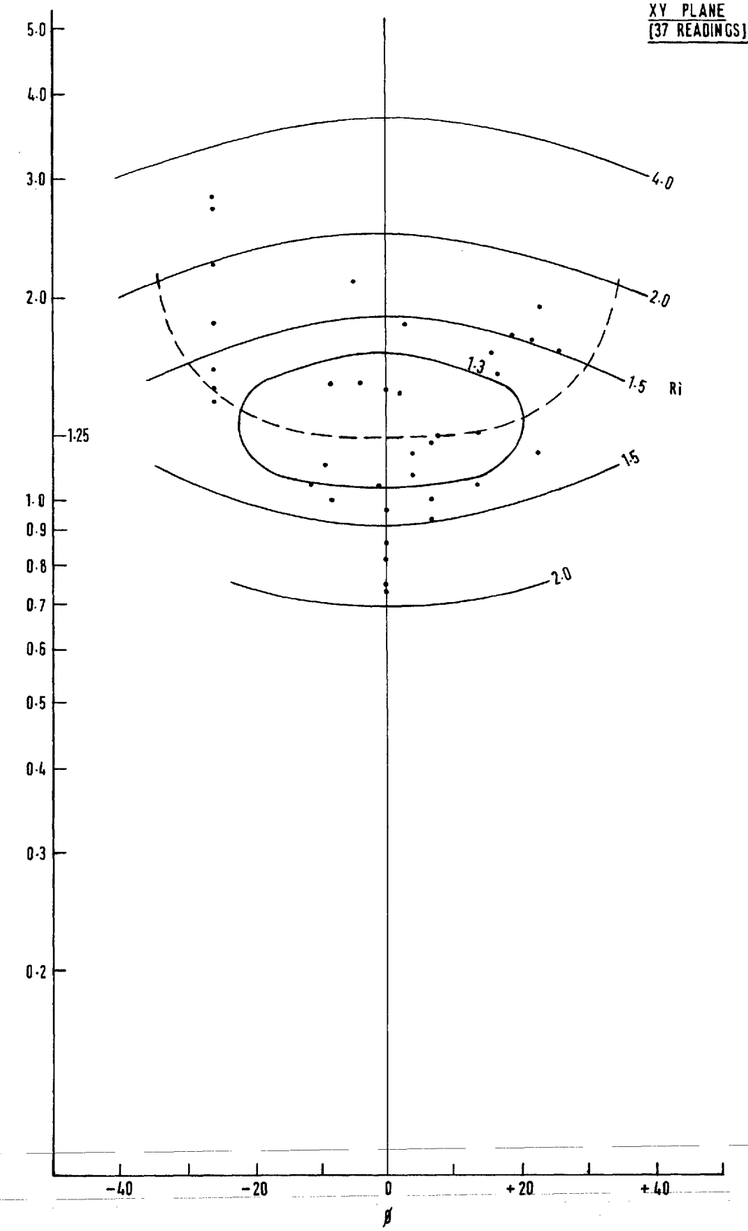
(c) XY plane Rf = 1.26 calculated from the formula YZ/X = 1, and Rf = 1.25 from the diagram with 37 readings. The maximum fluctuation is 90°, and the Rs 2.28. Twentynine of the xenoliths were elongated in the X direction, two had 1:1 axial ratios, and the remaining six were elongated in the Y direction. 73% of the Ri's were between 1:1 and 1.3:1.

Rf/ϕ DIAGRAMS WOLFSTAFFEL XENOLITHS

FIGURE 46

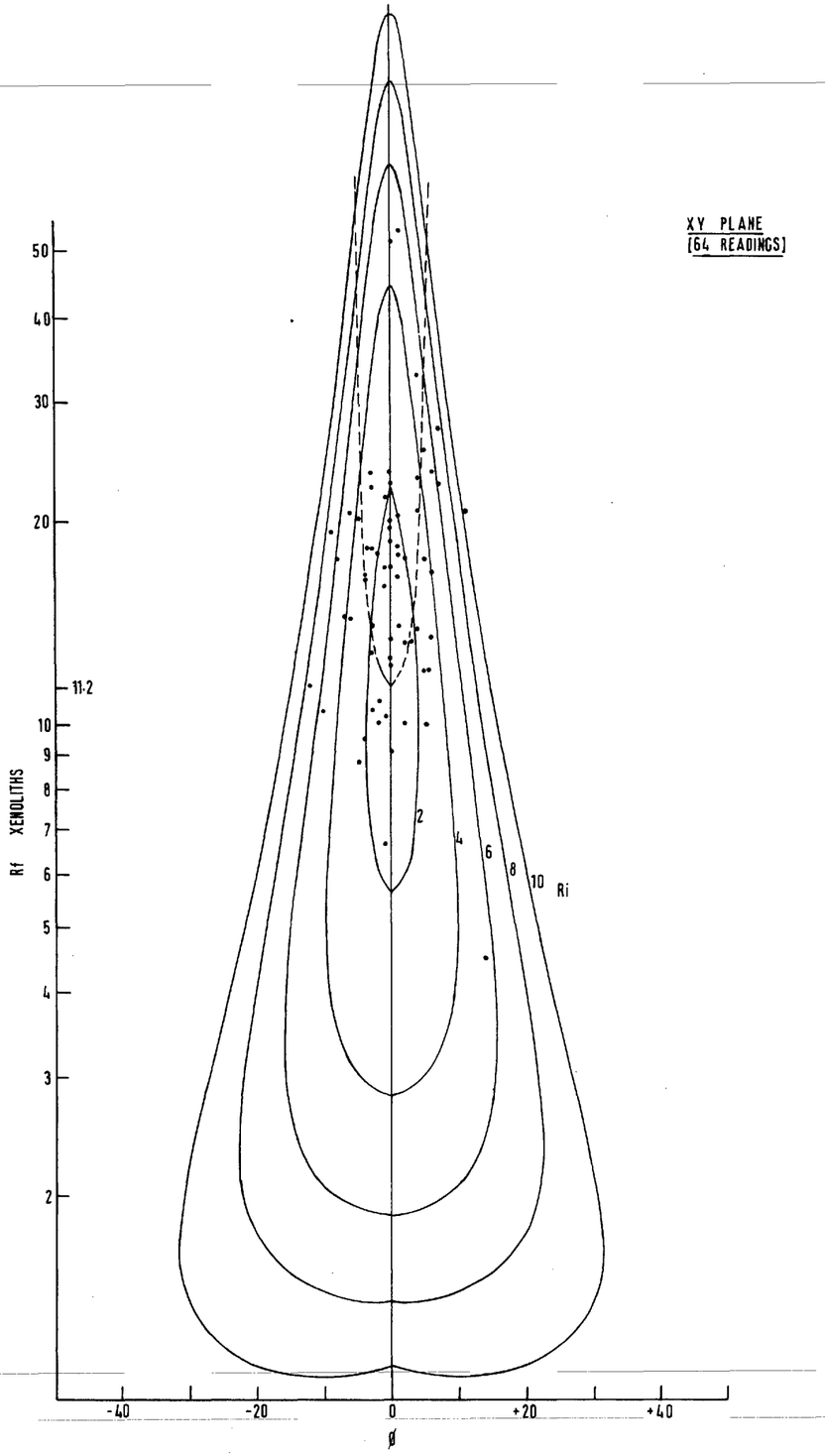


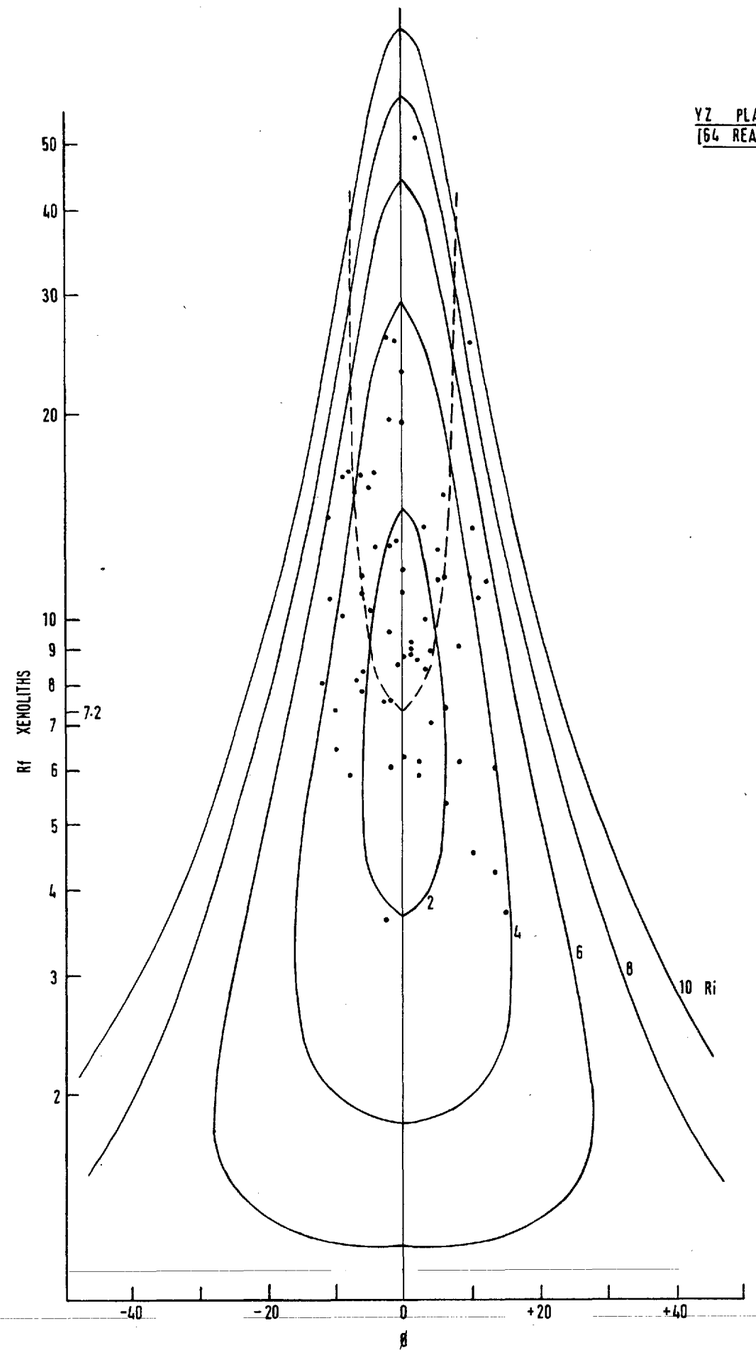


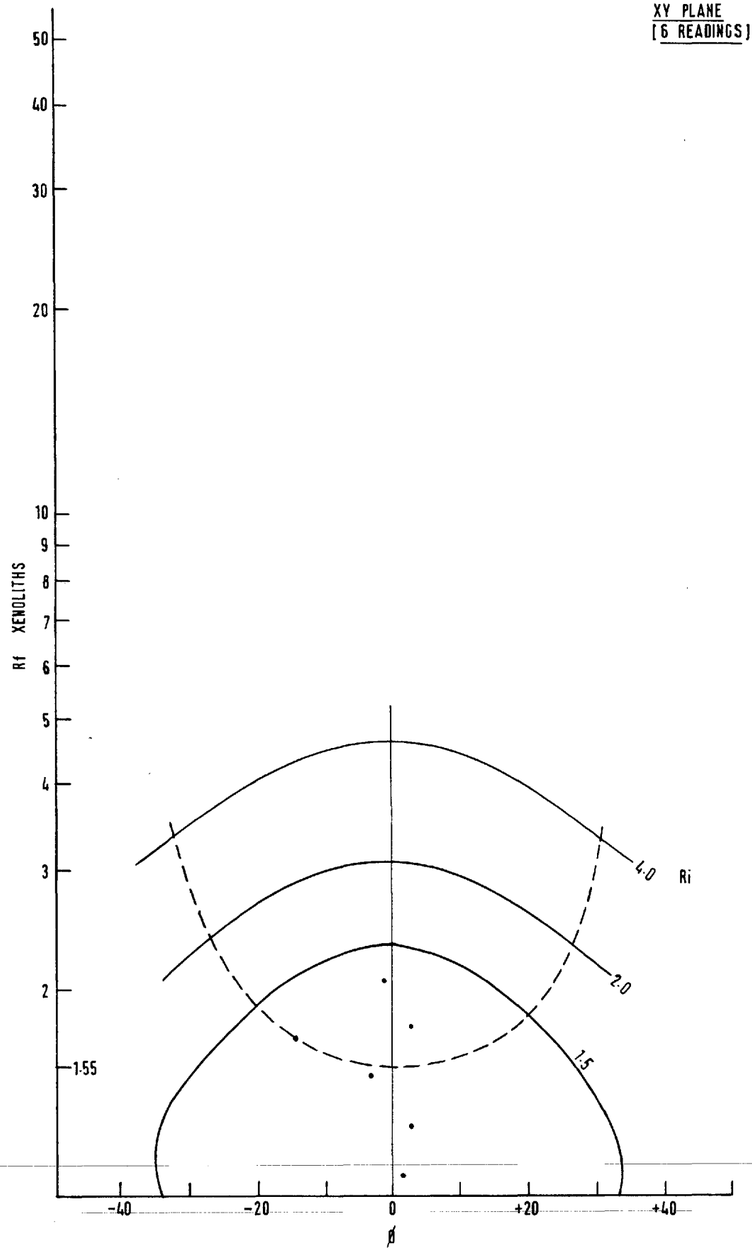


Rf / ø DIAGRAMS WANDFLUHHORN XENOLITHS

FIGURE 47







2. Wandfluhhorn (fig.47)

(a) XZ plane Rf = 11.2 from 64 readings, which had a maximum fluctuation of 13° and a maximum Rs of 53.3:1. 44% of the Ri's were between 1:1 and 2:1, and 33% were between 2:1 and 4:1.

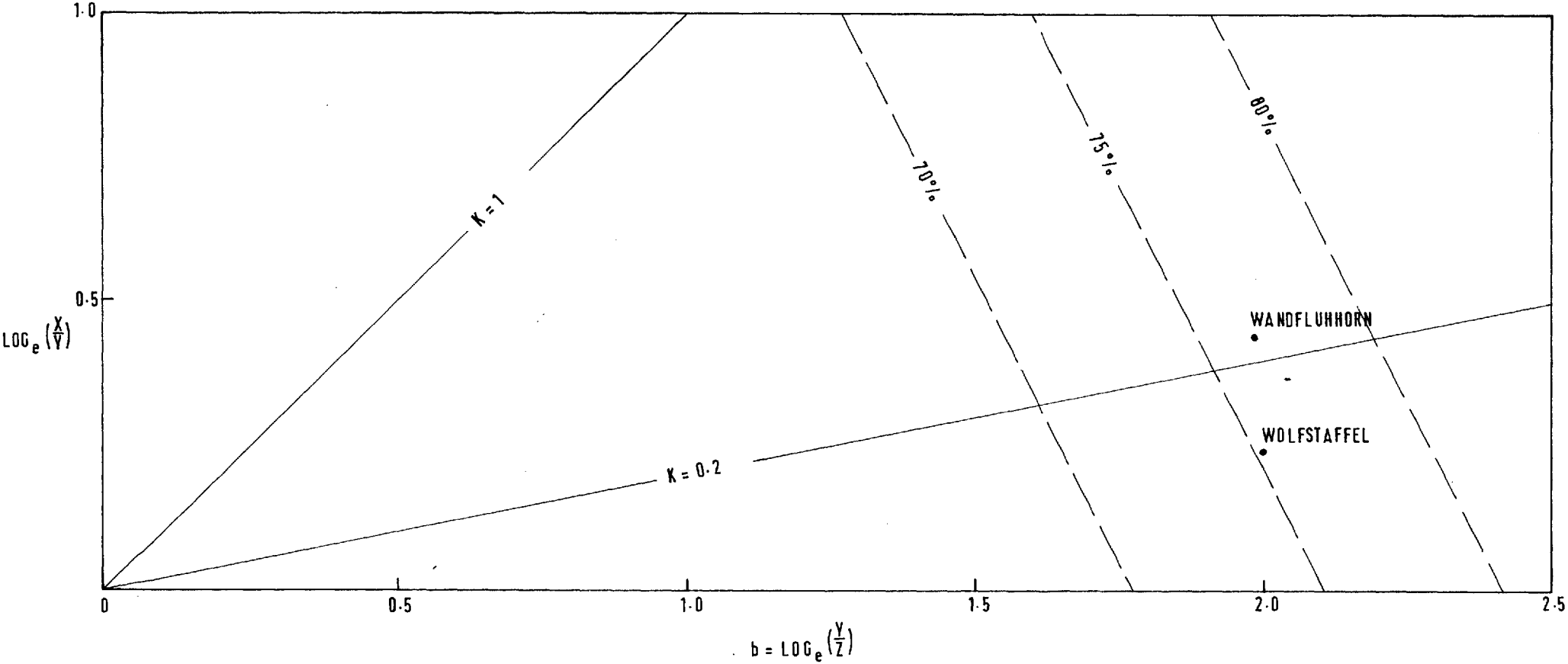
(b) YZ plane Rf = 7.2 from 64 readings, including a maximum fluctuation of 13° and a maximum Rs of 50:1. 35% of the Ri's of the xenoliths lay between 1:1 and 2:1, and 50% between 2:1 and 4:1.

(c) XY plane Rf = 1.56 when calculated, but there were only six readings, which coincidentally give an Rf value of 1.55. All the xenoliths showed a preferred orientation in the X direction. The maximum fluctuation is 15° and the maximum Rs is 2.08. All the Ri's were between 1:1 and 2:1.

The strain values from each area were converted to their best fit ellipsoids by utilising the computer programme adapted by Siddans. The best fit ellipsoid for the Wolfstaffel strain data has X, Y and Z axes of 2.28, 1.79 and 0.25 units respectively, and a K value (Flinn, 1962, Ramsay 1967:136-9), of 0.122 (fig.48). This results from shortening a 1:1:1 sphere 75% in the Z direction. Examination of an infinitesimally thin slab of material in the YZ plane, parallel to the direction of maximum shortening, reveals that, if constant volume deformation is assumed, only 45% of the original material now occurs in this plane. The remaining 55% appears to have been displaced parallel to the X axis, causing the preferred elongation in that direction. The X axis has consequently undergone an extension of 128% (fig.49a). Calculations also show that theoretically no material moved in the X direction until the Z axis had been shortened 44%.

The best fit ellipsoid for the Wandfluhhorn strain data has axes of 2.59, 1.66 and 0.23 units, and results from a 77% shortening in the Z direction. The K value is 0.225 (fig.48). Only 33% of the original material remains in the YZ plane, the remaining 67% having been displaced in the X direction which has been extended 159% (fig. 49b). A theoretical constant volume deformation of 40% is required before material was displaced in the X direction.

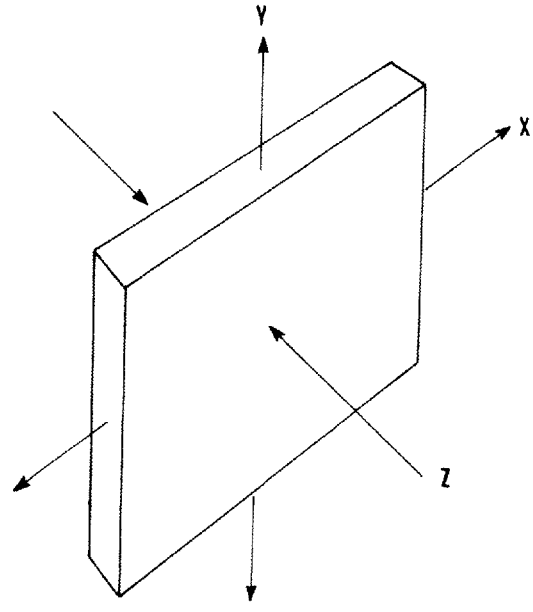
As the gneiss becomes finer grained and more schistose towards its outer margin the xenoliths become much thinner, and none were observed in

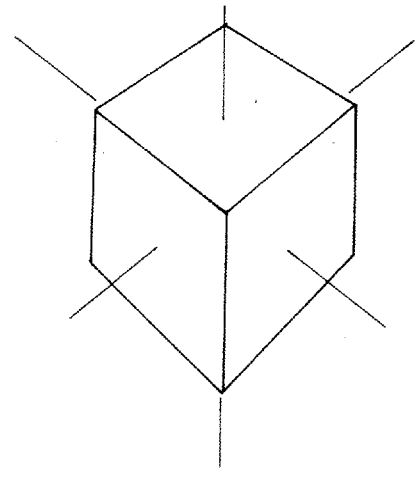


GRAPHICAL REPRESENTATION OF DEFORMED XENOLITHS IN RELATION TO RATIOS OF PRINCIPAL STRAINS AND AMOUNT OF FLATTENING (IN %) $K = \frac{a-1}{b-1}$

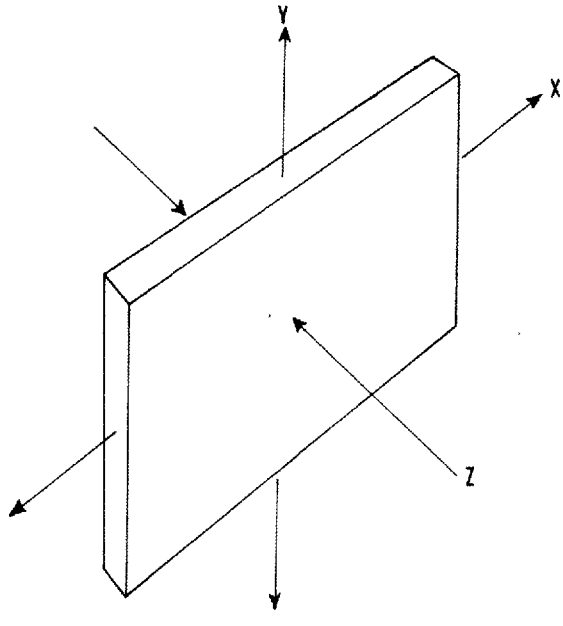
FIGURE 48

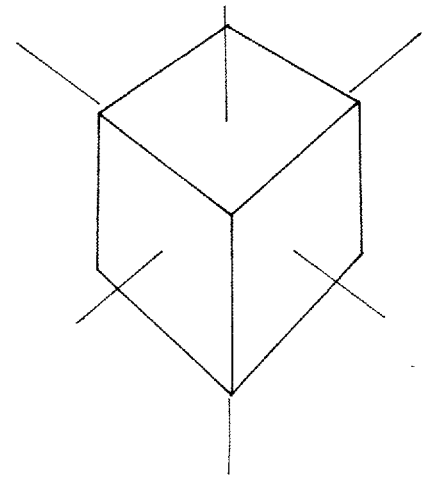
FIGURE 49
DEFORMED XENOLITHS





(a) DIAGRAMMATIC SHAPE CHANGE INDICATED BY WOLFSTAFFEL XENOLITHS





(b) DIAGRAMMATIC SHAPE CHANGE INDICATED BY WANDFLUHHORN XENOLITHS

the marginal 70 m. The most strongly deformed xenoliths observed occur on the western side of Hendar Furggu, approximately 75 m. above the Mesozoic rocks of the Stella Syncline. They are extremely thin, and only their XZ and YZ planes could be measured, but insufficient readings were obtained for Rf / ϕ diagrams to be constructed. In the XZ plane the long axes of the xenoliths were parallel to the schistosity trace (i.e. $\phi = 0^{\circ}$). The axial ratios varied from 36:1 to 150.5:1, the average of 12 readings being 70.4:1 and the mean 63.7:1. Only four readings were made in the YZ plane. These range from 9:1 to 13:4:1, and have angular fluctuations up to 12°.

These observations suggest that there has been considerably more extension in the X strain direction in the schistose margins of the gneiss than in the more massive interior. It is thus highly significant that a strong lineation, parallel to the X direction, occurs in the schistose margins of the Antigorio Gneiss.

9:3 Deformed Dykes and Veins

The Antigorio Gneiss is cut by aplite and pegmatite dykes and quartz veins up to 40 cms thick (fig. 50a). The aplite dykes have the same composition and mineralogy as the granitic gneiss, but are finer grained. They pre-date the pegmatites. The dykes and veins deformed with the gneiss, and biotite flakes in the aplite dykes lie parallel to the schistosity in the surrounding gneiss.

Most of the dykes and veins described occur in the Wolfstaffel area. They were never common enough at any one locality to be used to construct a minimum strain ellipsoid devised by Talbot (1970). A few were folded, but most had a tabular form (fig. 50b) and lay at angles of up to 66° from the schistosity.

A very good example of a folded aplite dyke, at the northern end of the ridge north of Rota Balmu (68011318), had interlimb angles of 30° to 60°, and strongly thickened hinges and thin limbs. A number of deformed xenoliths lying in the axial plane schistosity were elongated parallel to the axial planes of the folds. The tabular dyke observed lying at the highest angle to the schistosity (66°) had very small lobe and cusp structures along its boundaries. The lobes consisted of dyke material,



Fig.50(a) Aplite dykes in Antigorio Gneiss cut by thin pegmatite dyke. Note slightly irregular boundaries of dyke. Wolfstaffel (68241315).



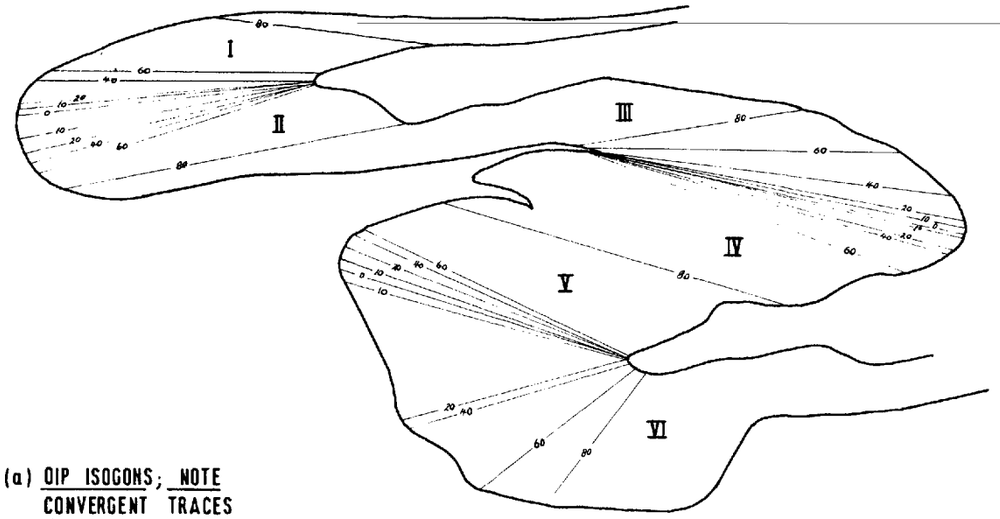
Fig.50(b) Aplite dyke subparallel to F2 schistosity in Antigorio Gneiss. Note straight boundaries of dyke. West of Lago Superiore. (67791318).

showing that the dyke was more competent than the enclosing gneiss. A minimum of 41% shortening along the dyke was calculated by comparing the arc length of one boundary with the distance between the same two points in a straight line.

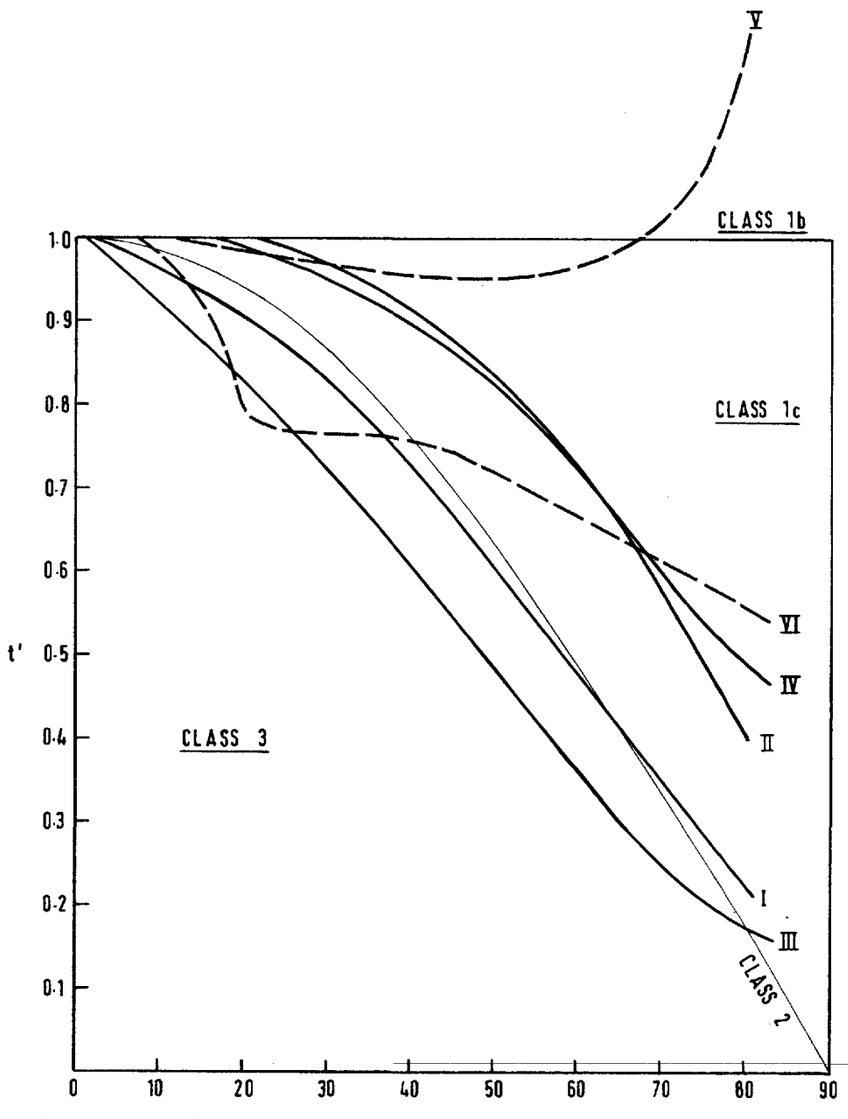
The pegmatite dykes are usually less than 10 cms thick, and lie at angles of up to 58° from the schistosity. They retain their tabular form with one exception. The exceptional dyke lay at 55° to 60° from the schistosity for most of its length, but at one point changed abruptly to lie at 20°from the schistosity. The boundaries of the steep portion were deformed into small lobes and cusps, the lobes being composed of dyke material. The folded portion of the dyke had been shortened at least 35%, but the portion lying closer to the schistosity was deformed into pinch and swell structures and was only a quarter the thickness of the steep portion.

Deformed quartz grains were rare, and only two were discovered. One was ptygmatically folded, and shortened at least 38%, but its thickness varied irregularly along its length. The other quartz vein consisted of a series of boudinaged folds, the limbs of which extended parallel to the schistosity. The boudinaged folds have thick hinges and thin, sub-parallel limbs (fig. 51a, c). One limb was generally one and a half to two times thicker than the other. Plots of t'a (fig. 51b, d) show that the thin limbs fall in the class 3 field close to the class 2 (similar) line, while the thick limbs lie in the class 1c field between $\sqrt{\frac{\lambda_2}{\lambda_1}} = 0.5$ and 0.7 (Ramsay, 1967; 411-5). The plot of $\sqrt{\frac{\lambda_2}{\lambda_1}} = 0.1$ lies approximately half way between the plots for the different limbs, and is also closest to that calculated from the Wolfstaffel strain data ($\sqrt{\frac{\lambda_2}{\lambda_1}} = 0.116$).

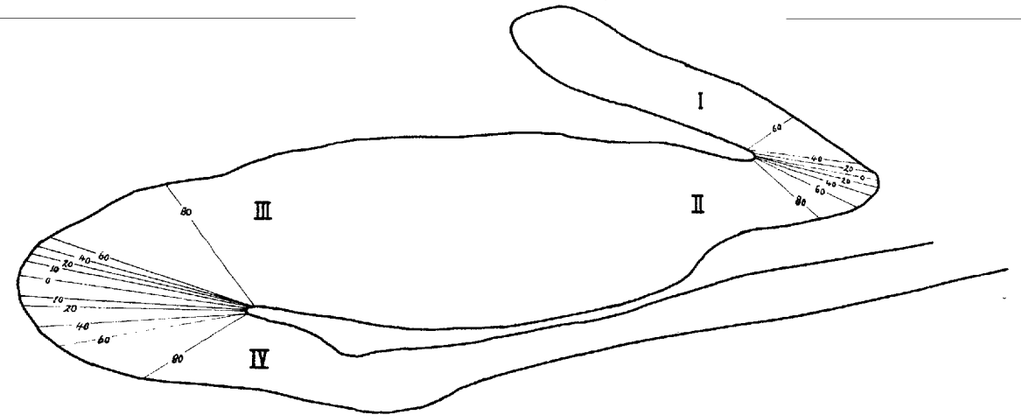
The t'a plots show that the folded quartz veins deformed by buckles flattened normal to their axial planes (Ramsay, 1962; 314). De Sitter (1958) has shown that boudinaged folds develop in the flattening field, and as they become tighter during progressive deformation their limbs are rotated into the extension field and stretched parallel to their lengths. The different limb thicknesses reflect the asymmetry of the folds.



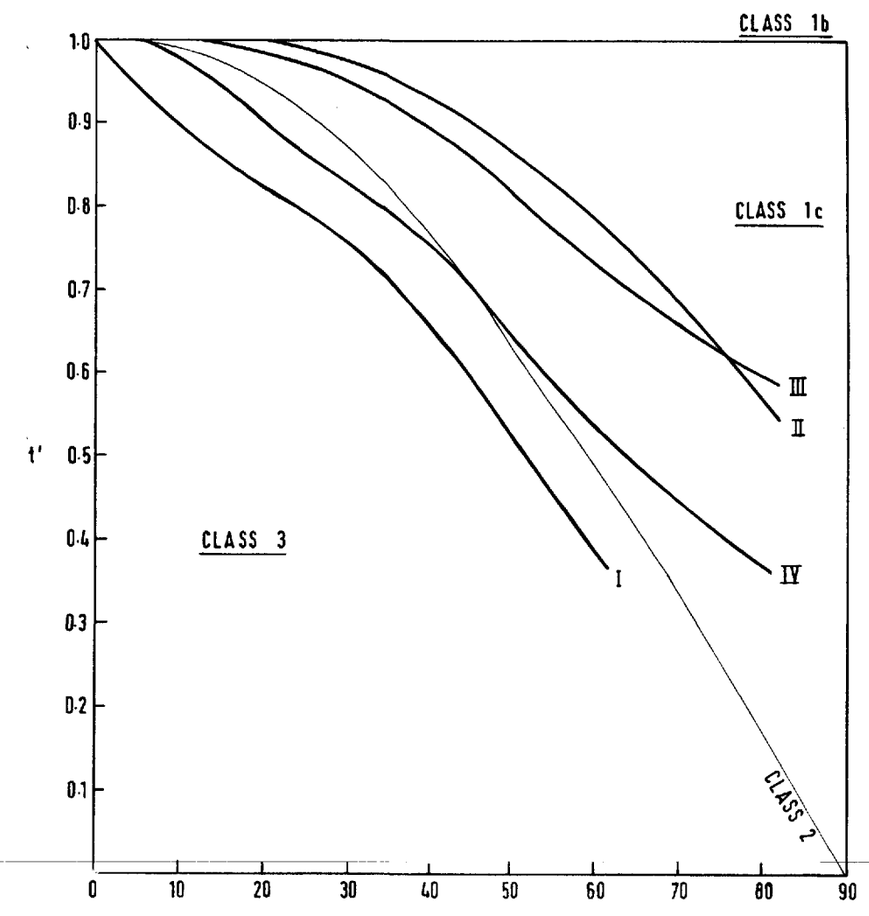
(a) DIP ISOGONS; NOTE CONVERGENT TRACES



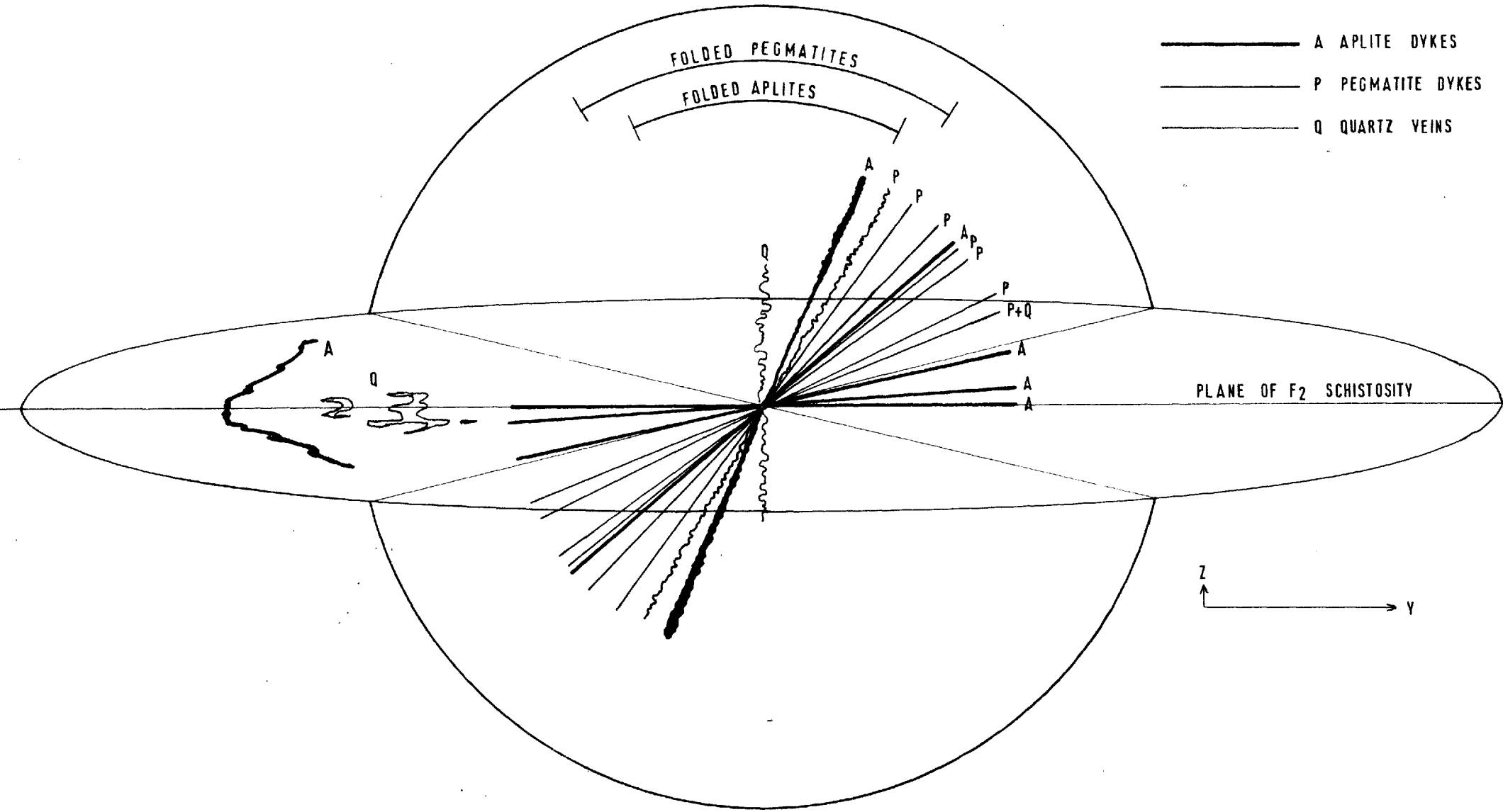
(b) t'∝ PLOTS OF FOLDS IN (a)



(c) DIP ISOGONS



(d) t'∝ PLOTS OF FOLDS IN (c)



DIAGRAMMATIC REPRESENTATION OF DYKES AND VEINS IN RELATION TO YZ PLANE OF WOLFSTAFFEL DEFORMED XENOLITHS SHOWN BY ELLIPSE. CIRCLE REPRESENTS UNDEFORMED SHAPE. NOTE SMALL SECTOR CONTAINING FOLDED DYKES

FIGURE 52

The orientations of the deformed dykes and veins from Wolfstaffel have been plotted on an elliptical diagram (fig. 52) derived from the YZ Wolfstaffel strain data. The ellipse has an axial ratio of 7.3:1, representing a 75% shortening in the Z direction. Lines of no finite longitudinal strain are located at 14° from the long axis, and there is consequently only a small extension field. A notable feature of the diagram is the wide angular distribution of tabular dykes. Dykes at angles of 46° and less from the schistosity trace are straight-edged, while pegmatites at 58° and aplites at 66° have only slightly folded boundaries.

During deformation the dykes, contained in a relatively homogeneous mass, were sufficiently thin and well-spaced to behave independently. The style of deformation of the dykes would therefore have followed the laws of single layer buckling, being dependent on their thickness and viscosity contrasts with the surrounding gneiss (Biot, Ode, and Roever, 1961), and their orientation with respect to the principal strains (Ramsay, 1967, ch. 9). As so few dykes are folded it is thought that their viscosities were very close to that of the gneiss, and only those initially subparallel to the principal shortening direction were folded. Dykes at a slightly higher angle to the shortening direction contracted along their lengths, developing small boundary lobes while rotating to lie closer to the XY plane. Dykes at moderate angles to the shortening direction rotated towards the XY plane without undergoing obvious contraction or extension. Dykes lying within the extension field rarely exhibit stretching features, again indicating a lack of viscosity contrast between the dykes and the surrounding gneiss. The dykes and veins with the greatest quartz content show the strongest deformation features, suggesting that the viscosity contrast between them and the Antigorio Gneiss was greater than that between the gneiss and the aplitic rocks.

9:4 Grain Size and Textures

This section examines the progressive changes in the grain size and texture of the Antigorio Gneiss during its transformation from a coarse grained granitic rock to a fine grained schist. It is based largely on a microscopic study of thin sections cut in the XZ and YZ planes, determined from the deformed xenoliths. The optic orientation of the grains in the thin sections was not considered, as the quartz and feldspar grains in a section exhibiting a very strong dimensional preferred orientation were

shown by J. Starkey (pers. comm.) to have no preferred orientation of c axes.

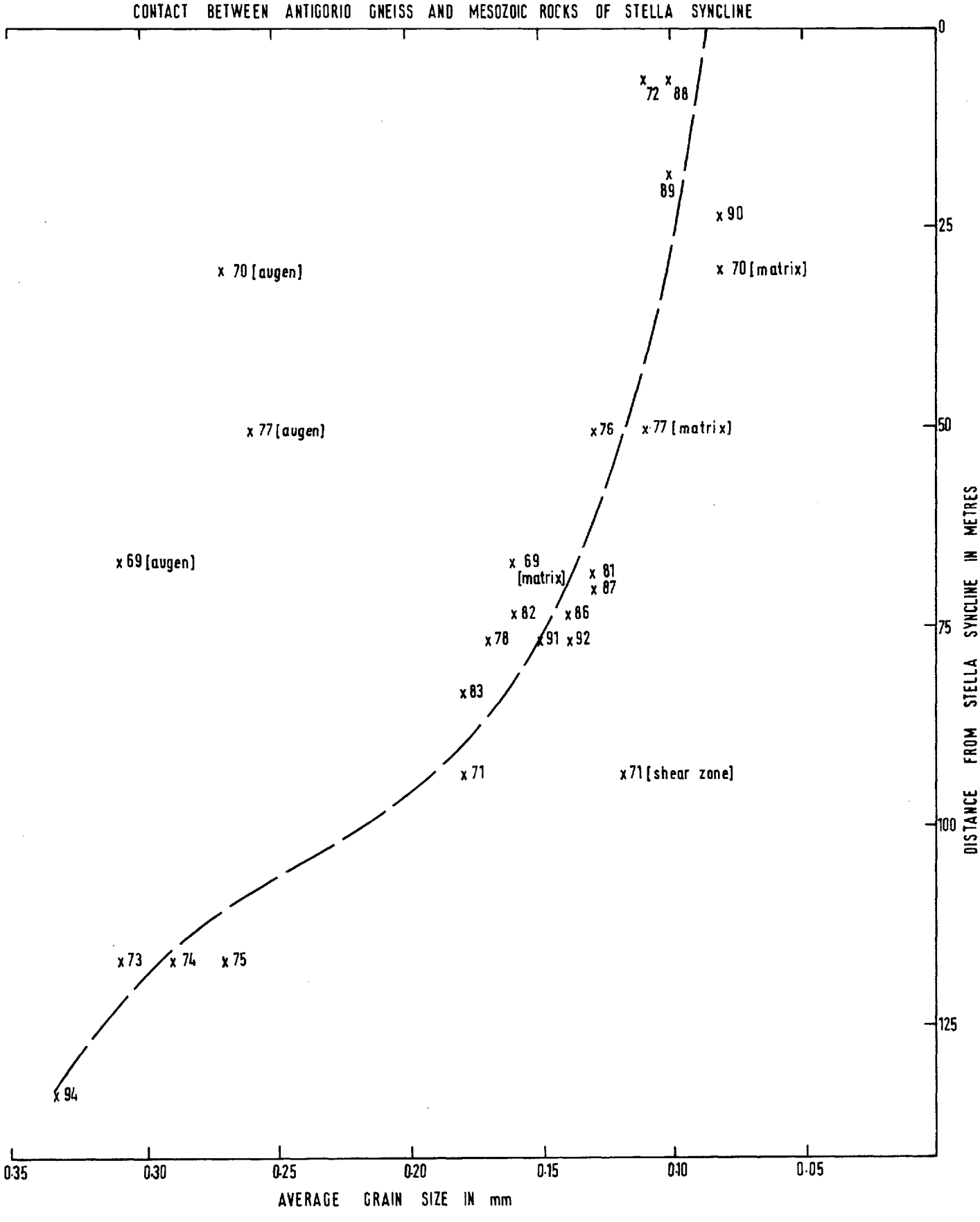
The average grain size of the quartz and felspar components was derived from a count of the number of grains along a series of lines of known length across the thin sections, both parallel to and normal to the long edge of the thin section. Between 1,000 and 1,200 grains were counted in each section. A graphical representation of the reduction in grain size is shown in Fig.53.

To determine the degree of dimensional preferred orientation of the grains a thin section, magnified approximately 1,000 times, was projected onto a paper covered screen. The outlines of randomly selected grains, evenly distributed over the entire section, were traced onto the paper. The traced outlines were then modified slightly to the elliptical shapes best fitting the outlines. The principal axes of the ellipses were measured, and the axial ratio of each grain (Ra) calculated. The angles from the trace of the mica fabric to the long axes were also measured, and recorded as positive or negative fluctuations (ϕ) depending on whether the right hand end of the long axes projected above or below the mica fabric.

Between 70 and 160 quartz and feldspar grains were measured in each thin section, and the results plotted in exactly the same way as similar data from the deformed xenoliths were recorded on Rf/ϕ diagrams. Where possible the points on the diagram were contoured in 20% intervals, so that the 100% contour enclosed all the points on the diagram and the 20% contour enclosed the most densely concentrated number of points equal to 20% of the total. In all examples which it was possible to contour it was found that the symmetric mid-point of the data fell within, and usually close to the centre of the area enclosed by the 20% contour. The symmetric mid-point also lay on or close to the line representing the trace of the mica fabric.

These diagrams are termed Ra/ϕ diagrams (from axial ratio v. angular fluctuation), and provide a useful method of comparing the degree of dimensional preferred orientation of the grains in rocks collected across the marginal zone of the Antigorio Gneiss. Selected diagrams, shown in figs. 55, 57, 59, 61 and 63, illustrate clearly that the dimensional preferred orientation of the grains increases progressively as the grain size decreases. It should be stressed that the values shown in the diagrams

FIGURE 53



GRAPHICAL REPRESENTATION OF GRAIN SIZE REDUCTION IN ANTIGORIO GNEISS

[Numbers refer to thin sections 34377, etc]

do not represent the finite strain, although they provide a guide to the finite strain when considered together with other deformed objects. The Ra/ϕ values were always greater when measured in the XZ plane, parallel to the lineation, than in the YZ plane.

The least deformed and most common Antigorio Gneiss is an even grained rock with an average grain size close to 0.30 mm., and a typically granitic texture (fig. 54a). The only indication of deformation is that many of the grains are cracked and strained, and their boundaries are commonly sutured. The few biotite flakes have a roughly parallel orientation (fig. 54b). An Ra/ϕ value of 1.37 was measured in one thin section (fig. 55 b).

Between 115 and 85 metres from the Mesozoic rocks of the Stella Syncline there is a marked decrease in the average grain size of the gneiss from 0.30 mm. to 0.17 mm. (fig. 53). This is accompanied by the development of narrow shear zones with strongly oriented quartz and feldspar grains with an average size of 0.12 mm. (fig. 56), and an Ra/ϕ value of 2.1 (fig.57b). The shear zones are outlined by concentrations of aligned biotite flakes along their margins, and contain common grains of epidote and ilmenite. The remainder of the rock retains its granitic texture, and the only indications of a fabric are aligned biotite flakes and weakly oriented quartz and feldspar grains (Ra/ϕ value of 1.5 in section 34371) (fig. 57a). The quartz and feldspar grains are strained and cracked, and often have irregular, sutured boundaries. The K feldspars are sericitic. There are a few grains of ilmenite and epidote, but the most notable mineralogical change is the appearance of minute quantities of muscovite, now partly altered to chlorite.

As the grain size decreases from 0.16 mm. to 0.13 mm. the granitic texture with aligned biotite flakes is replaced by a schistose texture with more common, strongly oriented biotite, muscovite, quartz and feldspar (fig.58). The average amount of muscovite increases slightly up to 6%, and is accompanied by a marked decline in the amount of K feldspar from between 30% and 50% to less than 10%. Ra/ϕ values are up to 2.7 (fig. 59).

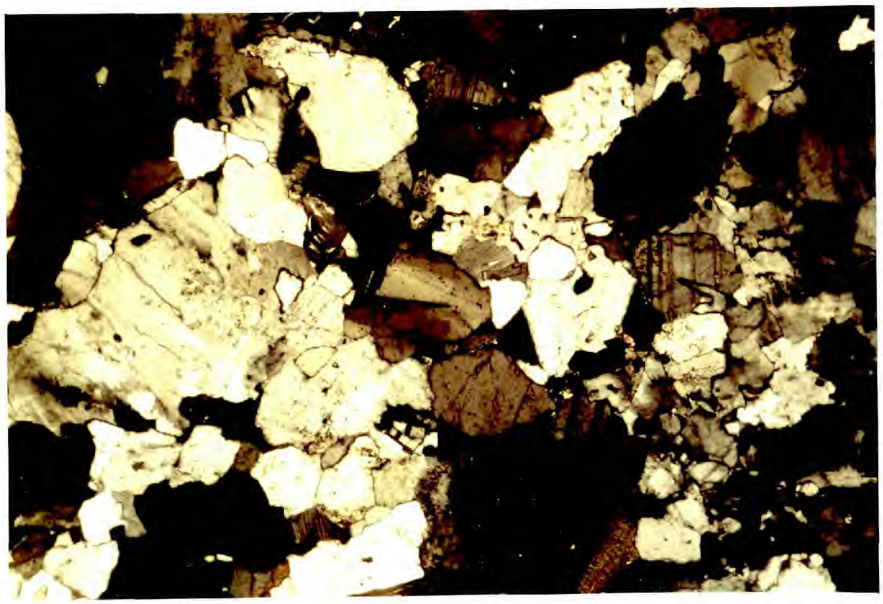


Fig. 54(a) Coarse-grained Antigorio Gneiss with original granitic texture. Note strained quartz grains at centre and on right hand side. X 30.

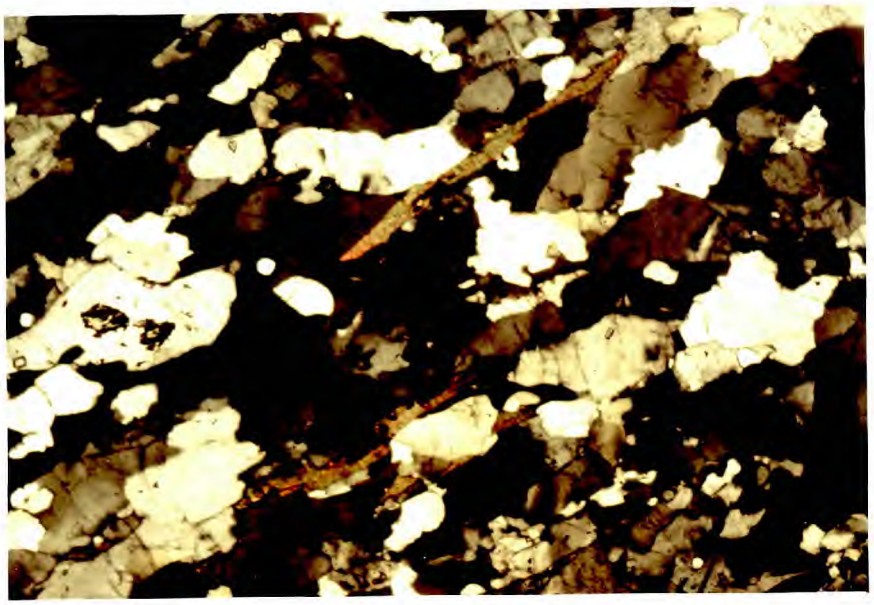
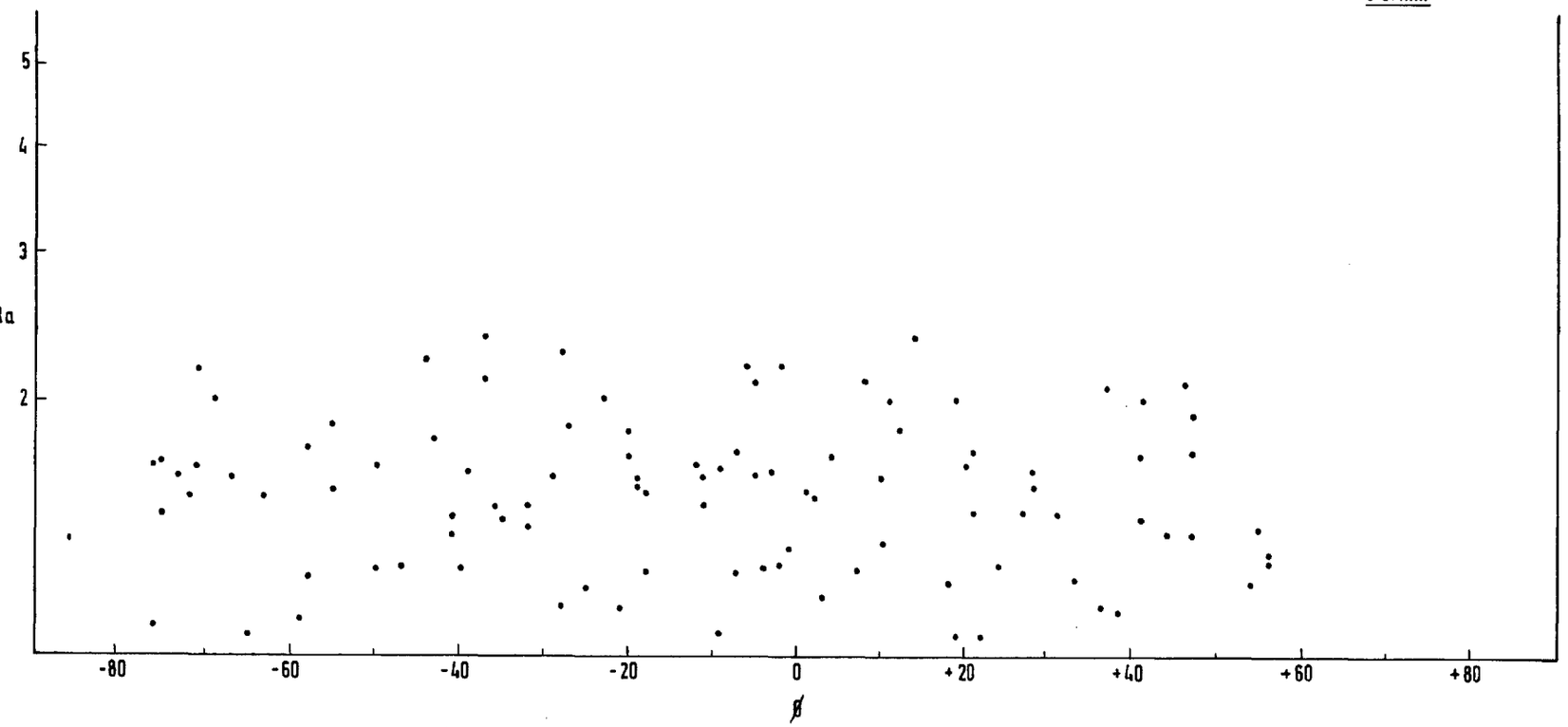


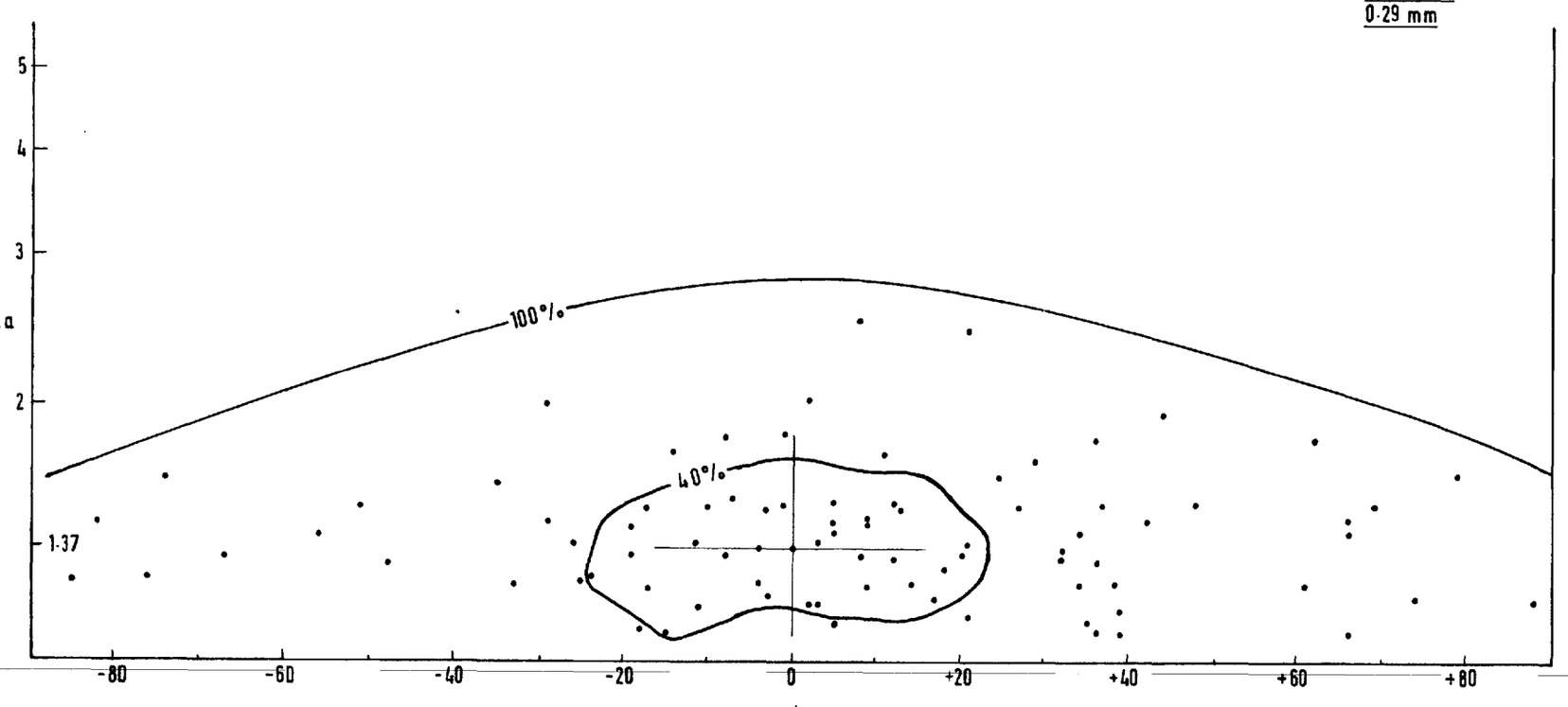
Fig. 54(b) Coarse-grained Antigorio Gneiss with aligned biotite flakes. Note strained quartz grains with serrated boundaries. X30.

Ra / ø DIAGRAMS ANTIGORIO GNEISS

(a) 34373
[101 READINGS]
YZ PLANE
0·31 mm



(b) 34374 A
[87 READINGS]
XZ PLANE
0·29 mm



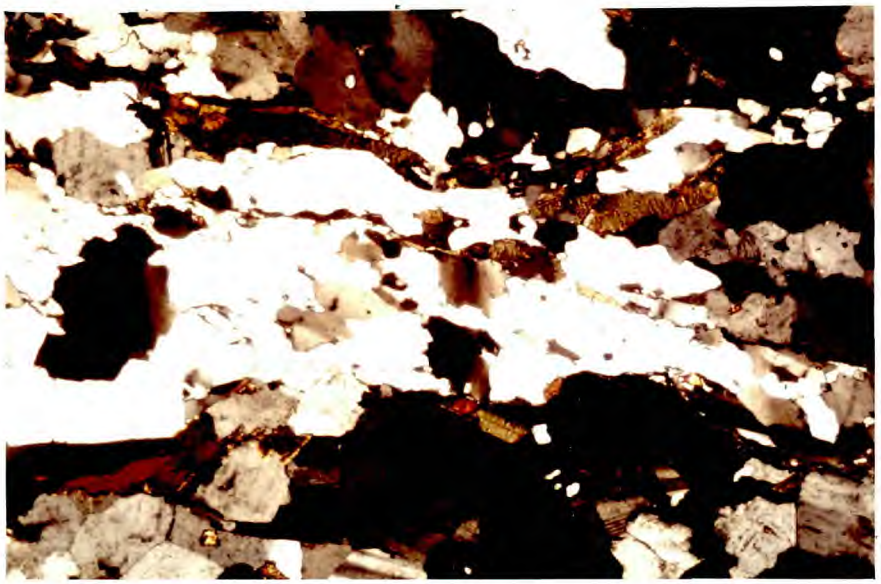


Fig.56(a) Shear zone in coarse grained Antigorio Gneiss. Quartz grains in shear zone are small and have serrated boundaries, largely subparallel to the sides of the shear zone. X 30.

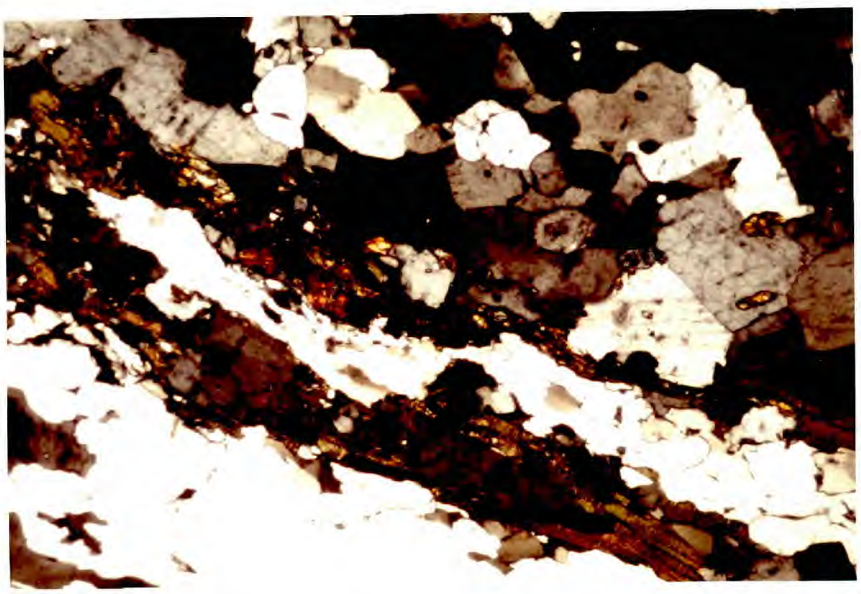
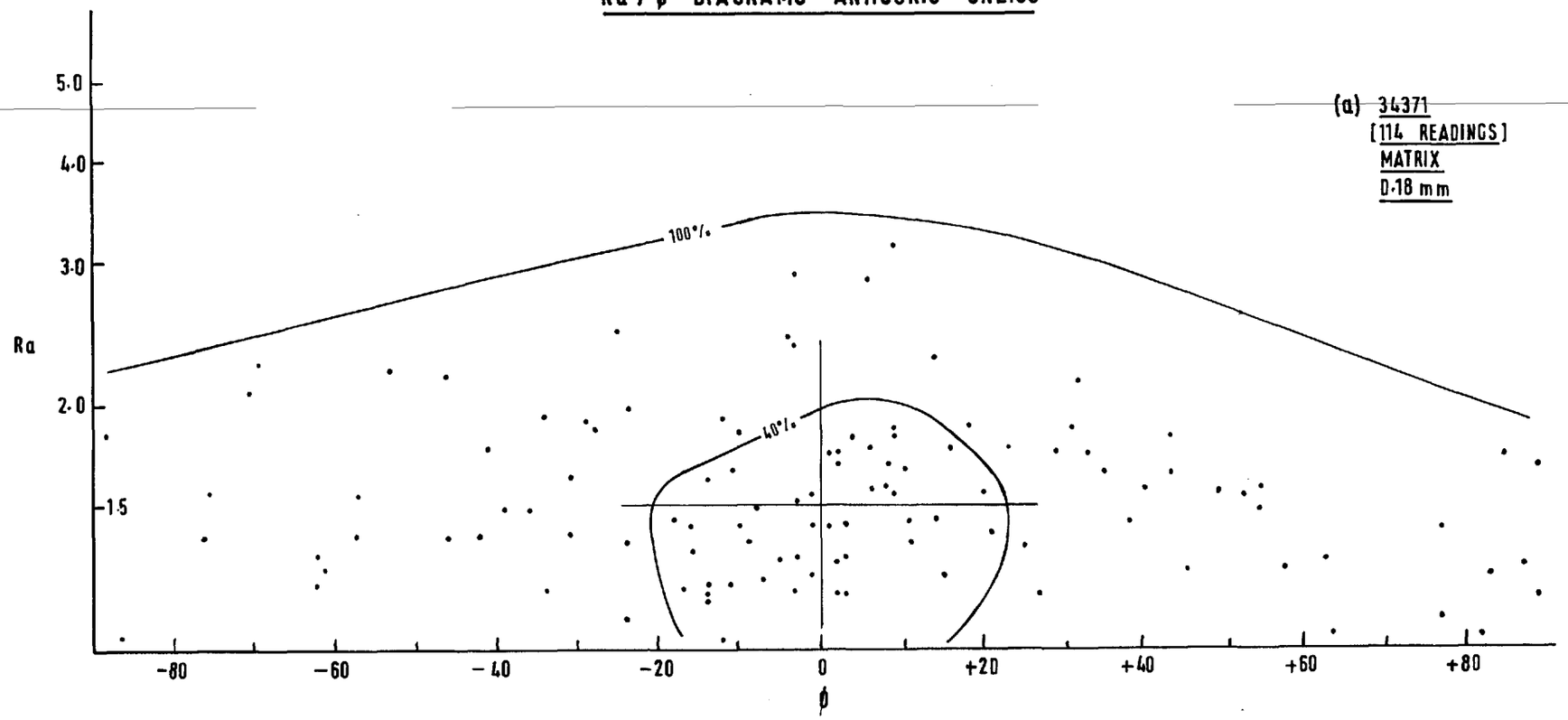


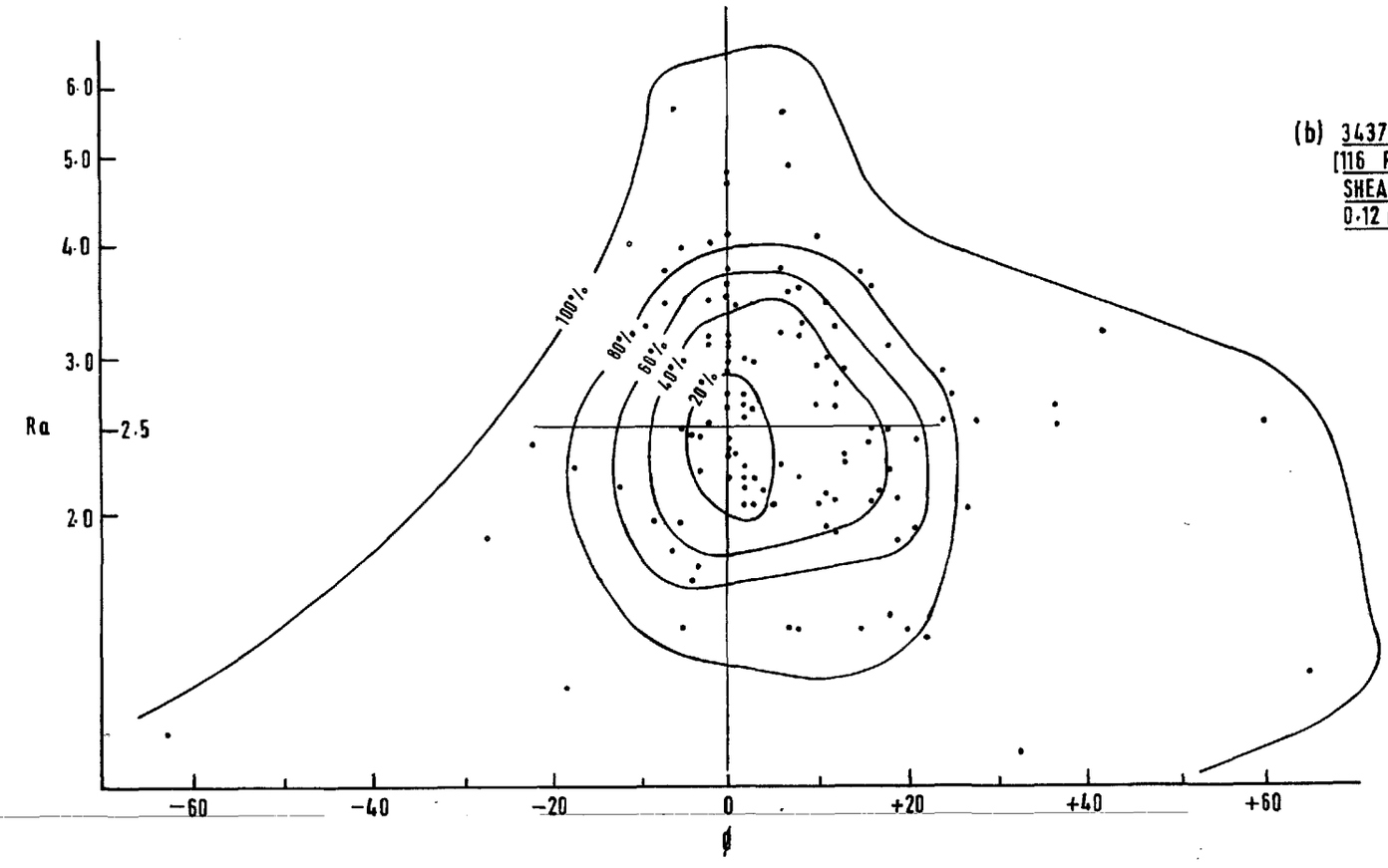
Fig.56(b) Narrow shear zones in coarse-grained Antigorio Gneiss, outlined by biotite and epidote. Note contrast in size and shape of grains in and above shear zone. X 30.

FIGURE 57

Ra / ϕ DIAGRAMS ANTIGORIO GNEISS



(a) 34371
[114 READINGS]
MATRIX
0·18 mm



(b) 34371
[116 READINGS]
SHEAR ZONE
0·12 mm

In the marginal 65 metres of the gneiss the grain size decreases only slightly to an average of about 0.09 mm. against the Mesozoic rocks of the Stella Syncline. Muscovite and biotite form a conspicuous fabric (fig. 60), and quartz and feldspar grains show strong dimensional orientation with Ra/$\emptyset$ values up to 3.07 (fig. 61).

Small lenticular quartz-feldspar augen in the schistose gneiss lie in the plane of the schistosity, and are elongated both parallel to and normal to the lineation. They have axial ratios of between 2:1 and 3:1, similar to those of individual grains. Grains within the augen are strained, but the granitic texture is largely preserved. The ends of the augen are cracked and granulated (fig. 62). An Ra/$\emptyset$ plot of quartz grains from an auge in section 34369 (fig.63a) gives a random distribution, but those from the schistose matrix have a value of 2.7 (fig. 59a). There is an abrupt change in grain size from 0.31 mm. in the auge to 0.16 mm. in the schist. A few small quartz augen persist in the finest grained schist. In section 34370, for example, the grain size of the schist is 0.08 mm. and that of the grains in the augen 0.27 mm.

Some schists have long thin bands of coarser grained quartz lying parallel to the mica fabric. In section 34377 the average grain size of the quartz changes abruptly from 0.26 mm. in the bands to 0.11 mm. in the schist groundmass. The Ra/$\emptyset$ value for the schist groundmass is 2.1 (fig. 61c), but the grains in the coarsely crystalline bands have a random orientation (fig. 63b).

In schists with an average grain size below 0.13 mm. individual grains are apparently less cracked, and their boundaries less sutured. Metamorphic minerals, especially biotite and muscovite, become more abundant and locally make up to 30% of some sections, but are largely in the 15% to 20% range. Ilmenite and epidote grains are common, and there are a few small almandine garnet porphyroblasts.

The reduction in grain size, the development of a strong schistosity and the appearance of metamorphic minerals in the marginal zone of the Antigorio Gneiss have also been observed by the writer in the upper Valle Bavona and along the Val Antabbia. Similar features were noted by Milnes (1965) in the Monte Cistella area, and by Grutter (1929) who correctly attributed them to "reworking" along the "edge zone" of the gneiss.

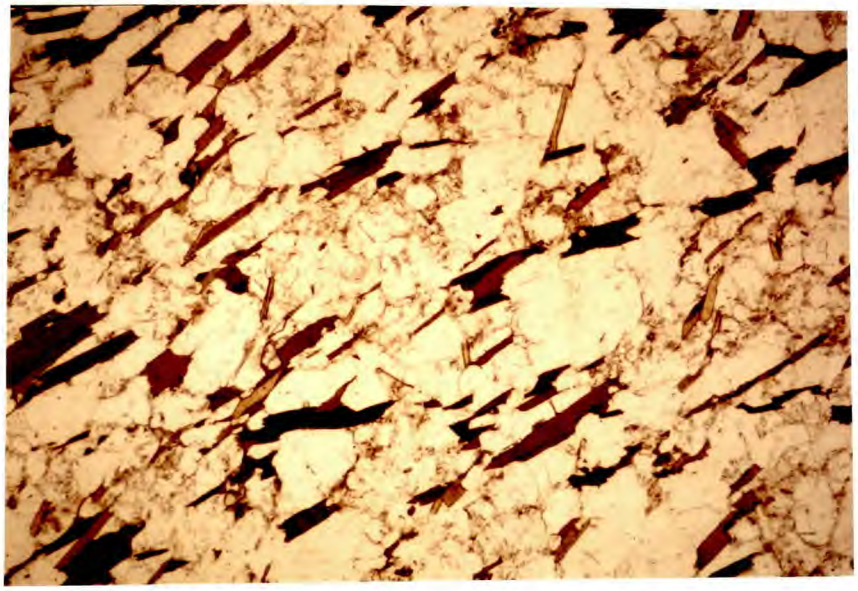


Fig.58(a) Antigorio Gneiss showing development of schistosity. Note oriented biotite flakes. X 30.

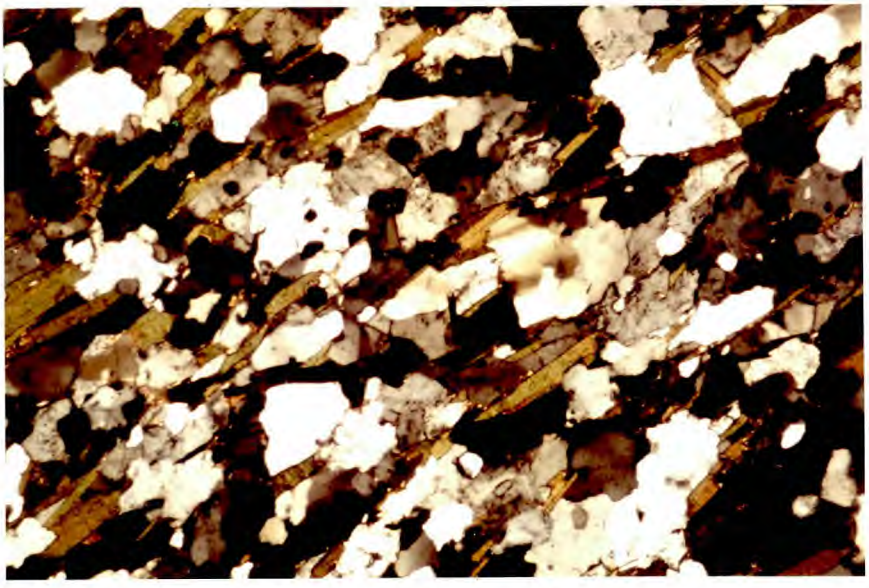
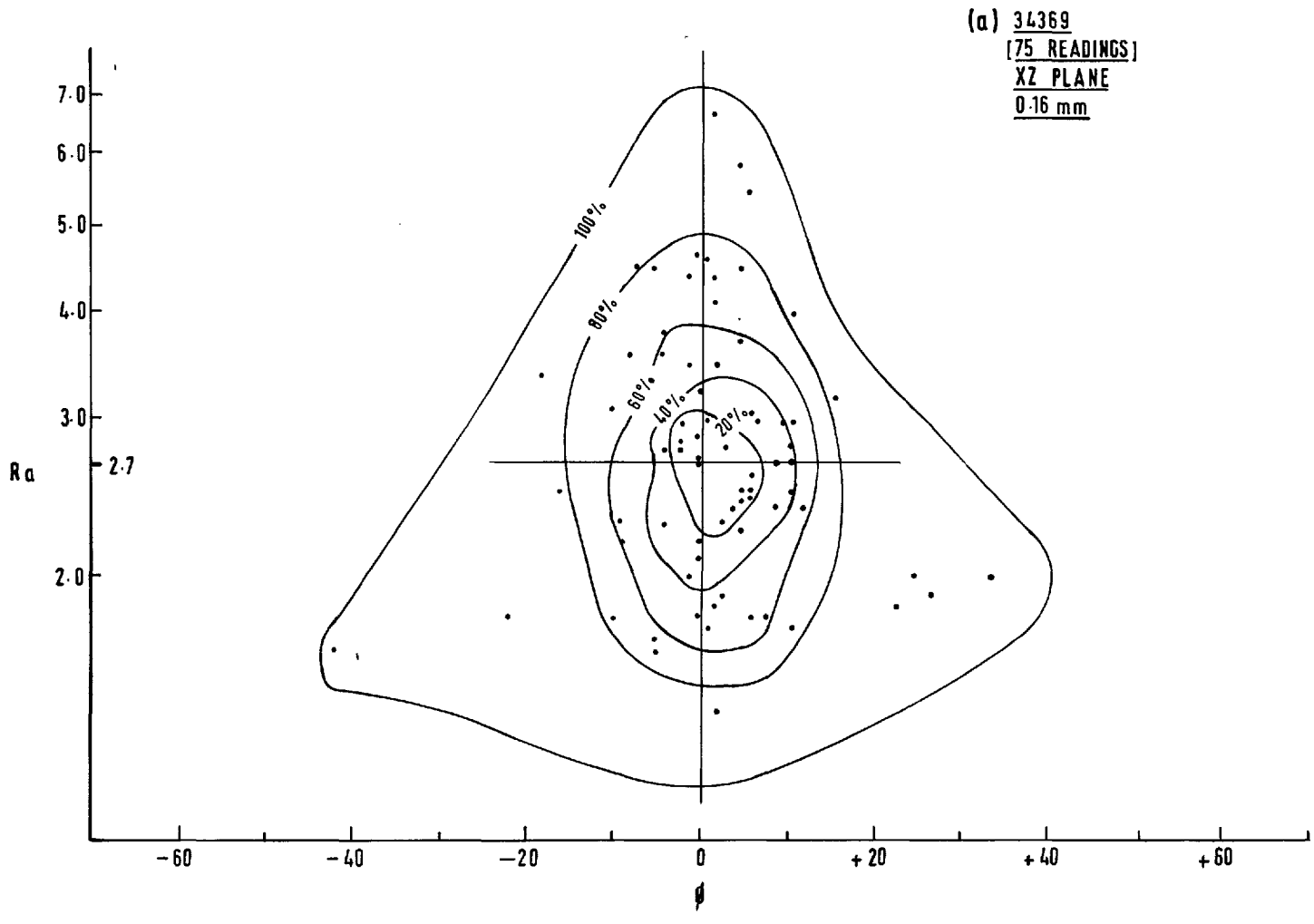
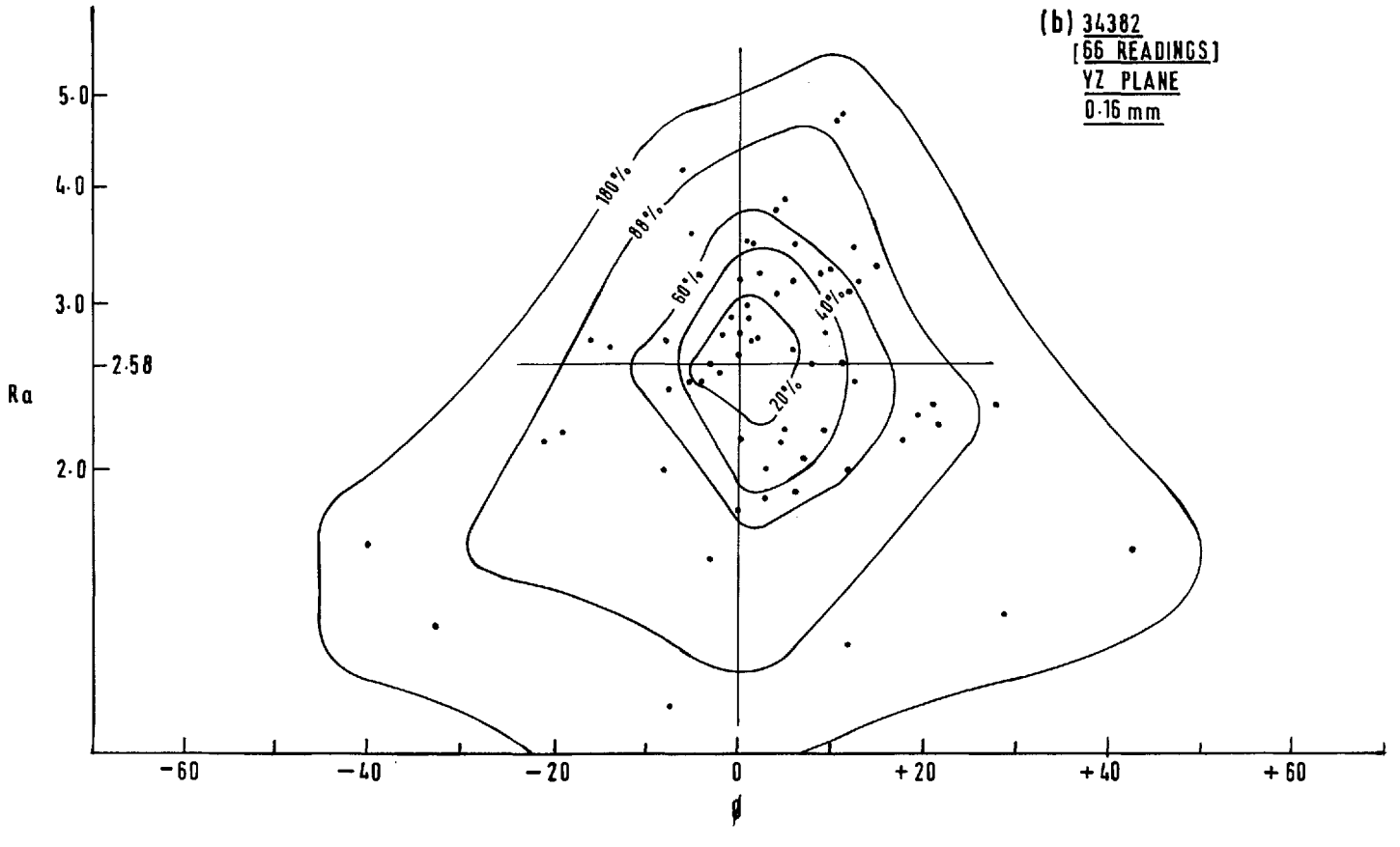


Fig.58(b) Same as above on polarised light. Note that many of the quartz grains have their longest dimension subparallel to the mica flakes.

FIGURE 59

Ra / ϕ DIAGRAMS ANTIGORIO GNEISS





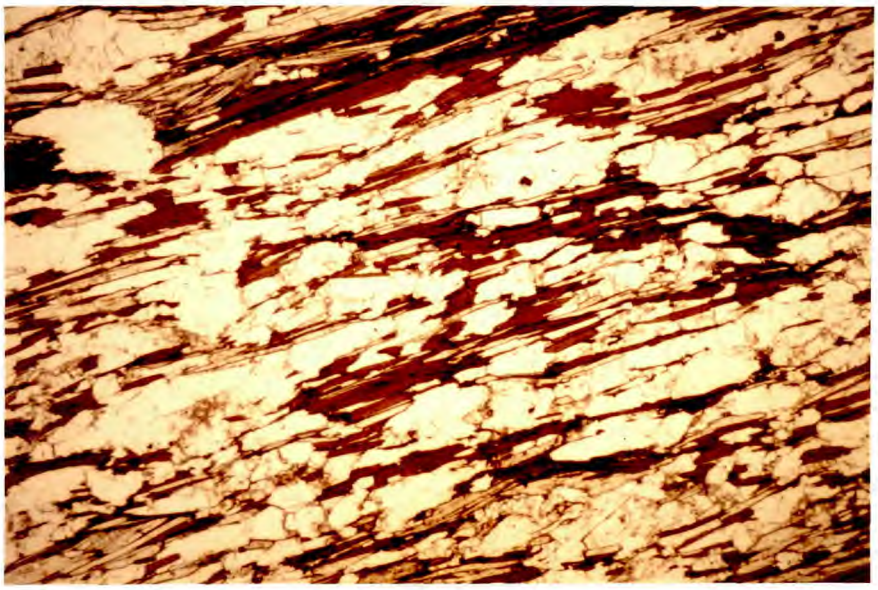


Fig.60(a) Fine-grained, schistose Antigorio Gneiss. Schistosity outlined by thin muscovite and biotite flakes. X 30.

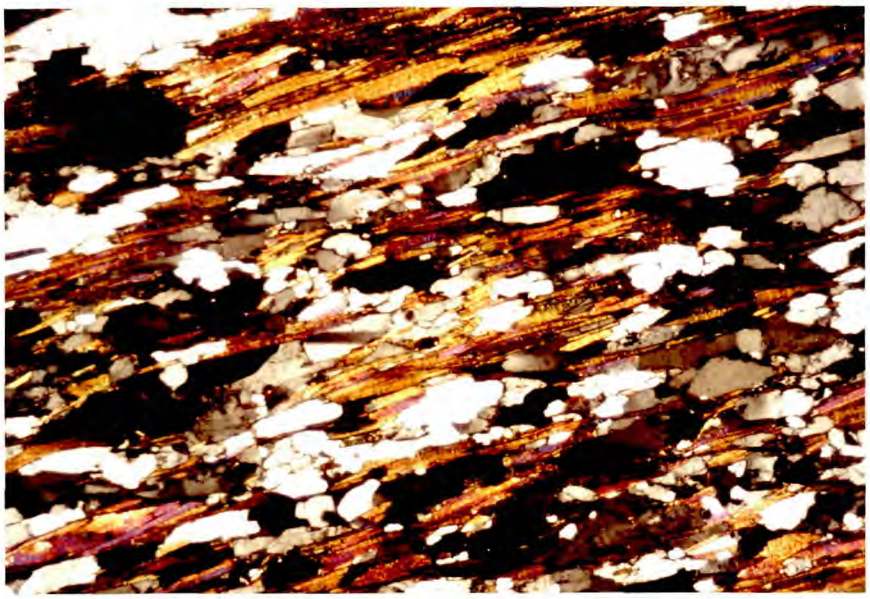
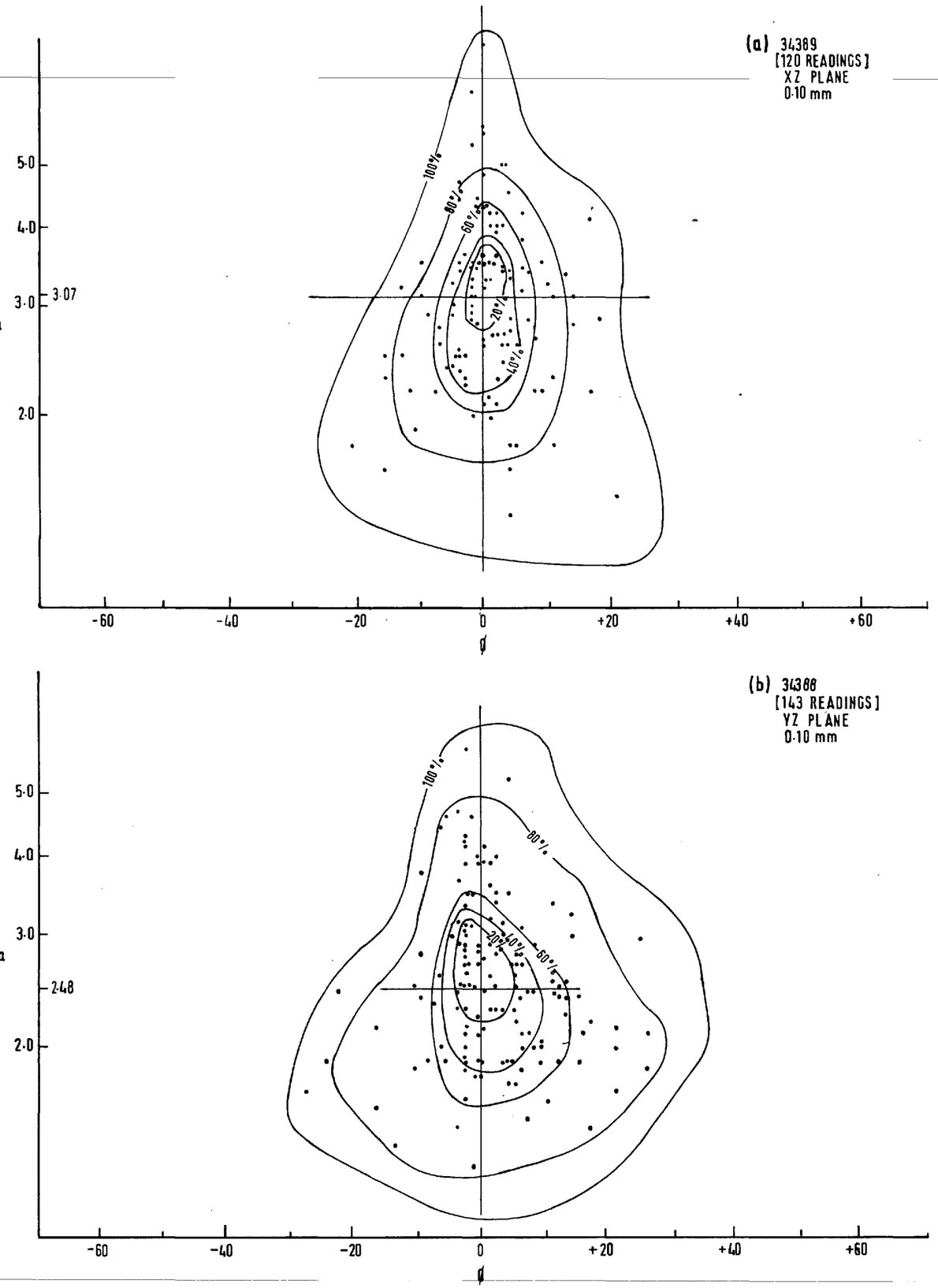


Fig.60(b) Same as above in polarised light. Note strong dimensional orientation of quartz and albite grains.

Ra / ϕ DIAGRAMS SCHISTOSE ANTIGORIO GNEISS



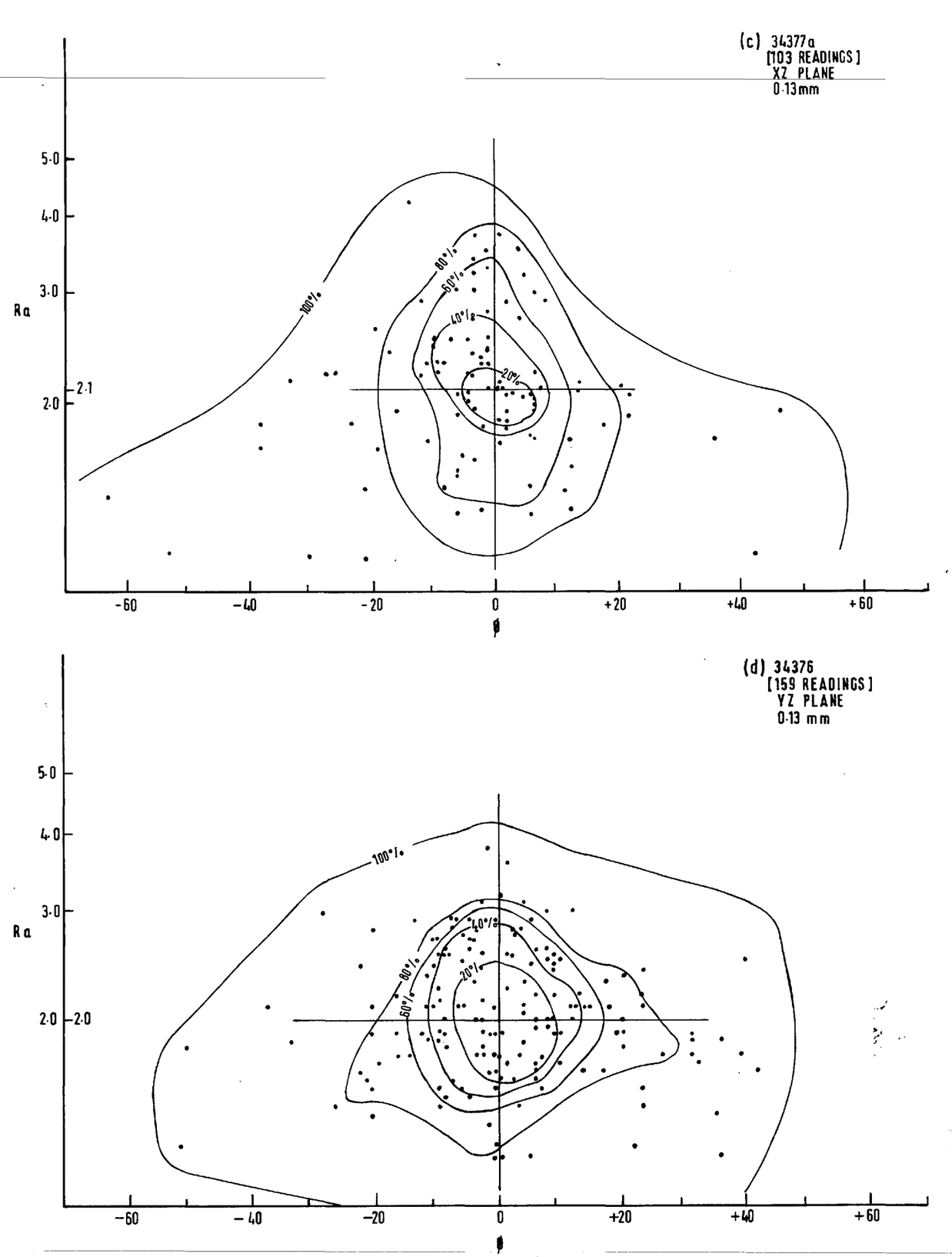




Fig. 62(a) Quartz auge in schistose Antigorio Gneiss. Note cracking and reduction in grain size towards end of auge. X 30.

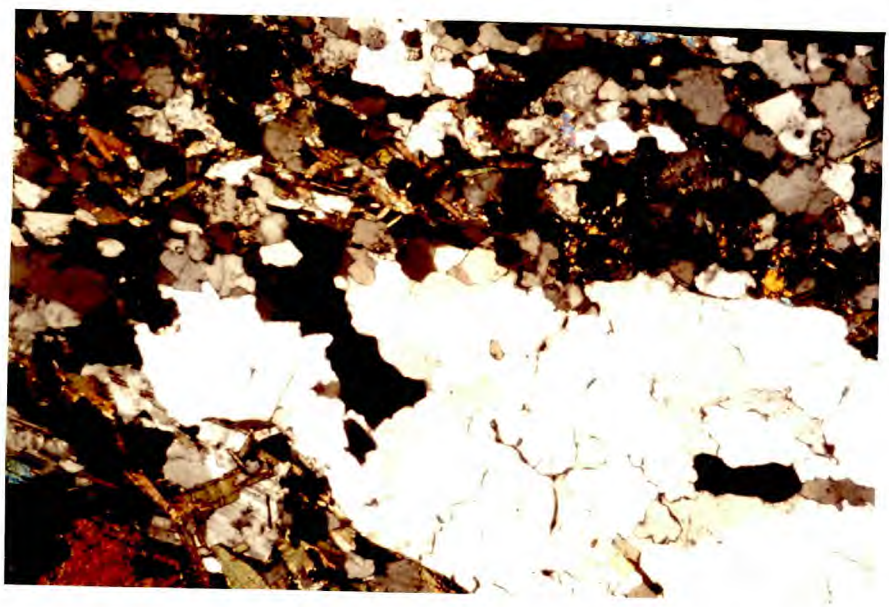
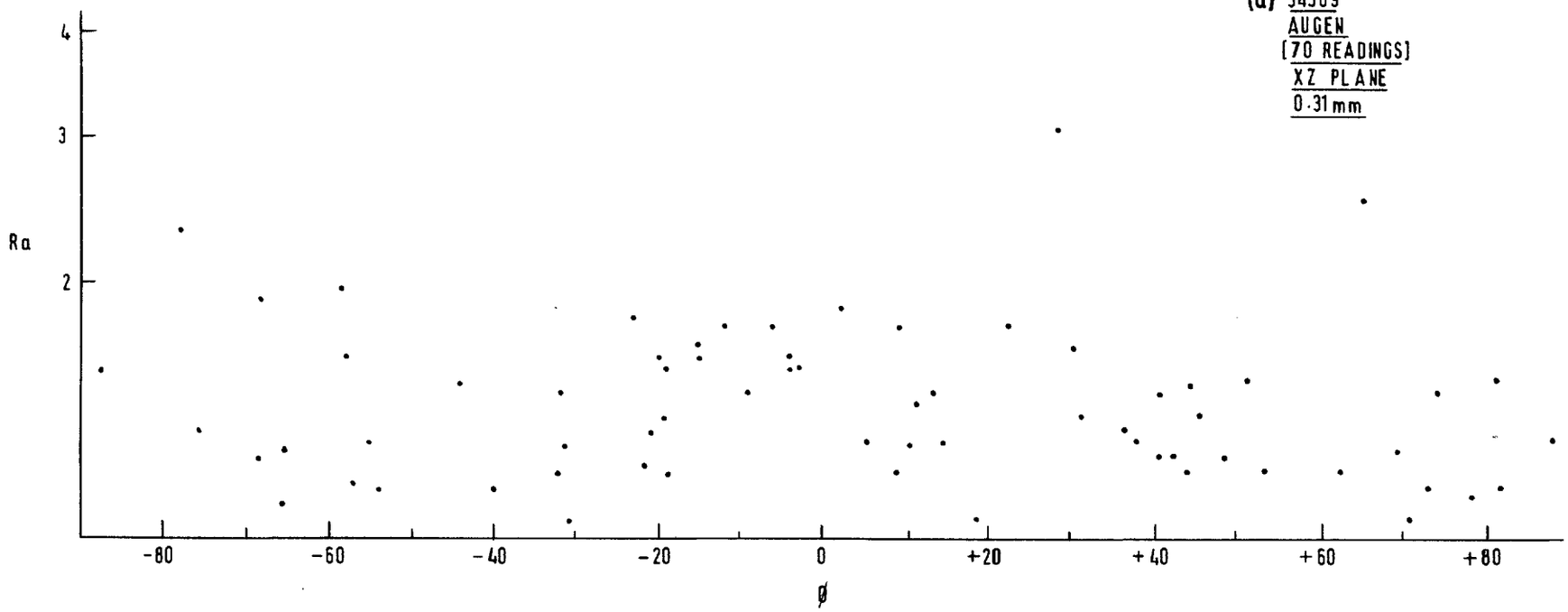
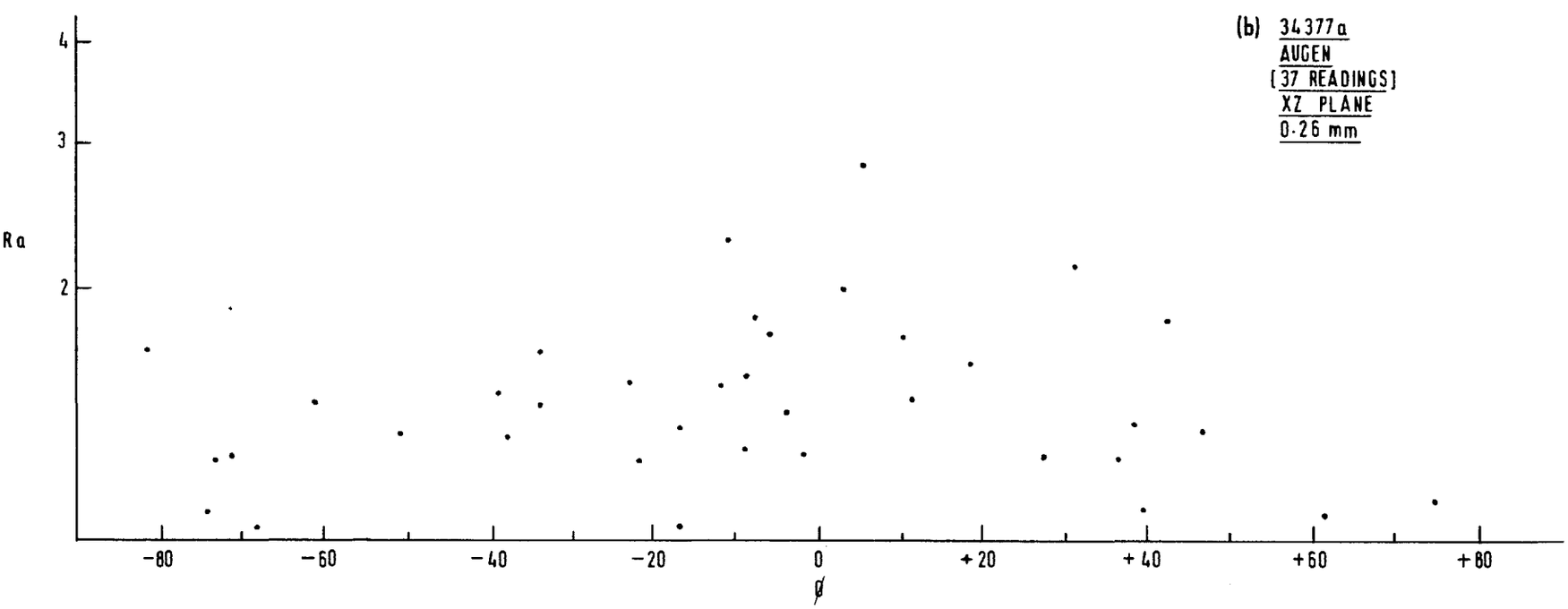


Fig.62(b) Quartz auge in schistose Antigorio Gneiss. X 30.

FIGURE 63

Ra / ø DIAGRAMS ANTIGORIO GNEISS





9:5 Metamorphic Textures

The Antigorio Gneiss is notable for its simple mineral assemblages and metamorphic textures. There appears to be a direct correlation between the grain size and appearance of new minerals. The mineral assemblage changes from quartz-orthoclase-microcline-oligoclase/andesine-biotite in the coarse grained gneiss to quartz-albite-biotite-muscovite-epidote (-ilmenite-chlorite-almandine-hornblende) in the fine grained schist. The method of examining the metamorphic textures of the rocks follows that outlined by Spry (1963), and is described in Chapter 13.

The minerals present in the coarse grained gneiss are probably the original igneous constituents. Feldspars include large plagioclase crystals (An_{24-35}), some with bent twin lamellae, slightly sericitic orthoclase, and very prominent microcline with perthitic intergrowths. Myrmekitic and graphitic intergrowths with quartz are common. Large quartz grains are often cracked and polygonised, and most have undulose extinction. The smaller grains have ragged, sutured boundaries. The minor biotite in the gneiss has a pale yellow (X), very dark olive green to green brown (Z) pleochroic scheme, but is often altered to secondary green chlorite. The biotite flakes show a preferred orientation, and as they are parallel to the F2 schistosity they probably recrystallized syntectonically during F2 from nucleii provided by original igneous biotite, resembling those grown experimentally by Means and Paterson (1966).

With increasing reduction in grain size metamorphic minerals become more common. Quartz has a strong dimensional preferred orientation, probably resulting from syntectonic recrystallization (Hobbs, 1968). Microcline is almost completely absent, and only a few small twinned plagioclase grains were observed. Most plagioclase occurs as untwinned grains with a composition An_{3-8}. Biotite and muscovite are common, although biotite is usually more dominant. Biotite forms thin, often needle-like flakes outlining the strong fabric. The pale yellow-dark olive green biotite continues into the schist, where a variety with a pale yellow (X) to medium red-brown (Z) pleochroic scheme appears. These two varieties never occur together. Most biotite crystallized syntectonically, but a few stubbier flakes, randomly oriented over the parallel fabric, probably grew post-tectonically.

Muscovite first appears along the edges of the biotite flakes, but eventually forms distinct, long thin cleavage flakes which are the dominant mica in some portions of the schist. Most muscovite is syntectonic, but there are a few larger, randomly oriented post-tectonic flakes.

Minute pale yellow epidote grains become common when the grain size is reduced below approximately 0.20 mm. The grains are initially associated with biotite along the edges of shear zones, but eventually become peppered through the matrix of the schist, and make up to 5% of some thin sections.

Rare small almandine garnet porphyroblasts occur in a few of the schists as both minute euhedral grains and larger skeletal grains. They grow post-tectonically across the fabric. One small post-tectonic hornblende porphyroblast occurs in one thin section of schist.

The following generalised reactions are considered the most likely to have generated new minerals: breakdown of microcline and orthoclase liberating K and Al, aiding the growth of muscovite and biotite; breakdown of plagioclase liberating Ca for the growth of epidote; orthoclase breakdown also liberating Na to combine with the Ca-depleted plagioclase, producing albite.

These reactions are essentially isochemical, but are dependent on the addition of water to the metamorphic system. This was probably introduced from an external source, as suggested by Beach (1971) when describing a similar problem of metamorphic regeneration in shear zones. The most likely source of water appears to have been the Mesozoic rocks which form an envelope around the Antigorio Gneiss.

9:6 Correlations and Conclusions

The Antigorio Gneiss has undergone intense strain resulting in the transformation of each unit cube into a thin rectangular slab (fig.49). The strain is considered to be largely the result of the F2 deformation, as xenoliths contained in the gneiss are flattened in the plane of the F2 schistosity and elongated in the direction of the F2 lineation. It is difficult to determine how much of the strain recorded from the xenoliths

results from the F3 deformation. Xenoliths deformed by F3 minor folds are only slightly thickened in the hinge regions, and do not appear to have undergone appreciable changes in shape on the fold limbs.

The strains determined from the xenoliths in the Antigorio Gneiss are comparable to those described by Higgins (1964b) and Chadwick (1965). In the Basodino area Higgins used conglomerate pebbles in the Lebendun Group to calculate a 55% to 70% flattening strain, and in the Lukmanier region Chadwick used deformed ooids in the Mesozoic rocks and xenoliths in the Gotthard Gneiss also to calculate a 55% to 70% flattening normal to F2 schistosity. The principal extension directions of the deformed objects were parallel to the F2 lineation. In the Basodino area, as in the Valle di Bosco, the F2 lineation was parallel to the F2 fold axes, but in the Nufenen and Lukmanier regions it was oriented approximately north-south, perpendicular to the major F2 fold axes. Sibbald (1971) and Thakur (1971) also recognised that the F2 lineation was perpendicular to the F2 fold axes in the Val Piora and Molare areas.

The change in the direction of principal extension during the F2 deformation, between the southerly area where it was parallel to F2 fold axes and the northerly area where it was perpendicular to the fold axes, appears to occur in the frontal zone of the Lower Pennine Nappes. The reason for the change in extension direction may be a result of the apparent decrease in strain northwards (compare the results from the Valle di Bosco and Lukmanier). If sufficient deformed objects could be found, the correlation of principal extension direction with tectonic position in the nappe pile, and possibly rock type, may provide a fruitful line of research.

It is suggested that during the F2 deformation the Antigorio Gneiss behaved in a ductile, "non-linear" manner, such that a small increase in stress would have caused a large increase in strain (Rutter, 1970; P. Cobbold, pers. comm.). A steep deformation gradient would have been set up, with a concentration of strain in the marginal zones of the gneiss. The results of this very high strain can be seen in the strong schistosity and lineation, the extreme thinning of the xenoliths, and the fine grain size leading to the homogenisation of the rock and the obliteration of the dykes.

Beach (1971; 181-2) has suggested that shear zones, with which the margins of the Antigorio Gneiss may be compared, result from an initial phase of fracturing, granulating the rock, followed by the coallescing of fractures by further shears and tensile failure. He also suggests (p. 200) that water would move out from the source area in the direction of the maximum compressive stress. It is considered that water would thus have been introduced into the highly sheared margins of the Antigorio Gneiss, initiating the metamorphic reactions previously described.

CHAPTER 10

UNDEFORMED PRE-ALPINE BASEMENT ROCKS

10:1 Introduction

This section concerns the unexpected occurrence of relatively undeformed, pre-Mesozoic basement in the intensely deformed rocks of the Valle di Bosco. Both field observations and the results of a petrographic examination are used to draw some conclusions on the pre-Alpine history of the area, and the nature of the Alpine deformation.

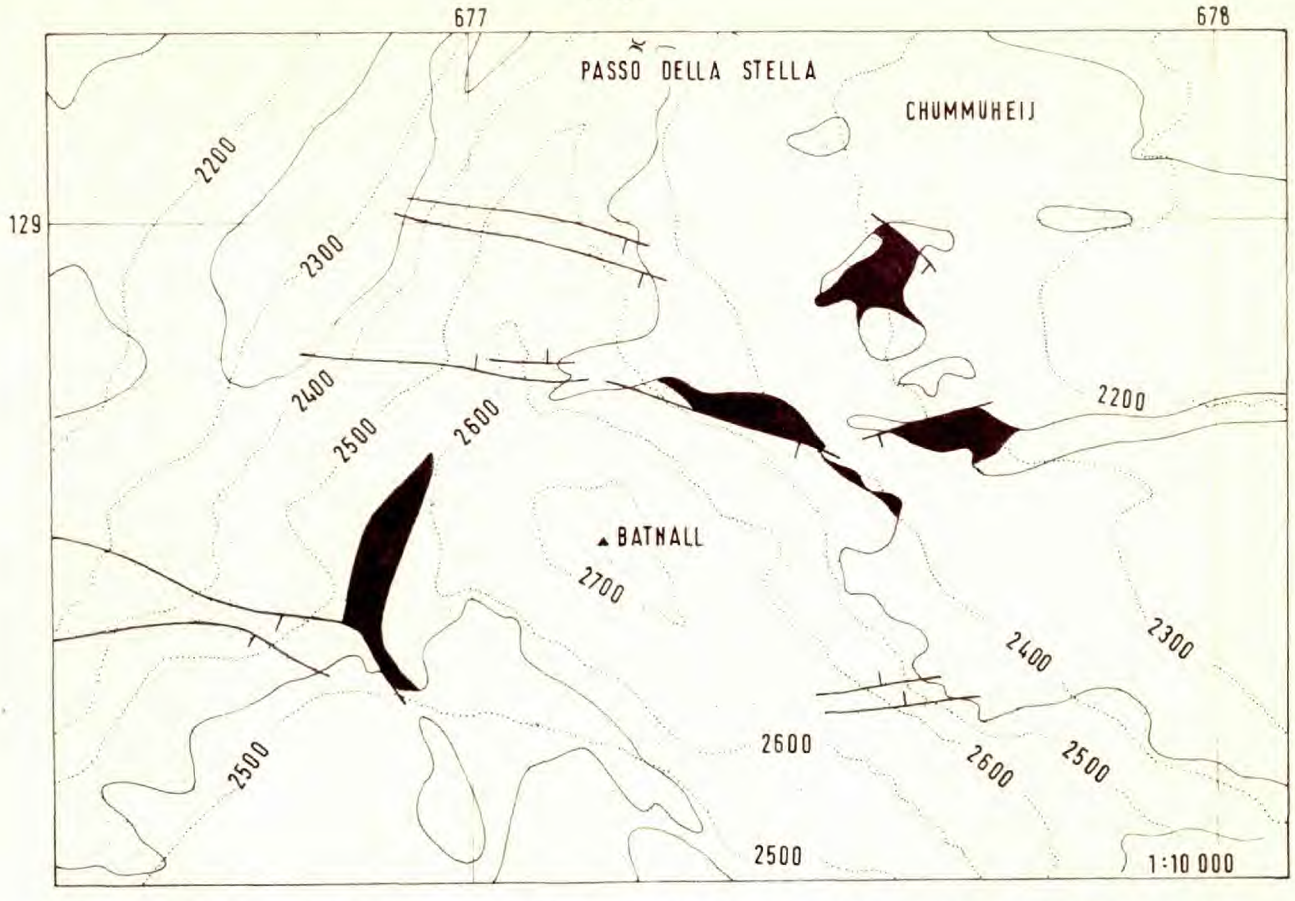
10:2 Field Relations

A number of large lenses of rocks macroscopically unaffected by any Alpine deformation occur in the vicinity of the Batnall at the head of the Valle di Bosco (fig.64a). They are recognised by their distinctive rock types, which are unlike those seen elsewhere in the region, and by their strong discordance with rocks containing a definite Alpine fabric. The lenses are completely enveloped by the Alpine F2 schistosity, and resemble very large augen.

The most accessible and best exposed of these lenses are at the foot of the cliffs immediately northeast of the summit of the Batnall. The largest, 400 m. long, is exposed vertically for 90 m.. Two smaller lenses are exposed 100 m. to the ENE and 200 m. to the northeast. That to the ENE has a vertical exposure of 80 m., and best illustrates the discordant relationship with the Alpine schistosity (fig.64b). A further lens, exposed on the western slopes of the Batnall 200 m. below the summit, extends over 400 m. in a north-south direction and has a maximum vertical exposure of 60 m.

Two distinct rock types, schist and aplitic granite, occur in these lenses. The granite is a medium to fine grained, mottled leucocratic rock, while the schist is a fine grained, semi-pelitic rock with a marked white and dark grey compositional banding. The white, quartz-rich bands often stand out as small ridges. Although the schist contains a few small almandine garnets it lacks the abundant large porphyroblasts of the semi-pelitic rocks with a strong Alpine schistosity.

FIGURE 64



(a) LOCATION MAP. LENSES IN WHICH PRE-ALPINE GEOLOGY IS PRESERVED ARE SHOWN IN BLACK OUTCROPS DOTTED CONTOURS ARE IN METRES ——›— FAULTS



(b) BASEMENT ROCKS UNDEFORMED DURING ALPINE OROGENY OCCUR IN LARGE BODY AT RIGHT ALPINE F_2 SCHISTOSITY AT LEFT IS DEFLECTED AROUND BODY CONTAINING UNDEFORMED BASEMENT ROCKS ENE OF BATNALL (677712 87)

The granite intrudes the schist as thin stringers, dykes up to 60 cms thick with clear marginal contact effects (fig.65a), and larger homogeneous masses with abundant small rafts of schist (fig. 65b). There are also a few very thin dykes of muscovite pegmatite. Nowhere in the region does the granite, or its gneissic equivalent, cut the Mesozoic rocks, and its youngest possible age is therefore Late Palaeozoic.

The semi-pelitic schist is deformed by two generations of coaxial minor folds, but because of the dislocation effects of the granite intrusions there is no consistency in the direction and angle of plunge of the folds from outcrop to outcrop. Both sets of folds deform a pre-existing schistosity (fig.66), but there is little evidence for their age other than Palaeozoic, as they clearly pre-date the granite.

Macroscopically the transition from pre-Alpine to Alpine-deformed rocks is very abrupt, although in one of the lenses northeast of the Batnall the near vertical granite dykes and schist gradually turn over until they are almost parallel with the Alpine schistosity. Across the boundary the clearly discordant relationship between the granite and the schist is largely obliterated, and the rocks are transposed and transformed into thin parallel bands of white muscovite-biotite gneiss and semi-pelitic schist with abundant staurolite and garnet porphyroblasts. Both of these rock types have a very strong planar fabric, which, from the regional evidence and detailed work in the Valle di Bosco, can only be the Alpine F2 schistosity.

This lit-par-lit-like relationship of Alpine schist and gneiss occurs over a wide area adjacent to Rovana Stream west of Bosco-Gurin, and is particularly well exposed in the deeply incised north bank tributaries between Schwarza Brunna and Bosco-Gurin. However, the original discordance is locally preserved, despite the intensity of the Alpine deformation, in outcrops on the north bank of the stream 500 m. upstream from Chumma (67851288). The irregular boundary between gneiss and schist is crosscut by the strong F2 schistosity, and small schist xenoliths in the gneiss lie parallel to this fabric (fig.67).



Fig.65(a) Granite dyke with chilled margins cutting pre-alpine schist. ENE of Batnall (67771288).



Fig.65(b) Thin granite dykes cutting pre-alpine schist. Note small xenoliths in granite just above centre of photograph. NE of Batnall (67731288).



Fig.66 Strongly folded schist in area of basement rocks undeformed during Alpine Orogeny. The folds resemble alpine F3 minor folds, but are cut by granite dykes. NW of Batnall. (67771289).



Fig.67(a) F2 schistosity cutting obliquely across boundary between Bosco Group Gneiss and staurolite schist. West of Chumma. (67851288).



Fig.67(b) Thin band of gneiss lying oblique to F2 schistosity. Note small schist xenolith at centre of photograph is elongated parallel to schistosity. West of Chumma. (67851288).

Insufficient xenoliths were observed from which the strain could be determined, but the xenoliths show the same characteristics as those in the schistose Antigorio Gneiss; i.e. they are flattened in the schistosity plane, and elongated in the lineation direction. The axial ratios of xenoliths in the XZ plane vary from 5.9 to 112.8, the average being 47.9. In the YZ plane the axial ratios are between 4.8 and 6.6, and in the XY plane they vary from 2.6 to 8.0.

10:3 Microtextural Relations

Samples of granite from the dykes appears undeformed in hand specimen, but in thin section the most outstanding feature is the random development of mortar texture (Spry, 1963) making up 15%-20% of the slide (figs. 68,69). The areas unaffected by mortar texture have a typical granite texture with a relatively even grain size averaging 0.40 mm., and a mineral assemblage of quartz, K feldspar, muscovite, biotite and minor tourmaline and apatite. All the quartz and feldspar grains show undulose extinction, but a number are also cracked and a few have serrated boundaries. The muscovite and biotite (light to dark red-brown plechroism) occur as large plates.

The development of the mortar texture has resulted from the random, recrystallization of both entire grains and parts of grains. The minute polygonal grains of the mortared areas have a remarkably uniform size (0.03mm.) and shape. The pattern of recrystallization within large, partly deformed grains passes from a strained, uncracked portion, through a narrow, partly polygonised zone, to a region of complete recrystallization with a mosaic of minute, randomly oriented grains with straight boundaries. Associated with the areas of mortar texture are abundant minute needles of muscovite (sericite), and a few small biotite flakes and some very small almandine garnets (fig. 68). The granite thus shows clear evidence of its original, pre-Alpine texture as well as the incipient development of an Alpine deformation texture. The original mineral assemblage remains intact, except in the areas of mortar texture where it is replaced by Alpine metamorphic minerals.

Immediately outside the lenses containing the relatively undeformed basement rocks, the granite is transformed into a white to light grey gneiss (fig.70). The main microscopic changes are the development of a

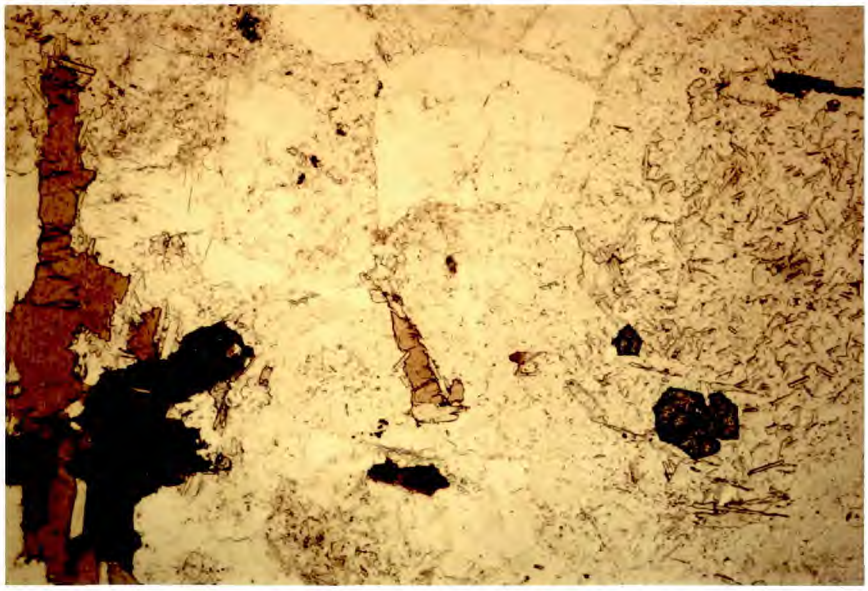


Fig.68(a) Mortar texture in granite. Large grain at right has completely recrystallized. Note minute sericite flakes associated with recrystallized areas. X 30.

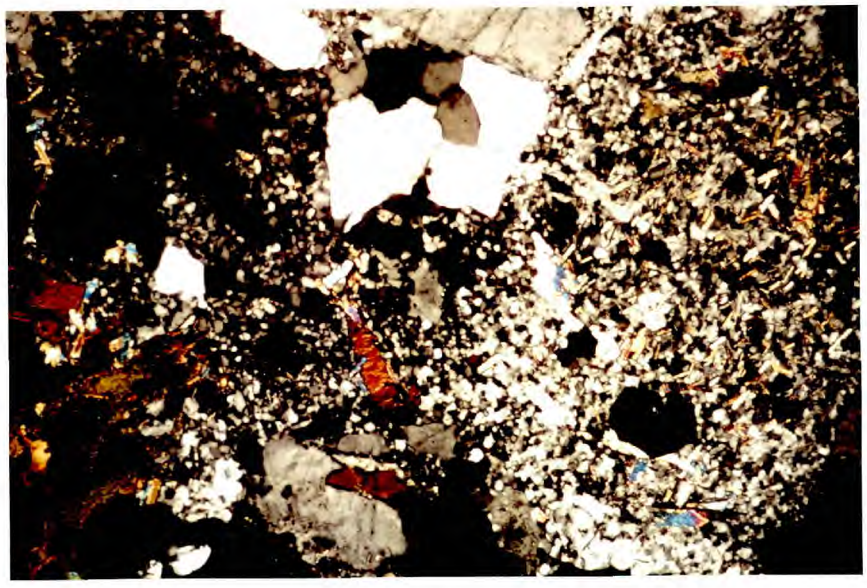


Fig.68(b) Same as above in polarised light.

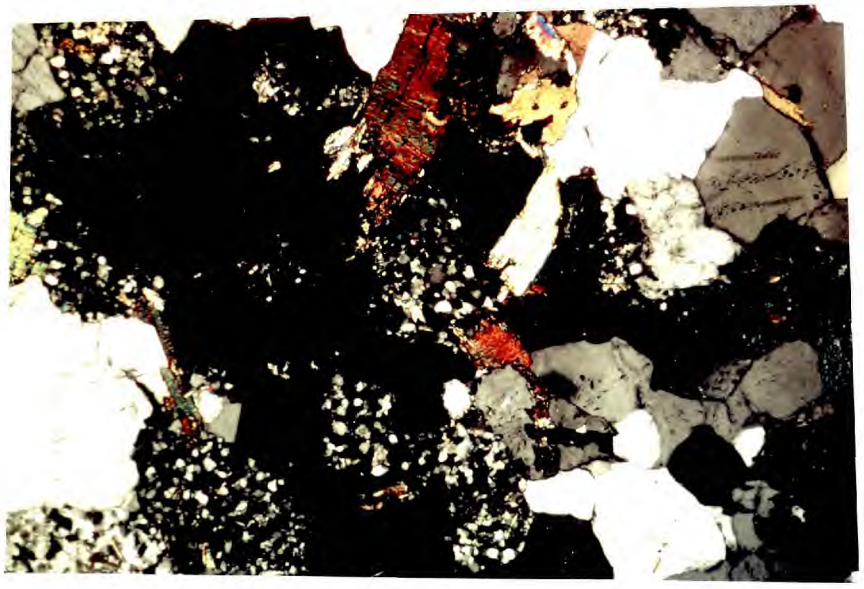


Fig.69 Mortar texture in granite. Granitic texture preserved at right, although quartz grains severely strained. X 30.

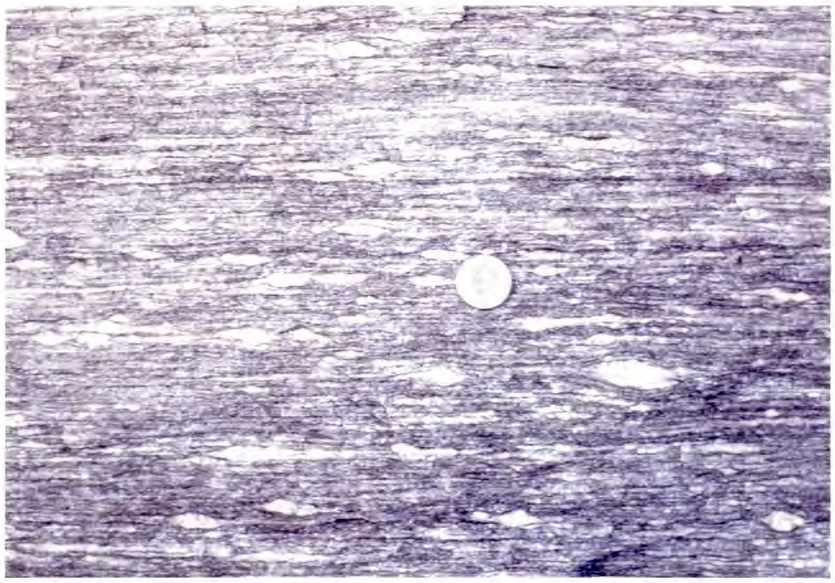


Fig.70(a) Bosco Group gneiss showing augen structure. Compare texture with that of granite in Fig.65.

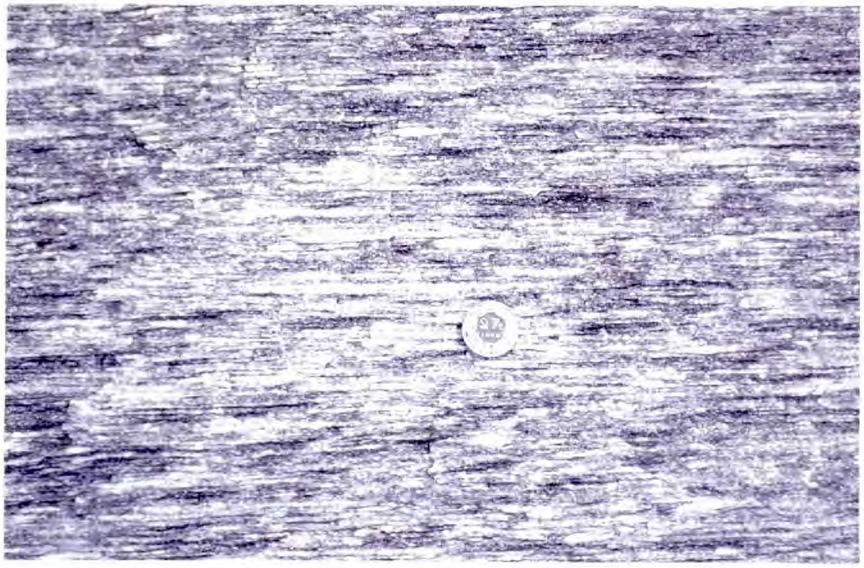


Fig.70(b) Bosco Group gneiss showing development of strong planar fabric.

much finer grain size (average 0.06 to 0.09 mm.), a prominent planar fabric, and the appearance of Alpine metamorphic minerals. The fabric consists of minute, polygonal quartz grains and aligned micas. In one section (36316) the micas enclose irregular patches of large, strained quartz grains and in another (36314) they lie between parallel bands of discontinuous quartz aggregates up to 3 mm. thick (fig. 71). The average size of the quartz grains in these augen is 0.40 mm., the same as that in the granite.

The mineral assemblage of the gneiss is essentially the same as that of the granite, but minerals in the gneiss are largely recrystallized. Muscovite and biotite (pale to medium brown pleochroism) occur as minute, aligned needles associated with the areas of mortar texture, and large plates growing randomly throughout the sections. Almandine garnet is present both as minute grains "peppering" parts of the mortar texture areas, and as larger, spongy porphyroblasts up to 0.25 mm. across, often with oriented inclusion trails of ilmenite and biotite. Ilmenite occurs both as small needles aligned with those of the muscovite and biotite, and as small, irregular grains, while tourmaline forms small euhedral grains, strongly pleochroic from neutral to olive-green.

The pre-Alpine schist in the lenses is a typical semi-pelitic rock with mineralogically distinct layers of oriented mica flakes and rectangular quartz grains. The layers are up to 2.5 mm. thick (fig. 72a). This strong compositional banding distinguishes the pre-Alpine schist from the Bosco Group semi-pelitic schists with their aligned, but generally separate micas and large garnet and staurolite porphyroblasts. The mineral assemblage of the pre-Alpine schist includes quartz, dominantly as elongate, ragged-edged grains, rare plagioclase, equal amounts of biotite and muscovite as long, narrow flakes, minute ilmenite, epidote and apatite grains, and very small almandine porphyroblasts. The average size of the quartz grains is between 0.10mm and 0.13mm.

In one thin section (36320) the mica layers are folded, and a second pre-Alpine fabric has developed parallel to the axial planes of the folds (fig. 72b). Polygonised quartz grains in the fold hinges have their longest edges subparallel to the second fabric, which is emphasised by isolated, oriented flakes of muscovite and biotite. Some muscovite and biotite has grown mimetically over the earlier mica layers on the fold limbs.

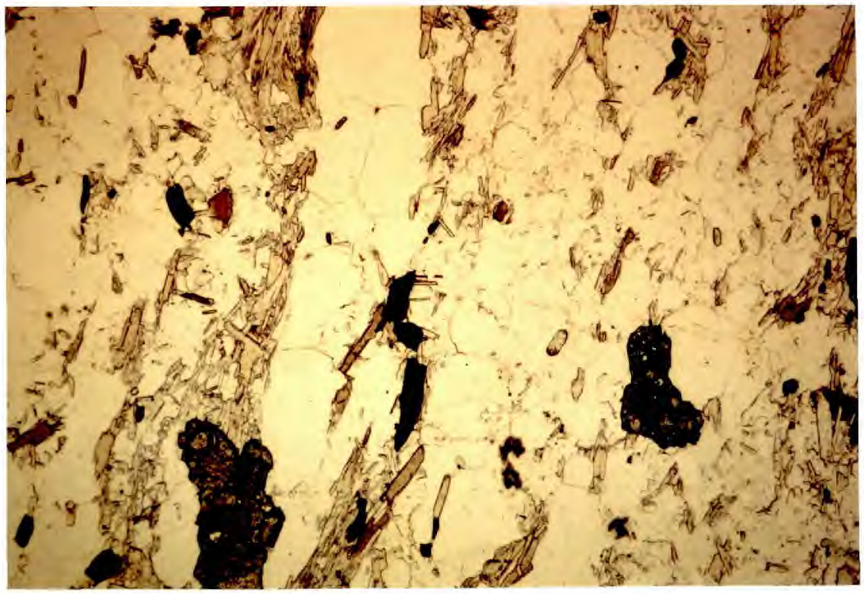


Fig.71(a) Texture of Bosco Group gneiss. Recrystallization much more widespread than in granite. Note partial development of bands of fine and coarse grained quartz, and strongly aligned muscovite and biotite flakes. X 30.

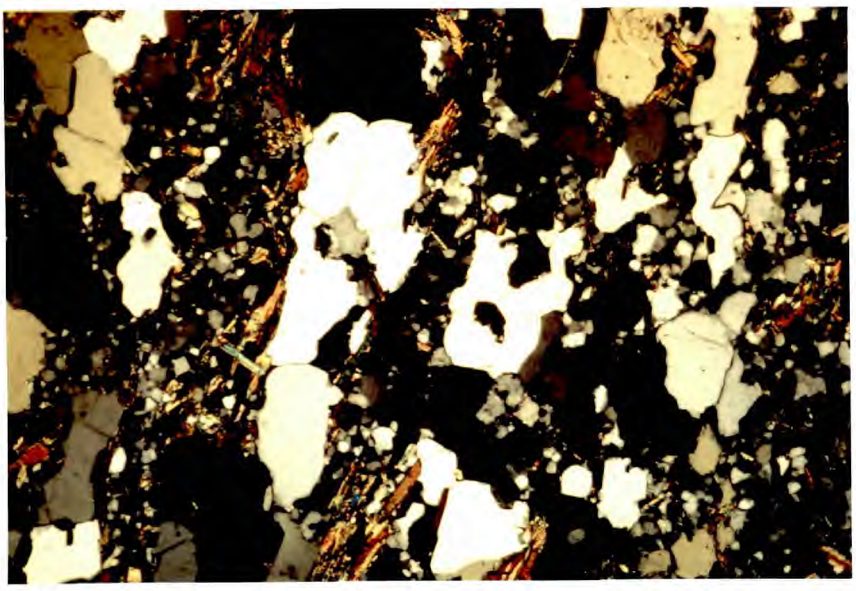


Fig.71(b) Same as above in polarised light.



Fig.72(a) Schist from area undeformed by alpine deformation. The conspicuous mica-quartz layering is in sharp contrast to the fabric development in the alpine schists. X 30.

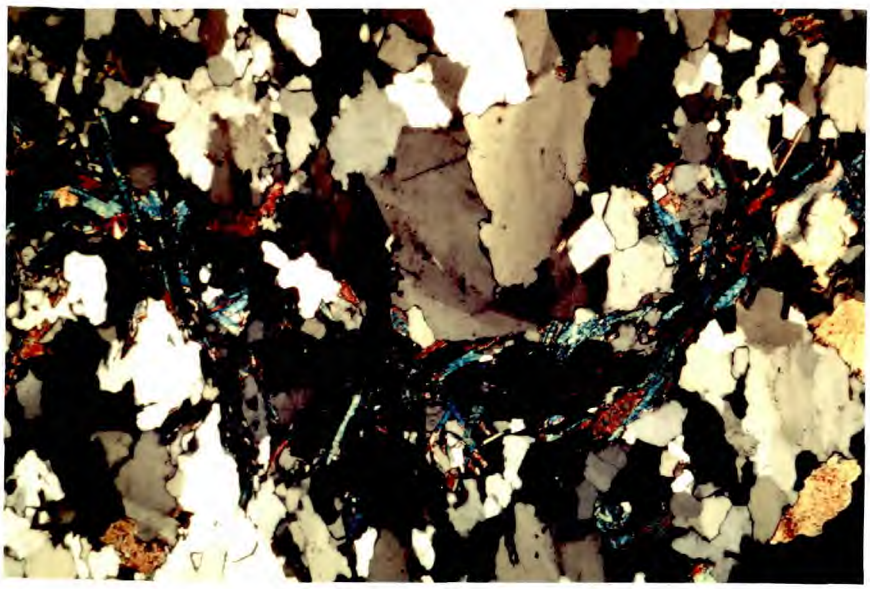


Fig.72(b) Pre-alpine schist showing folded mica layer and development of axial plane fabric. X 30.

10:4 Outline of structural and Metamorphic history.

Combining the evidence from the microscopic textures with the field data, the following history can be inferred from the rocks of the pre-Alpine lenses and their immediate surroundings:

1. Syntectonic fabric development, and crystallization of muscovite, biotite, quartz and ilmenite.

2. Post-tectonic crystallization of garnet, muscovite, biotite and epidote.

3. Folding of the fabric and development of a second, weaker schistosity, accompanied by the syntectonic crystallization of quartz, muscovite and biotite.

4. Further folding, without fabric development.

5. Granite intrusion.

These first five events are all pre-Alpine (i.e. Pre-Triassic).

6. Partial destruction and transposition of fabric by the development of mortar texture during the Alpine F2 deformation. Syntectonic recrystallization of quartz, muscovite, biotite and ilmenite.

7. Post-tectonic recrystallization of large, randomly oriented muscovite and biotite plates and very small garnet porphyroblasts.

The outstanding implication of this history is that after the granite intrusion the pre-Alpine basement rocks of the Valle di Bosco remained texturally undeformed until the Alpine F2 deformation. This suggests that during the Alpine F1 deformation, when the Mesozoic rocks were tectonically intercalated between the Antigorio Gneiss and the Bosco Group, the basement rocks were displaced without suffering large finite strains. The most likely form of this type of deformation would have been the development of large thrust sheets of basement rocks, similar to those described from the northern Aar Massif (Collet and Parejas, 1931).

CHAPTER 11

POST F3 DEFORMATION

11:1 Introduction

The youngest structural features observed in the rocks of the Valle di Bosco are chlorite-filled tension gashes and joints, quartz-filled and barren joints, faults and rare kink folds. Barren joints were distinguished from faults because they do not displace the rocks on either side. The kink folds, tension gashes and chlorite- and quartz-filled joints have a pronounced NNW-SSE trend, while the barren joints and faults have a dominant NNW-SSE trend and a secondary E-W trend.

11:2 Kink Folds

Kink folds are rare in the rocks of the Valle di Bosco. They are small, asymmetric structures deforming the schistosity planes of the metamorphic rocks. Their steep limbs invariably dip west, and their axial planes strike NW-SE. The hinge lines of the kink folds generally plunge gently southeast.

The majority of the kink folds occur in the hornblende schist and have amplitudes up to 1 cm. Most of the remainder occur in the semi-peltic schist and a few in the schistose gneiss and marble, and have amplitudes up to 5 cms. The orientation of the axial planes suggests that the kink folds formed while the area was subjected to a NE-SW directed compression.

11:3 Tension Gashes

Small, sigmoidal, chlorite-filled tension gashes occur in narrow zones trending between N.12 W. and N.26 W., and are most common in gneiss. Individual gashes within the zones are oriented between N.40 and N.45 W. They indicate an east-side-north (sinistral) sense of displacement across the zones (fig. 73a).

One example of chlorite-filled tension gashes indicated a west-side-north sense of displacement. The gashes, up to 50 cms in length, much longer than usual, were arranged en echelon and were oriented N.40 W. A

few centimetres to the east, a zone of typical small chlorite-filled tension gashes, indicating an east-side-north displacement sense, was oriented N. 16 W. The two sets of tension gashes are illustrated in fig. 73a.

11:4 Chlorite-Filled Joints

Long, chlorite-filled joints trend between N-S and NW-SE across the area (fig. 73b), and are most common in the Antigorio Gneiss. They are vertical or dip steeply west, and often occur in groups.

11:5 Quartz-Filled Joints

Long, thin quartz-filled joints are most common in the Antigorio Gneiss and Bosco Group Gneiss. The strikes of the joints are symmetrically distributed about a peak between N.20 W. and N.30 W (fig. 73c). All the quartz-filled joints observed dip towards the west, and 45% of the dips were greater than 80°.

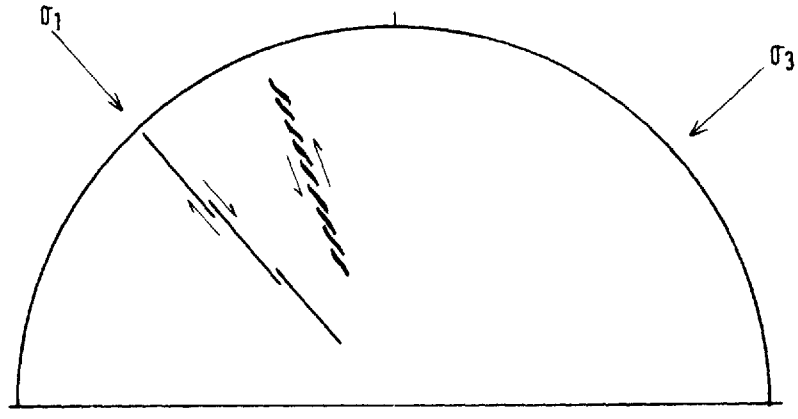
11:6 Development of Mineralised Joints

The small chlorite-filled tension gashes are thought to be the oldest post-F3 joints, and to have developed when the rocks were in a semi-brittle state, having cooled sufficiently to resist deformation by ductile shear. The east-side-north displacement sense along the NNW-SSE trending zones, and the NW-SE orientation of the individual gashes suggests that the principal stress, σ_1 in fig. 73a, was directed NW-SE. The 30° angle between the orientation of the gashes and the zones containing them is possibly equivalent to the 30° angle shown by Anderson (1951) to exist between the principal stress and line of fracture in brittle rocks.

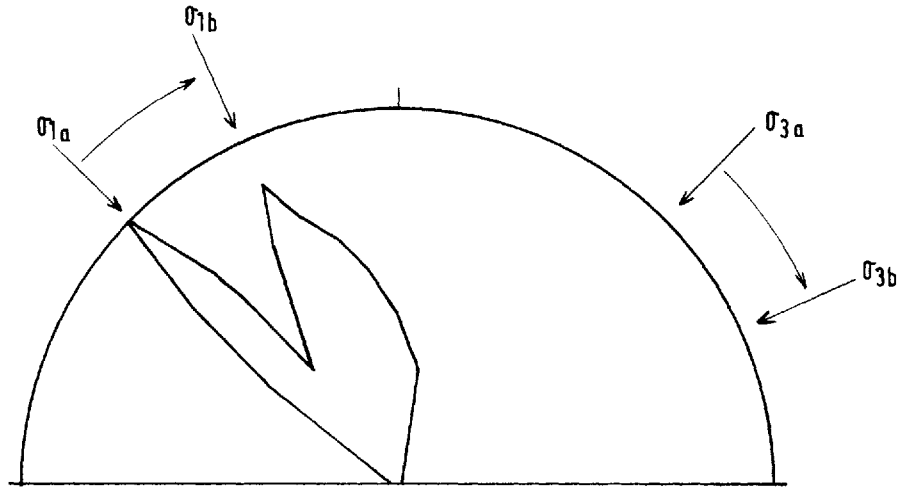
The tension gashes indicating a west-side-north displacement sense are oriented NW-SE, and as they are much longer than the typically small tension gashes they may indicate a greater component of tensile failure. They are considered to be slightly younger than the NNW-SSE oriented tension gash zones, and probably developed as the rocks cooled to the point at which they began to deform in a brittle manner.

FIGURE 73

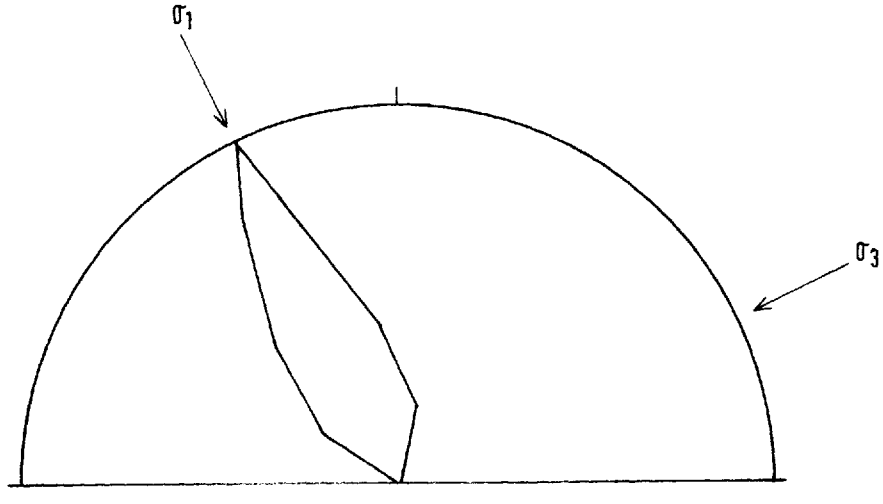
MINERALISED JOINTS



(a) CHLORITE FILLED TENSION GASHES



(b) CHLORITE FILLED JOINTS



(c) QUARTZ FILLED JOINTS

The dominant trend of the chlorite-filled joints is also NW-SE. These are thought to have developed as tensile fractures, under the same stress system as the tension gashes, while the temperature remained sufficiently elevated for chlorite crystallization. The vein filling material is locally derived, as the rocks immediately adjacent to the joints are depleted of ferromagnesian minerals for a distance of 1 to 2 cms, and the feldspars are distinctly potassic. The probable metamorphic reaction, resulting from the introduction of hot water along the open fractures, was the breakdown of biotite forming chlorite and liberating potassium. The chlorite migrated to the open fracture space, while the potassium combined with the feldspars of the country rock. To satisfy this reaction the feldspar would have first had to liberate Na and Ca.

During the formation of the chlorite-filled joints the principal stress appears to have swung slightly from NW-SE to become directed NNW-SSE, parallel to the dominant trend of the quartz-filled joints. Examples of joints filled with both chlorite and quartz occur in Bosco Group gneiss just southwest of Passo Quadrella. The chlorite filling material usually occurs at one end of the fractures, suggesting that the fractures were reopened to enable quartz deposition.

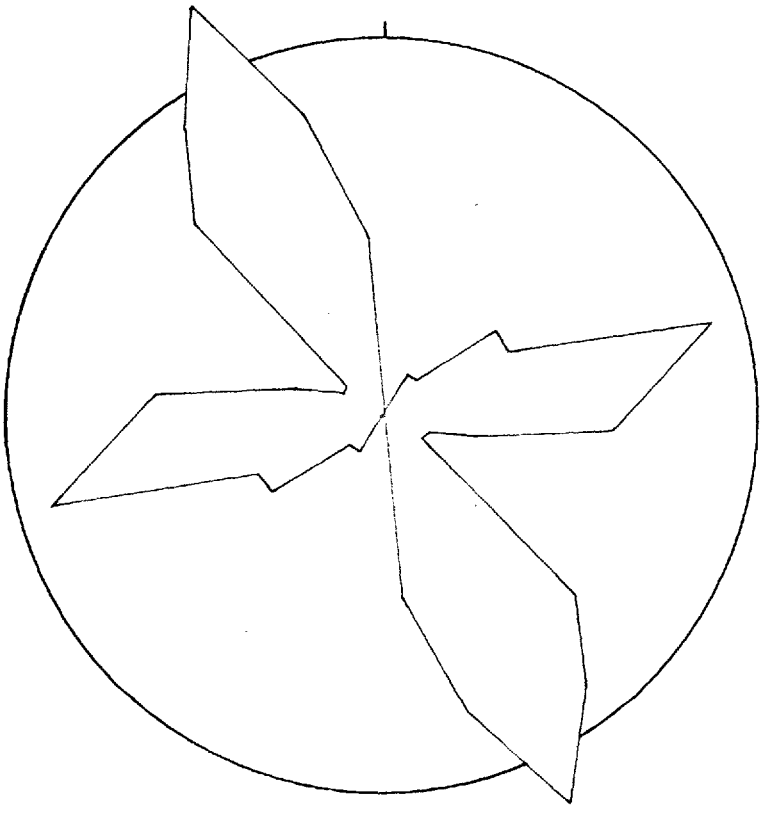
A few quartz-filled joints have well developed steeply plunging slickensides on their surfaces, suggesting that the fractures were re-sheared when the principal stress was near vertical.

Higgins (1964b) recognised a sequence of mineralised joint development similar to that just described. Chlorite-filled tension gashes, in zones striking between NW and NNW, indicated a west-side-north (dextral) displacement sense, the opposite to that indicated in the Valle di Bosco. Chlorite- and quartz-filled joints in the Basodino area also strike between NW and NNW, and dip steeply SW, and Higgins considered that these and the tension gashes were related to a NW-SE directed principal stress.

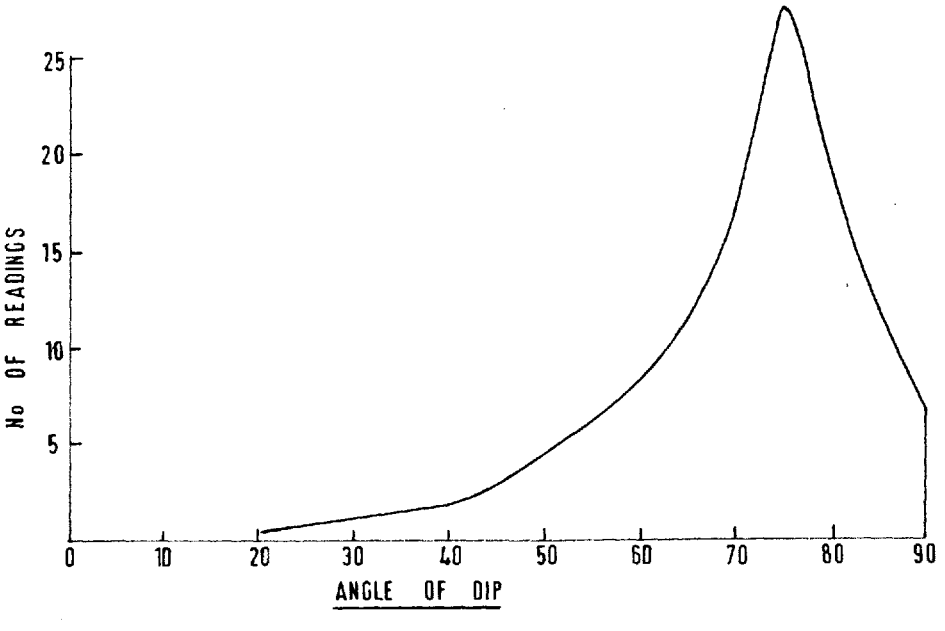
11:7 Barren Joints

Barren joints are considerably more common than both quartz- and chlorite-filled joints. They cut all rocks types and occur in two dominant trends, each of which has a conspicuous statistical peak (fig.74a).

FIGURE 74
BARREN JOINTS

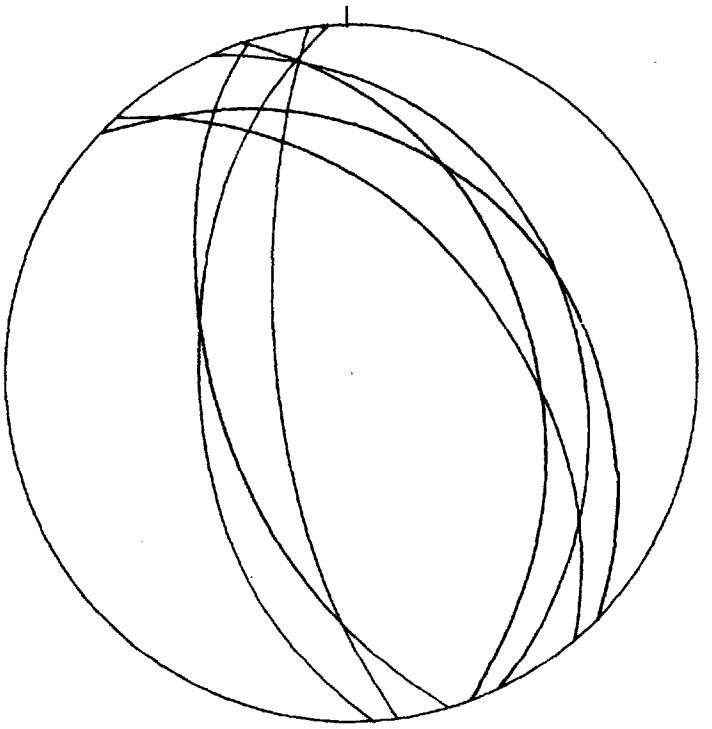


(a) ORIENTATION OF BARREN JOINTS
(67 READINGS)

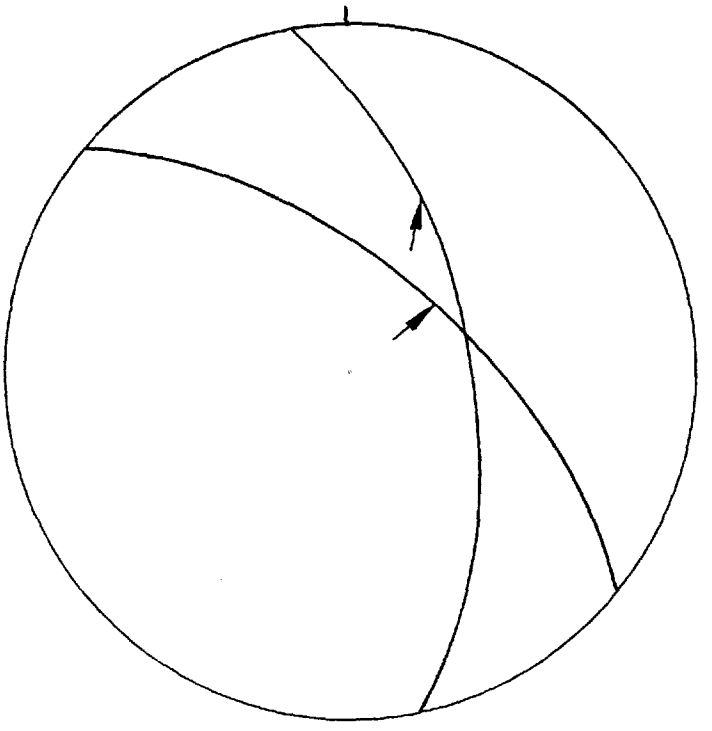


(b) GRAPH OF DIP FREQUENCY OF BARREN JOINTS
(67 READINGS)

FIGURE 75
BARREN JOINTS



(a) CONJUGATE BARREN JOINTS, SCHISTOSE GNEISS
SOUTH FACE OF MARTSCHENSPITZ (6793 1311)



(b) SLICKENSIDE DIRECTIONS IN BARREN JOINTS

The NNW-SSE trend, containing 55% of the readings, occupies a 60° sector between north and N.60 W with a strong peak between N.17 W and N.27 W. The E-W trend occupies a broader, 80° sector between N.30 E. and N.70 W. with a peak between N.72 and N.82 E. In both trends the readings lie symmetrically on either side of the statistical peak.

The plot of the frequency of the dip angles of all the barren joints measured (fig. 74b) gives an asymmetric, unimodal distribution about a peak between 70° and 80°, containing 46% of the total number of readings. The same distribution pattern emerged when the dip frequencies of the NNW-SSE and E-W trending joints were examined separately. The NNW-SSW trending joints showed a tendency to dip northeastwards, while the E-W set showed a tendency to dip southwards. At most localities examined the joints of both sets had consistent directions of dip, but in a few outcrops (e.g. fig. 75a) joints of one or both sets had a conjugate relationship.

There is no obvious evidence for the relative ages of the barren joint sets. Their very steep dips suggest that they developed as tensile fractures under different stress systems, and at different times. The NNW-SSE joints possibly represent the continuation of fracturing by the same stress system as that under which the chlorite- and quartz-filled joints formed. The formation of the E-W trending joints, by contrast, suggests a reoriented stress system with the principal stress becoming directed approximately ENE-WSW.

Steep NNW-SSE and ENE-WSW to E-W trending joints have been described throughout the lower Pennine area by Chadwick (1968), Gunthert (1956 and 1970), Higgins (1964b), Joos (1969), Knup (1958), Kobe (1956), Milnes (1965), Reinhardt (1966), Thakur (1971) and Wenk (1966), and are clearly of regional significance. In most cases the NNW-SSE trending set is the more dominant. Reinhardt recognised two sets of NNW-SSE trending joints, the earlier one being mineralised and the later barren.

11:8 Faults

Faults were distinguished from barren joints in the field by having observable displacements across them, nearly always in a normal sense. Most of the displacements are less than 4 m., but a few faults with throws greater than 50 m. were recorded. The strikes of the faults fall into two

distinct groups, (figs. 76, 77a). A dominant NNW-SSE trend between N.55 W. and N.10 E contains 64% of the readings, and includes a very strong peak between N.20 W. and N.40 W. A secondary E-W trend, between N.50 E. and N.75 W, has a main peak between N.70 E. and N.80 E., and a minor peak between N.70 W. and N.80 W. The two fault trends show up in a most spectacular manner on the gently sloping Bann area, and are illustrated in fig. 78a.

The frequency of the dips of all fault planes measured are statistically distributed about a unimodal peak between 60° and 70° (fig. 77b). The dips range from 27° to 90°, but 35% occur in the 60° to 70° group. The same pattern emerges when the faults of the different trends are treated separately. The NNW-SSE trending faults show a greater tendency to dip northeast, while the E-W trending faults show a tendency to dip south, and are generally steeper. Both the NNW-SSE and E-W trending faults include conjugate sets.

As the faults show the same general trends as the barren joints there may be a close genetic relationship. The main statistical difference between the faults and barren joints is the steeper dips of the joints.

The NNW trending faults are best exposed on the ridge between the Valle di Bosco and the Valle di Campo (fig. 78b). They commonly form gullies on the northern slope, while on the southern slope the fault planes are exposed on steep cliff faces. Deep gullies also follow many of the NNW trending faults on the northern slopes of the Valle di Bosco. Many of the faults along which gullies had formed have surprisingly little displacement across them, frequently less than one metre.

A number of fault planes were observed with slickensided surfaces (see fig. 76). The slickensides generally plunged in the direction of dip of the fault planes, confirming the normal displacement sense indicated by the offsetting of lithological boundaries. The slickensides on the very steep plane (70° to 80°) of the Grosshorn Fault were an exception to the general observations. They plunge at 40° towards the SSE, and indicate a substantial component of horizontal movement.

64 DIP OF FAULT PLANE

(15m) VERTICAL DISPLACEMENT IN METRES (ON DOWN THROWN SIDE OF FAULT)

37 PLUNGE OF SLICKENSIDES ON FAULT PLANE

Wandfluhhorn

Hendar Furggu Fault

Martschenspitz

Ritzberg

Guriner Furka Fault

Bosco - Gurin

Kleinhorn Fault

Grasshorn Fault

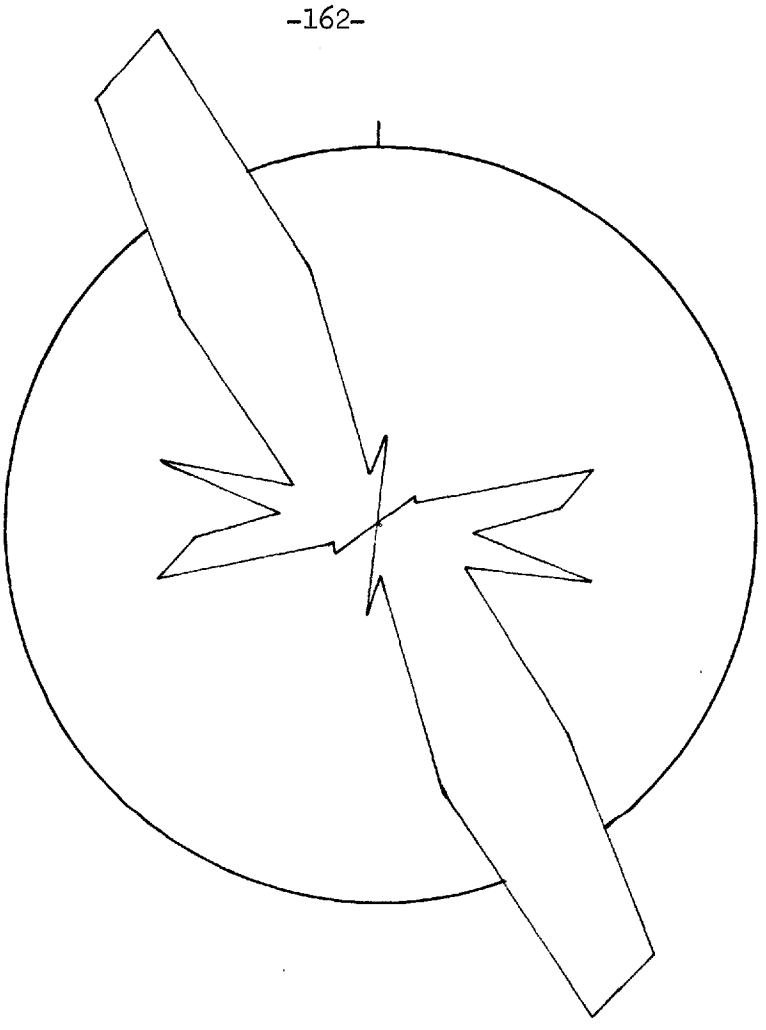
Batnall

P Bombogn

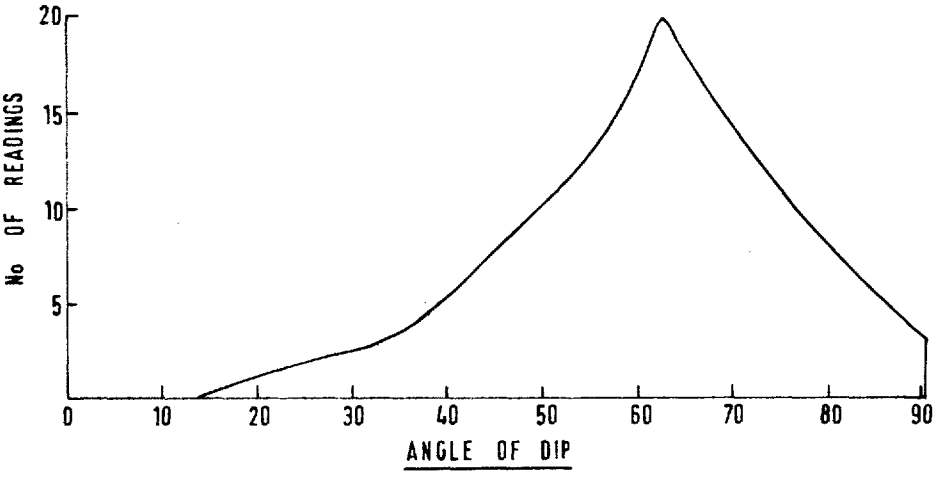
Cerentino

1:25,000

FIGURE 77
FAULTS



(a) ORIENTATION OF FAULTS
(65 READINGS)



(b) GRAPH OF DIP FREQUENCY OF FAULT PLANES

The major NNW trending fault, the Kleinhorn Fault, crosses the divide separating the Valle di Bosco and the Valle di Campo between the Kleinhorn and the Sasso Rosso. The fault plane, dipping between 65° and 80° to the northeast, and with steeply plunging slickensides, is exposed on a cliff face below the Sasso Rosso. On the north side of the ridge a deep gully has formed along the line of the fault. The base of the hornblende schist east of the gully is downthrown approximately 80 metres. On the ridge crest a small east facing scarp up to 45 cms high and 6.5 ms long marks the trace of the fault, and may indicate a very young surface displacement. To the north, across the valley of Rovana Stream, the fault can be followed as a fairly distinct line marking the western boundary of the large area of Bosco Group gneiss exposed on Grossalp. The Kleinhorn Fault appears to end abruptly where it meets the Guriner Furka Fault, and no sign of it could be found in the area to the north.

The major E-W striking fault, the Guriner Furka Fault, crosses the international boundary ridge at Passo di Bosco, and extends eastwards as a deep gully along the southern boundary of the hornblende schist exposed on the slopes of the Martschenspitz. It appears to lie just north of Bosco-Gurin, and continues east along the valley of Rovana Stream. Lithological boundaries exposed on the north side of the stream are displaced up to 250 metres east on the south side of the stream. West of Corino lack of exposures in the heavily wooded area make the fault difficult to trace.

At Passo di Bosco the fault splays, enclosing a narrow block just over a kilometre long and up to 70 metres wide. The base of the Bosco Group is upthrown 70 m. to 80 m. on the south side of the south branch of the fault, and is downthrown 15 m. on the north side of the north branch. Unfortunately the fault plane is not clearly exposed, but the trace of the fault over the topography suggests that the fault plane is vertical or dips very steeply south.

Another major E-W trending fault, the Hendar Furggu Fault, crosses into the Valle di Bosco at the high pass between the Wandfluhhorn and Martschenspitz massifs. West of the pass a deep gully has eroded along the



Fig.78(a) View west across Bann showing the NNW and E-W striking faults. Martschenspitz top left, Hendar Furggu lowest point on skyline ridge. Cliff along left hand side separates Bann from Bort.



Fig.78(b) View southwest to ridge between Valle di Bosco and Valle di Campo showing gullies formed along NNW striking faults. Grossalp village bottom right, Pizzo Bombogn top right. Skyline ridge is south of Valle di Campo.



Fig.79 View west along trace of Hendar Furggu Fault from Usser See, (68271323) above Wolfstaffel.

fault plane, and lithological units to the south are approximately 35 m. higher than their equivalents to the north. To the east the fault follows the foot of a line of cliffs before being marked by a conspicuous deep gully across the rugged gneiss terrain (fig.79). Three small lakes are evenly spaced along the fault trace at Wolfstaffel. The fault plane is concealed, but the trace of the fault over the topography indicates that it dips steeply northwards.

CHAPTER 12

REGIONAL METAMORPHIC HISTORY

12:1 Regional Setting

The Lower Nappes occupy an area of high grade, regional metamorphism. The existence of high grade minerals has been known for a considerable time, but it was not until the work of Niggli (1960) and Niggli and Niggli (1965) that the regional distribution of stilpnomelane, chloritoid, glaucophane, kyanite and sillimanite was outlined. These index minerals occur in a series of semi-concentric zones, the innermost being occupied by sillimanite and centred on the north side of the Insubric Line at Lago Maggiore (fig. 80a) Niggli (1970) suggested that the metamorphism was caused by a load of 4 to 8 kilobars (corresponding to a nappe pile 15 to 30 kilometres thick) and post-dated the major Alpine folding.

Meanwhile, Bearth (1958) had recognised zones of increasing anorthite content in plagioclase in the cover rocks of the upper Pennine Nappes just west of the region of high grade metamorphism. Later Bearth (1962) outlined the distribution of glaucophane, lawsonite, pumpellyite, chloritoid, and garnet in the Mesozoic ophiolites. He recognised an external lawsonite-pumpellyite zone and an internal garnet-chloritoid zone, and considered that the isograd separating them was parallel to the tectonic trend. He also suggested that isograds of a greenschist facies metamorphism in the lower Pennine area cut across the tectonic trend, overprinting the earlier, "parallel" metamorphism.

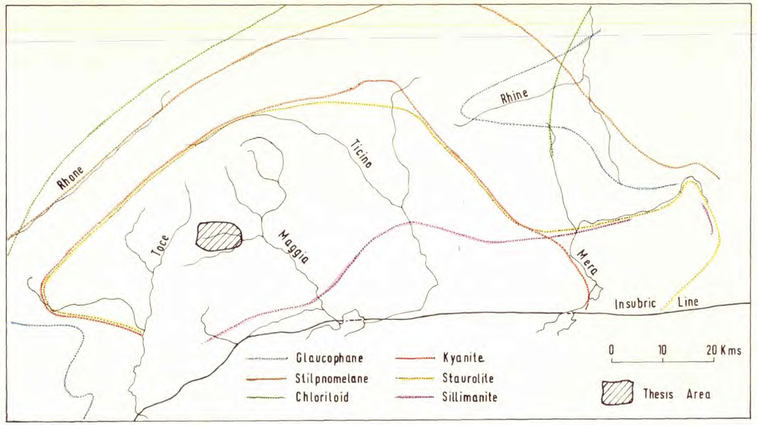
Bearth (1966) amplified these conclusions by showing that basic volcanics with a greenschist facies albite-epidote-chlorite-actinolite mineral assemblage were associated with glaucophane-lawsonite schists and basic bodies with eclogite facies mineral assemblages. The glaucophane schists are usually in the process of replacement, and contain "mixed" glaucophane-almandine-epidote (zoisite)-paragonite-rutile-muscovite-chloritoid assemblages in which the zoisite commonly occurs as pseudomorphs after lawsonite. A similar metamorphic history has been described by Nicolas (1969) from the southwest portion of the Alps.

Wenk (1962) based his subdivision of the central, high grade area on the southward increase in the An content of plagioclase in Mesozoic calcareous schists. Isograds were drawn defining the outer limits of plagioclase with compositions of An_{17}, An_{30}, An_{50} and An_{70} (fig. 80b). Schwander and Wenk (1967) later established an An_{85} isograd. Wenk considered that the isograd boundaries dipped outwards from a central "thermal dome" and introduced the concept of dynamo-thermal metamorphism, rather than the load metamorphism hypothesis previously described.

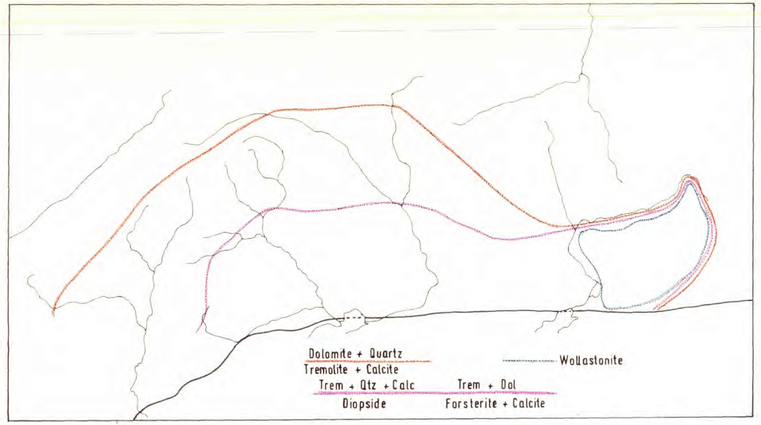
Trommsdorff (1966) based his subdivision of the same area on the first appearances of talc, tremolite, diopside, forsterite and wollastonite in the mineral assemblase of siliceous marbles (fig. 80c). The first appearance of tremolite+calcite was found to coincide with Wenk's (1962) An_{30} plagioclase+calcite isograd and the kyanite isograd, while the appearances of diopside+calcite and forsterite+calcite were just inside the An_{85} plagioclase+calcite isograd. Wollastonite occurs only in the area surrounding the small Tertiary granite pluton in the Bergell Alps at the head of Lake Como (Trommsdorff, 1968). In the centre of the lower Pennine area, Trommsdorff envisaged a maximum temperature of between 570°C. and 620°C., and a pressure of 3 to 5 kilobars.

More recently Wenk and Keller (1969) based their subdivision of the lower Pennine area on the mineral assemblages and An content of plagioclase in amphibolites. Isograde boundaries were defined for plagioclase of composition An_{20}, An_{30}, An_{40} and An_{50}, and an innermost zone of pyroxene-bearing amphibolite was delineated (fig. 80d). The isograds show a generally semi-concentric pattern, but in detail the inner boundaries are very irregular.

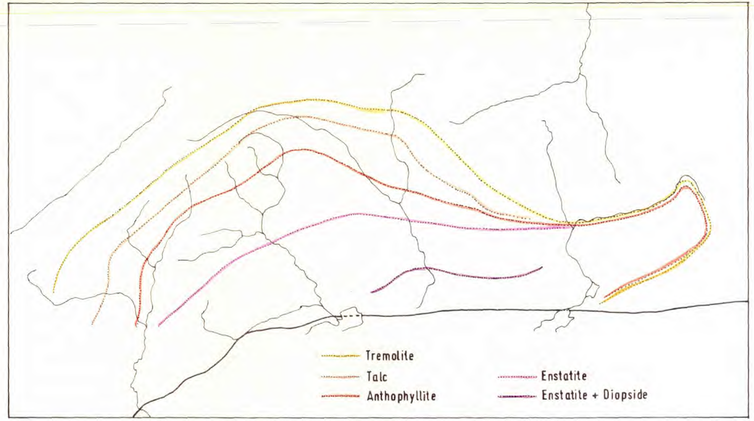
The most recent subdivision of the area was based by Evans and Trommsdorff (1970) on the first appearances of diopside, forsterite, tremolite, talc, anthophyllite, enstatite and the couple diopside-enstatite in the mineral assemblages of ultramafic rocks (fig. 80e). Tremolite appears close to the kyanite isograd and enstatite appears just before the sillimanite isograd is reached. Trommsdorf and Evans (1969) considered that enstatite appeared in the ultramatic rocks in relatively dry conditions just above 600°C., and at a pressure of 4 kilobars.



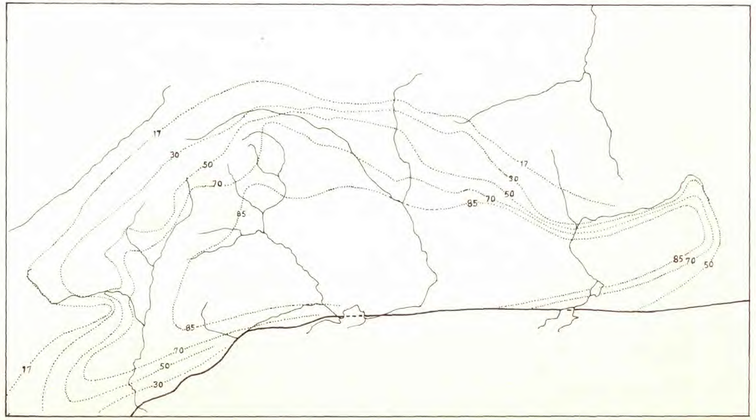
(a) INDEX MINERALS IN PELITIC ASSEMBLAGES (NIGGLI AND NIGGLI 1965)



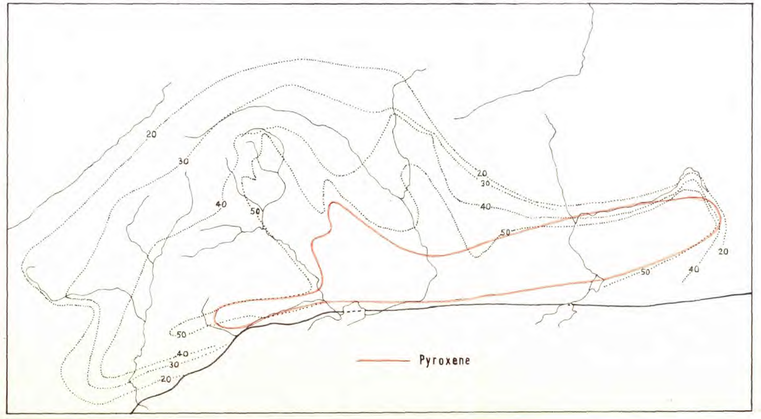
(c) MINERAL ASSEMBLAGES OF SILICEOUS MARBLES (TROMMSDORFF 1966, 1968)



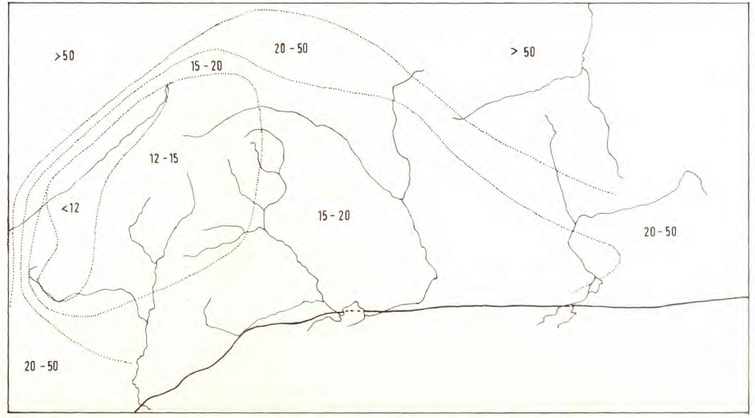
(e) FIRST APPEARANCE OF MINERALS IN OLIVINE BEARING ULTRAMAFIC SCHISTS (BASED ON EVANS AND TROMMSDORFF 1970)



(b) An CONTENT OF PLAGIOCLASE IN MESOZOIC CALCAREOUS SCHISTS (WENK 1962; SCHWANDER AND WENK 1967)



(d) An CONTENT OF PLAGIOCLASE IN AMPHIBOLITES (WENK AND KELLER 1969)



(f) BIOTITE COOLING AGES IN MILLIONS OF YEARS (JÄGER, NIGGLI AND WENK 1967)

The area of high grade metamorphism is significantly outlined by the contour drawn around the outer limits of biotites with 20 to 50 million year cooling ages (Jäger, Niggli and Wenk, 1967) (fig.80f). The youngest biotites, with cooling ages from less than 12 to 15 millions old, occur in the northwest corner of the lower Pennine area. The peak of Alpine metamorphism (i.e. when the highest temperatures prevailed) has been dated by Hunziker (1969) as occurring 38 $\pm$ 2 millions ago.

The rocks of the Valle di Bosco fall just within the area containing biotite cooling ages younger than 15 million years old. It is well within the kyanite zone, about mid-way between the kyanite and sillimanite isograds. The isograds marking the first appearances of forsterite in siliceous marbles, and plagioclase with an An_{85} content in calcareous schists, pass ENE-WSW along the southern edge of the area. The isograd for plagioclase with an An_{40} content in amphibolite passes in the same direction through the centre of the area. Correlation with Evans and Trommsdorff's (1970) mineral assemblages of ultramafic rocks suggests that enstatite should appear in the southeast corner of the thesis area. The area also lies just inside the isograd defining the outer limit of muscovite with a 45% phengite content (Schwander, Hunziker and Stern, 1968).

The maximum metamorphic conditions to which the rocks of the Valle di Bosco were subjected were approximately 600°C. and 4 kilobars, equivalent to a depth of 15 kms at a temperature gradient of 40° km. These figures are based on Trommsdorff's (1966) estimate of the P/T conditions represented by siliceous marble assemblages, and Trommsdorff and Evan's (1969) estimate for the conditions under which enstatite appears in forsterite-bearing ultramafic rocks. They do not represent the maximum metamorphic conditions prevailing in the lower Pennine area, as these were higher to the south and east.

12:2 Metamorphic Textures

Despite the remarkable wealth of mineralogical data, age determinations and structural detail, investigations of the timing of the metamorphism in relation to the various phases of deformation are still in their infancy. The object of this section of the work is to further that investigation, but without examining the detailed geochemistry of the metamorphic systems.

It has generally been asserted (e.g. Wenk and Trommsdorff, 1965) that crystallization outlasted deformation, but recent studies of the metamorphic textures (e.g. Higgins, 1964b; Chadwick, 1968) have shown that the F2 schistosity, across which the main porphyroblasts grew, has been strongly folded. Chatterjee (1961), who studied the Simplon region, was the first worker to realise that Alpine crystallization and deformation were not simple, single phase events. He recognised six stages of crystallization and two phases of movement. During the first stage of crystallization, in the waning phase of the first movement, prochlorite, muscovite, clinozoisite, biotite, quartz and calcite formed. These continued to form during the second stage of crystallization. During the third stage of crystallization, occurring syntectonically during the second movement phase, prochlorite, muscovite, biotite, calcite, amphiboles, epidote and garnets with sigmoidal trails formed. After the second movement had ceased phlogopite, chloritoid, garnet, staurolite and kyanite porphyroblasts, and a second generation of muscovite, chlorite and biotite grew across the schistosity during the fourth stage of crystallization. The climax of the metamorphism occurred during Chatterjee's fifth stage of crystallization when plagioclage porphyroblasts were added to those already formed. The final, sixth, stage is indicated by weak, retrograde growth of secondary chlorite, tourmaline and further plagioclase.

More recent work has shown that although Chatterjee's stages of crystallization seem unnecessarily numerous, the main importance of his work was in recognising that the metamorphic peak occurred after two major movements, and that plagioclase porphyroblasts were among the last to crystallize.

Higgins (1964b) established a detailed movement and metamorphic history for the Mesozoic rocks of the Basodino-Nufenenpass area to the north of the Valle di Bosco. He found that the textural relations changed across the area due to the northward migration of deformation phases relative to stationary metamorphic conditions. In the northern, Nufenen zone the first recognisable crystallization was the syntectonic growth of micas and rare garnets during the F2 deformation. This was followed by the post-tectonic growth of biotite, plagioclase, hornblende and garnet porphyroblasts. These were rotated during the F3 deformation, but no new mineral growth occurred. In the central Bedretto zone and southern Teggiolo zone most of the porphyroblasts again post-date the deformations F2 and were rotated during the F3 deformations.

Higgins (p.205) suggested that garnets with gently folded inclusion trails grew during the early stages of the F3 deformation and were slightly rotated as the fabric continued to be folded. Crystallization ceased during the F3 deformation. Similarly, Chadwick (1968) found that in the north of the Lukmanier Pass area the metamorphic peak occurred during the F2 deformation, but in the south it was between the F2 and F3 deformations.

Sibbald (1971), from textural work in the Val Piora region, between Nufenenpass and Lukmanier Pass, considered that garnet, staurolite and kyanite porphyroblasts commenced crystallization at a late stage during the F2 deformation, and continued to grow post-tectonically. The schistosity across which the porphyroblasts grew was later deformed by small F3 folds. Plagioclase porphyroblasts were the last to appear, and are generally deformed by the F3 folds, but rare porphyroblasts continued to crystallize after the F3 deformation.

In the Molare area, south of Lukmanier Pass, Thakur (1971) also showed that garnet, staurolite, kyanite, plagioclase and biotite porphyroblasts crystallized after the F2 deformation, and were rotated during the F3 deformation. A few with slightly curved internal inclusion trails were interpreted as having crystallized during the early stage of the F3 deformation.

A regional textural picture is gradually emerging of a narrow northern zone in which porphyroblasts commenced crystallization during the F2 deformation and an extensive southern zone in which crystallization did not commence until after the F2 deformation and continued until the early stages of the F3 deformation. The metamorphic zones, described earlier, must therefore have been established over most of the Lower Pennine region during the metamorphic peak in the static interval between the F2 and F3 deformations. It would be remarkable if the isograds delineating these zones escaped displacement during the F3 deformation, and this should be seriously considered in any regional metamorphic-structural interpretation. For instance, the crowding together of the kyanite, staurolite, garnet and chloritoid isograds along the southern edge of the Gotthard Massif, and the large gap between the kyanite and sillimanite isograds in the central lower Pennine area, may be reflections of post-metamorphic folding. Also, plagioclase has generally

been found to be the last crystallizing porphyroblast, confirmed in the textural study of the Valle di Bosco rocks, and the possibility arises that the metamorphic zones described by Wenk (1962) may post-date the F3 movement. Any consideration of the conditions of metamorphism must account for the strong possibility that in the lower Pennine region the nappe pile was thickest after the F3 deformation, and the conclusions of Niggli (1970) should therefore be treated with caution.

CHAPTER 13

METAMORPHIC TEXTURES, VALLE DI BOSCO

13:1 Introduction

In examining the metamorphic textures I have followed the method of Spry (1963). This consists of establishing, initially from field evidence, the structural surfaces (schistosity, crenulation cleavage) present in the rocks, and relating the time of growth of minerals to these surfaces. The principal surface in the rocks of the Valle di Bosco is the F2 schistosity. Microscopically this is outlined by strongly aligned micas and quartz grains with a distinct dimensional preferred orientation. These minerals are considered to have crystallized syntectonically during the F2 deformation. Larger, randomly oriented porphyroblasts which grow across the schistosity are considered to have grown under static, post-tectonic conditions. They often enclose straight inclusion trails continuous with the schistosity. Porphyroblasts with curved inclusion trails are considered to have grown syntectonically during the F2 deformation. When the schistosity was seen to be folded this was considered to be an F3 effect. During the F3 deformation the porphyroblasts were sometimes slightly rotated so that their inclusion trails lie at a slight angle to the schistosity, and the schistosity is commonly deflected around them. Where the schistosity became detached from the porphyroblasts, the triangular spaces (pressure shadows) are filled by minerals considered to have grown syntectonically during the F3 deformation. Porphyroblasts not deformed during the F3 deformation are considered to have crystallized post-tectonically in the static interval after the F3 deformation has ceased. Such porphyroblasts are rare, and only confidently recognised where they grow over schistosity deflected around pre-F3 porphyroblasts during the F3 deformation.

The following section does not attempt a detailed petrographic description, as this has already been adequately undertaken by Grutter (1929), Hunziker (1966) and Wieland (1966). It shows that the metamorphic textures exhibited by the rocks of the Valle di Bosco are generally simple, and confirms that the main growth time of the porphyroblasts was in the static interval between the F2 and F3 deformations.

13:2 Mesozoic Rocks

The Mesozoic rocks of the Valle di Bosco consist largely of marble and calcareous schist, with very minor quartzite and pelitic garnet-kyanite schist. They are the only rocks in the area to have been affected solely by the Alpine Orogeny, and are therefore the most reliable indicators of the metamorphic and structural events associated with the orogeny. The pelitic schist, despite its very restricted occurrence, is by far the most useful for determining the textural relationships.

(a) Pelitic Schist

The pelitic schist consists typically, of quartz, biotite, muscovite, ilmenite, tourmaline, garnet, kyanite, plagioclase and graphite. Kyanite and tourmaline do not occur in all sections, and occasionally either muscovite or biotite is absent. Staurolite, epidote, calcite, rutile and sphene also occur, but are rare. The average size of the quartz grains is about 0.13 mm.

A prominent schistosity is formed by aligned mica flakes and ilmenite and graphite grains in a fine-grained mosaic of rectangular quartz crystals. The schistosity is often slightly deflected around the larger porphyroblasts, and the inclusion trails of the porphyroblasts may be slightly rotated with respect to the schistosity. In a few cases the schistosity has been detached from the porphyroblasts, and small quartz fringes now link the schistosity to the porphyroblasts. These pressure shadows are usually very small, and often developed at only one end of the porphyroblasts. It is not uncommon for there to be no quartz fringes although the schistosity is deflected. Curving, hematitic pressure solution lines occur above and below some of the porphyroblasts, and the quartz removed from these high strain areas was presumably deposited in the pressure shadows during the F3 deformation (Durney, 1972).

Quartz occurs as rectangular grains aligned parallel to the schistosity, and as larger, rounded grains in the pressure shadows of large garnet porphyroblasts. It is usually strained and sometimes polyganised, and has irregular, sutured boundaries.

Biotite has a straw yellow (X) to red-brown (Z) pleochroic scheme. It occurs as long narrow flakes lying parallel to the schistosity, and less commonly as shorter, randomly oriented flakes. Some of the larger randomly oriented flakes contain straight inclusion trails of minute graphite, ilmenite and epidote grains, and a few are associated with quartz in the pressure shadows.

Muscovite is much less common than biotite. The long, narrow flakes aligned parallel to the schistosity lie along the boundaries between adjacent quartz grains. A second generation of muscovite is randomly oriented in small pressure shadows.

Ilmenite occurs as small black needles parallel to the schistosity, and as larger, rectangular grains in a few pressure shadows.

Tourmaline is represented by the iron-rich variety schorlite. It is strongly pleochroic from light to dark olive-green, and occurs as zoned euhedral grains. The grains always grow across the schistosity, and have minute biotite inclusions. A few occur in some of the small pressure shadows.

Almandine garnet occurs as cracked euhedral crystals up to 5 mm. across. Most have graphitic inclusion trails which, in sections cut parallel to the F2 lineation, are continuous with the schistosity on either side (fig. 81a). In sections normal to the lineation the graphitic trails are strongly folded (fig. 81b). Less commonly garnet porphyroblasts contain inclusion trails of minute quartz needles. These are straight in sections parallel to the F2 lineation (fig.82a) but slightly curved in sections normal to the lineation (fig. 82b). Porphyroblasts with trails showing both S and Z symmetry occur in the same thin section. The outer portion of these garnets consists of up to five euhedral rims without inclusion trails, and only minor, randomly oriented inclusions of quartz, biotite, tourmaline, epidote, rutile and ilmenite. A zone of small, circular quartz blebs often occurs at the junction of the two portions of the porphyroblasts. Smaller zoned garnets, without a core containing inclusion trails, occur in the same thin sections.



Fig.81(a) Post-tectonic (F2) garnet porphyroblast in Mesozoic pelitic schist. Note straight inclusion trails, and schistosity deflected around porphyroblast during F3. Section cut parallel to F2 lineation. X 30.

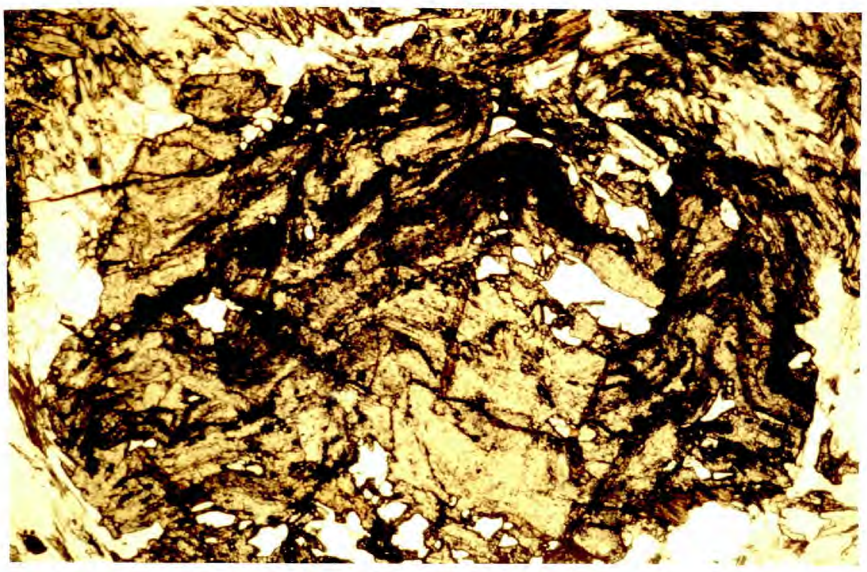


Fig.81(b) Post-tectonic (F2) garnet porphyroblast in Mesozoic pelitic schist. Note folded inclusion trails (= F2 folds). Section cut normal to F2 lineation. X 30.

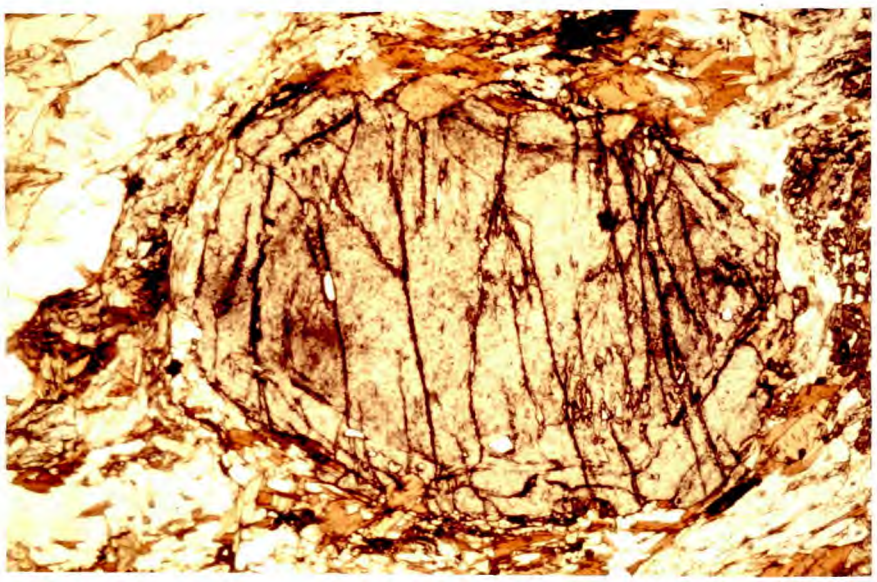


Fig.82(a) Garnet porphyroblast in Mesozoic pelitic schist. Note core with straight inclusion trails of aligned quartz needles, and euhedral, post-tectonic (F2)rims. Section cut parallel to F2 lineation. X 30.

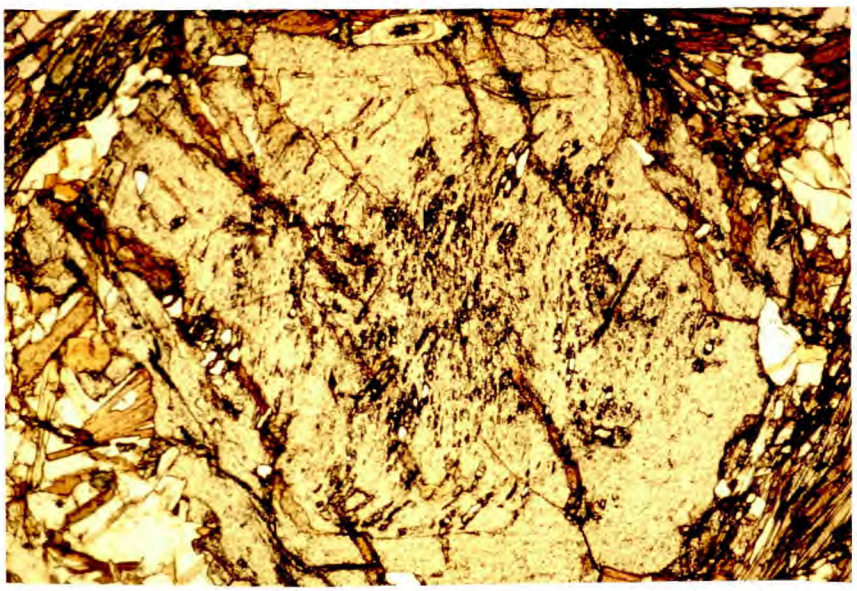


Fig.82(b) Garnet porphyroblast in Mesozoic pelitic schist. Core contains slightly curved, syntectonic (F2) inclusion trails of quartz needles. Post-tectonic, euhedral rims surround core. Section cut normal to F2 lineation. X 30.

Kyanite forms large, blade-like crystals with a very pronounced cleavage, and smaller skeletal grains. It contains quartz, calcite and biotite inclusions, as well as straight ilmenite and graphite trails continuous with the schistosity.

Plagioclase occurs as very large porphyroblasts which appear as irregular graphitic-sericitic patches in plane light (fig.83a), and large twinned crystals in polarised light (fig.83b). It contains inclusions of all other minerals in the same thin section, and has internal mica-graphite trails which are straight or very gently curved. The composition, determined from albite and carlsbad-albite twins, varies from An_{42} to An_{67}.

Calcite occurs as a minor constituent of a few thin sections, and is usually intergrown with biotite, while sphene and staurolite form rare, small grains which grow across the schistosity.

The mineral parageneses of the pelitic schist are illustrated in fig.87a. The straight inclusion trails of the garnet, kyanite, tourmaline and larger biotite porphyroblasts, suggests that the porphyroblasts crystallized under static conditions. They post-date the F2 deformation, as their trails are continuous with the schistosity, and pre-date the F3 deformation, as they have been slightly rotated and the schistosity is deflected around them. The schistosity is occasionally slightly deflected around plagioclase porphyroblasts, suggesting that they also crystallized prior to the F3 deformation. However, positive evidence that plagioclase continued to crystallize after the F3 deformation is found where the porphyroblasts grow across schistosity that has been deflected around pre-F3 porphyroblasts. In this case the inclusions trails are slightly curved, but continuous with the schistosity.

The most interesting textural relationships are portrayed by the garnet porphyroblasts. Those with internal sigmoidal inclusion trails and zoned rims probably began to crystallize at a late stage of the F2 deformation, each growth increment enclosing a portion of the schistosity before being slightly rotated (Powell and Treagus, 1970). The rims grow across the schistosity, and are post-tectonic features. The porphyroblasts which contain strongly folded, graphitic inclusion trails are also considered to have crystallized post-tectonically. The internal trails may represent insoluble material outlining the original sedimentary

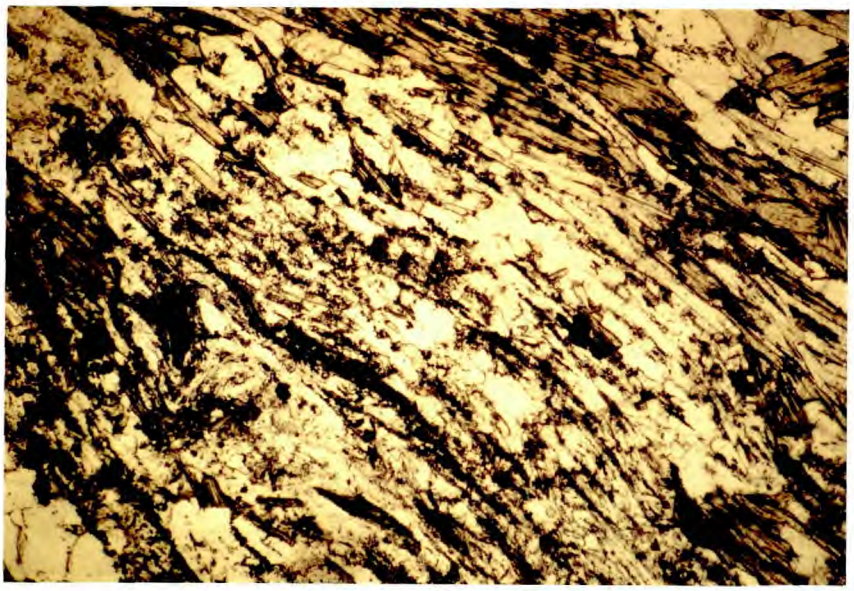


Fig.83(a) Post-tectonic (F2) plagioclase in Mesozoic pelitic schist. Note inclusion trails parallel to the F2 schistosity. X 55.

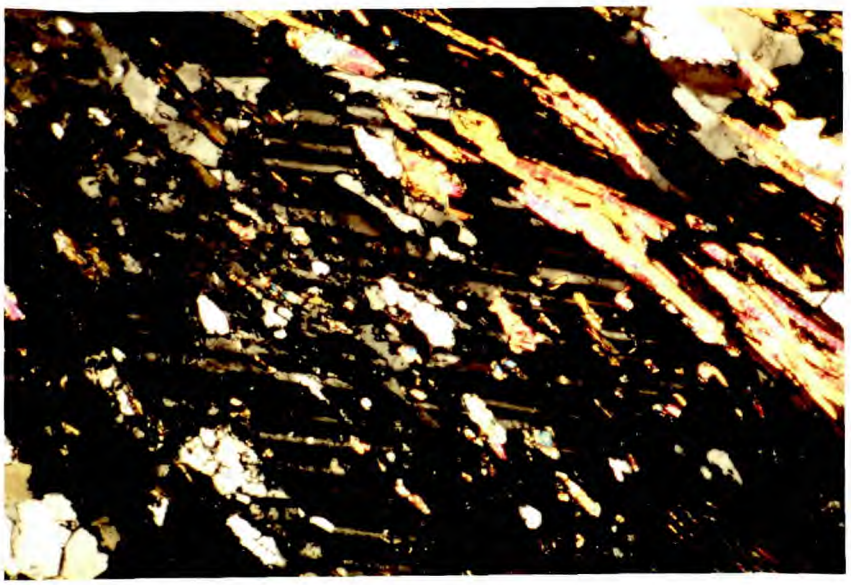


Fig.83(b) Same as above in polarized light

bedding, which is otherwise masked by the strong schistosity. During the F3 deformation many of the garnet porphyroblasts were slightly rotated, and the schistosity deflected around them. The random orientation of the inclusion trails in garnets in sections cut normal and parallel to the lineation (fig.84) shows that there was apparently no consistency in the direction and amount of rotation of the porphyroblasts.

(b) Calcareous Schist

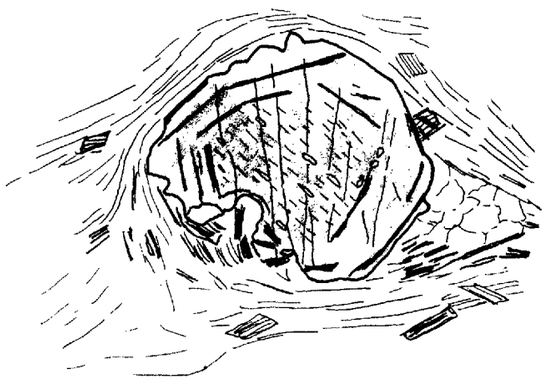
The calcareous schist is the most common of the Mesozoic rocks. It differs from marble by being finer grained, and more micaceous and quartz rich, and from pelitic schist by containing more common calcite and having a less strongly developed schistosity. The texture is largely granoblastic but the micas are strongly aligned. Occasionally mica layers alternate with layers of slightly elongate quartz grains. The average grain size varies from 0.11 mm to 0.15 mm, and increases with calcite content. The typical mineral assemblage includes quartz, calcite, plagioclase, biotite and sphene. Ilmenite, muscovite, garnet, phlogopite and chlorite are sometimes present in very small amounts.

Quartz grains have angular, elongate to smooth, rounded outlines. They are strained and frequently have very sutured boundaries. Calcite usually occurs as small untwinned grains containing ilmenite and muscovite inclusions. The few large grains have common twin lamellae. Plagioclase occurs as both small, twinned, and relatively clear porphyroblasts, and larger sericitic patches with abundant inclusions. A composition of An_{64} was determined from the twin lamellae of one porphyroblast, and Grutter (1929: 127) recorded An_{65} from another. Schwander and Wenk (1967) have shown that the composition of the most basic plagioclase in the calcareous schists in this area lies between An_{70} and An_{85}. Biotite has a pale brown (X) to rich red-brown (Z) pleochroic scheme, but some is partly altered to chlorite. Most flakes have a strong preferred orientation. Sphene forms common, elongate grains altering to ilmenite around the edges.

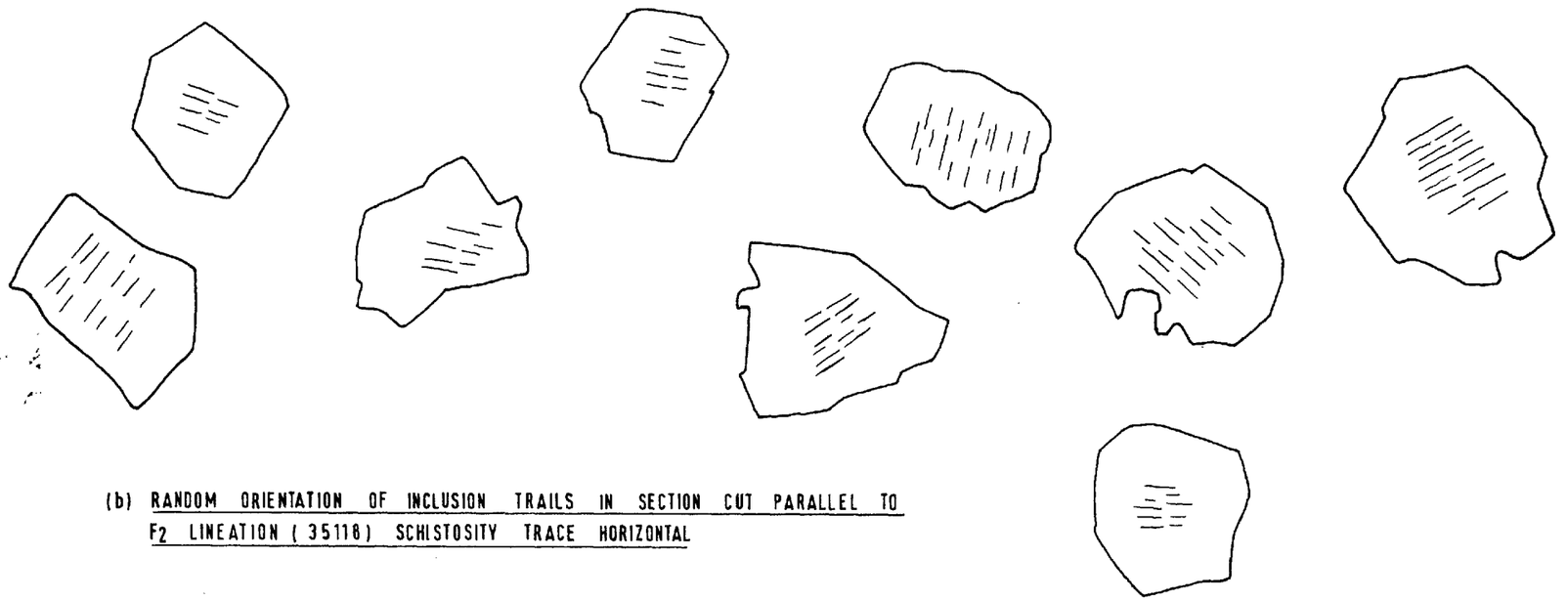
Because of the poor development of schistosity and the absence of evidence of the F3 deformation in the thin sections examined, the time relations between the minerals are not especially clear. Biotite

FIGURE 84

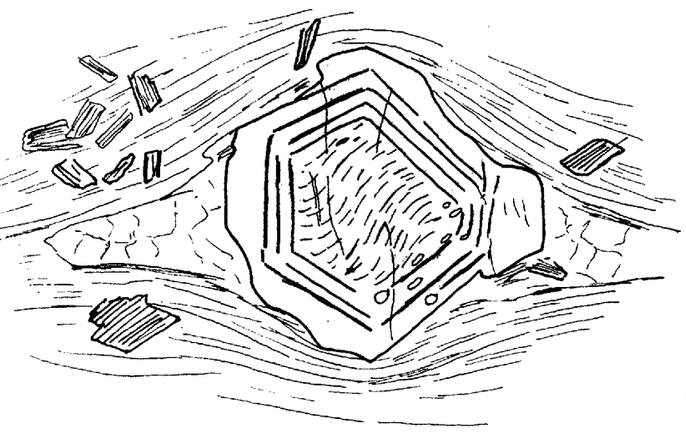
ORIENTATION OF INCLUSION TRAILS IN GARNET PORPHYROBLASTS IN MESOZOIC PELITIC SCHIST



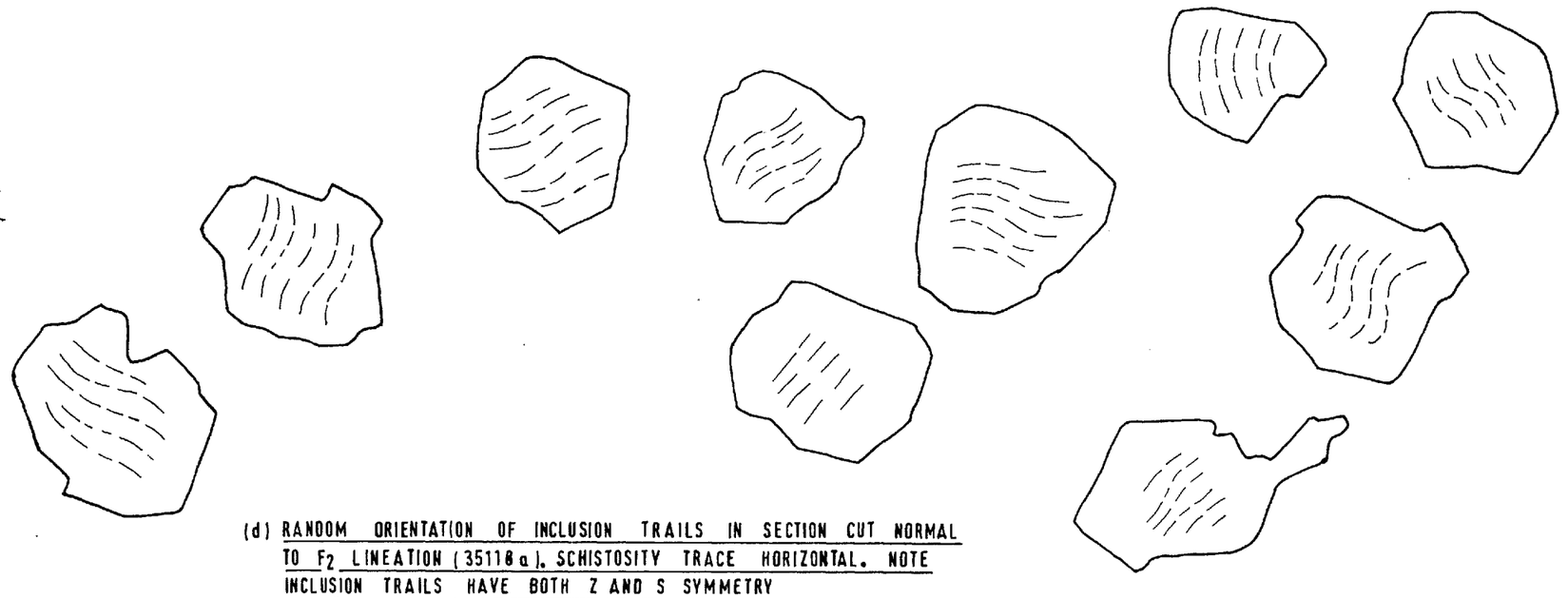
(a) SECTION CUT PARALLEL TO F_2 LINEATION (35118) NOTE STRAIGHT INCLUSION TRAILS, AND DEFLECTED SCHISTOSITY AND QUARTZ FILLED PRESSURE SHADOW DEVELOPED DURING F_3



(b) RANDOM ORIENTATION OF INCLUSION TRAILS IN SECTION CUT PARALLEL TO F_2 LINEATION (35118) SCHISTOSITY TRACE HORIZONTAL



(c) SECTION CUT NORMAL TO F_2 LINEATION (35118a) NOTE CURVED INCLUSION TRAILS, AND DEFLECTED SCHISTOSITY AND QUARTZ FILLED PRESSURE SHADOWS DEVELOPED DURING F_3. POST F_2 MUSCOVITE GROWS ACROSS SCHISTOSITY



(d) RANDOM ORIENTATION OF INCLUSION TRAILS IN SECTION CUT NORMAL TO F_2 LINEATION (35118a). SCHISTOSITY TRACE HORIZONTAL. NOTE INCLUSION TRAILS HAVE BOTH Z AND S SYMMETRY

appears to have crystallized both during and after the F2 deformation. Sphene is also a post-tectonic mineral, as is plagioclase, since it contains straight inclusion trails of all the other minerals. The most definite conclusion is that plagioclase was the last mineral to crystallize, and grew under static conditions.

The mineral parageneses of the calcareous schist are shown in fig.87b.

(c) Marble

The Mesozoic marbles are dominantly quartz-calcite rocks with very simple mineral assemblages and textures. They vary from coarsely crystalline rocks with little quartz and no plagioclase, to finer grained, quartz rich types with a poor schistosity outlined by isolated phlogopite flakes (fig.85) and thin strings of ilmenite grains. The average grain size varies from 0.25 mm to 0.13 mm, but is commonly between 0.16 mm and 0.17 mm.

Typical mineral assemblages include calcite, quartz, ilmenite, phlogopite, plagioclase and sphene. Muscovite, tremolite, graphite and dolomite occasionally occur in very small amounts. Quartz is typically undulose and often polygonised and cracked. Individual grains are usually rounded but their boundaries are often very irregular. Calcite occurs as large, twinned grains with irregular boundaries. The twin lamellae in adjacent grains are randomly oriented. Phlogopite forms large rectangular flakes which are pleochroic from pale brown (X) to light brown (Z). They show a distinct preferred orientation. A few flakes are strained and slightly bent. Others have small ilmenite inclusions and a number are partly altered to secondary chlorite. Plagioclase generally occurs as large porphyroblasts containing abundant inclusions of all other minerals in the same thin section. In plane light the porphyroblasts appear as irregular patches of ilmenite, sericite and graphite, but are much clearer in polarised light. The smaller porphyroblasts are strongly twinned. Sphene is most common as small prismatic or pyramidal grains, but occasionally forms large, twinned rhombic porphyroblasts. Its colour varies from dark brown to neutral.

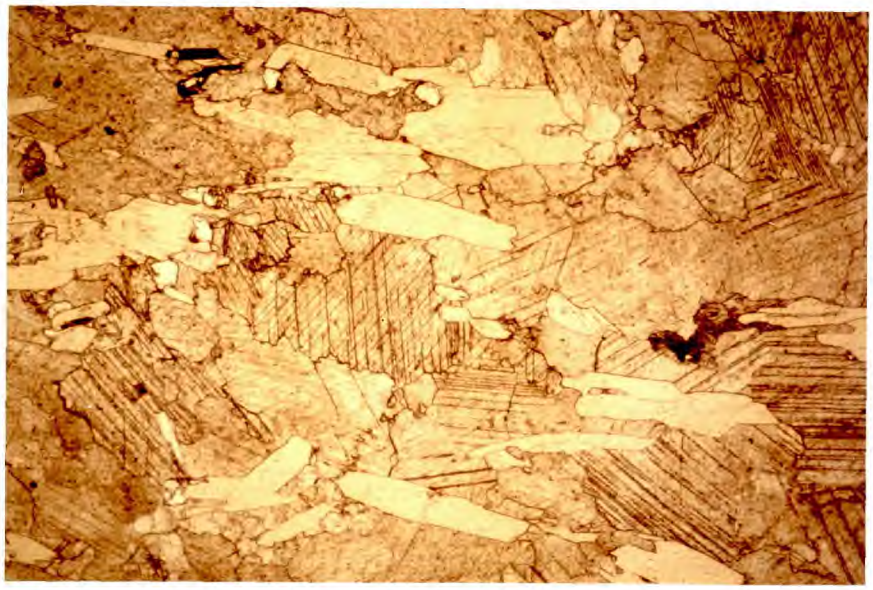


Fig.85(a) Mesozoic marble with oriented phlogopite micas. X 30.

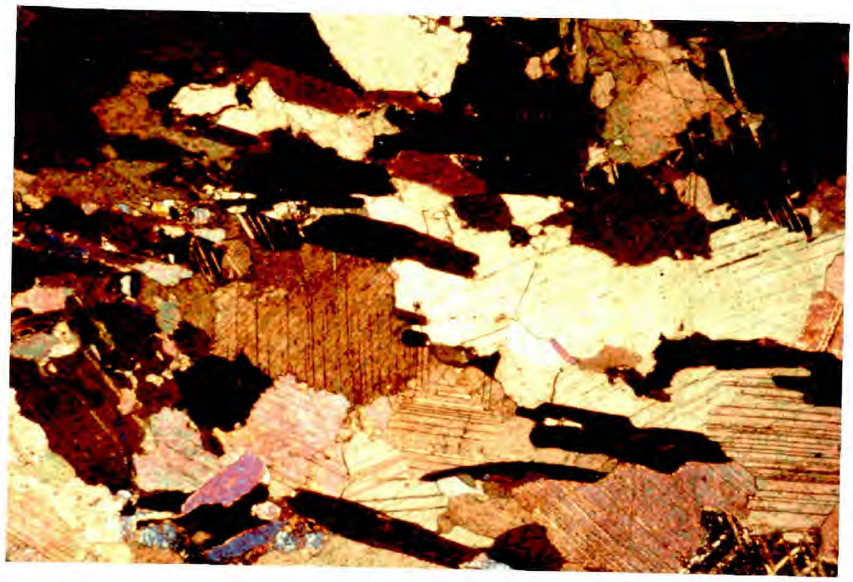


Fig.85(b) Same as above in polarised light.

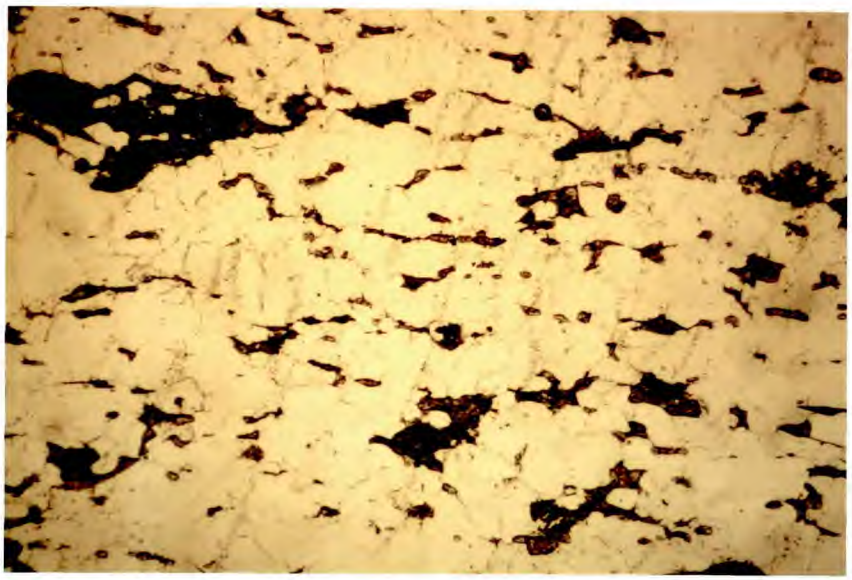


Fig.86(a) Mesozoic quartzite. Note common, skeletal garnets and poor schistosity. X 30.

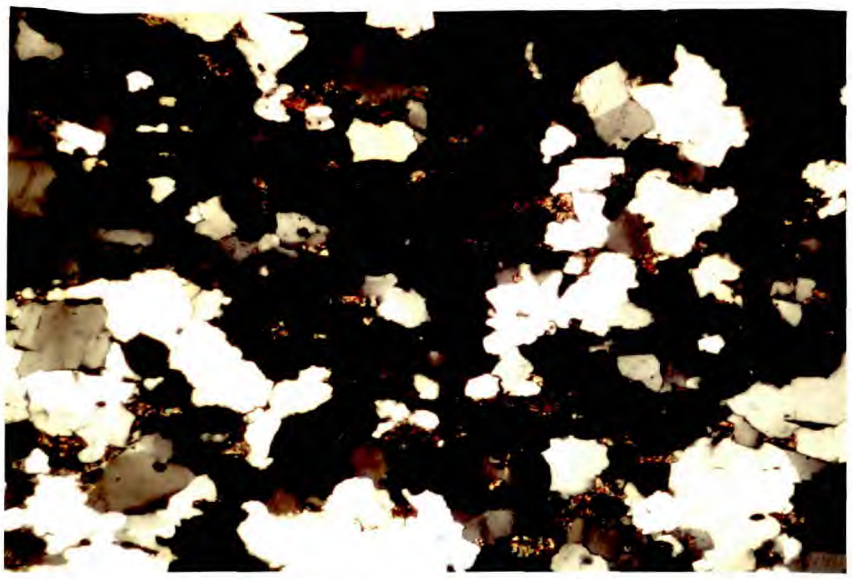


Fig.86(b) Same as above in polarised light. The quartz grains have very serrated boundaries.

FIGURE 87

MINERAL PARAGENESES OF MESOZOIC ROCKS

(a) PELITIC SCHIST

MINERAL		F_2		F_3	
QUARTZ		—	—	—	
BIOTITE		—	—	—	
MUSCOVITE		—	—	—	
ILMENITE	—	—		—	
TOURMALINE			—	—	
GARNET			—		
KYANITE			—		
PLAGIOCLASE			—		—
CALCITE		—?—			
SPHENE			—		
STAUROLITE			—		
EPIDOTE	—	—			

(b) CALCAREOUS SCHIST

MINERAL		F_2		F_3	
QUARTZ		—	—		
CALCITE		—	—		
PLAGIOCLASE					—
BIOTITE		—	—		
SPHENE			—		
CHLORITE			—		—
ILMENITE			—		—

(c) MARBLE

MINERAL		F_2		F_3	
QUARTZ		—	—		
CALCITE		—	—		
PHLOGOPITE		—			
TREMOLITE			—?—		
PLAGIOCLASE					—?—
CHLORITE					—
ILMENITE		—			
SPHENE			—?—		

(d) QUARTZITE

MINERAL		F_2		F_3	
QUARTZ		—	—		
GARNET			—		
BIOTITE		—			
EPIDOTE			—		

The mineral parageneses of the marble, shown in fig.87c, cannot be determined with certainty because of the lack of a definite reference surface. By anologue with the pelitic and calcareous schists the aligned phlogopites must have grown syntectonically during F2. Quartz and calcite recrystallization may largely coincide with or postdate the phlogopite, as phlogopite sometimes occurs as inclusions in calcite. Quartz, calcite and phlogopite have all been strained (probably during F3), but the plagioclase which post-dates them is undeformed. Plagioclase porphyroblasts are thus inferred to have crystallized after the F3 deformation.

(d) Quartzite

The Mesozoic quartzite is an uncommon rock in the Valle di Bosco. It has a quartz-biotite-epidote-garnet-ilmenite mineral assemblage, with minor calcite and chlorite. A strong schistosity is outlined by aligned biotite-chlorite patches in a mosaic of ragged-edged quartz grains (fig.86). The average grain size is 0.21 mm.

Garnet is represented by very small almandine grains which are either irregularly shaped or skeletal. Some are elongate and parallel to the schistosity. Ilmenite and epidote occur as small grains, while the dominant quartz grains have a marked undulose extinction and are sometimes cracked. Garnet and biotite are both partly altered to chlorite.

There are no clear time relations between the minerals, but the biotite probably crystallized syntectonically and garnet and epidote post-tectonically to F2 (fig.87d).

13:3 Bosco Group

The Bosco Group is composed of basement schist and gneiss, strongly deformed and intensely metamorphosed during the Alpine Orogeny. The dominant semi-pelitic schist is divided, in the field, into members with garnet and staurolite porphyroblasts. Except in the southwest these two members are conveniently separated by a hornblende schist formation, which contains pods of amphibolite and ultramafic schist. Microscopically the semi-pelitic schist

members are identical, and they are consequently treated together in this section. The only difference, a minor one, is that while garnet always occurs with staurolite, staurolite is sometimes absent in garnet-bearing rocks. The textures of the muscovite-gneiss member of the Bosco Group have been described in Chapter 10.

(a) Semi-Pelitic Schist

The semi-pelitic rocks of the Bosco Group are composed of mineral assemblages typical of high grade, quartz-mica schists. These include quartz, muscovite, biotite, garnet and ilmenite which are always present, and variable amounts of staurolite, kyanite, tourmaline, plagioclase and chlorite. No calcite occurs in any of the semi-pelitic schists examined. In hand specimen garnets occur as large euhedral knots up to 2.5 cms. across. They are usually cracked and the mica fabric is slightly deflected around them. Staurolite forms thin, short prisms aligned parallel to the mica lineation, and larger, stubby prisms up to 2 cms long and randomly oriented. Kyanite blades up to 2 cms long, and tourmaline needles just over 1 cm. long are both randomly oriented and aligned on the schistosity surfaces. In thin section these porphyroblasts all grow across a strong schistosity.

The schistosity consists of long, thin muscovite and biotite flakes and ilmenite needles and grains, set in a fine mosaic of quartz and plagioclase grains. The mica flakes occur separately or in long thin trains, but occasionally pack together into bands. Muscovite and biotite occur in about equal amounts. The quartz grains have a very uniform grain size averaging 0.10 mm, and their boundaries are usually straight. In sections cut parallel to the lineation the quartz grains show a dimensional preferred orientation, but this was never as strongly developed as that in the schistose edges of the Antigorio Gneiss.

The schistosity is an F2 feature. During the F3 deformation it was folded into small chevrons with rounded hinges and straight limbs. The micas have been strained, and are bent around the fold hinges, but no new micas were observed growing parallel to the axial planes. Quartz grains in the hinge regions of the folds have been

severely strained and polyganised into subgrains elongated parallel to the axial planes of the folds. The subgrain boundaries are slightly serrated. On the limbs of the folds and in unfolded zones the schistosity is deflected around the porphyroblasts. Infrequent, small pressure shadows adjacent to the porphyroblasts are filled with quartz and minor biotite and ilmenite. A few thin pressure solution lines, represented by hematitic streaks, occur where the schistosity has been compressed against some of the garnet porphyroblasts, and a few also extend parallel to the schistosity along the limbs of small F3 folds.

Biotite forming the schistosity has a very pale yellow-brown (X) to rich, medium red-brown (Z) pleochroic scheme. It occurs as long thin flakes which are often altered to chlorite and ilmenite along the edges. A few larger, stubby flakes are randomly oriented across the schistosity, while others occur in the pressure shadows adjacent to garnet porphyroblasts.

Muscovite also occurs as long, thin flakes parallel to the schistosity, and less commonly as stubbier, randomly oriented flakes. Ilmenite forms minute needles parallel to the schistosity, and larger grains in a few pressure shadows. Chlorite occurs principally as a secondary mineral replacing biotite, muscovite and garnet, but also as a few primary flakes with medium green to almost colourless pleochroism. These contain ilmenite and quartz inclusions.

Garnet, represented by pink almandine, is the most common porphyroblast. Very small euhedral crystals up to 0.5 mm across commonly occur in quartz layers. They have spongy interiors with minute quartz inclusions, but clear rims (fig.88a). The medium sized garnets, 0.25 mm to 1.2 mm across, also have euhedral outlines. They are commonly spongy (fig. 88b), but often skeletal, containing irregular to elliptical quartz and feldspar inclusions continuous with the schistosity (fig.89). The largest garnet porphyroblasts, up to 6 mm across in the thin sections examined, generally have rounded outlines. Internally they are much clearer than the smaller garnets, but are usually crossed by a number of cracks along which chloritization has occurred. The

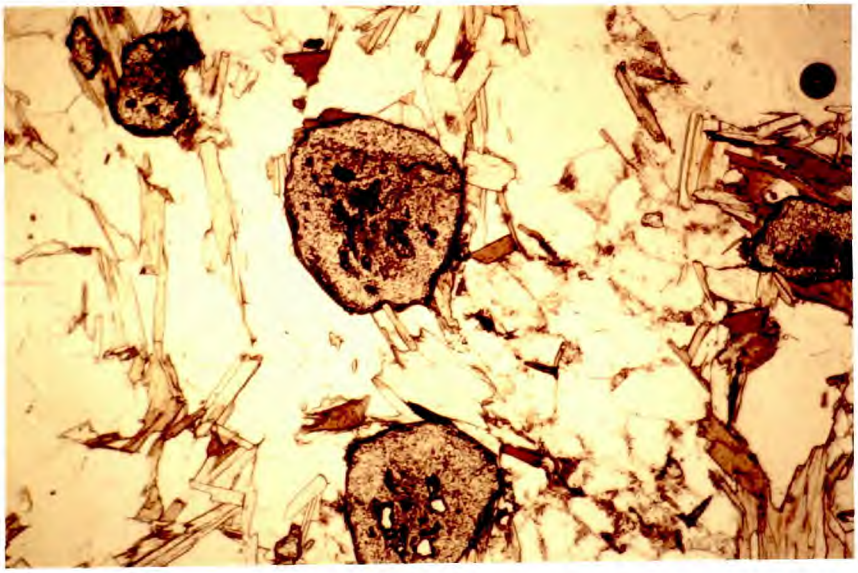


Fig.88(a) Small euhedral garnets in semi-pelitic schist of the Bosco Group. X 55.

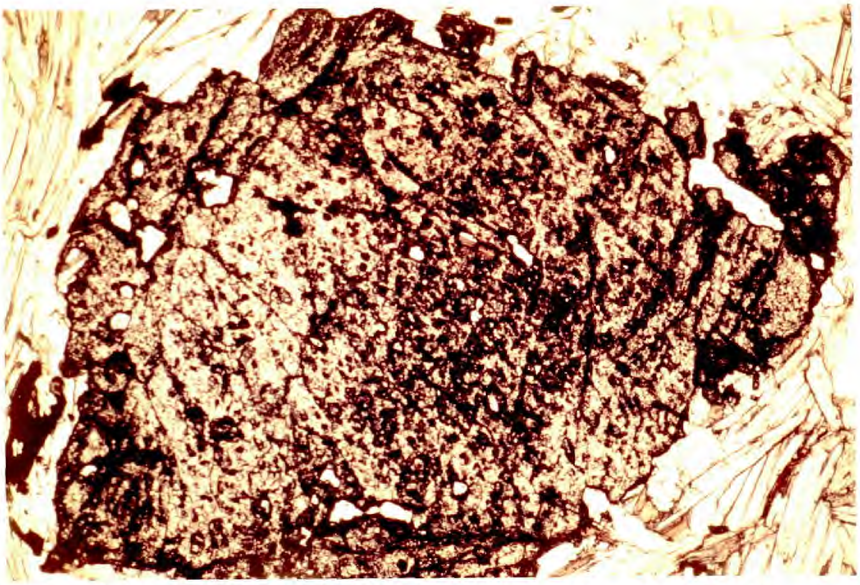


Fig.88(b) Medium sized spongy garnet of Bosco Group semi-pelitic schist. X 55.

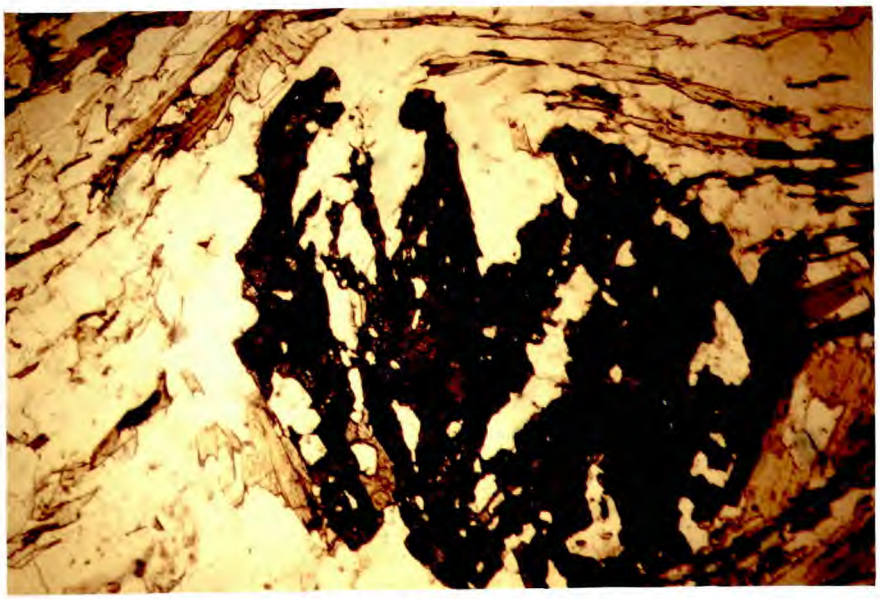


Fig.89(a) Post-tectonic (F2) garnet in Bosco Group semi-pelitic schist. Straight internal inclusion trails rotated during F3 so that they lie at a steep angle to the external F2 schistosity. X 30.



Fig.89(b) Same as above in polarised light. Note micas outlining F2 schistosity deflected around top right corner of porphyroblast

few internal trails observed in the largest garnets are straight, and formed by aligned ilmenite needles and minute quartz grains and muscovite flakes continuous with the schistosity (fig. 90a). In sections cut normal to the F2 lineation a very small number of large garnets contain tightly folded trails of ilmenite needles. These are probably F2 folds, as they predate the porphyroblasts enclosing them.

Garnets of all three sizes may occur together in the same thin section, but it is usual to find only the smallest and largest varieties coexisting. They all crystallized during the static interval between the F2 and F3 deformations. During the F3 deformation some were rotated so that their internal inclusion trails now lie at an angle to the schistosity, but because so few have well developed trails it was impossible to determine if there was any consistency in the direction of rotation. The schistosity is often deflected around the garnets, and small quartz-filled pressure shadows occur where the schistosity has become detached.

Staurolite occurs as elongate euhedral grains up to 4 mm long and 1.5 mm across. These are moderately pleochroic from pale to medium yellow. Like the garnet porphyroblasts they post-date the F2 schistosity, and contain straight inclusion trails of ilmenite needles, quartz grains, and muscovite and biotite flakes (figs. 90b, 91). Individual porphyroblasts lie both parallel to the schistosity and obliquely across it, and a few have been slightly rotated during the F3 deformation. Occasionally the schistosity is deflected around them, but no pressure shadows have developed.

Kyanite is less common than either garnet or staurolite. It occurs as broad, elongate plates with a very strong cleavage parallel to the longest side. The larger porphyroblasts, up to 4 mm long in thin section, are usually skeletal and have abundant needle-like inclusions of quartz and ilmenite continuous with the schistosity (fig.92). Small plates up to 2 mm long rarely



Fig. 90(a) Edge of large post-tectonic (F2) garnet in semi-pelitic schist of Bosco Group, showing internal inclusion trails continuous with F2 schistosity. X 30.

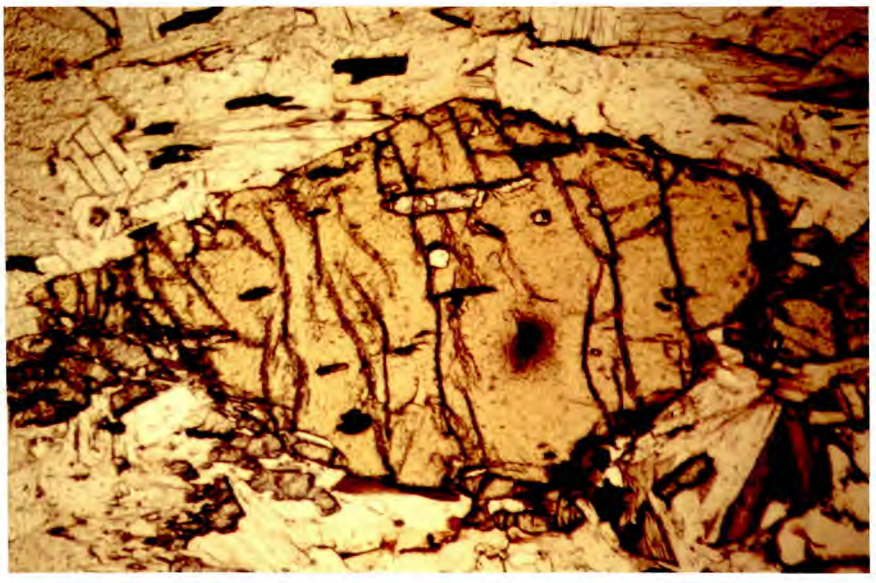


Fig. 90(b) Euhedral post-tectonic (F2) staurolite porphyroblast in semi-pelitic Bosco Group schist growing across F2 schistosity. X 30.

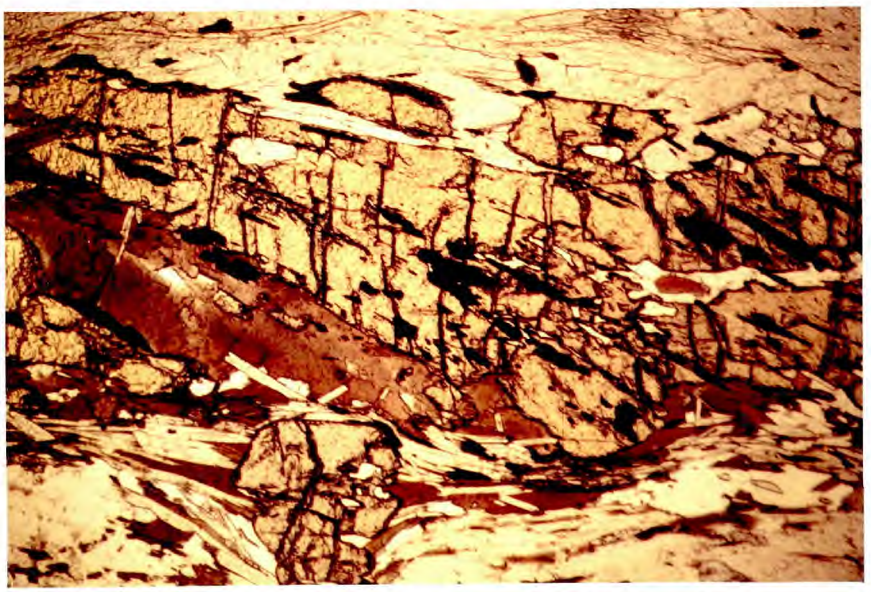


Fig.91(a) Post-tectonic (F2) staurolite porphyroblasts in semi-pelitic Bosco Group Schist, growing across F2 schistosity. Note schistosity deflected around small porophyroblast at bottom centre. X 30.

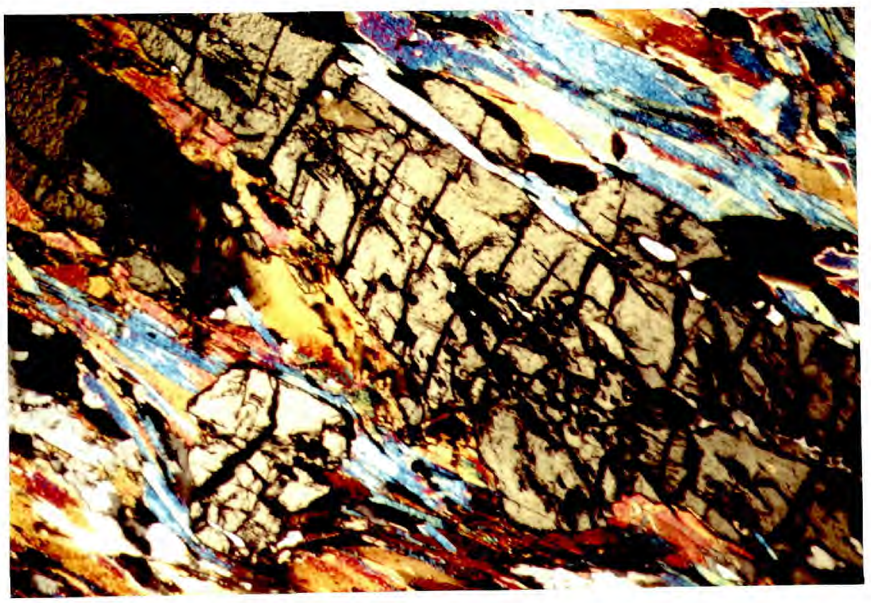


Fig.91(b) Same as above in polarized light.

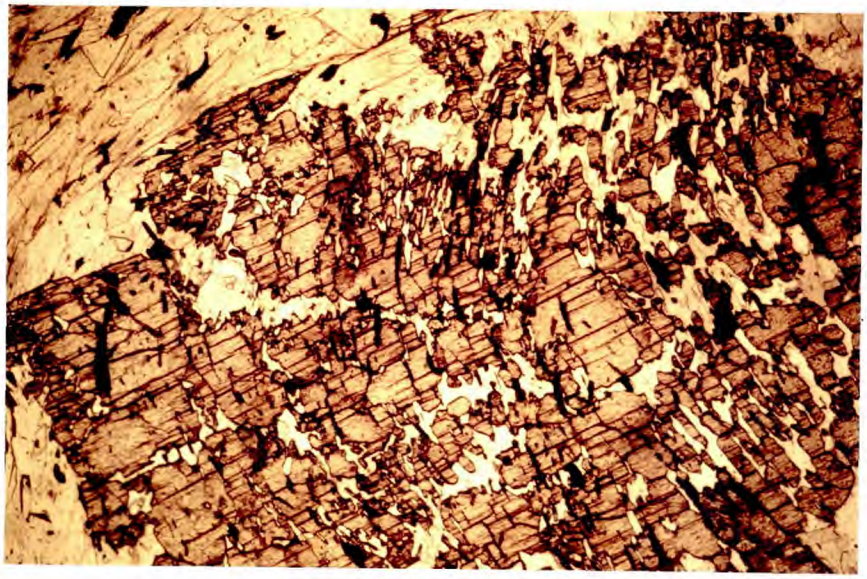


Fig.92(a) Post-tectonic (F2) Kyanite porphyroblast in Bosco Group semi-pelitic schist, growing across F2 schistosity. Schistosity has been deflected around left-hand side of porphyroblast during F3. X 30.

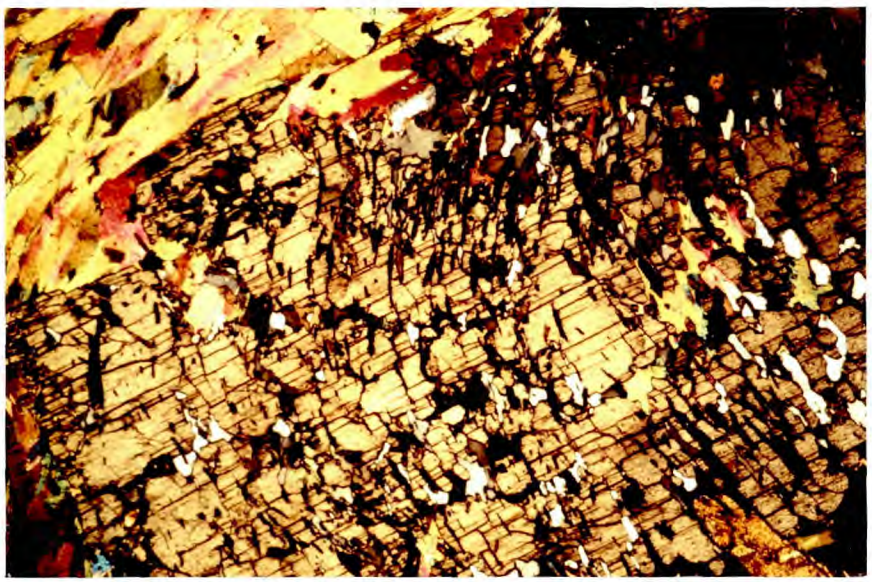


Fig.92(b) Same as above in polarized light.

have inclusion trails and are often oriented parallel to the schistosity. The grains oriented at the highest angles to the schistosity have the schistosity slightly deflected around them. A few grains were also bent during F3.

Tourmaline occurs as minute euhedral grains. It is pleochroic from almost colourless to yellow-green, and was identified as the iron-rich variety schorlite. In common with the other porphyroblasts, tourmaline post-dates the F2 schistosity. It was also observed both included in garnet and containing minute garnet inclusions.

Plagioclase was the last prominent porphyroblast forming mineral to crystallize, and is the least common. It forms large, usually untwinned plates which are clear in polarised light and slightly cloudy in plain light. These contain straight inclusion trails of graphite, ilmenite, muscovite and biotite, and occasionally enclose garnet, muscovite and biotite porphyroblasts (fig.93). A few plagioclase porphyroblasts have the schistosity slightly deflected around them, suggesting that they were deformed during F3. The composition, determined from twin lamellae, varies from An_{22} to An_{43}.

The mineral parageneses of the semi-pelitic schists of the Bosco Group are illustrated in fig.97a. The textural relationships are similar to those observed in the Mesozoic peltic schist, except that no syntectonic garnets were discovered. The main period of porphyroblast growth was in the static interval between the F2 and F3 deformations. During F3 many of the porphyroblasts were rotated and the schistosity was deflected around them. There is no evidence that plagioclase continued to crystallize after the F3 deformation. Minor, secondary chlorite was the last mineral to form.

(b) Hornblende Schist

The hornblende schist member of the Bosco Group is a fine grained rock with a granular mosaic dominated by minute basal sections and laths of hornblende. The most common mineral assemblage

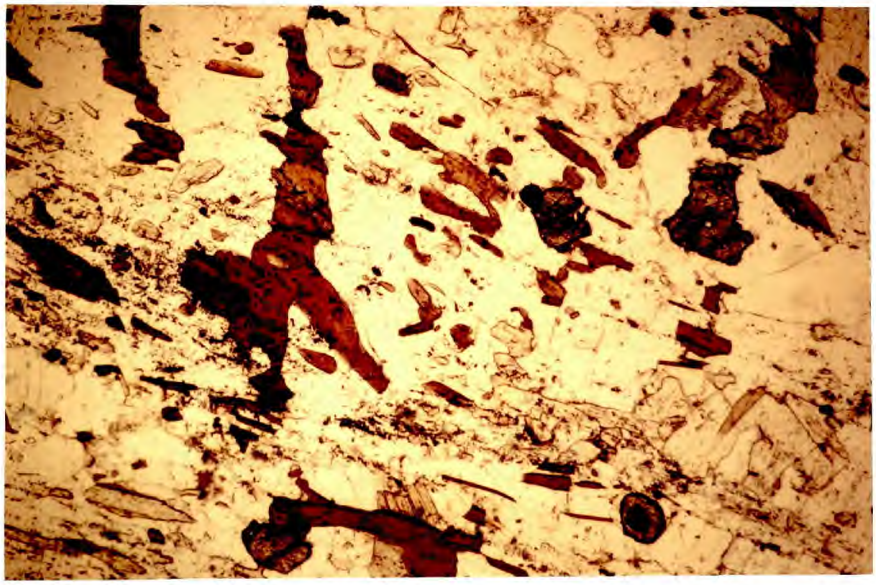


Fig.93(a) Late crystallizing plagioclase in Bosco Group semi-pelitic schist, showing straight inclusion trails outlining F2 schistosity, and biotite, muscovite, garnet and tourmaline inclusions post-dating schistosity. X 30.



Fig.93(b) Same as above in polarized light.

includes hornblende, plagioclase, quartz, epidote, biotite and ilmenite. Biotite and epidote are not always present, and the amount of epidote appears to increase as the grain size of the schist increases. Garnet and rutile also occur, but are uncommon.

In sections cut both parallel to and normal to the strongly oriented hornblende needles the schist shows gradations between an even-grained, granoblastic texture to one with a moderately well developed schistosity. The schistosity is made up of alternating thin layers of quartz - plagioclase and hornblende, and scattered, strongly oriented biotite flakes. Locally the schistosity was folded during the F3 deformation into small chevrons with rounded hinges and straight limbs (fig.94). The hornblende laths are sometimes bent and cracked in the hinge regions of the folds. The schistosity is deflected around the large garnet and plagioclase porphyroblasts, but no pressure shadows formed.

Hornblende occurs as both basal sections with a 56° angle between the cleavages, and as laths up to 2 mm long with 14° to 27° extinction angles. It has a very pale yellow-green (X), olive green (Y) to dark olive green and sometimes medium blue-green (Z) pleochroic scheme. A few small patches of hornblende have altered to mossy brown biotite. The laths often have minute needle-like inclusions of quartz, rutile and ilmenite parallel to their longest edge. They also include rare biotite flakes. No clear time relationships can be determined from the interlocking hornblende laths, but their strong orientation in hand specimen, and the presence of aligned laths and basal sections in the same thin section suggest that they crystallized both during and after the F2 deformation.

Plagioclase occurs as small, straight-sided twinned grains parallel to the schistosity, and larger poikilitic plates up to 3 mm across. Some of the large plates are partly twinned, and others appear as aggregates of small grains with randomly oriented twin lamallae. They are slightly cloudy in plane light, but in polarised light the many small, rounded quartz inclusions give the appearance of sieve structure. Inclusions of all other minerals in the same

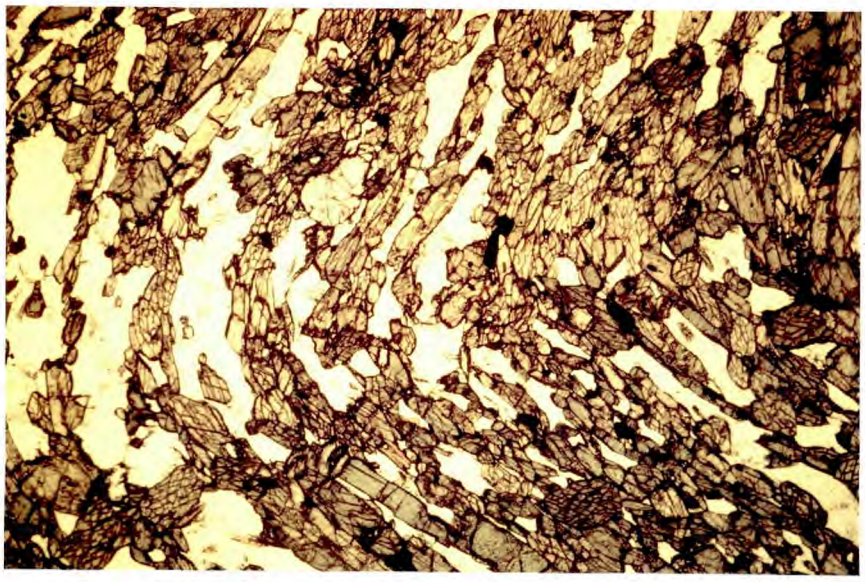


Fig.94(a) Bosco Group hornblende schist showing F2 schistosity composed of quartz-plagioclase and hornblende bands, deformed by F3 minor fold. Note hornblende crystals occur as laths parallel to the schistosity and basal section parallel to F2 lineation. X 30.

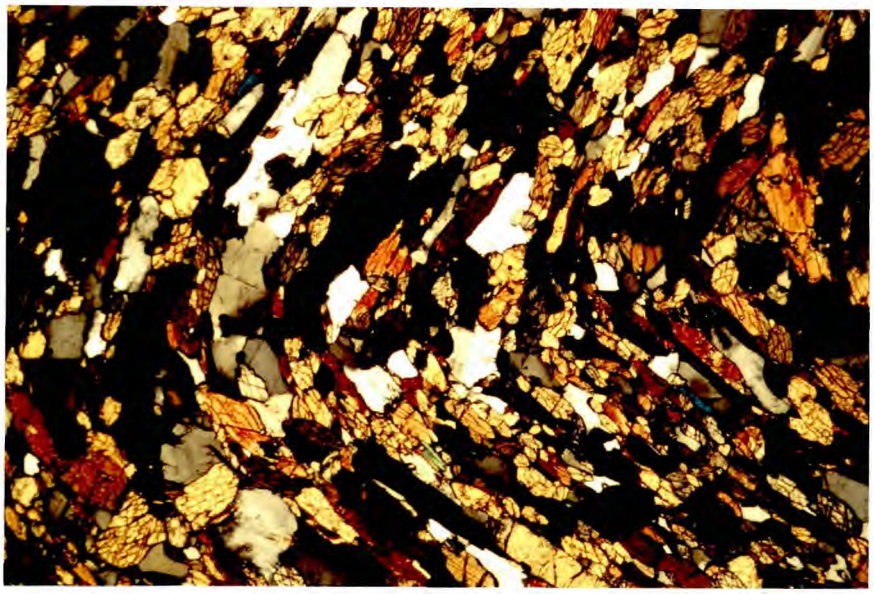


Fig.94(b) Same as above in polarized light.

thin sections occur in the plagioclase porphyroblasts. The schistosity is slightly deflected around them, showing that they crystallized in the static interval between the F2 and F3 deformations. The most calcic composition, determined from a porphyroblast in a rock collected from Alpe Bobna, was An_{42}.

Quartz occurs as very small grains with undulose extinction and slightly irregular boundaries. A few long thin quartz layers are strongly strained and polyganised.

Epidote is generally colourless or mildly pleochroic from neutral to pale green. It occurs as small grains and stubby laths up to 0.5 mm long, with a good cleavage parallel to the longest edge. There is no clear indication of the time of crystallization of the epidote but it predates the large plagioclase porphyroblasts, and probably grew at the same time as the hornblende with which it is interlocked.

Biotite has a pale brown (X) to dark red-brown (Z) pleochroic scheme. It is uncommon, occurring as relatively stout flakes parallel to the schistosity and folded with it, but is occasionally randomly oriented. A number of flakes are partly altered to chlorite.

Garnet is represented by very pale pink, almost colourless almandine. It occurs as minute subhedral grains up to 0.5 mm across, and large skeletal crystals up to 7 mm across. The small grains have a slightly mossy appearance and are usually cracked, while the skeletal crystals have straight inclusion trails of ilmenite, hornblende and biotite. The schistosity is slightly deflected around the garnets. The textural evidence suggests that the garnets crystallized under static conditions, after the hornblende and biotite, but before the large plagioclase plates.

The mineral parageneses of the hornblende schist are illustrated in fig.97b. They show that the main period of crystallization was under static conditions between the F2 and F3 deformations.

Associated with the hornblende schist are small pods of coarse grained, mottled amphibolite and ultramafic schist. The amphibolite grades into the hornblende schist as its grain size decreases and the schistosity develops. It is probably the recrystallized equivalent of the rock type from which the hornblende schist was derived.

(c) Amphibolite

The amphibolite is a coarse grained rock consisting of stout, interlocking plates of hornblende, epidote and minor plagioclase and rutile (fig.95). The hornblende has a pale yellow-green (X), olive green (Y), blue-green (Z) pleochroic scheme. It occurs as large plates up to 8 mm long and 2 mm wide, and also as small needles. Epidote occurs as laths up to 2 mm long and as minute euhedral grains, while rutile is present as very small brown to yellow grains. Plagioclase forms small, straight sided, simply twinned grains. A composition of An_{28-30} was determined from a grain in a rock collected just north of the Kleinhorn.

By comparison with the other rock types of the Bosco Group it is suggested that the minerals present in the amphibolite crystallized during the static interval between the F2 and F3 deformations (fig.97c). Judged from the inclusion pattern rutile and the minute hornblende needles appear to have crystallized first, and were followed by epidote and the main hornblende phase. Plagioclase crystallized last, as it contains inclusions of all the other minerals but never occurs as inclusions.

(d) Ultramafic Schist

The ultramafic schist consists of large, prismatic crystals of tremolite in a talc matrix (fig.96). Only two minerals were present in the thin sections examined. Tremolite is slightly pleochroic from neutral (X) to pale green (Z). It occurs as randomly oriented blades up to 5 mm long, and as basal sections with a 56° angle between the two cleavage directions. The blades have cleavage traces parallel to their longest sides, and extinction angles of 4° to 18°. Talc forms stout, colourless cleavage flakes with very shadowy extinction. They are strongly aligned to form a distinct

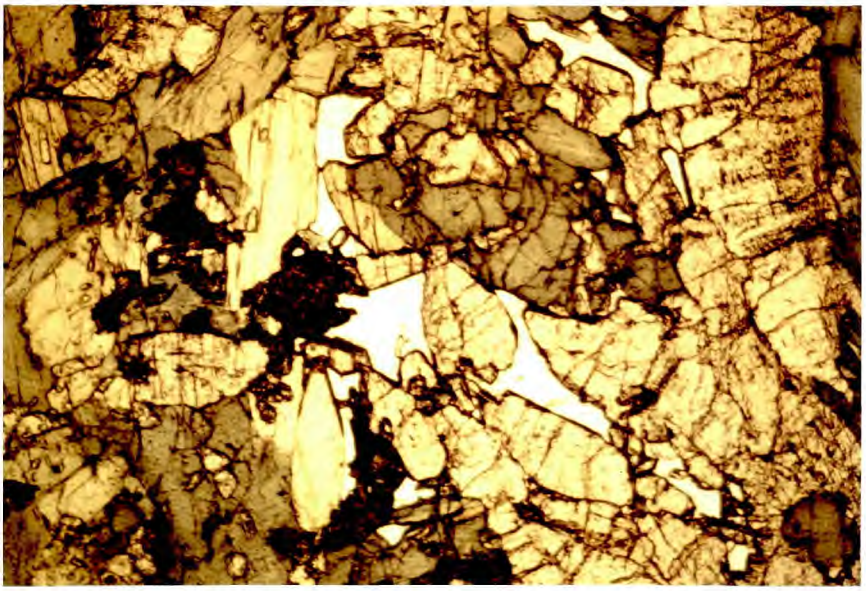


Fig.95(a) Coarse-grained amphibolite, associated with hornblende schist member of the Bosco Group. Composed of hornblende(green) epidote (pale yellow), plagioclase (off-white) and rutile (dark brown). X 30.

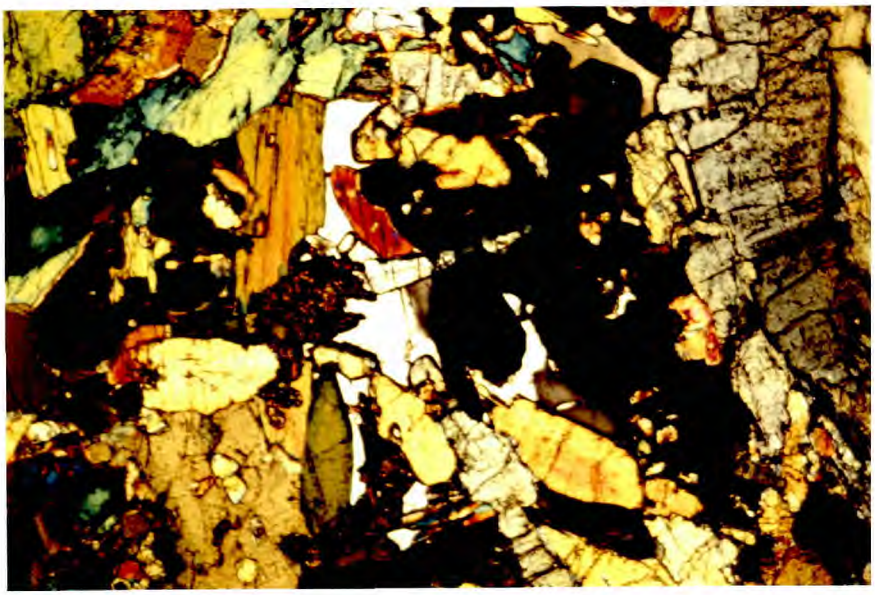


Fig.95(b) Same as above in polarized light.

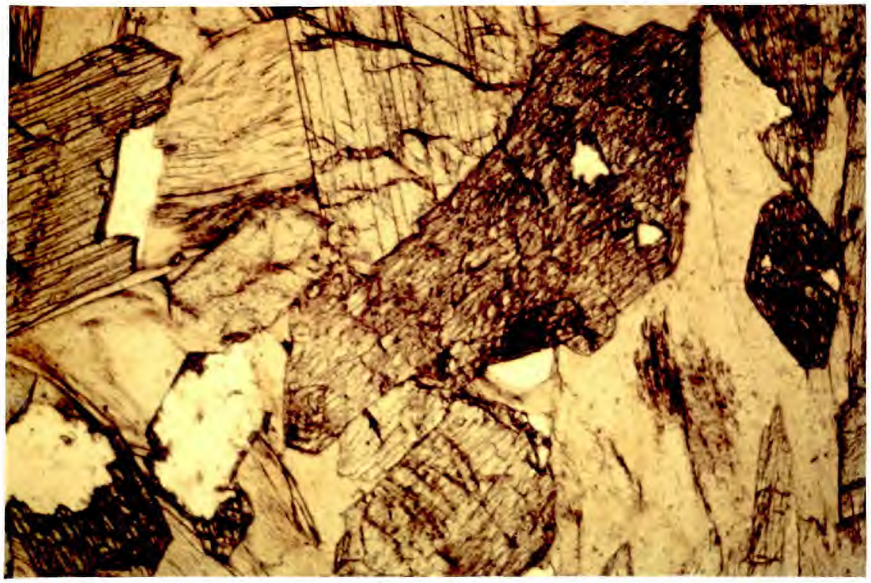


Fig.96(a) Ultramatic schist, associated with hornblende schist member of Bosco Group. Tremolite porphyroblasts grow across talc flakes outlining F2 schistosity. X 30.



Fig.96(b) Same as above in polarized light.

MINERAL PARAGENESES OF BOSO GROUP

FIGURE 97

(a) SEMI-PELITIC SCHIST

MINERAL		F_2		F_3	
QUARTZ		—	—	—	
BIOTITE		—	—	—	
MUSCOVITE		—	—		
ILMENITE		—		—	
PLAGIOCLASE			—		
GARNET			—		
STAUROLITE			—		
KYANITE			—		
TOURMALINE			—		
EPIDOTE			—		
CHLORITE					—

(b) HORNBLENDE SCHIST

MINERAL		F_2		F_3	
HORNBLENDE		—	—		
BIOTITE		—	—		
QUARTZ			—?—		
PLAGIOCLASE			—		
EPIDOTE			—?—		
GARNET			—		

(c) AMPHIBOLITE

MINERAL		F_2		F_3	
HORNBLENDE			—		
EPIDOTE			—		
PLAGIOCLASE			—		
RUTILE			—		

(d) ULTRAMAFIC SCHIST

MINERAL		F_2		F_3	
TALC		—	—		
TREMOLITE			—		

schistosity, which is locally kinked or slightly folded. A few rare flakes grow randomly over the schistosity.

The tremolite porphyroblasts grow over the schistosity formed by the talc flakes, and include a few ghost-like forms which have only partly developed. The schistosity is considered to be an F2 feature that was folded during the F3 deformation and sometimes slightly deflected around tremolite porphyroblasts. Tremolite crystallized under static conditions before the F3 deformation, but after the randomly oriented flakes of talc (fig.97d).

13.4 Antigorio Gneiss

The Antigorio Gneiss consists largely of granite gneiss with minor diorite gneiss and hornblende schist. The metamorphic textures of the granite gneiss have been dealt with in an earlier section, and only the diorite gneiss and hornblende schist are described here.

(a) Diorite Gneiss

The diorite gneiss is a dark, mottled rock with a moderately strong schistosity. It occurs as thin bands in the granitic gneiss which end in a train of dark xenoliths. The mineral assemblage consists of hornblende, biotite, quartz, plagioclase, epidote, and minor rutile and sphene. The average grain size of the quartz and plagioclase grains varies from 0.18 mm to 0.26 mm in different thin sections. The texture is typically gneissic, with strongly oriented, interlocking hornblende and biotite in a granular quartz-plagioclase groundmass (fig.98). The quartz and plagioclase sometimes form large augen which include common epidote grains, but are free of hornblende and biotite.

Hornblende occurs as both basal sections with a 57° angle between the cleavages, and blades up to 2 mm long with 19° to 27° extinction angles. It has a pale brown to pale green (X), olive green (Y), dark

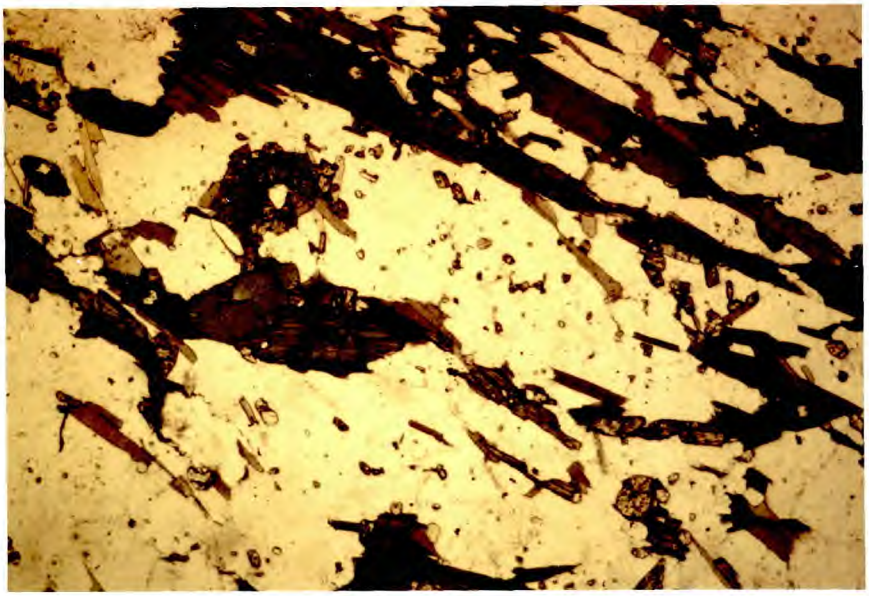


Fig.98(a) Diorite gneiss, from Antigorio Gneiss, F2 schistosity outlined by biotite and hornblende. Note common epidote grains. X 30.

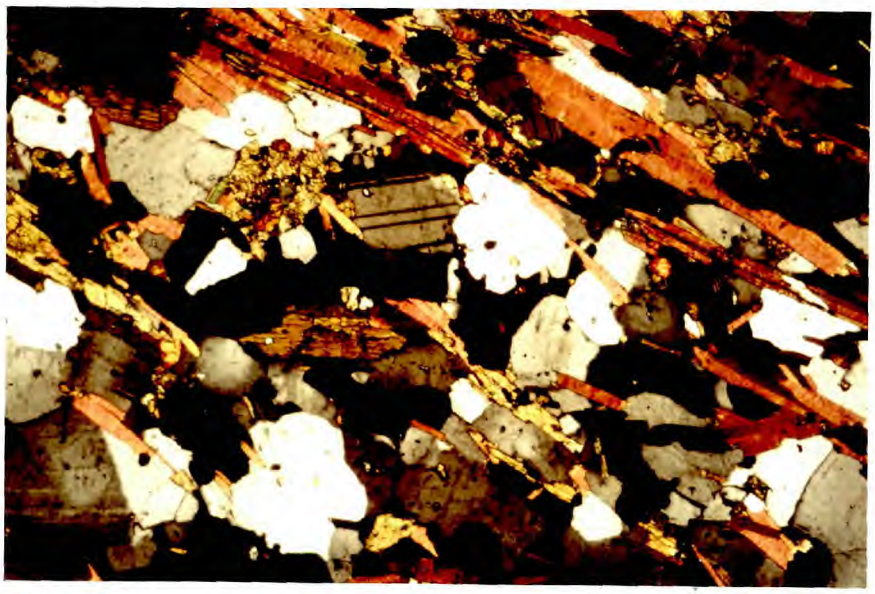


Fig.98(b). Same as above in polarized light. Note undeformed "granitic" texture of quartz and plagioclase grains.

blue-green pleochroic scheme. The blade-like crystals are generally strongly aligned, and contain inclusions of rutile and epidote.

Biotite occurs as long, thin and strongly aligned cleavage flakes outlining the schistosity. They are pleochroic from straw yellow (X) to dark brown or dark green-brown (Z), but are sometimes chloritized. Only a few randomly oriented biotite flakes were observed.

Epidote forms minute grains, scattered throughout the diorite gneiss. They are colourless in plane light, but have a very conspicuous birefringence in polarised light.

Quartz and plagioclase form angular grains with only a few sutured boundaries. Quartz is more common, and generally has undulose extinction and is sometimes cracked. Large grains are often polyganised. The plagioclase (composition An_{20-35}) is commonly twinned, and the larger grains are usually cloudy and sericitic.

Rutile and sphene occur as minute grains, commonly included in hornblende and biotite.

The textures and mineral parageneses of the diorite gneiss are very similar to those of the granitic gneiss. Hornblende and biotite began crystallizing during the F2 deformation and continued to grow post-tectonically. The quartz and plagioclase are probably the original igneous components, and only partially recrystallized during the Alpine metamorphism.

(b) Hornblende Schist

The hornblende schist occurs as a long thin band enclosed by granitic gneiss on the ridge west of the Martschenspitz. In the field and in thin section it is identical to the hornblende schist of the Bosco Group. It is a fine grained rock with a poorly developed schistosity but strong lineation. The mineral assemblage consists of hornblende, epidote, quartz, plagioclase and rutile.

Hornblende, the dominant mineral, occurs as basal sections and aligned and randomly oriented blades up to 1.5 mm long. It is

typically pleochroic from pale yellow-green (X) to olive green (Z) and sometimes medium blue-green. Epidote occurs as small colourless grains and a few randomly oriented blades. The remainder of the rock consists of a fine mosaic of straight-edged quartz and plagioclase grains. The plagioclase is generally twinned, and has a composition of An_{13-33}. There are also a few minute prismatic grains of yellow-brown rutile.

CHAPTER 14

TIME, TEMPERATURE AND TECTONICS

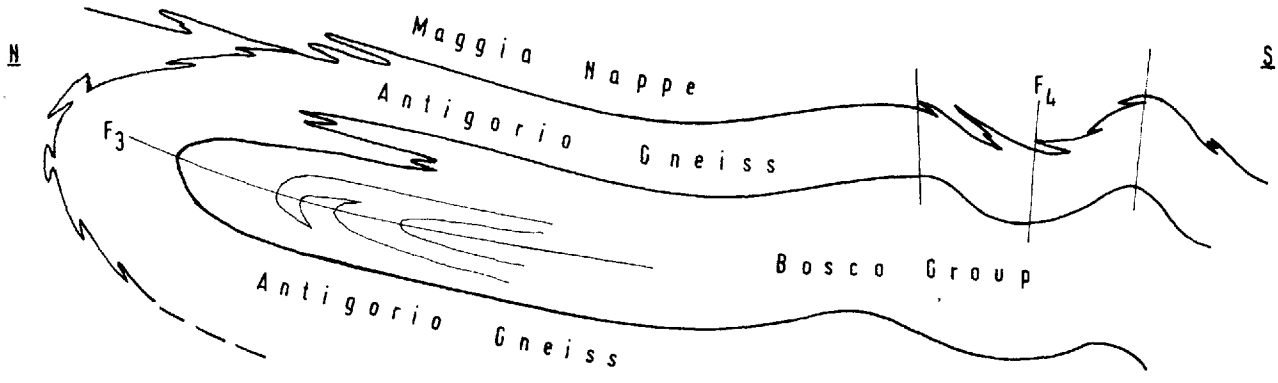
The discovery of the relative age and nature of the Wandfluhhorn Antiform throws a completely new light on the structural geology of the Lower Pennine nappes. The existence of the antiform creates as many problems as it solves; for instance, what effect does it have on the assumed tectonic order of the nappes?; are there any complimentary structures tectonically above or below?; what were the rheological conditions of the basement rocks during its formation?

The first significant answer is that there do not appear to be any complimentary structures tectonically above or below the Wandfluhhorn Antiform. Examination of the 1:200,000 Ticino geological map shows that on the upper limb of the antiform the band of Mesozoic rocks between the Bosco Group and Antigorio Gneiss (i.e. Stella Syncline) and between the Antigorio Gneiss and basement of the overlying Maggia Nappe, extend south towards the Insubric Line and are not refolded by any large, post F2 recumbent structures. Kobe (1956), Knup (1958) and Wieland (1966) found only open, east-west tending folds on the upper limb of the Wandfluhhorn Antiform between the Valle di Bosco and the Insubric Line. In the classification used in this thesis these folds could probably be designated F4 (fig.99a).

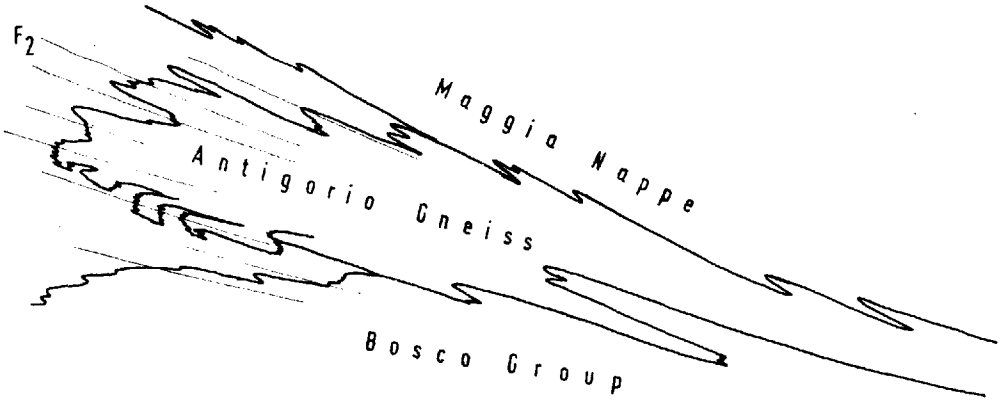
No complimentary structures appear below the Wandfluhhorn Antiform. This is hardly surprising as the rocks on the lower limb, exposed on the floor of the Valle Antigorio, are the lowest tectonic units in the Alps (i.e. Verampio-Baceno complex; Milnes, 1968).

As there appear to be no complimentary major F3 structures in the Lower Pennine region between the Valle Antigorio and the Valle Maggia, it becomes a simple exercise to unfold the Wardfluhhorn Antiform, restoring the rocks to their pre-F3 position (fig.99b). This leads to the conclusion that before the F3 deformation the rocks were fairly flat-lying, as they could not otherwise have folded into a large recumbent form with a subhorizontal axial plane, and also that the

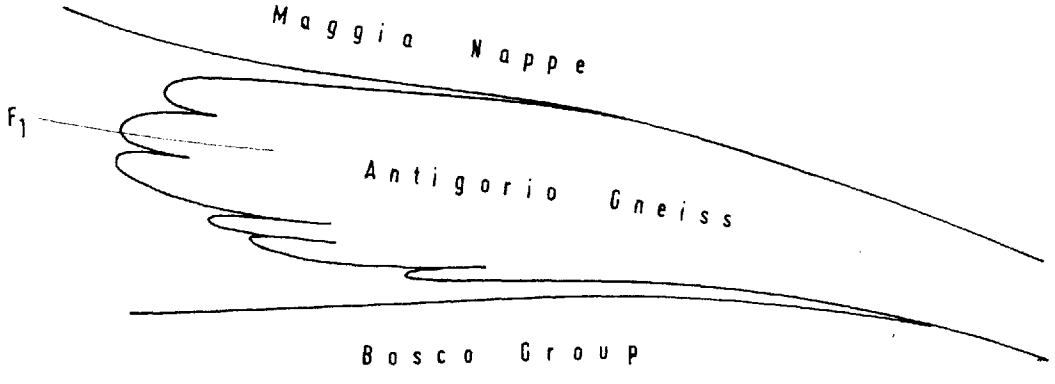
FIGURE 99



(a) POST-F_3-



(b) POST-F_2-



(c) POST-F_1-

DIAGRAMMATIC RECONSTRUCTION OF TECTONIC HISTORY

[Not to scale]

Antigorio Gneiss overlay the Bosco Group.

It has been shown in this thesis that during the F2 deformation the Antigorio Gneiss was strained about 75%, and that the Mesozoic rocks separating the Antigorio Gneiss and Bosco Group were refolded into recumbent, isoclinal structures with a powerful axial plane schistosity. Restoring the rocks to their pre-F2 position requires unstraining them so that each thin slab of material becomes a cube (e.g. fig.49). This reconstruction (fig.99c), to the position at the end of the F1 deformation, still leaves the Antigorio Gneiss on top of the Bosco Group. Since it is recognised that the direction of tectonic transport in the Alps was northwards (e.g. Argand. 1916; Trumpy, 1960), it seems likely that during the F1 deformation a nappe composed of Antigorio Gneiss was thrust over the Bosco Group from the south (see Chapters 3 and 10). This implies that the Antigorio Nappe, far from being the lowest tectonic unit of the Lower Pennine Nappes, overlies the Monte Leone Nappe (=Bosco Group?).

The three phase deformation history seems fairly well established in the Lower Pennine Nappes (Chapter 8), and there is now sufficient evidence available from which the time and temperature of each deformation may be estimated (fig.100). Trumpy (1960) considered that the beginning of the Alpine orogeny was marked by the appearance of flysch sediments in the ultrahelvetic rocks, derived from "rising cordilleras" to the south. The flysch, commencing in the early Palaeocene, records the time that the F1 nappes of the Lower Pennine region, immediately south of the ultrahelvetic zone, were exposed to erosion. Judged from the appearance of the flysch, the F1 deformation occurred about 60 million years ago during the latest Cretaceous and earliest Tertiary.

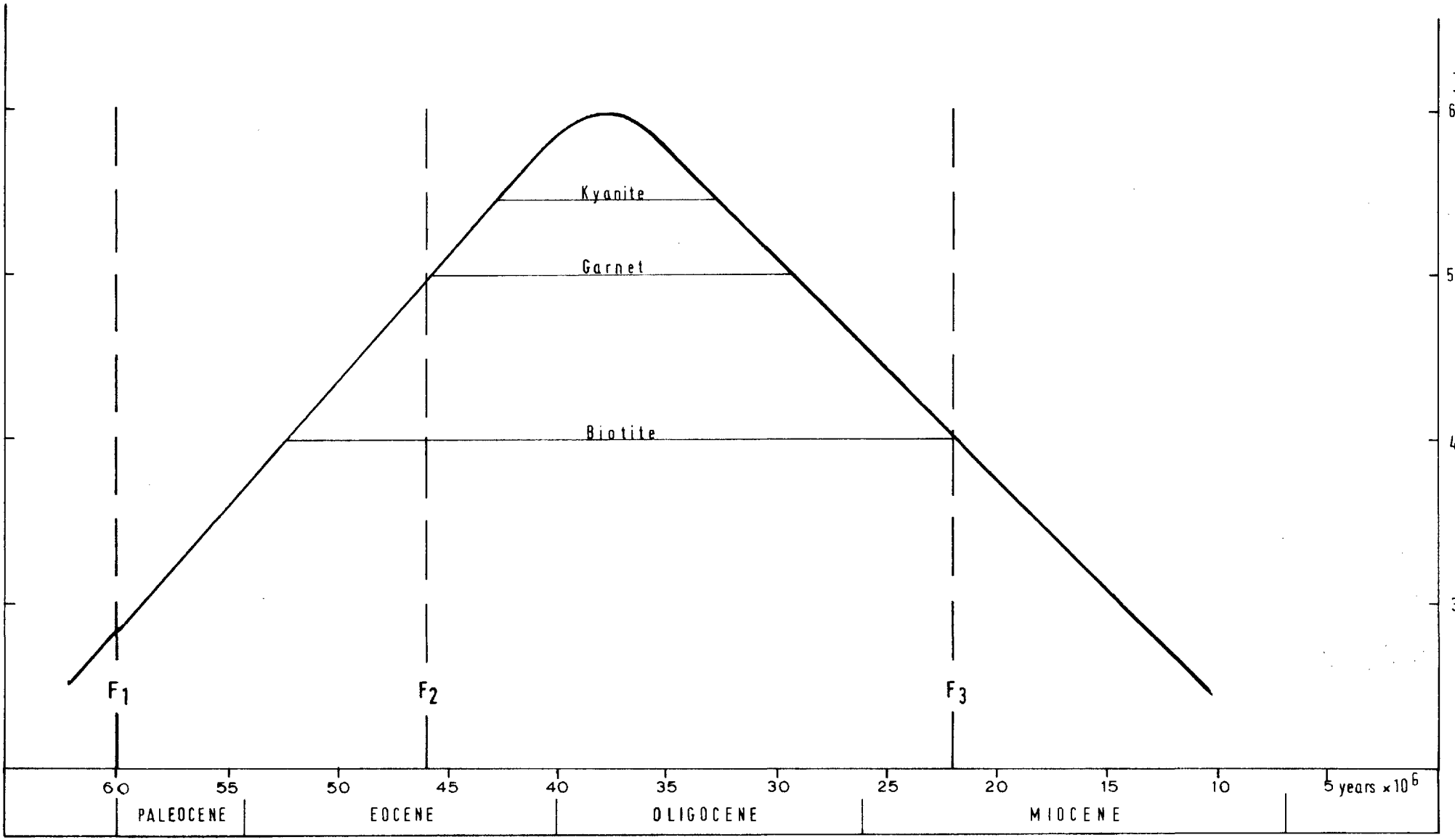
There is no evidence for any metamorphism in the Lower Pennine region during the F1 deformation. The mineral assemblages of the Mesozoic rocks do not exhibit the replacement textures described by Bearth (1966) and Nicolas (1969), and it can only be inferred, from lack of evidence, that the temperature and pressure were below those necessary to initiate blue schist metamorphism.

During the F2 deformation the F1 nappes were strongly refolded. The most reliable estimate of the time of the time of the deformation has been made by Steiger (1964) who dated hornblende from the southern Gotthard massif, immediately north of the Lower Pennine region. The hornblende, aligned parallel to the F2 lineation, gave K-Ar ages of 46 million years (i.e. middle to late Eocene), and is believed to have crystallized syntectonically. As Chadwick (1968) and Higgins (1964b) have shown the deformation "pulses" migrated northwards, and the 46 million year date must be considered as the youngest possible age of the F2 deformation in the Lower Pennine region.

The results of the strain analysis (Chapter 9) suggest that the F2 deformation occurred under extremely ductile conditions. The temperature during the deformation may be estimated from the syntectonic crystallization of common muscovite and biotite and rare garnet, and was probably about 500°C (Winkler, 1967).

The peak of metamorphism in the Simplon area, west of the Valle di Bosco, has been dated as occurring 38 ± 2 million years ago, during the late Eocene - early Oligocene (Hunziker, 1969). In all but the frontal portion of the Lower Pennine Nappes the metamorphic peak occurred during static conditions between the F2 and F3 deformations. At this time the rocks reached their highest temperature of about 650°C in the south, adjacent to the Insubric Line, and 530°C in the north, along the southern edge of the Gotthard Massif. (Chapter 12). The rocks of the Valle di Bosco, roughly in the centre of the Lower Pennine region, were heated to about 600°C and confined beneath a 15 km thick nappe pile.

The F3 deformation post-dated the metamorphic peak. The timing of the deformation may be estimated from the cooling ages of biotite (13 - 15 million years in the Valle di Bosco; Jäger et al., 1967), the temperature at which biotite becomes isotopically stable (300°C; Jäger et al.; 1967) and the crystallization temperature of biotite (c. 400°C; Winkler, 1967). The latest biotite to crystallize in the rocks of the Valle di Bosco occurs in very small amounts in the axial plane fabric of a few F3 minor folds (Chapter 7). The rare occurrence of biotite suggests that the temperature of the rocks during the F3 deformation was close to the crystallization temperature of 400°C.



TIME-TEMPERATURE GRAPH

FIGURE 100

During the 21 to 27 million years between the metamorphic peak and the time the biotite attained isotopic stability, the temperature dropped about 300°C. Assuming a constant cooling rate of 11 - 14°C/ million years, the temperature would have dropped to 400°C 14 - 18 million years after the metamorphic peak (i.e. between 20 and 24 million years ago). The time of the F3 deformation is therefore placed at 22 $\pm$ 4 million years ago, during the early Miocene.

REFERENCES

American Geological Institute, 1962: Dictionary of Geological Terms. Doubleday and Co., New York, 545 p.

ANDERSON, E.M., 1951: The Dynamics of Faulting. Oliver and Boyd, Edinburgh.

ARGAND, E., 1916: Sur l'arc des Alpes Occidentales. Eclogae geol. Helv., 14(1): 145 -191.

ARNOLD, A., 1970: On the history of the Gotthard Massif (Central Alps, Switzerland). Eclogae geol. Helv., 63(1) 29 - 30.

BEACH, A., 1971: The relation between metamorphic reactions and tectonic structure at Scourie, Sutherland: A Study of Regeneration. Unpub. Ph.D. thesis, Imp. Coll., Univ. London.

BEARTH, P., 1958: Ueber einen wechsel der Mineralfacies in de Wurtzelone des Penninikums. Schweiz. Min. Pet. Mitt., (S.M.P.M.) 38: 363 - 373.

_____, 1962: Versuch einer Gliederung alpin-metamorpher Serien der Westalpen. S.M.P.M., 42: 127-137.

_____, 1966: Zur mineralfaziellen Stellung der Glaucophangesteine der Westalpen. S.M.P.M., 46:13 - 24.

BERTRAND, M., 1884: Rapports de structure des Alpes de Glaris et du Bassin haviller du Nord. Bull. Soc. geol. Fr. 3eme Ser. 12.

BIOT, M.A., ODE, H., and ROEVER, W.L., 1961: Experimental verification of the folding of stratified viscoelastic media. Geol. Soc. Am. Bull., 72: 1621 - 1630.

BOLLI, H.M., and NABHOLZ, W.K., 1958: Bundnerschiefer, ähnliche fossilarme serie und ihr Gehalf an Mikrofossilien. Eclogae geol. Helv., 52(1): 237 - 270.

CHADWICK, B., 1965: The structural and metamorphic geology of the Lukmanier Region, Ticino-Grisons, Switzerland. Unpub. Ph.D. thesis, Imp. Coll., Univ. Lond.

_____, 1968: Deformation and metamorphism in the Lukmanier Region, Central Switzerland. Geol. Soc. Am. Bull., 79:1123-1150.

CHATTERJEE, N.D., 1961: The alpine metamorphism in the Simplon Area, Switzerland and Italy. Geol. Rundschau, 51: 1 - 72.

COBBOLD, P.R., COSGROVE, J.W., and SUMMERS, J.M., 1971. Development of internal structures in deformed anisotropic rocks. Tectonophysics, 12: 23 - 53.

COLLET, L.W., and PAREJAS, E., 1931: Geologie de la chaine de la Jungfrau. Beit. Geol. Karte Schweiz. N.F. 63, Lieferung.

Commissione Geologica Svizzera, 1955: Carta geologica generale della Svizzera, 1:200,000, Foglio 7, Ticino. Kümmerly and Frey, Bern.

DE SITTER, L.U., 1954: Schistosity and shear in micro and macro-fabrics. Geol. Mijnbouw., 16: 429 - 439.

_____, 1958: Boudins and parasitic folds in relation to cleavage and folding. Geol. Mijnbouw, 20: 277 - 286.

DESOR, E., 1865: Der Gebirgsbau der Alpen. Wiesbaden.

DUNNET, D., 1969: A technique of finite strain analysis using elliptical particles. Tectonophysics, 7(2): 117 - 136.

DURNEY, D.W., 1972: Solution - transfer, an important geological deformation mechanism. Nature, 235 (5337):315-6.

EVANS, B.W., and TROMMSDORFF, V., 1970. Regional metamorphism of ultrabasic rocks in the central Alps: Parageneses in the system CaO - MgO - SiO_2 - H_2O. S.M.P.M., 50(3): 481 - 492.

FLINN, D., 1962: On folding during three-dimensional progressive deformation. Quart. J. Geol. Soc. 118: 385 - 433.

FRANKS, G.D., 1968: A study of the upper Palaeozoic sediments and volcanics in the northern part of the eastern Aar Massif. Eclogae geol. Helv., 61: 49 - 140.

GAY, N.C., 1968: Pure shear and simple shear deformation of inhomogeneous viscous fluids. 1. Theory. Tectonophysics, 5(3): 211 - 234.

GRUTTER, O., 1929: Petrographische und geologische untersuchungen in der Region von Bosco (Valle Maggia) Tessin. Verh. Natf. Ges. Basel, Bd. 40(1):78 - 152.

GÜNTHERT, A., 1957: Geologischer Atlas der Schweiz, 1:25,000, Blatt 1271, Basodino. Schweiz. Geol. Komm.

_____, 1958. Geologischer Atlas der Schweiz, 1:25,000, Blatt 1271, Basodino (Erläuterungen). Schweiz Geol. Komm.

_____, 1971: Klufttypen im nordwestlichen Tessin und westlichen Gotthardmassiv, eine Übersicht. S.M.P.M., 64(1): 105 - 131.

HEIM, A., 1878: Mechanisms der Gebirgsbildung im Auschluss an die geologische Monographie der Todi-Windgallen Gruppe. 2 vols., Basel.

HIGGINS, A.K., 1964a: Fossil remains in staurolite-kyanite schists of the Bedretto Mulde Bundnerschiefer. Eclogae geol. Helv., 57: 151 - 6.

_____, 1964b: The structural and metamorphic geology of the area between Nufenenpass and Basodino, Tessin, Switzerland. Unpub. Ph.D. thesis, Imp. Coll., Univ. Lond.

HOBBS, B.E., 1968: Recrystallization of single crystals of quartz. Tectonophysics, 6(5):353 - 401.

HUNZIKER, J.C., 1966: Zur Geologie und Geochemie des Gebietes zwischen valle Antigorio (Provincia di Novara) und Valle di Campo (Kt. Tessin). S.M.P.M., 46: 473 - 552.

_____, 1969: Rb - Sr Alterstimmungen aus den Walliser Alpen Hellglimmer und Gesamtgestein-salterwerte. Eclogae geol. Helv., 62(2):527 - 542.

JAGER, E., NIGGLI, E., and WENK, E., 1967: Rb - Sr Altersbestimmungen an Glimmer der zentralalpen. Beit. Geol. Kart. Schweiz, N.F. 134.

JOOS, M.G., 1969: Zur Geologie und Petrographie der Monte Giove-Gebirgsgruppe im östlichen Simplon Gebiet (Novara Italia). S.M.P. M., 49(2): 277 - 323.

KNUP, P., 1958: Geologie und Petrographie des Gebietes zwischen Centovalli - Valle Vigezzo und Onsernone. S.M.P.M., 38: 83 - 236.

KOBE, H.W., 1956: Geologisch - Petrographische untersuchungen in der Tessiner werzelone zwischen Vergeletto-Onsernone und Valle Maggia. S.M.P.M., 36: 244 - 238.

_____, 1966: Struktur des Gebietes zwischen Gresso und Passo della Garina, Tessin. (Mit Deutungsversuch der tektonisch-structurellen Verhältnisse des Gebietes vom Valle di Vergeletto bis zum untersten Val Verzasca). Eclogae geol. Helv., 59(2):789 - 802.

LUGEON, M., 1901: Les grandes nappes de recouvrement des Alpes du Chablais et de Suisse. Bull. Soc. geol. Fr. 4eme. Ser.1, 723 - 825.

_____, 1902: Sur la coupe geologique du massif du Simplon. C.R. Acad. Sci. Paris, 134: 726 - 727.

_____, and ARGAND, E., 1905: Sur les grandes nappes de la recouvrement de la zone du Piedmont. C.R. Acad. Sci. Paris, 140: 1364-1367.

MEANS, W.D., and PATERSON, M.S., 1966: Experiments on preferred orientation of platy minerals. Contrib. Min. Pet., 13: 108 - 120.

MILNES, A.G., 1965: Structure and history of the Antigorio Nappe (Simplon Group, North Italy). S.M.P.M., 45(1):167-177.

_____, 1968: Strain analysis of basement nappes in the Simplon region, Northern Italy. XXIII Int. Geol. Congress, 3:61-76.

NABHOLZ, W.K., 1945: Geologie der Bundnerschiefergebirge zwischen Rheinwald, Valser und Satiental. Eclogae geol. Helv., 38(1): 1-119.

NICOLAS, A., 1969: Tectonique et metamorphose dans les Stura di Lanzo (Alpes Piedmontaises). S.M.P.M., 49(2) 359-377.

NIGGLI, E., 1960: Mineralzonen der alpinen Metamorphose in den Schweizer Alpen. XXI Int. Geol. Congress, 13:132-138.

_____, 1970: Alpine Metamorphose und alpine Gebirgsbildung. Fortschr. Miner., 47(1): 16-26.

_____, and NIGGLI, C.R., 1965: Karten der Verbreitung einiger Mineralien der alpidisch Metamorphose in den Schweizer Alpen. (Stilpnomelane, Alkali-Amphibol, Chloritoid, Staurolith, Disthen, Sillimanit). Eclogae geol. Helv., 58:3335-368.

NIGGLI, P., PREISWERK, H., GRUTTER, O., BOSSHARD, L., and KUNDIG, E., 1936: Geologische Beschreibung der Tessiner Alpen Zwischen Maggia - und Bleniotal. Beit. Geol. Karte Schweiz., N.F. 71.

PATERSON, M., and WEISS, L.E., 1961: Symmetry concepts in the structural analysis of deformed rocks. Geol. Soc. Am. Bull., 77: 343-374.

POWELL, D., and TREAGUS, J.E., 1970: Rotational fabrics in metamorphic minerals. Mineral. Mag., 37: 801-14.

PREISWERK, H., 1918: Geologische Beschreibung der lepontinischen Alpen. Oberes Tessin - und Maggiagebiet. 1:50,000. Beit XXVI. Geol. Spezialkarte Nr. 116.

_____, 1921: Die zwei Deckenkulminationen Tosa - Tessin und Tessinerquerfalte. Eclogae geol. Helv., 16: 177-187.

RAMSAY, J.G., 1962: The Geometry and mechanics of formation of "similar" type folds. J. Geol., 70:309-327.

_____, 1967: Folding and fracturing of rocks. McGraw-Hill, New York.

REINHARDT, B., 1966: Geologie und Petrographie der Monte Rosa-Zone, der Sesia-Zone und des Canavese im Gebiet zwischen Valle d'Ossola und Valle Loana. S.M.P.M., 46: 553-679.

RENEVIER, E., 1879: Notice of Prof. Heim's work on the mechanism of the formation of mountains. Geol. Mag., Dec. II, 6, 4 pp.

RUTTER, E.H., 1970: An experimental study of the factors affecting the rheological properties of rocks in simulated geological environments. Unpub. Ph.D. thesis, Imp. Coll., Univ. Lond.

SCHMIDT, C., 1894: Geologische Exkursionen durch die zentraren Schweizer Alpen. Livret-Guide geol., Paris-Lousanne, 136-142.

_____, 1907: Uber die Geologie des Simplon-gebietes. Eclogae geol. Helv., 9:484-584.

_____, PREISWERK, H., and STELLA, A., 1908: Geologische Karte der Simplongruppe mit Profilen und Erläuterungen. Beit. XXVI, 1:50,000. Spezial-Karte Nr. 48.

SCHWANDER, H., HUNZIKER, J.C., and STERN, W., 1968: Zur Mineralchemie von Hellglimmern in dem Tessinalp. S.M.P.M., 48(2) 357-390.

_____, and WENK, E., 1967: Studien mit der Röntgen-Mikrosande an basischen Plagioclasen alpiner Metamorphite. S.M.P.M., 47: 225-234.

SIBBALD, T.I.I., 1971: The structural and metamorphic geology of the Val Piora region, Ticino, Switzerland. Unpub. Ph.D. thesis, Imp. Coll., Univ. Lond.

SIDDANS, A.W., 1971: The origin of slaty cleavage. Unpub. Ph.D. thesis, Imp. Coll., Univ. Lond.

SPRY, A., 1963: Chronological analysis of crystallization and deformation of some Tasmanian Precambrian rocks. J. geol. Soc. Aust., 10(1): 193-208.

STEIGER, R., 1964: Dating of orogenic phases in the central Alps by K-Ar ages of hornblende. J. Geophys. Res., 69(24):5407-5412.

TALBOT, C.J., 1970: The minimum strain ellipsoid using deformed quartz veins. Tectonophysics, 9:47 - 76.

THAKUR, V.C., 1971: The structural and metamorphic history of the Mesozoic and pre-Mesozoic basement rocks of the Molare region, Switzerland. Unpub. Ph.D. thesis, Imp. Coll., Univ. Lond.

TROMMSDORFF, V., 1966: Progressive metamorphose Kieseliger Karbonategestein in den Zentralalpen. S.M.P.M., 46: 431-460.

_____, 1968: The Wollastonite reaction in the Western Bergell Alps. S.M.P.M., 48: 828-829.

_____, and EVANS, B.W., 1970: The stable association of enstatite-forsterite-chlorite in amphibolite facies ultramafics of the Lepontine Alps. S.M.P.M., 49(2): 325-332.

TRUMPY, R., 1954: La zone de Sion-Courmayeur dans le haut Val Ferret valaisan. Eclogae geol. Helv., 47(2):315-359.

_____, 1960: Palaeotectonic evolution of the central and western Alps. Geol. Soc. Am. Bull., 71:843-907.

WENK, E., 1943: Ergebrisse und Problem von Gefügeuntersuchunger in Verzascatal (Tessin). S.M.P.M., 23: 265-294.

____, 1962: Plagioklas als Indexmineral in den Zentralalpen. S.M.P.M., 42: 139-152.

____, 1963: Das reaktivierte Grundgebirge der Zentralalpen. Geol. Rundschau, 52: 754-766.

____, and KELLER, F., 1969: Isograde im Amphibolitserien der Zentralalpen. S.M.P.M., 49(1): 157-198.

____, and TROMMSDORFF, V., 1965. Parallelgefüge und Glimmerregelund im Südöstlichen Teil der Simplongruppe. Eclogae geol. Helv., 58: 417-422.

WENK, H.R., 1966: Die Geologische Abbildung, erläutert am Beispiel der Zentralalpen. Eclogae geol. Helv., 59(2) 777-788.

____, 1970: Geologische Beobachtungen im Bergell 1. Gedanken zur Genese des Bergeller Granits. (Rückblick und Ausblick) S.M.P.M., 50(2): 321-348.

WIELAND, H., 1966: Zur Geologie und Petrographie der Valle Isorno (Novara, Italia). S.M.P.M., 46: 189-303.

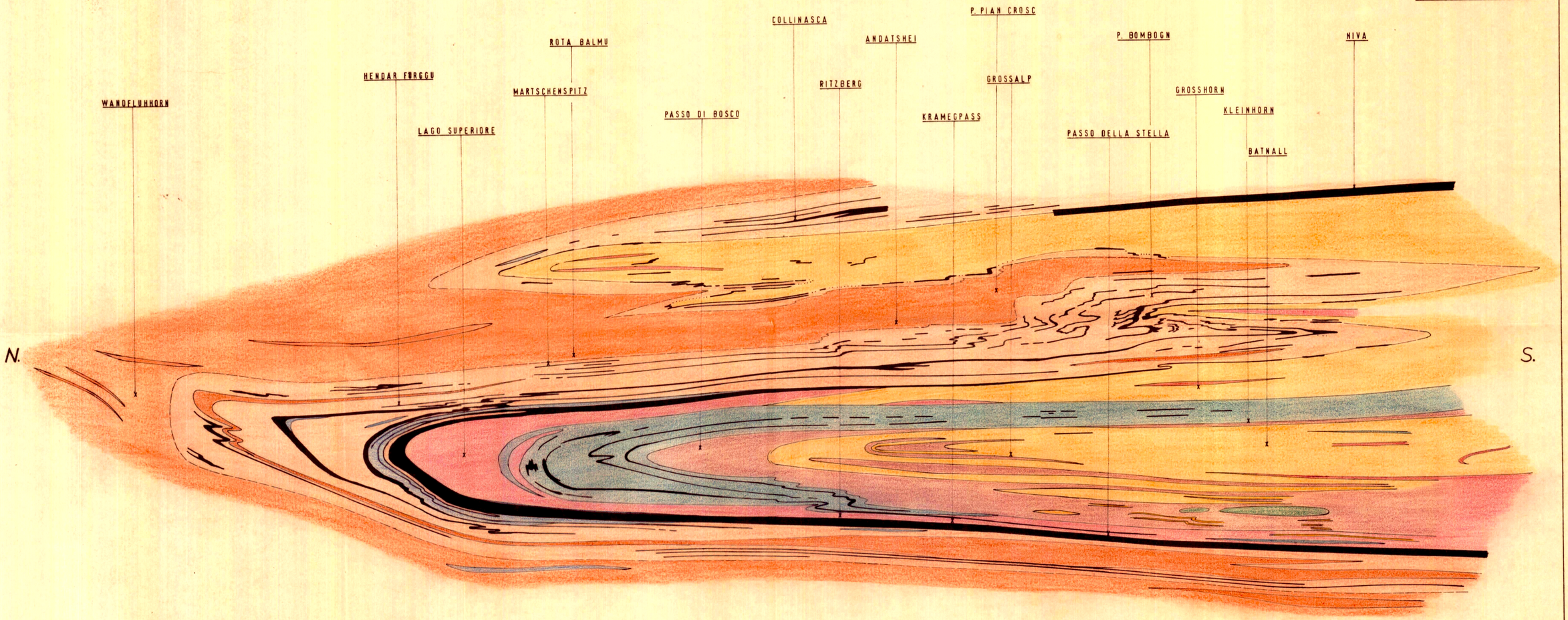
WINKLER, H.G.F., 1967: Petrogenesis of Metamorphic Rocks. Springer-Verlag, Berlin, 237 p.

STRUCTURAL PROFILE - VALLE DE BOSCO

SCALE 1:10,000

FAULTS NOT SHOWN

LEGEND AS FOR GEOLOGICAL MAP



WDMH 6/72

GEOLOGICAL MAP - VALLE DI BOSCO

SCALE 1:10.000

LEGEND

MESOZOIC
- Calc Schist, Marble, Petitic Schist, Quartzite.

ANTIGORIO GNEISS
- Biotite Gneiss
- Muscovite Gneiss
- Diorite Gneiss
- Hornblende Schist
- Schistose Gneiss

BOSCO GROUP
- Garnet Schist
- Hornblende Schist
- Amphibolite, Ultramafic Schist
- Staurolite Schist
- Muscovite Gneiss

PRE-ALPINE ROCKS
- Schist, Granite

/23 Strike and Dip of F_2 Schistosity

Wandfluhhorn
Strahlbann
P. d'Orsalia
Hendar Furgga
Lago Superiore
Bann
Bort
Martschenspitz
Rota Balma
Wolfstaffel
Passo di Bosco (Guriner Furka)
Ritzberg
Grossalp
Krameggpass
Lago del Cramec
Passo della Stella
Chummuheij
Batnall
P. Quadro
Passo Quadrella
Kleinhorn
Sassa Rosso
Grosshorn
SCHWARZA BRUNNA
BOSCO-GURIN
UBARAG
ALP BORMA
ANDATSCHEI
P. Bamboga
P. Pian Crosc
Piano dei Vitetti
CORINO
CAMANDI
CERENTINO
COLLINASCA
NIVA
RITANA
POGGA
CIOS

WDMH 6/72